https://doi.org/10.15388/vu.thesis.949
https://orcid.org/0000-0002-6171-6913

VILNIUS UNIVERSITY
NATURE RESEARCH CENTRE

Justė Aželytė

Avian Malaria Parasites: Interaction with Gut Microbiome and Factors Shaping Parasite Development

DOCTORAL DISSERTATION

Natural Sciences,
Zoology (N 014)

VILNIUS 2026

The dissertation was prepared between 2021 and 2025 (Nature Research Centre). The research was supported by the Research Council of Lithuania (Nr. S-MIP-20-25, S-MIP-22-52), and the Research Council of Lithuania, European Social Fund (Nr. 09.3.3-LMT-K-712-01-0016).

Academic Supervisor – Dr. Vaidas Palinauskas (State Scientific Research Institute Nature Research Centre, Natural Sciences, Zoology N 014)
Academic Consultant – Dr. Alejandro Cabezas-Cruz (National Research Institute for Agriculture, Food and Environment, France).

This doctoral dissertation will be defended in a public meeting of the Dissertation Defence Panel:

Chairman – Dr. Maria Fernanda Torres Jimenez (Vilnius University, Natural Sciences, Zoology N 014).
Members:
Dr. Rasa Binkienė (Nature Research Centre, Natural Sciences, Zoology N 014),
Dr. Kasun Harshana Bodawatta (Lund University, Natural Sciences, Zoology N 014),
Prof. Dr. Jana Radzijevskaja (Vytautas Magnus University, Natural Sciences, Zoology N 014),
Dr. Bazilė Ravoitytė (Nature Research Centre, Natural Sciences, Biology N 010).

The dissertation shall be defended at a public meeting of the Dissertation Defence Panel at 13h on 29th June, 2026, in meeting room 101 of the Nature Research Centre.
Address: Akademijos str. 2. LT-08412, Vilnius, Lithuania.
Tel. +37052729257; e-mail: sekretoriatas@gamtc.lt

https://doi.org/10.15388/vu.thesis.949
https://orcid.org/0000-0002-6171-6913

VILNIAUS UNIVERSITETAS
GAMTOS TYRIMŲ CENTRAS

Justė Aželytė

Paukščių maliarijos parazitai: sąveika su žarnyno mikrobiota ir veiksniai darantys įtaką parazito vystymuisi

DAKTARO DISERTACIJA

Gamtos mokslai,
Zoologija (N 014)

VILNIUS 2026

Disertacija rengta 2021–2025 metais (Gamtos tyrimų centras).
Mokslinius tyrimus rėmė Lietuvos mokslo taryba (Nr. S-MIP-20-25, S-MIP-22-52), Lietuvos mokslo taryba, Europos socialinis fondas (Nr. 09.3.3-LMT-K-712-01-0016)

Mokslinis vadovas – dr. Vaidas Palinauskas (Gamtos tyrimų centras, gamtos mokslai, zoologija, N 014).
Mokslinis konsultantas – dr. Alejandro Cabezas-Cruz (Nacionalinis žemdirbystės, maisto ir aplinkos mokslinis institutas, gamtos mokslai, zoologija, N 014, Prancūzija).

Gynimo taryba:
Pirmininkė – dr. Maria Fernanda Torres Jimenez (Vilniaus universiteto, gamtos mokslai, zoologija, N 014).
Nariai:
Dr. Rasa Binkienė (Gamtos tyrimų centras, gamtos mokslai, zoologija, N 014),
Dr. Kasun Harshana Bodawatta (Lundo universitetas, gamtos mokslai, zoologija, N 014),
Prof. dr. Jana Radzijevskaja (Vytauto Didžiojo universitetas, gamtos mokslai, zoologija N 014),
Dr. Bazilė Ravoitytė (Gamtos tyrimų centras, gamtos mokslai, biologija, N 010).

Disertacija ginama viešame Gynimo tarybos posėdyje 2026 m. birželio 29 d. 13 val. Gamtos tyrimų centro 101 posėdžių salėje.
Adresas: Akademijos g. 2, LT-08412, Vilnius, Lietuva).
Tel. +37052729257; el. p. sekretoriatas@gmatc.lt

TABLE OF CONTENTS

ABBREVIATIONS

α1,3GT – α-1,3-galactosyltransferase

α-Gal – galactose-α-1,3-galactose

Abs – antibodies

ANOVA – analysis of variance

ASV – amplicon sequence variant

BLAST – basic local alignment search Ttol

Cyt b – mitochondrial cytochrome b gene

COG - clusters of orthologous groups

DPI – days post-infection

DNA – deoxyribonucleic acid

EC - enzyme commission

ELISA – enzyme-linked immunosorbent assay

HAS – human serum albumin

HRP – horseradish peroxidase

IgG – immunoglobulin G

IgY – immunoglobulin Y

IgM – immunoglobulin M

IMD – immune deficiency

KEGG- kyoto encyclopedia of genes and genomes

KO – KEGG orthologs

NCBI – The National Center for Biotechnology Information

OD – optical density

PERMANOVA – permutational multivariate analysis of variance.

PBS – phosphate-buffered saline

PBST – phosphate-buffered saline with Tween-20

PCR– polymerase chain reaction

PGRP – peptidoglycan recognition proteins

QIIME – quantitative insights into microbial Eeology

RNA – ribonucleic acid

rRNA – ribosomal ribonucleic acid

TRIzol LS – total RNA isolation reagent

LIST OF ORIGINAL PUBLICATIONS

This dissertation is based on the following co-authored original publications, published in six journals indexed in the Clarivate Analytics Web of Science (CA WoS) database. Throughout the dissertation, publications are cited using Roman numerals.

I. Palinauskas V, Mateos-Hernandez L, Wu-Chuang A, de la Fuente J, **Aželytė J**, Obregon D, Cabezas-Cruz A. Exploring the Ecological Implications of Microbiota Diversity in Birds: Natural Barriers Against Avian Malaria. *Front Immunol* (Q1; IF 6.4) (2022) 13:807682. doi: 10.3389/fimmu.2022.807682

II. **Aželytė J**, Maitre A, Abuin-Denis L, Wu-Chuang A, Žiegytė R, Mateos-Hernández L, Obregón D, Palinauskas V, Cabezas-Cruz A. Nested Patterns of Commensals and Endosymbionts in Microbial Communities of Mosquito Vectors. *BMC Microbiology* (Q2; IF 4.2) (2024) 24(1), 1-13, doi: 10.1186/s12866-024-03593-x

III. **Aželytė J**, Wu-Chuang A, Žiegytė R, Platonova E, Mateos-Hernandez L, Maye J, Obregon D, Palinauskas V, Cabezas-Cruz A. Anti-Microbiota Vaccine Reduces Avian Malaria Infection Within Mosquito Vectors. *Front Immunol* (Q1; IF 6.4) (2022) 13:841835. doi: 10.3389/fimmu.2022.841835

IV. **Aželytė J**, Wu-Chuang A, Maitre A, Žiegytė R, Mateos-Hernández L, Obregón D, Palinauskas V, Cabezas-Cruz A. Avian Malaria Parasites Modulate Gut Microbiome Assembly in Canaries. *Microorganisms* (Q2; IF: 4.5) (2023) 11:563. doi: 10.3390/microorganisms11030563

V. **Aželytė J**, Maitre A, Abuin-Denis L, Piloto-Sardiñas E, Wu-Chuang A, Žiegytė R, Mateos-Hernández L, Obregón D, Cabezas-Cruz A, Palinauskas V. Impact of *Plasmodium relictum* Infection on the Colonization Resistance of Bird Gut Microbiota: A Preliminary Study. *Pathogens* (Q2; IF: 3.3) (2023), 13(1), 1-14. doi: 10.3390/pathogens13010091

VI. García-Longoria L, Palinauskas V**, Aželytė J**, Marzal A, Ovelleiro D, Hellgren O. Generalist Malaria Parasites and Host Imprinting: Unveiling Transcriptional Memory. *Mol Biol Evol* (Q1; IF 5.3) (2025), 1;42(9):msaf198. doi: 10.1093/molbev/msaf198

All authors made editorial contributions and revised and accepted the final versions of the manuscripts.

I. AC-C (Alejandro Cabezas-Cruz) and VP (Vaidas Palinauskas) conceived the study. LM-H (Lourdes Mateos-Hernández), AW-C (Alejandra Wu-Chuang), VP, and **JA (Justė Aželytė)** performed the experiments and acquired the data. DO, AW-C, LM-H, and AC-C analyzed the data. DO (Dasiel Obregón), AW-C, and AC-C prepared figures. AC-C, VP, and JF (José de la Fuente) contributed reagents and other resources. AC-C, VP, and DO supervised the work. AC-C, LM-H, and VP drafted the first version of the manuscript.

II. AC-C and VP conceived the study and supervised the work. **JA**, AM (Apolline Maitre), LA-D, DO, AW-C, LM-H, VP, and RŽ (Rita Žiegytė) performed the analyses. **JA** and AM prepared the figures. **JA**, AM, and AC-C drafted the manuscript.

III. AC-C and VP conceived the study. **JA**, RŽ, JM (Jennifer Maye), EP, LM-H, and VP performed the experiments and acquired the data. **JA**, AW-C, and DO analyzed the data. **JA**, AW-C, and AC-C prepared the figures. AC-C, VP, and JM contributed reagents and other resources. AC-C, VP, and DO supervised the work. **JA**, AW-C, AC-C, and VP drafted the first version of the manuscript.

IV. VP and AC-C conceived the study. **JA**, RŽ, and VP performed the experiments and acquired the data. **JA**, AW-C, DO, AM, and LM-H analyzed the data. **JA**, DO, and AC-C prepared figures and Supplementary Materials. VP and AC-C contributed reagents and other resources. VP, AC-C and DO supervised the work. **JA**, AW-C, AM and AC-C drafted the first version of the manuscript.

V. AC-C and VP conceived the study and supervised the work. **JA**, AM, LA-D, EP-S (Elianne Piloto-Sardiñas), DO, AW-C, LM-H and RŽ performed the analyses. **JA**, AM, LA-D and EP-S prepared the figures. LA-D, AW-C and DO provided software. **JA** and AC-C drafted the manuscript.

VI. OH (Olof Hellgren) and VP conceived the study, designed the overall experiment, and contributed to the conceptual development. VP and **JA** performed all experimental work, including experimental infections and laboratory procedures. OH, VP, and A.M. (Alfonso Marzal) secured funding for the research. LG-L (Luz García-Longoria) conducted bioinformatics analyses and statistical assessments, drafted the manuscript, and contributed to the conceptual

development and interpretation of results. D.O. (David Ovelleiro) provided support and assistance with bioinformatics.

LIST OF CONFERENCE PRESENTATIONS ON THE DISSERTATION TOPIC

1. **Aželytė, J**., Wu-Chuang, A., Žiegytė, R., Platonova, E., Mateos-Hernandez, L., Maye, J., Obregon, D., Palinauskas, V. ir Cabezas-Cruz, A. (2022). Microbiota modulation reduces *Plasmodium relictum* infection in mosquitoes *Culex quinquefasciatus.* In the 15th International Congress of Parasitology (ICOPA 2022). Copenhagen, Denmark.
2. Palinauskas, V., Mateos-Hernandez, L., Wu-Chuang, A., De La Fuente, J., **Aželytė, J.,** Obregon, D., & Cabezas-Cruz, A. (2022). Can gut microbiota enhance immunity against avian malaria? In Fifth international conference on malaria and related haemosporidian parasites of wildlife: book of abstracts (pp. 87-87). Bielefeld, Germany.
3. **Aželytė, J**., Wu-Chuang, A., Žiegytė, R., Platonova, E., Mateos-Hernandez, L., Maye, J., Obregon, D., Palinauskas, V. ir Cabezas-Cruz, A. (2022). The impact of mosquito microbiota on sporogony of avian malaria parasites. Biofuture: Perspectives in Natural and Life Sciences. The 15th Conference of Young Scientists in Lithuania: book of abstracts (pp. 7-7). The Lithuanian Academy of Sciences, Vilnius, Lithuania.
4. **Aželytė, J.,** Wu-Chuang, A., Maitre, A., Žiegytė, R., Mateos-Hernandez, L., Obregon, D., Cabezas-Cruz, A., & Palinauskas, V. (2023). Can avian malaria disrupt microbiome of the host? In The COINS 2023: International Conference of Life Sciences: book of abstracts (pp. 96-96). Vilnius, Lithuania.
5. **Aželytė, J.,** Wu-Chuang, A., Maitre, A., Žiegytė, R., Mateos-Hernandez, L., Obregon, D., Cabezas-Cruz, A., & Palinauskas, V. (2023). Changes in bird gut microbiome during avian malaria infection. In 10th Conference of the Scandinavian- Baltic Society for Parasitology (SBSP): book of abstracts (pp. 68-68). Tartu, Estonia.
6. **Aželytė, J.,** Maître, A., Abuin-Denis, L., Piloto-Sardiñas, E., Wu-Chuang, A., Žiegytė, R., Mateos-Hernandez, L., Obregon, D., Cabezas-Cruz, A. ir Palinauskas, V. (2023). The impact of avian malaria infection on the gut microbiota of vertebrate hosts. Biofuture: Perspectives in Natural and Life Sciences. The 16th Conference of Young Scientists in Lithuania: book of abstracts (pp. 9-9). The Lithuanian Academy of Sciences, Vilnius, Lithuania.
7. **Aželytė, J.,** Maitre, A., Abuin-Denis, L.,Piloto-Sardiñas, E., Wu-Chuang, A., Žiegytė, R., Mateos-Hernández, L., Obregón, D., Cabezas-Cruz, A., Palinauskas, V. (2024). The impact of avian malaria infection on the gut microbiota of the vertebrate host. In the COINS 2024:

International Conference of Life Sciences: book of abstracts (pp. 253-253). Vilnius, Lithuania.

8. **Aželytė, J**., Maitre, A., Abuin-Denis, L., Piloto-Sardiñas, E., Wu-Chuang, A., Žiegytė, R., Mateos-Hernández, L., Obregón, D., Cabezas-Cruz, A., Palinauskas, Vaidas. (2024). Exploring the effects of avian malaria on bird gut microbiota. In the 6th International Conference on Malaria and Related Haemosporidian Parasites of Wildlife: book of abstracts. Medellin, Colombia.

SCIENTIFIC PROBLEM

Avian malaria has long been recognized as a significant threat to wild bird populations with serious ecological and evolutionary consequences (Valkiūnas, 2005). Avian malaria parasites with noticeable ecological flexibility, such as *Plasmodium relictum* and *Plasmodium homocircumflexum*, can negatively impact avian health (Simberloff & Rejmanek, 2011; Martinez de la Puente et al., 2021; Palinauskas et al., 2015). Infections may reduce host fitness, affecting survival, reproduction, and long-term population stability (Santiago-Alarcon & Marzal, 2020). As a result, it makes avian malaria not only a threat to biodiversity but also a valuable model system for studying host–parasite interactions in a natural context.

The outcomes of parasite infections are shaped not only by parasite genetics but also by a complex interplay between host biology and environmental pressures (Ruiz-Lopez, 2020; Gabrieli et al., 2021; Cansado-Utrilla et al., 2021). In particular, host and vector microbiota are increasingly recognized as key contributors to parasite dynamics. The microbiota – including bacteria, fungi, and viruses – interacts directly and indirectly with the host and parasites (Palinauskas et al., 2024; Ipollito et al., 2018). These microorganisms influence host immune responses and homeostasis, mediate susceptibility or resistance to infection, and affect pathogen development, vector competence, and transmission efficiency (Cansado-Utrilla et al., 2021; Gutierrez-Lopez et al., 2020; Ippolito et al., 2018; Belkaid et al., 2014).

In mosquitoes, microbiota colonize multiple organs, including the gut, salivary glands, and reproductive tissues (Romoli & Gendrin, 2018). These communities profoundly influence mosquito biology by affecting survival, immune function, and pathogen development within the vector (Romoli & Gendrin, 2018; Palinauskas et al., 2024). Importantly, mosquito microbiota also come into contact with host blood components during feeding, creating interactions that can influence both the mosquito and the parasite (Yilmaz et al., 2014). Studies further show that parasite infections can alter mosquito microbiota, while the microbiota itself can determine the success of parasite development (Romoli et al., 2021). The implications are substantial, since such interactions directly influence vector competence and the efficiency of malaria transmission.

The vertebrate host microbiome is equally important in this tripartite relationship. In wild birds, gut microbial communities are shaped by both intrinsic factors, such as genetics and immune status, and extrinsic factors, such as diet, habitat, and parasite infection (Waite & Tailor, 2014). Next-generation sequencing approaches have greatly expanded our understanding

of avian gut microbiota diversity and their functional roles in host physiology (Sun et al., 2022). Several studies further indicate that malaria parasites can alter host microbiota, with consequences for immunity and even host behaviour (Taniguchi et al., 2015; Mooney et al., 2015; Gabrieli et al., 2021). Notably, there is evidence that parasite-induced changes in the microbiome may modify host odor profiles, thereby increasing mosquito attraction to infected individuals and facilitating transmission (Ruiz-Lopez et al., 2020).

However, taxonomic composition alone cannot fully explain how microbiota influence parasite development or respond to infection (Gabrieli et al., 2021; Ruiz-Lopez et al., 2020). Microbial network stability, resilience to colonization, and functional metabolic pathways may be as important as taxonomic composition in shaping host–parasite interactions (Cansado-Utrilla et al., 2021; Ruiz-Lopez et al., 2020).

While host and vector microbiota represent one layer of complexity, parasite plasticity provides another. Generalist parasites such as *Plasmodium* spp. must cope with widely varying environments when transmitted across phylogenetically distinct host species. These environments differ in immune defences, body temperature, metabolic processes, and nutrient availability – all factors that pose challenges for parasite survival and replication (Agosta et al., 2010; Gupta et al., 2020; Prati et al., 2022). However, it remains unclear whether adaptation to new host environments is driven primarily by genetic divergence or by rapid transcriptional responses that allow parasites to adjust to different host physiologies and immune systems (Prati et al., 2022; Turnbull et al., 2022). Understanding these mechanisms is key to explaining the ecological success of generalist parasites such as *P. relictum* or *P. homocircumflexum*.

Despite growing recognition of the importance of microbiota in host-parasite systems, many aspects of these interactions remain insufficiently understood. In particular, it was unclear how microbial communities associated with vertebrate hosts and mosquito vectors influence malaria parasite development and transmission, or whether host-derived immune responses can indirectly affect parasite success through microbiota-mediated mechanisms. It also remained uncertain whether malaria parasites adapt to new host environments primarily through genetic divergence or rapid transcriptional responses. This dissertation therefore addressed the following questions: (1) can the bird-malaria parasite-microbiota system serve as an experimental model to identify natural barriers that restrict parasite development and transmission; (2) can host-derived immune factors modulate mosquito gut microbiota and thereby affect parasite development in the vector; (3) how do malaria parasites affect vertebrate host gut microbiota

composition and community structure, and how might these microbial communities influence parasite infection dynamics; and (4) how do avian malaria parasites genetically and transcriptionally respond to changes in vertebrate host environments?

THE AIM AND MAIN TASKS OF THIS DISSERTATION

The aim of this dissertation is to investigate host and vector microbiota and their alterations during avian malaria infections, assess their impact on parasite sporogonic development, and examine how avian malaria parasites genetically and transcriptionally respond to changes in the vertebrate host environment.

Main tasks:

1. To investigate the bird-malaria parasite-microbiota system as an experimental model to identify natural barriers that may restrict malaria parasite development.
2. To estimate the microbiota composition of *Culex pipiens* f. *molestus* and *Culex quinquefasciatus* and evaluate the impact of *Plasmodium relictum* infection on vector gut microbial communities.
3. To evaluate whether host-derived antibodies can modulate *Culex quinquefasciatus* gut microbiota and influence the sporogonic development of *Plasmodium relictum*.
4. To assess the impact of *Plasmodium relictum* and *Plasmodium homocircumflexum* infections on the gut microbiota composition, community assembly, and colonization resistance in canaries (*Serinus canaria domestica*);
5. To determine the genetic and transcriptional response of *Plasmodium homocircumflexum* to changes in the vertebrate host immune environment, using experimentally infected canaries (*Serinus canaria domestica*) and Eurasian siskins (*Spinus spinus*).

STATEMENTS TO BE DEFENDED

1. The bird-malaria parasite-microbiota system represents an innovative experimental framework that integrates host gut microbiota diversity as an important factor influencing avian malaria infection dynamics, particularly through modulation of anti-α-Gal immunity and host resistance to *Plasmodium* spp.

2. *Culex quinquefasciatus* and *Culex pipiens* f. *molestus* differ in the assembly and dynamics of their midgut microbial communities despite similar diversity, and *Plasmodium relictum* infection alters the microbial composition and network topology in *C. quinquefasciatus.*

3. Modulation of *Culex quinquefasciatus* midgut microbiota by antibodies induced in birds by *Escherichia coli* O86:B7 reduces *Plasmodium relictum* oocyst formation, indicating a functional link between vertebrate immunity and vector competence.

4. Infection with avian malaria parasites, *Plasmodium relictum* and *Plasmodium homocircumflexum*, modulates the avian gut microbiota, causing deviations from its normal developmental trajectory and reducing colonization resistance, thereby compromising microbial community stability.

5. During *Plasmodium homocircumflexum* infection, parasites inherit transcriptional profiles from the previous host and gradually adapt them to the new host's immune and physiological conditions.

NOVELTY AND SIGNIFICANCE

1. For the first time, the bird-malaria parasite-microbiota system was proposed as an experimental framework to investigate the links between gut microbiota composition, anti-α-Gal antibody responses, and malaria infection after demonstrating the presence of α-Gal in protein extracts from three avian malaria parasites, *Plasmodium ashfordi*, *Plasmodium relictum*, and *Plasmodium homocircumflexum*, obtained from experimentally infected Eurasian siskins (*Spinus spinus*).
2. A high similarity in microbiota composition was observed between two avian malaria vectors, *Culex pipiens* f. *molestus* and *Culex quinquefasciatus*, reared under controlled laboratory conditions; however, network analyses revealed that despite this similarity, microbial communities of these mosquito species exhibit distinct responses in their structural dynamics under simulated perturbations, highlighting that microbiota organization – not only composition – may be relevant for understanding vector-parasite interactions.
3. For the first time, antibodies induced in birds by α-Gal-expressing bacteria were shown to modulate mosquito microbiota, providing a mechanism by which vertebrate immunity can influence vector microbial communities.
4. Host-derived antibodies directed against specific bacterial antigens were shown to remain functional within mosquito tissues, where they modulate *Plasmodium*-induced changes in the vector microbiota, leading to gut microbial restructuring and reduced parasite infectivity.
5. A study of the avian gut microbiota provides the first experimental evidence that avian malaria infection induces mainly transient changes in the vertebrate host gut microbiome, affecting the abundance of specific bacterial taxa.
6. For the first time, functional profiling of the gut microbiota in *Plasmodium*-infected birds demonstrated that infection can alter microbial metabolic pathways. Some of these pathways are likely to contribute to the microbial response against malaria infection, suggesting that microbiome functionality, not only composition, may play a role in host-parasite-microbiota interactions.
7. *Plasmodium* infection affects interactions among bacterial species, leading to changes in microbial network structure. *In silico* experiment revealed that these alterations reduce network stability and resilience to colonization, highlighting a previously unrecognized layer of host-parasite-microbiota interaction.

8. For the first time, a generalist parasite, *Plasmodium homocircumflexum,* was tested for its adjustment to different host species. Results indicate epigenetic inheritance, with transcriptional profiles initially retained from the donor and gradually adjusting to the recipient host, while selection-driven genetic divergence was not supported.

1. BRIEF LITERATURE REVIEW

1.1. Avian malaria parasites

Avian haemosporidian parasites (order Haemosporida) are globally distributed protozoans, with malaria-causing *Plasmodium* species actively circulating in the Baltic region. The order comprises three main genera – *Haemoproteus, Leucocytozoon*, and *Plasmodium*. Morphologically, more than 50 species of avian *Plasmodium* have been described to date (Valkiūnas, 2005; Valkiūnas and Iezhova, 2018). These parasites have a complex life cycle that requires two hosts: a vertebrate host and an insect vector (Valkiūnas, 2005). In birds, *Plasmodium* infections can cause severe disease and, occasionally, host mortality (Valkiūnas, 2005; Palinauskas et al., 2011, 2016). Research on avian malaria has demonstrated that infection severity and host susceptibility vary widely among species and even between individuals (Bensch et al., 2009; Hellgren et al., 2013; Palinauskas et al., 2011).

Complex interactions occur within the host-parasite-vector system. To complete its life cycle, *Plasmodium* undergoes multiple developmental stages in both the avian host and the mosquito vector. Following transmission, sporozoites enter the host through the skin during a mosquito blood meal, circulate briefly in the bloodstream, and invade reticuloendothelial cells, where exoerythrocytic development occurs (Valkiūnas, 2005). Throughout its development within the avian host, *Plasmodium* must overcome immune defenses and oxidative stress at multiple life-cycle stages (Palinauskas et al., 2020). Merozoites released into circulation initiate the erythrocytic cycle within red blood cells, and a subset of these differentiate into macro- and microgametocytes, which are taken up by mosquitoes during blood feeding. In mosquito midguts, fertilization and sporogony occur. After fertilization, zygotes develop into motile ookinetes that penetrate the midgut epithelium and transform into oocysts, where sporozoites mature and migrate to the salivary glands, ready to infect a new avian host. The sporogonic stage in the mosquito midgut represents a key point of interaction between the parasite and the vector microbiota, which can influence parasite development and transmission efficiency (Bando et al., 2013; Wang et al., 2021).

The progression of infection in vertebrate hosts is influenced primarily by parasite origin and the host's immune response, with environmental factors likely contributing as well, although their roles remain poorly understood (Palinauskas et al., 2020). Based on their ability to infect different hosts, *Plasmodium* species can be classified as specialists, with a narrow host range, or generalists, capable of infecting a broad spectrum of avian species

(Valkiūnas, 2005). Generalist parasites face a unique challenge with each host shift, encountering different immune responses that demand rapid physiological adaptation to survive and reproduce (Agosta et al., 2010). Two avian malaria parasites, *Plasmodium relictum* and *Plasmodium homocircumflexum*, exemplify this flexibility. Both can infect multiple host species, producing variable infection outcomes that range from low parasitemia and low virulence to high virulence and host mortality (Ilgūnas et al., 2016; Martínez-de la Puente et al., 2021; Palinauskas et al., 2015). These differences likely reflect host-specific adaptations in parasite gene expression (García-Longoria et al., 2020). Understanding the relationships between parasite genetic diversity, host specificity, and immune adaptation is essential for explaining the evolutionary success of avian malaria parasites. However, successful transmission also depends on parasite development within the insect vector, where interactions with the mosquito microbiota may further influence infection outcomes.

1.2. Vector microbiota

The mosquito midgut harbors a complex and dynamic microbiota composed of bacteria, fungi, viruses, and other microorganisms that colonize the digestive tract and influence host physiology and pathogen interactions. The term microbiome encompasses this microbial community and its collective genetic content (Ippolito et al., 2018). The composition of the mosquito gut microbiota varies across developmental stages, species, and environmental conditions, and its members interact with one another and with the mosquito host (Romoli & Gendrin, 2018). Over the past decade, growing research has shown that these interactions can significantly modulate vector competence by affecting the survival and development of pathogens within the mosquito (Ippolito et al., 2018). In the case of avian *Plasmodium*, the parasite enters the mosquito during a blood meal, and its early developmental stages take place in the midgut, where the resident microbiota can directly influence parasite establishment and sporogonic development (Cirimotich et al., 2011).

Microbiota can influence parasite development in mosquitoes through both immune-mediated and direct mechanisms. Certain bacterial taxa activate mosquito immune pathways, such as the immune deficiency (IMD) pathway, via peptidoglycan recognition proteins (PGRP-LC), leading to the production of antimicrobial peptides that suppress *Plasmodium* development (Cirimotich et al., 2011). In parallel, midgut microorganisms can directly inhibit parasite survival by generating reactive oxygen species, competing for nutrients, or

secreting antiparasitic metabolites (Ippolito et al., 2018; Cirimotich et al., 2011).

Understanding the composition and functional diversity of the mosquito microbiota is therefore essential, as different bacterial species can exert contrasting effects on *Plasmodium* development. Experimental studies on human and rodent malaria systems have demonstrated that antibiotic treatment, which disrupts the native microbiota, can increase mosquito susceptibility to infection (Ramirez et al., 2014). Identifying bacterial taxa that inhibit or promote parasite development is therefore critical for the development of microbiota-based vector control strategies.

Several studies have highlighted species-specific microbial effects on *Plasmodium* sporogony. For instance, in rodent malaria, *Asaia bogorensis* bacteria in *Anopheles stephensi* alters midgut glucose metabolism, raising pH levels and enhancing *Plasmodium berghei* gametogenesis, which leads to higher oocyst counts compared to controls (Wang et al., 2021). Conversely, the introduction of certain gut bacteria has been shown to reduce the intensity of *Plasmodium falciparum* infection in mosquitoes (Cirimotich et al., 2011). Gram-negative bacteria from the families Enterobacteriaceae, Yersiniaceae, and Pseudomonadaceae generally exhibit inhibitory effects on *Plasmodium*, whereas Gram-positive bacteria rarely affect parasite development (Boissiere et al., 2012). However, most of these studies have focused on *Anopheles* species transmitting human malaria, while the microbiota-parasite interactions in avian malaria vectors remain poorly explored.

1.3. Avian host microbiota

Despite growing interest in host-microbiota interactions, knowledge of vertebrate host microbiota in relation to avian malaria remains limited. The composition of bird gut microbiota is shaped by ecological niche, diet, and host genetics, but interactions with the host immune system are only beginning to be understood (Grond et al., 2018). The gut microbiota can indirectly affect host health through its influence on pathogen colonization and immune modulation, yet data on its role in avian malaria are still sparse. Some studies suggest that gut bacteria can colonize the bursa of Fabricius, potentially contributing to the development of the adaptive immune system in young birds (Videvall et al., 2021a). Moreover, observational studies from malaria-endemic regions indicate that differences in microbiota composition may correlate with reduced malaria risk (Villarino et al., 2016), implying that microbial communities could play a protective role against infection.

The core avian gut microbiota typically consists of bacterial taxa from the phyla Proteobacteria, Firmicutes, Fusobacteria, Actinobacteria, and Bacteroidetes (Hird et al., 2015; Grond et al., 2019). Waite et al.'s (2014) study has shown that microbial communities cluster according to gastrointestinal tract regions, following patterns similar to those observed in mammals and reptiles. Environmental factors, such as habitat, migratory behavior, and diet, further contribute to interspecific variation in gut microbiota structure (Hird et al., 2015; Grond et al., 2019). Although relatively stable within individuals, these communities can shift under physiological stress, infection, or changes in diet, potentially altering host immune homeostasis (Kreisinger et al., 2015; Grond et al., 2018; Videvall et al., 2018).

Evidence from experimental models suggests that the microbiota can influence malaria infection outcomes through both immune-mediated and metabolic mechanisms (Villarino et al., 2016; Videvall et al., 2018). In mice, increased abundance of *Lactobacillus* and *Bifidobacterium* species has been associated with resistance to *Plasmodium yoelii* infection, while other bacterial groups may exacerbate disease severity (Villarino et al., 2016). Microbial metabolites also play a role. For example, propionate produced by *Bacteroides* has been shown to inhibit the growth of certain pathogens, suggesting that similar mechanisms could influence *Plasmodium* development (Villarino et al., 2016). These findings highlight the potential for gut microbial composition and metabolic activity to modulate host-parasite interactions.

Of particular interest are bacteria expressing α1,3-galactosyltransferase (α1,3GT) genes, including *Escherichia*, *Haemophilus*, *Pediococcus*, and *Lactobacillus*. These taxa can produce the disaccharide Galα1-3Gal (α-Gal), a carbohydrate antigen absent in birds, fish, and humans due to inactivation of the *ggta1* gene. The presence of α-Gal–expressing bacteria in the gut stimulates the production of natural anti-α-Gal antibodies, which may confer protection against α-Gal-bearing pathogens, including *Plasmodium* (Mateos-Hernández et al., 2020). This microbiota-driven immune response represents a potential natural defense mechanism linking gut microbial composition to malaria resistance.

The role of the avian gut microbiota in shaping immunity and infection dynamics is critical for interpreting patterns of susceptibility and resistance in wild and captive birds. *Plasmodium* infections can negatively affect reproduction and physiological performance, suggesting that shifts in microbiota composition may also influence host fitness with broader ecological and evolutionary consequences. Further research on the interactions among host microbiota, immune responses, and malaria parasites

will improve our ability to predict infection dynamics and may help identify new approaches to mitigate the impact of avian malaria.

1.4. Parasite gene expression

Gene regulation in haemosporidian parasites underpins their capacity to adapt to diverse hosts and to the internal environmental conditions they encounter within host organisms. In avian malaria, increasing evidence suggests that infection success and host range are determined not only by genetic diversity but also by transcriptional and epigenetic plasticity (García-Longoria et al., 2020; Kalbskopf et al., 2021; Videvall et al., 2017). Such regulatory flexibility allows parasites to modulate gene expression in response to host-specific immune pressures, metabolic constraints, and ecological variability, supporting their persistence across heterogeneous environments.

Recent transcriptomic investigations have revealed that avian *Plasmodium* species exhibit extensive gene-expression plasticity, reflecting adaptation to diverse host environments. In both *Plasmodium ashfordi* and *Plasmodium homocircumflexum*, genetically identical parasites show distinct transcriptional profiles depending on the avian host species (García-Longoria et al., 2020; Videvall et al., 2017). In *P. ashfordi*, expression patterns remained consistent across infection stages within the same host but differed substantially among host species, suggesting that gene regulation is finely adjusted to specific host physiological and immunological contexts rather than to temporal progression alone (Videvall et al., 2017). Similarly, in *P. homocircumflexum*, differential expression analyses across two passerine species identified gene sets associated with cell-invasion, apoptosis, and oxidative stress, indicating host-specific modulation of transcriptional programs (García-Longoria et al., 2020).

Complementing these between-host species observations, *Plasmodium relictum* displayed pronounced transcriptional shifts within a single host species across the course of infection (Kalbskopf et al., 2021). In experimentally infected Eurasian siskins (*Spinus spinus*), early and late infection stages exhibited distinct expression profiles, reflecting gene-regulatory adjustments to parasite development and the host's changing immune environment. Moreover, increased inter-individual variation in gene expression at the post-peak stage suggested that parasites in different hosts follow divergent transcriptional trajectories, possibly driven by variable immune responses or within-host selection pressures (Kalbskopf et al., 2021).

Research on human malaria parasites has provided evidence for similar patterns of transcriptional and epigenetic regulation. In *Plasmodium*

falciparum, transcription is influenced by stage-specific regulation and by genetic and environmental factors, with epigenetic mechanisms such as histone modification, chromatin remodeling, and DNA methylation playing central roles in controlling gene expression (Turnbull et al., 2022; Serrano-Duran et al., 2022). These processes generate phenotypic variation within clonal parasite populations, enabling rapid acclimation to changing host conditions and immune evasion without requiring underlying genomic change (Turnbull et al., 2022). Although direct molecular evidence remains limited in avian *Plasmodium*, analogous regulatory systems are likely conserved across the genus.

Overall, current evidence suggests that transcriptional and epigenetic plasticity play central roles in shaping the ecological versatility of avian malaria parasites. These dynamic regulatory strategies likely contribute to the success of generalist lineages such as *P. relictum* and *P. homocircumflexum*, which thrive across phylogenetically and immunologically diverse hosts. Nevertheless, transcriptomic data for avian *Plasmodium* remain limited, highlighting the need for additional comparative and experimental studies to better understand how regulatory flexibility influences host specificity, immune evasion, and parasite adaptation.

2. METHODS AND MATERIALS

A comprehensive description of the materials collected and the methodologies applied in this dissertation is presented in the published papers (**PAPERS I–VI**). A brief overview of the main methodologies used is provided below and in Figure 1.

2.1. Experimental immunization

Live and heat-inactivated *Escherichia coli* strains, which are known to have abundant α1,3GT genes responsible for α-Gal production, were prepared for oral immunization of domestic canaries (*Serinus canaria domestica*). Bacteria were cultured in Luria Broth (LB; Sigma-Aldrich, St. Louis, MO, USA) at 37 °C, washed, and resuspended in phosphate-buffered saline (PBS; 10 mM NaH_2PO_4, 2.68 mM KCl, 140 mM NaCl, pH 7.2; Thermo Scientific). Heat-inactivated bacteria were obtained by incubation at 70 °C for one hour. Each bird received 50 µL of bacterial suspension orally, with booster doses administered one and two weeks later; controls received PBS only. For protein quantification, bacterial lysates were prepared in Triton X-100, centrifuged, and analyzed using the Bradford assay (**PAPER III**).

2.2. Experimental infection of birds via inoculation

Juvenile domestic canaries and Eurasian siskins (*Spinus spinus*) used in the experiments were bought from commercial vendors and kept at the State Scientific Research Institute Nature Research Centre vivarium (License No. LT-61-13-003) under standard living conditions for birds.

Birds were experimentally infected with *Plasmodium homocircumflexum* (**PAPERS IV**, **VI**) or *Plasmodium relictum* (**PAPERS III, V**) following the protocol of Palinauskas et al. (2008). Each bird received 0.10 mL of infected blood mixed with 3.7% sodium citrate and 0.9% saline (4:1:5) injected into the pectoral muscle (Figure 1).

2.3. Experimental transmission of *Plasmodium* spp. via mosquito bite

For mosquito exposure and experimental bird infection, each donor bird was gently restrained in a paper tube with only the legs exposed to allow mosquito feeding (Kazlauskienė et al., 2013). The tube was placed in a cage with laboratory-reared female *Culex quinquefasciatus* mosquitoes. Birds were exposed for up to 10 minutes until mosquitoes had fed. Blood-fed mosquitoes

were kept in smaller cages (17.4 × 17.5 × 17.5 cm) for 17 days under standard conditions with water provided for oviposition. Following the blood feeding, mosquitoes were dissected and salivary glands were examined microscopically for sporozoites (**PAPER III**) (Figure 1).

2.1. Blood collection and microscopy

Blood samples were collected from birds via brachial vein puncture using sterile microcapillaries (**PAPERS III-VI**). A small droplet was used to prepare thin blood smears, which were air-dried, fixed in absolute methanol, and Giemsa-stained following Valkiūnas et al. (2008). Approximately 20 – 30 μL of blood was preserved in SET buffer (0.05M Tris, 0.15M NaCl, 0.5M EDTA, pH 8.0) for molecular analysis (**PAPERS III, IV, VI)**, and an additional 50 – 100 μL was collected for serum isolation (**PAPERS III, IV)**. For RNA studies, samples were stored in TRIzol LS reagent (**PAPER VI**).

Serum samples were allowed to clot at room temperature, then centrifuged at 5000×*g* for 5 min and stored at -15 °C until further use (**PAPERS III, IV**).

Microscopic examination of blood smears and mosquito-derived preparations was performed with an Olympus BX61 light microscope. Parasitemia was expressed as the percentage of infected erythrocytes based on counts of 10,000 red blood cells (Godfrey et al. 1987) (**PAPERS III, IV, VI**). Successful mosquito infection and parasite development (sporogony) were confirmed by observing sporozoites in dissected salivary gland preparations (**PAPER III**).

2.2. Collection of mosquito midguts and salivary glands

Mosquitoes were euthanized by vigorous shaking in an insect aspirator to stun them. Wings and legs were removed, and dissections were performed under a stereomicroscope. Each mosquito was separated into two parts: the thorax with the head and the abdomen. Midguts were extracted from abdomens in a drop of saline; some were stained following Kazlauskienė et al. (2013) to count *Plasmodium* oocysts (**PAPER III**), while others were left unstained, pooled, and frozen at -20 °C for microbiota analysis **(PAPERS II, III)**. Salivary glands were dissected from thoraxes, placed in saline, and crushed to prepare smears for detecting sporozoites (**PAPER III**). The remaining thorax tissues and salivary gland remnants were fixed in SET buffer for PCR analysis. To prevent contamination, new dissecting needles were used for each mosquito (**PAPER III**).

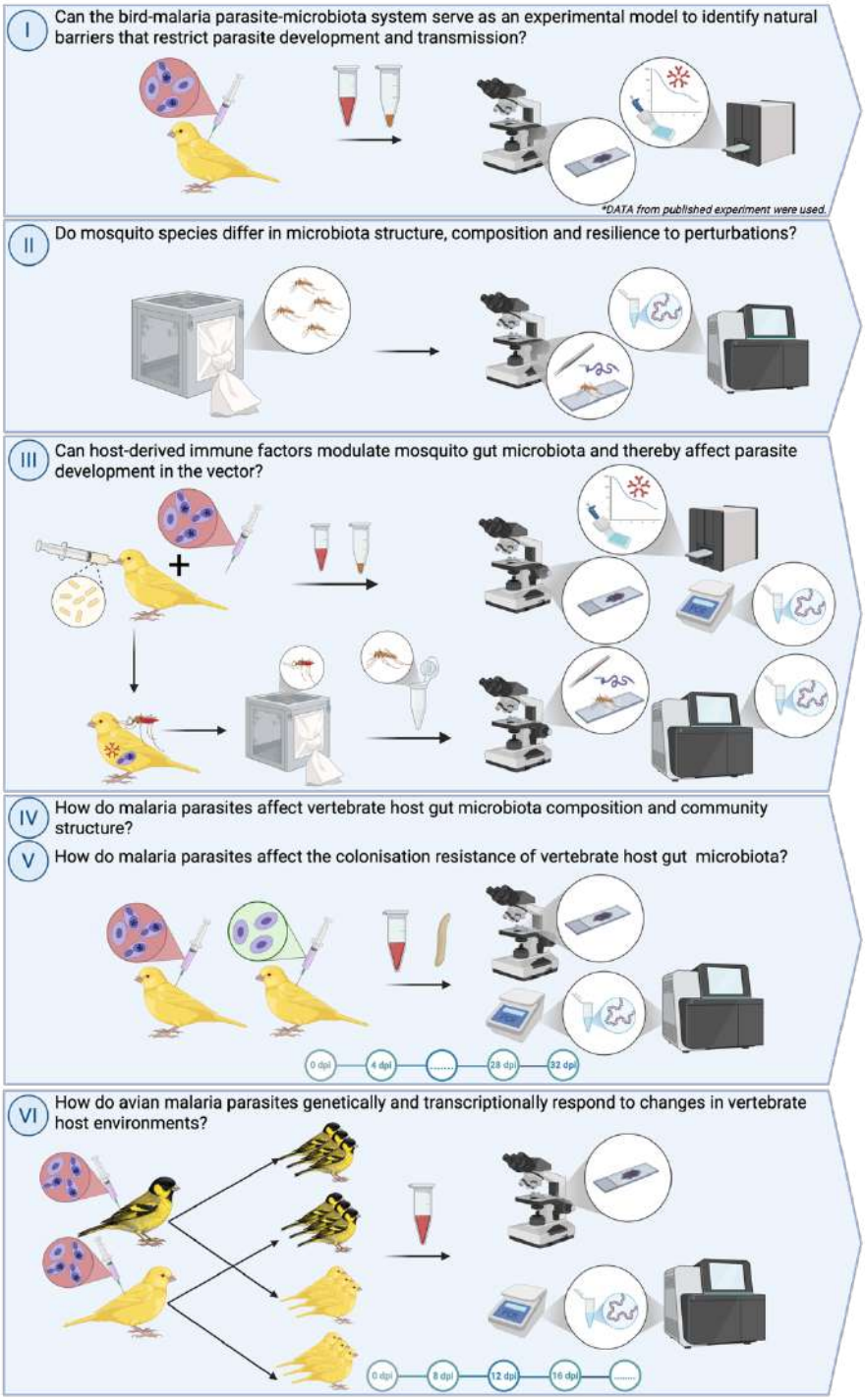

Figure 1. Schematic overview of the experimental workflows used in PAPERS I-VI. Roman numerals correspond to the respective papers. The schemes summarize the main research questions, experimental procedures, and methods used across the studies. Created in BioRender. Aželytė, J. (2026)

2.3. Molecular diagnostics

Genomic DNA from avian blood samples was extracted using the ammonium acetate protocol (Sambrook et al., 2001) (**PAPERS III, IV, VI**). Haemosporidian infections were detected using a nested PCR assay targeting a 478 bp fragment of the mitochondrial cytochrome b gene (Bensch et al., 2000; Hellgren et al., 2004). Amplification products were visualized on 2% agarose gels, and positive samples were sequenced using the primer HaemF on an ABI PRISM™ 3100 capillary sequencer (Applied Biosystems, USA). Resulting sequences were edited in BioEdit (Hall, 1999) and identified through BLAST searches against the NCBI database (**PAPERS III, IV, VI**).

Genomic DNA was extracted from frozen fecal samples or mosquito midguts using the PureLink™ Microbiome DNA Purification Kit (Invitrogen, Thermo Fisher Scientific, USA) and eluted in 70 µL of buffer. Extraction reagent controls were included by following the same DNA extraction steps as for the samples, using water instead. DNA quality (OD260/280 = 1.8–2.0) was verified with a NanoDrop™ One spectrophotometer (Thermo Scientific, USA) (**PAPERS III, IV**).

Library preparation and sequencing were performed by Novogene Bioinformatics Technology Co. (London, UK). DNA libraries were prepared with the NEBNext® Ultra™ II DNA Library Prep Kit (New England Biolabs, USA) using ≥ 200 ng of DNA (20 ng/µL). Amplicons of the V4 region of the 16S rRNA gene were generated using barcoded primers (515F/806R) and sequenced on an Illumina MiSeq platform (251 bp paired-end). Raw reads are available in the SRA repository (**PAPERS III, IV**).

Total RNA was extracted from 20µL of whole blood using 1 mL TRIzol LS, followed by phase separation with 200 µL chloroform (Merck, Germany) and purification using the RNeasy Mini Kit (Qiagen, Germany) according to the manufacturer's protocol. RNA samples were shipped on dry ice to Novogene Bioinformatics Technology (Hong Kong) for quality control, DNase treatment, rRNA depletion, and library preparation using the SMARTer Ultra Low Kit (Clontech, USA). Sequencing was performed on an Illumina HiSeq 2000, and read quality was assessed with FastQC (v0.10.1) (Andrews, 2010) (**PAPER VI**).

Sequencing data from fecal samples were used to characterize the bird gut microbiota, as fecal sampling provides a non-invasive longitudinal approach that most closely reflects the lower intestinal microbiome while yielding sufficient microbial biomass (Davies et al., 2026).

2.4. ELISA

Antibody levels in bird sera against *Escherichia coli* proteins were quantified using an indirect ELISA adapted from established protocols (Mateos-Hernández et al., 2021; Mateos-Hernández et al., 2020). Ninety-six-well plates (Thermo Scientific, USA) were coated with *E. coli* BL21 protein extract (50 ng/mL) in carbonate–bicarbonate buffer (0.05 M, pH 9.6) and incubated for 2 h at room temperature (RT) followed by overnight incubation at 4 °C. After washing with PBST (PBS + 0.05% Tween-20), wells were blocked with 1% human serum albumin (HSA) in PBS for 1h at RT. Serum samples diluted 1:200 in 0.5% HSA/PBS were added and incubated for 1 h at 37 °C. Bound antibodies were detected using HRP-conjugated goat anti-turkey IgG (MyBioSource, USA; 1:1000 in 0.5% HSA/PBST), followed by TMB substrate (Promega, USA) for 20 min. The reaction was stopped with 4% H_2SO_4, and absorbance was measured at 450 nm using a Filter-Max F5 microplate reader (Molecular Devices, USA). All samples were analyzed in triplicate, and mean optical density (OD) values were blank-corrected. The cut-off value was defined as twice the mean OD of the blanks (**PAPER III**).

2.5. Bioinformatic microbiota analysis

Amplicon sequence variants were generated based on 251-base paired-end reads from the V4 variable region of the 16S rRNA gene using barcoded universal primers (515F/806R). Sequencing data were processed using the QIIME 2 pipeline (v.2021.4). Unless otherwise stated, default parameters were used. Parameters for read trimming and rarefaction depth were adjusted based on sequence quality and sequencing depth across samples. Reads were demultiplexed, quality-filtered, denoised, and merged with DADA2, and chimeric sequences were removed. Amplicon sequence variants (ASVs) were aligned with MAFFT, and a phylogenetic tree was constructed using FastTree2. Taxonomic classification was performed using a naïve Bayes classifier trained on the SILVA database (release 132) for the V4 region (515F/806R). Taxonomic tables were collapsed at the genus level and filtered to remove taxa with fewer than 10 total reads or present in <30% of samples (**PAPERS II-V**).

Functional metagenomic predictions were generated using PICRUSt2, aligning ASVs to a reference tree (NSTI cut-off = 2) to infer gene family abundances. KEGG Orthologs (KO), Enzyme Commission (EC) numbers, and Clusters of Orthologous Groups (COG) were used as gene family

references, and metabolic pathways were reconstructed using the MetaCyc database (**PAPERS III, IV**).

2.6. Bacterial co-occurrence networks

Network construction and analysis were carried out using the Sparse Correlations for Compositional Data (SparCC) method, implemented in R ver. 4.2. Co-occurrence bacterial networks were generated for each condition based on genus-level taxonomic profiles. ASVs that could not be classified at the genus level were assigned to higher taxonomic ranks. These networks served to visually represent bacterial community structure and to assess the relative importance of bacterial taxa within the community. In this framework, taxa are represented as nodes, while significant co-occurrence interactions, either positive or negative, represented by different colors, are shown as edges connecting them. The resulting networks were visualized with Gephi 0.9.5, which was also used to calculate key topological properties, including the number of nodes and edges, network diameter, average degree, weighted degree, average path length, modularity, eigenvector centrality, and the number of modules.

2.7. Differential gene expression analysis

To analyze transcriptional responses of *Plasmodium homocircumflexum* to different avian hosts, parasite RNA reads were processed using both reference-based and *de novo* approaches. Reads mapping to the canary (serCan2020) and siskin (ASM3478079v1) genomes were removed, while those aligning to the *P. relictum* genome (GCA_900005765.1; Böhme et al., 2018) and a published *P. homocircumflexum* transcriptome (García-Longoria et al., 2020) were retained. Alignments were performed with STAR (Dobin et al., 2013) and Bowtie (Langmead & Salzberg, 2012), and *de novo* assembly with Trinity (v.2.15.1; Grabherr et al., 2011) yielded 14,649 contigs. To minimize host contamination, transcripts with GC content <23% (n = 12,058) were retained, consistent with the AT-rich nature of the *Plasmodium* genome. Gene expression was quantified using Salmon (v.1.3.2; Patro et al., 2017) and normalized by regularized log transformation in R (v.4.5.0), with visualizations produced in ggplot2 (Wickham, 2016) (**PAPER VI**).

The single-nucleotide polymorphism (SNP) analysis was performed with RNA-seq data. Parasite reads were isolated by sequentially removing host reads and using available *Plasmodium* references, together with a

previously published *P. homocircumflexum* transcriptome, to retain parasite sequences. A *de novo* transcriptome assembly was generated, and variant calling was performed on the mapped RNA-seq reads (**PAPER VI**).

2.8. Statistical analysis

All analyses were performed in R (versions 4.0-4.5) (R Core Team), Anaconda Python environment (v3.9.17) (Anaconda Software Distribution), and QIIME2 (v. 2021.4-2023.5) (Bolyen et al., 2019). Statistical tests were selected based on data normality and variance homogeneity. Differences in infection prevalence (oocyst and sporozoite frequency) were analyzed using Fisher's exact test with Bonferroni correction (**PAPER III**), while Mann–Whitney U and Kruskal–Wallis tests with Benjamini-Hochberg correction were applied to compare oocyst counts (**PAPER III**) and parasitemia levels (**PAPER VI**), respectively. Infection incidence and survival were compared using Chi-square and log-rank (Mantel–Cox) tests (**PAPER VI**).

For immunological assays, differences in antibody levels (OD values) among treatments and sampling days were assessed using two-way ANOVA with Bonferroni post hoc tests, or non-parametric tests (Mann–Whitney U or Kruskal–Wallis with Benjamini-Hochberg correction) when data deviated from normality (**PAPER III**).

Microbiota analyses were based on rarefied ASV tables processed in QIIME2 (Bolyen et al., 2019). Alpha diversity (Faith's phylogenetic diversity, Shannon index, Pielou's evenness) was compared using Kruskal–Wallis tests with Benjamini-Hochberg correction, while beta diversity (Bray–Curtis dissimilarity) was evaluated via PERMANOVA and betadisper ANOVA. Longitudinal variation was examined using first distances and random forest regression within the q2-longitudinal pipeline (**PAPERS II-V**).

Differentially abundant taxa and pathways (**PAPERS II-V)** and expressed genes (**PAPER VI**) were identified using DESeq2 (Love et al., 2014) or ALDEx2 (Wald test or t-test, $p < 0.05$) (Fernandes et al., 2014) with log fold-change normalization. Shared taxa and pathways were visualized using Venn diagrams (**PAPERS II-V**).

Bacterial co-occurrence networks were constructed using SparCC and visualized in Gephi (v. 0.9.2-0.9.5) (Bastian et al., 2009). Network topology and similarity between groups were assessed with NetCoMi (Peschel et al., 2021) using Jaccard's index ($p < 0.05$). Robustness to node removal or addition was evaluated with NetSwan (Lhomme, 2015) and igraph (Csardi et al., 2006), applying Wilcoxon signed-rank tests and Benjamini–Hochberg correction for multiple comparisons (**PAPERS II-V**).

All tests used a significance threshold of $p = 0.05$, and data visualization was performed in R Studio (R Studio Team), Anaconda Python environment (v3.9.17) (Anaconda Software Distribution), and Adobe Illustrator (**PAPERS II-VI**).

2.9. Permits, ethical statements and experimental animals.

All procedures were conducted at the State Scientific Research Institute Nature Research Centre (Vilnius, Lithuania) in compliance with Lithuanian national legislation and the International Guiding Principles for Biomedical Research Involving Animals (2012). Ethical approval for infection experiments and all associated protocols was granted by the Lithuanian State Food and Veterinary Service (Ref. Nos. 2015/05/07-G2-27, 2018/05/03-G2-84). (**PAPERS I-VI**).

Animal procedures were performed by licensed professionals (licenses 2012/02/06-No-208, 2016/01/29-No-344, and 2021/02/05-No-527). Domestic canaries and siskins were housed under standard husbandry conditions (License No. LT-61-13-003) at 21 ± 1 °C with *ad libitum* access to food and water (**PAPERS I, III-VI**).

Experiments involving *Culex pipiens* f. *molestus* and *Culex quinquefasciatus* were performed in accordance with ethical standards for animal research; however, mosquitoes are not protected under Lithuanian legislation (**PAPER II**).

3. RESULTS AND DISCUSSION

3.1. The bird-malaria parasite-microbiota system as an experimental model

The bird-malaria parasite-microbiota system provides a promising experimental model for investigating natural barriers that limit malaria parasite development. One such barrier involves immune responses against the oligosaccharide galactose-α-1,3-galactose (α-Gal), a carbohydrate epitope synthesized by certain Gram-negative bacteria in the avian gut, hypothesized to induce anti-α-Gal antibodies in birds (**PAPER I**). Structurally similar α-Gal glycans are present on the surface of *Plasmodium* sporozoites (Yilmaz et al., 2014), suggesting that gut microbiota may indirectly shape immunity and limit parasite development in the vertebrate host (**PAPER I**, Figure 4).

Experimental research in the mammalian malaria model has shown that anti-α-Gal antibodies can inhibit *Plasmodium berghei* ANKA sporozoites in mice lacking endogenous α-Gal, mediating complement-dependent lysis before parasites reach hepatocytes and preventing blood-stage infection (Yilmaz et al., 2014). Notably, α-Gal was detected in the salivary glands of both infected and uninfected mosquitoes, indicating that vector-derived glycans may contribute to the induction or maintenance of anti-α-Gal immunity in vertebrate hosts (Yilmaz et al., 2014).

Preliminary experimental data support this framework. Galactose-α-1,3-galactose was detected in protein extracts from blood stages of three avian *Plasmodium* species – *Plasmodium ashfordi* (GRW2), *Plasmodium relictum* (SGS1), and *Plasmodium homocircumflexum* (COLL4) – obtained from experimentally infected Eurasian siskins (*Spinus spinus*) (**PAPER I**, Figure 1). Gut microbiota analyses across a range of wild and domestic bird species revealed that, among over 140 bacterial taxa, *Escherichia-Shigella*, *Herbaspirillum*, *Megamonas*, and *Serratia* contributed most to α1,3GT gene abundance, confirming that α-Gal–producing bacteria are prevalent in avian hosts (**PAPER I**, Figure 3).

To assess the immunogenicity of avian *Plasmodium* α-Gal, IgY antibody responses were measured against two glycan epitopes – Galα1-3Gal and Galα1-3Galβ1-4GlcNAc – in experimentally infected domestic canaries (*Serinus canaria domestica*). Birds infected with *P. homocircumflexum* showed no significant change in circulating IgY levels, whereas *P. relictum* infection induced a significant increase in anti-Galα1-3Gal IgY titers by day 38 post-infection (**PAPER I**, Figure 2). This demonstrates that avian malaria

infection can elicit a microbiota-mediated humoral response analogous to that observed in mammalian systems.

These findings demonstrate the value of the bird-malaria parasite-microbiota experimental model for studying how gut microbiota composition and microbiota-induced antibodies may act as natural barriers to malaria infection. They also provide a basis for future experimental and field studies examining microbiota-associated resistance mechanisms and their ecological drivers in avian malaria systems (**PAPER I**).

3.2. Vector microbiota and malaria parasite development

Previous studies have shown that symbiotic bacteria in the mosquito midgut modulate vector competence by either facilitating (Hajkazemian et al., 2021) or constraining (Wang et al., 2021; Bando et al., 2013) pathogen colonization and development. Because *Plasmodium* parasites undergo sporogonic development within the mosquito midgut (Valkiūnas, 2005), direct interactions can occur between the parasite and resident microbiota. To better understand vector-microbiota-pathogen interactions, the gut microbiota of two avian malaria vectors, *Culex pipiens* f. *molestus* and *Culex quinquefasciatus*, which were laboratory reared, were analyzed to identify natural similarities and differences between the species and to determine how their microbial communities respond to perturbations such as parasite infection (**PAPER II**). In addition, the vector microbiota was modulated using specific host-derived antibodies, which remain functional within the mosquito midgut following blood feeding (Noden et al., 2011; Maitre et al., 2021), to assess how *Cx. quinquefasciatus* microbiota influences the development of *Plasmodium relictum* (**PAPER III**).

The composition and network dynamics of the gut microbiota in two avian malaria vectors, *Cx. pipiens* f. *molestus* and *Cx. quinquefasciatus*, reared under controlled laboratory conditions, were analyzed to assess their potential influence on parasite development. Using 16S rRNA gene profiling and network analyses, distinct microbial community structures were observed between the two mosquito species, despite most of the taxa being shared (**PAPER II**, Figure 1). The similarity in mosquito microbial diversity across species is expected under the same ecological setting (Muturi et al. 2018). The differences were shown by analyzing the nested patterns of *Wolbachia* endosymbiont and *Escherichia-Shigella* commensal bacteria within the microbiota of mosquitoes. In both species, *Escherichia-Shigella* acted as a keystone taxon, forming major network modules and contributing substantially to microbial connectivity (**PAPER II**, Figure 2). As a keystone

taxon, *Escherichia-Shigella* may play a central role in regulating community structure and ecological relationships, consistent with findings in other systems (Banerjee et al., 2018). In contrast, *Wolbachia* displayed species-specific modular organization. It was embedded in a major *Cx. pipiens* f. *molestus* module, but formed a small, distinct module in *Cx. quinquefasciatus* (**PAPER II**, Figure 2). The reduced connectivity of *Wolbachia* suggests a specialized ecological function within the mosquito microbiota, potentially linked to its pathogen-blocking properties, modulation of host reproductive biology by activating host immune pathways, competition for intracellular resources, and manipulation of reproduction through cytoplasmic incompatibility (Moreira et al., 2009; Bian et al., 2010). *In silico* network perturbation experiments using node removal revealed differential sensitivity of the microbial network. In *Cx. pipiens* f. *molestus*, disruption of *Wolbachia* reduced network connectivity, whereas in *Cx. quinquefasciatus*, *Escherichia-Shigella* removal led to decreased network stability (**PAPER II**, Figure 4). These findings indicate species-specific differences in microbial network robustness and resilience to perturbations.

To evaluate the impact of host antibody-mediated microbiota modulation on parasite development, *Cx. quinquefasciatus* mosquitoes were allowed to feed on canaries immunized against *E. coli* antigens and/or infected with *P. relictum*. Circulating anti-*E. coli* IgY remained active in the mosquito midgut after blood feeding (**PAPER III,** Figure 2A). Overall microbial richness and evenness in the mosquito midgut were largely unchanged across experimental groups (**PAPER III**, Figures 2B and 2C). However, the taxonomic composition differed significantly (**PAPER III**, Figure 2D). *Plasmodium*-infected mosquitoes displayed a distinct microbial profile compared to controls, and those feeding on birds with anti-*E. coli* antibodies showed altered abundances of multiple bacterial taxa (**PAPER III**, Figures 3 and 4). Network analyses revealed pronounced shifts in community structure, including reduced co-occurrence of *Escherichia-Shigella* with other taxa and changes in topological parameters such as connectivity, modularity, and hub centrality (**PAPER III**, Figures 6 and 7; Table 1). A similar reduction in *Escherichia* connectivity and changes in the abundance of specific bacterial taxa were reported by Mateos-Hernández et al. (2021) in ticks ingesting host-derived anti-*E. coli* antibodies. These findings demonstrate that host-derived antibodies can modulate vector microbiota and disrupt microbial interactions.

Functionally, host antibody-mediated modulation of mosquito microbiota had a measurable impact on parasite development. The prevalence of *P. relictum* oocysts in the midgut was significantly lower in mosquitoes fed on birds with anti-*E. coli* antibodies, and sporogonic stages were less frequently

observed (**PAPER III**, Figure 9). The *E. coli* O86:B7 strain, which expresses high levels of α-Gal (Yilmaz et al., 2014), had a particularly strong negative effect on *P. relictum* development in *Cx. quinquefasciatus*. Differences in mosquito survival between experimental groups were also noted, with the highest mortality in mosquitoes that fed on birds immunized with *E. coli* BL21 and infected with *P. relictum* (**PAPER III**, Figure 8), suggesting that immune-mediated microbial perturbations can influence vector fitness. Overall, these findings indicate that host antibodies targeting specific gut bacteria can interfere with the development of avian malaria parasites, revealing a mechanism by which vertebrate immunity indirectly affects vector competence and pathogen transmission.

Together, these results show that both the natural structure of the mosquito microbiota and external factors such as host antibody-mediated modulation influence the stability of microbial communities in avian malaria vectors. These interactions affect mosquito fitness and parasite development, emphasizing the close link between host immunity, the vector microbiota, and malaria transmission (**PAPERS II, III**).

3.3. Avian host microbiota and malaria infection

Interactions between avian hosts, their gut microbiota, and malaria parasites are increasingly recognized as key factors shaping infection outcomes and host health. Previous studies have shown that parasite infections can alter the composition and structure of host-associated microbial communities, disrupt immune homeostasis, and influence disease severity (Videvall et al., 2021; Taniguchi et al., 2015). Despite advances in avian microbiome research, the effects of *Plasmodium* infections on the gut microbiota of birds and on the ecological stability of these microbial communities remain poorly understood.

To address this, experimental infections with both *Plasmodium homocircumflexum* (**PAPER IV**) and *Plasmodium relictum* (**PAPER V**) were conducted in domestic canaries (*Serinus canaria domestica*). The objective was to assess how infection influences gut microbiota composition, community assembly, and colonization resistance, using 16S rRNA amplicon sequencing of fecal samples collected throughout the course of infection.

Across both infections, alpha and beta diversity metrics did not differ significantly between infected and control birds, indicating that overall microbiota richness and evenness remained relatively stable. These results are consistent with previous malaria studies showing that infection has a limited impact on overall microbial diversity (Rohrer et al., 2023; Macdonald et al.,

2017). Although overall diversity remained unchanged, both infections were associated with compositional variation in specific bacterial taxa. Taxonomic profiling revealed a shared core microbiota and taxa that differed across sampling points. Functional profiling, conducted for *P. homocircumflexum*, further showed associations between specific taxa and infection stages, suggesting temporal dynamics in microbial composition.

Network-based analyses provided further insight into the effects of infection on community structure. In both *P. homocircumflexum* and *P. relictum* infections, bacterial co-occurrence networks of infected birds showed reduced connectivity and altered patterns of bacterial associations compared to controls (**PAPER IV, V**). Infected birds exhibited fewer correlations between nodes and more fragmented network modules, whereas control networks contained larger, cohesive clusters with highly connected taxa displaying high eigenvector centrality (**PAPER IV**). Network structural states, expressed as relationships between taxa inventory and connectivity (nodes and edges), also differed between infected and control groups, indicating that infection affected overall network structure and organization (**PAPER V**).

Analysis of network stability supported these findings. In both infections, removal of nodes caused greater network disruption in infected birds, while node addition did not improve the overall network stability, indicating lower resilience of the microbial community. These results suggest that *Plasmodium* infection influences microbial interaction networks and weakens colonization resistance without substantially altering overall community diversity.

When considered together, the results of both *Plasmodium* species demonstrate that avian malaria induces structural reorganization of gut microbial communities rather than broad changes in taxonomic composition (**PAPER IV, V**). Despite stable alpha and beta diversity, infection was consistently associated with reduced network complexity and connectivity, reflecting transient but measurable effects on community assembly.

Findings from murine malaria models (Taniguchi et al., 2015; Mooney et al., 2015) similarly indicate that malaria infection induces primarily transient alterations in the microbiome, affecting specific bacterial taxa. Such compositional shifts may, in turn, influence the organization of microbial communities and their interaction networks (Li et al., 2021). In line with observations from other parasite systems (Mammeri et al., 2020), avian *Plasmodium* infection was also associated with reduced network complexity and connectivity, suggesting that reorganization of microbial communities may represent a common response to parasitic infection. These alterations can

reduce colonization resistance and affect community resilience, with possible consequences for immune regulation and susceptibility to secondary infections.

Overall, the results indicate that avian *Plasmodium* infection alters the organization of the gut microbiota mainly through changes in community assembly and network structure rather than through major shifts in overall diversity. Similar patterns observed in both *P. relictum* and *P. homocircumflexum* suggest a shared mechanism by which malaria parasites disturb the ecological balance of the avian gut microbiota. Although the gut microbiota of canaries appears relatively stable in terms of diversity, the transient reorganization of microbial networks indicates that functional structure is sensitive to infection and may influence host-microbiota-parasite interactions and infection outcomes.

3.4. Parasite transcriptional responses to host immune environment

Generalist malaria parasites must rapidly adapt to the distinct immune environments of different hosts to ensure survival and transmission (Prati et al., 2022). This adaptability may arise not only from genetic variation but also from transcriptional plasticity that enables parasites to modulate gene expression in response to host-specific immune and physiological conditions (Turnbull et al., 2022; Hollin et al., 2023). To investigate how *Plasmodium homocircumflexum* responds at both the genetic and transcriptional levels to host immune variation, experimental cross-species infections were performed using canaries (*Serinus canaria domestica*) and Eurasian siskins (*Spinus spinus*), two avian hosts differing in immune background and physiology (Palinauskas et al., 2020).

The experiment aimed to determine how parasite gene expression adjusts to divergent host environments and immune responses. Parasitemia peaked at 8 days post-infection (dpi) in all experimental groups (**PAPER VI**, Figure 1). RNA expression profiling revealed that early transcriptional patterns were primarily influenced by the donor host species, with parasite gene expression reflecting the immune and physiological environment of the source host up to 8 dpi (**PAPER VI**, Figures 2 and 3). These results suggest that *P. homocircumflexum* may transiently retain donor host species-specific transcriptional signatures, possibly reflecting epigenetically inherited states carried over from the previous host environment (Abdrabou et al., 2021). As infection progressed, however, selective pressures exerted by the immune system of the new recipient host species appeared to drive a reconfiguration of parasite gene expression, with transcriptional profiles aligning with those

of the recipient host by 16 dpi (**PAPER VI**, Figures 2 and 3). While parasite transcriptional plasticity may be influenced by immediate host-mediated cues, the strong donor host species-specific transcriptional signatures observed early in infection suggest the involvement of inherited regulatory mechanisms, including epigenetic regulation (Llorà-Batlle et al., 2019).

Analysis of single-nucleotide polymorphisms (SNPs) revealed no clear clustering by donor or recipient species (**PAPER VI**, Figure 5), indicating that the observed transcriptional changes were not driven by genetic differentiation. Although SNP-based approaches have been widely used to investigate host-pathogen interactions and detect selection signatures (Maïga-Ascofaré et al., 2010), only a small fraction of SNPs exhibited divergence between groups, suggesting limited selection pressure at this infection stage. Thus, the transcriptional variation observed most likely reflects regulatory plasticity rather than sequence-level evolution.

Together, these findings demonstrate that *P. homocircumflexum* adapts to novel avian hosts primarily through transcriptional reprogramming rather than genetic divergence. This regulatory flexibility likely enhances the parasite's ability to persist across heterogeneous host environments, representing a key adaptive strategy underlying the ecological success of generalist malaria parasites. Such transcriptional flexibility may represent a widespread evolutionary mechanism among avian malaria parasites, enabling them to exploit hosts with contrasting immune profiles without requiring lineage-specific genetic adaptations. By relying on rapid transcriptional adjustments rather than slower genetic change, generalist parasites can respond flexibly to diverse host immune environments while maintaining a broad host range. These findings contribute to a better understanding of how plasticity influences host-parasite coevolution and may help explain the ecological success and widespread distribution of generalist *Plasmodium* parasites.

3.5. Toward a systems-level understanding of avian malaria dynamics

The results of this dissertation lead to a structured ecological interpretation of avian malaria. Rather than representing independent host-parasite or vector-parasite interactions, the evidence supports a system in which infection dynamics emerge from interconnected processes operating simultaneously within the host-vector-microbiota network.

At the core of this system lies the microbiota structure. Both vertebrate and mosquito-associated microbial communities constitute organized ecological networks whose connectivity, stability, and functional composition

shape the environment in which parasite development occurs. Microbial communities act as ecological filters, influencing parasite success through immune-mediated modulation and structural properties of microbial networks. These findings indicate that parasite development and transmission are contingent upon the ecological architecture of host and vector microbiota rather than occurring in a neutral biological background.

The interaction, however, is not unidirectional. *Plasmodium* infection itself induces measurable restructuring of microbial community organization, altering network topology and resilience without necessarily causing large shifts in overall diversity. This demonstrates that infection functions as an ecological perturbation capable of modifying microbial system stability. Consequently, the microbiota both constrain and are reshaped by the presence of the parasite, establishing a reciprocal feedback relationship within the host-vector system.

Superimposed on this ecological layer is parasite regulatory flexibility. The transcriptomic analyses show that generalist avian malaria parasites adjust gene expression in response to distinct vertebrate host environments. This transcriptional reprogramming allows parasites to accommodate variation in immune context without requiring rapid genetic differentiation. In ecological terms, such plasticity represents an adaptive response mechanism operating within heterogeneous host landscapes.

Taken together, these components define a tripartite ecological model characterized by: (i) microbiota-mediated modulation of parasite development, (ii) infection-driven restructuring of microbial network architecture, and (iii) parasite transcriptional adjustment to host-specific environments.

These processes operate concurrently and interactively within the host-vector system, forming a dynamic network of reciprocal modulation rather than a linear chain of causation. Within this framework, infection outcomes arise from the structural properties of microbial communities, immune-mediated interactions, and the parasite's adaptive capacity, acting in concert.

This integrative model provides a coherent ecological structure for interpreting the experimental findings of this dissertation and situates avian malaria within a systems-level biological context.

CONCLUSIONS

1. The bird-malaria parasite-microbiota system is a novel experimental model for identifying natural barriers that limit malaria parasite development, shaped by *Plasmodium* biology and microbiota-driven immunity.
2. *Plasmodium relictum* infection influences the gut microbiota composition and network structure of *Culex pipiens* f. *molestus* and *Culex quinquefasciatus*, thereby affecting vector–parasite interactions.
3. Targeted modulation of the avian malaria vector *Culex quinquefasciatus* gut microbiota negatively affects the sporogonic development of *Plasmodium relictum*.
4. Avian malaria infections with *Plasmodium relictum* and *Plasmodium homocircumflexum* alter the gut microbiota of vertebrate hosts, disrupting microbial community stability and reducing colonization resistance.
5. Upon infecting a new host, *Plasmodium homocircumflexum* demonstrates transcriptional plasticity – initially retaining donor-specific gene expression patterns, then gradually reprogramming to adapt to the immune and physiological conditions of the new host.

SANTRAUKA

MOKSLINĖ PROBLEMA

Paukščių maliarija yra laikoma didele grėsme laukinių paukščių populiacijoms ir gali sukelti rimtų ekologinių bei evoliucinių pasekmių (Valkiūnas, 2005). Paukščių maliarijos parazitai, pasižymintys ekologiniu lankstumu, tokie kaip *Plasmodium relictum* ir *Plasmodium homocircumflexum,* gali turėti neigiamą poveikį paukščių sveikatai (Simberloff & Rejmanek, 2011; Martinez de la Puente et al., 2021; Palinauskas et al., 2015). Infekcijos gali neigiamai veikti šeimininko sveikatos būklę, reprodukciją ir ilgalaikį populiacijos stabilumą, bloginant išlikimo galimybes (Santiago-Alarcon & Marzal, 2020). Paukščių maliarijos parazitai yra ne tik svarbi grėsmė biologinei įvairovei, bet ir vertinga modelinė sistema, suteikianti galimybę tirti šeimininko ir parazito sąveikas natūraliomis sąlygomis.

Parazitinės infekcijos eiga priklauso ne tik nuo parazitų genetikos, bet ir nuo daugiakomponentės šeimininko biologijos ir aplinkos veiksnių sąveikos (Ruiz-Lopez, 2020; Gabrieli et al., 2021; Cansado-Utrilla et al., 2021). Šeimininko ir vektoriaus mikrobiota vis dažniau išskiriama kaip vienas svarbiausių parazitų vystymosi dinamiką formuojančių veiksnių. Mikrobiota, įskaitant bakterijas, grybus ir virusus, tiesiogiai ir netiesiogiai sąveikauja su šeimininku ir parazitu (Palinauskas et al., 2024; Ipollito et al., 2018). Šie mikroorganizmai daro įtaką šeimininko imuniniam atsakui ir homeostazei, lemia imlumą ar atsparumą infekcijoms ir veikia patogenų vystymąsi, vektorių kompetenciją ir perdavimo efektyvumą (Cansado-Utrilla et al., 2021; Gutierrez-Lopez et al., 2020, Ippolito et al., 2018, Belkaid et al., 2014).

Uodų mikrobiota kolonizuoja daugelį organų, įskaitant žarnyną, seilių liaukas ir reprodukcinių organų audinius (Romoli & Gendrin, 2018). Šios mikroorganizmų bendrijos daro didelę įtaką uodų biologijai, veikdamos jų išgyvenimą, imuninę veiklą ir patogenų vystymąsi pernešėjuje (Romoli & Gendrin, 2018; Palinauskas et al., 2024). Svarbu tai, kad maitinimosi metu uodų žarnos mikrobiota kontaktuoja su šeimininko kraujo komponentais, o šios sąveikos gali paveikti uodus ir parazitus (Yilmaz et al., 2014). Tyrimai taip pat rodo, kad parazitų infekcijos gali pakeisti uodų mikrobiotą, o ši gali nulemti parazitų vystymosi sėkmę (Romoli et al., 2021). Tokios sąveikos tiesiogiai daro įtaką vektorių kompetencijai ir maliarijos perdavimo efektyvumui.

Paukščių, maliarijos parazitų, mikrobiotos sąveikoje lygiai taip pat svarbus yra stuburinių šeimininkų mikrobiomas. Laukinių paukščių žarnyno

mikrobiotos formavimąsi veikia vidiniai (genetika ar imuninė būklė) ir išoriniai (mityba, buveinė ir parazitų infekcijos) veiksniai (Waite & Tailor, 2014). Naujos kartos sekoskaitos metodai praplėtė mūsų žinias apie paukščių žarnyno mikrobiotos įvairovę ir jos funkcinius vaidmenis šeimininko fiziologijoje (Sun et al., 2022). Atlikti tyrimai rodo, kad maliarijos parazitai gali keisti šeimininko mikrobiotą, darydami įtaką imunitetui ir net šeimininko elgesiui (Taniguchi et al., 2015; Mooney et al., 2015; Gabrieli et al., 2021). Svarbu pažymėti, kad yra įrodymų, jog parazitų sukelti mikrobiotos pokyčiai gali modifikuoti šeimininko kvapo profilį, todėl uodus labiau traukia užsikrėtę individai, taip palengvinant parazito perdavimą (Ruiz-Lopez et al., 2020).

Tačiau vien taksonominė sudėtis negali iki galo paaiškinti, kaip mikrobiota veikia parazitų vystymąsi ar reaguoja į infekciją (Gabrieli et al., 202; Ruiz-Lopez et al., 2020). Mikroorganizmų tinklo stabilumas, atsparumas kolonizacijai ir funkciniai metaboliniai keliai gali būti tokie pat svarbūs kaip taksonominė sudėtis, formuojant šeimininko ir parazito sąveiką (Cansado-Utrilla et al., 2021; Ruiz-Lopez et al., 2020).

Šeimininko ir vektoriaus mikrobiotos mechanizmas bei parazitų plastiškumas yra labai sudėtingi ekologine prasme. Eurikseniniai parazitai, užkrečiantys įvairių rūšių šeimininkus, tokie kaip *Plasmodium* spp., turi prisitaikyti prie labai skirtingų aplinkos veiksių, kai yra perduodami tarp filogenetiškai skirtingų šeimininkų rūšių. Imuninė apsauga, kūno temperatūra, metaboliniai procesai ir maistinių medžiagų prieinamumas – tai veiksniai, keliantys parazitams iššūkių išlikti ir daugintis (Agosta et al., 2010; Gupta et al., 2020; Prati et al., 2022). Lieka neaišku, ar prisitaikymas prie naujos šeimininko aplinkos vyksta, pirmiausia, dėl genetinės divergencijos, ar dėl greitesnio transkripcinio atsako, leidžiančių parazitams prisitaikyti prie skirtingos šeimininko fiziologijos ir imuninio atsako (Prati et al., 2022; Turnbull et al., 2022). Šių mechanizmų supratimas yra esminis, norint paaiškinti eurikseninių parazitų, tokių kaip *P. relictum* ar *P. homocircumflexum*, ekologinę sėkmę.

Nors mikrobiotos svarba šeimininko ir parazito sistemose vis labiau pripažįstama, daugelis šių sąveikų aspektų vis dar išlieka nepakankamai ištirti. Visų pirma, nėra aišku, kaip su stuburiniais šeimininkais ir uodų vektoriais susijusios mikroorganizmų bendruomenės veikia maliarijos parazitų vystymąsi ir perdavimą; ar šeimininko žarnyno mikrobiotos sukeltas imuninis atsakas gali netiesiogiai paveikti parazito vystymosi sėkmingumą. Taip pat buvo neaišku, ar maliarijos parazitai prisitaiko prie naujo šeimininko, pirmiausia, per genetinę divergenciją ar greitus genų raiškos pokyčius. Todėl šioje disertacijoje nagrinėjami šie klausimai: (1) ar paukščių, maliarijos parazitų ir mikrobiotos sistema gali būti naudojama kaip eksperimentinis

modelis, galintis nustatyti natūralias kliūtis, ribojančias parazito vystymąsi ir perdavimą; (2) ar šeimininko imuniniai veiksniai gali moduliuoti uodų žarnyno mikrobiotą ir taip paveikti parazito vystymąsi vektoriuje; (3) kaip maliarijos parazitai veikia stuburinio šeimininko žarnyno mikrobiotos sudėtį ir bendrijos struktūrą, ir kaip šios mikroorganizmų bendruomenės gali paveikti parazitų infekcijos eigą; ir (4) kaip paukščių maliarijos parazitai genetiniame ir transkripciniame lygmenyse reaguoja į pokyčius stuburiniame šeimininke?

DISERTACIJOS TIKSLAS IR PAGRINDINIAI UŽDAVINIAI

Disertacijos tikslas – ištirti šeimininkų ir vektorių mikrobiotą bei jos pokyčius paukščių maliarijos infekcijų metu, įvertinti jų poveikį parazitų sporogoniniam vystymuisi ir nustatyti, kaip paukščių maliarijos parazitai genetiniame ir transkripciniame lygmenyse reaguoja į pasikeitusią aplinką stuburiniame šeimininke.

Pagrindiniai uždaviniai:

1. Ištirti paukščių, maliarijos parazitų ir mikrobiotos sistemą kaip eksperimentinį modelį, siekiant nustatyti natūralius barjerus, galinčius riboti maliarijos parazitų vystymąsi.
2. Įvertinti *Culex pipiens* f. *molestus* ir *Culex quinquefasciatus* mikrobiotos sudėtį ir nustatyti *Plasmodium relictum* infekcijos poveikį vektoriaus žarnyno mikroorganizmų bendrijoms.
3. Ištirti *Culex quinquefasciatus* žarnyno mikrobiotos poveikį paukščių maliarijos parazito *Plasmodium relictum* sporogoniniam vystymuisi.
4. Įvertinti *Plasmodium relictum* ir *Plasmodium homocircumflexum* infekcijų poveikį kanarėlių (*Serinus canaria domestica*) žarnyno mikrobiotos sudėčiai, bendrijų struktūrai ir atsparumui kolonizacijai.
5. Nustatyti *Plasmodium homocircumflexum* genetinį ir transkripcinį atsaką į pakitusią aplinką stuburiniame šeimininke, naudojant eksperimentiškai užkrėstas kanarėles (*Serinus canaria domestica*) ir eurazinius alksninukus (*Spinus spinus*).

GINAMIEJI TEIGINIAI

1. Paukščių, maliarijos parazitų ir mikrobiotos sistema yra novatoriškas eksperimentinis modelis, kuris integruoja šeimininko žarnyno mikrobiotos įvairovę kaip svarbų veiksnį, darantį įtaką paukščių maliarijos infekcijos dinamikai, ypač moduliuojant anti-α-Gal imunitetą, ir šeimininko atsparumui *Plasmodium*.
2. *Culex quinquefasciatus* ir *Culex pipiens* f. *molestus* skiriasi savo mikroorganizmų bendrijų sudėtimi ir dinamika, nepaisant panašios įvairovės, o *P. relictum* infekcija keičia mikrobiotos sudėtį ir tinklo topologiją *Cx. quinquefasciatus* uoduose.
3. *Culex quinquefasciatus* mikrobiotos moduliacija, kurią sukelia antikūnai, susiformavę *E. coli* O86:B7 imunizuotuose paukščiuose, sumažina *P. relictum* oocistų susidarymą, atskleisdama funkcinį ryšį tarp stuburinių šeimininkų imuniteto ir vektorių tinkamumo pernešti parazitus.

4. Paukščių maliarijos parazitų *P. relictum* (SGS1) ir *P. homocircumflexum* (COLL4) infekcija paveikia paukščių žarnyno mikrobiotą, sukeldama nukrypimus nuo normalios vystymosi trajektorijos ir sumažindama atsparumą kolonizacijai, taip pakenkdama mikroorganizmų bendrijos stabilumui.
5. *Plasmodium homocircumflexum* infekcijos metu parazitai paveldi ankstesnio šeimininko transkripcijos profilius ir palaipsniui juos pritaiko prie naujo šeimininko imuninės aplinkos.

NAUJUMAS IR REIKŠMĖ

1. Pirmą kartą paukščių, maliarijos parazitų ir mikrobiotos sistema buvo pateikta kaip eksperimentinis modelis, skirtas tirti ryšius tarp žarnyno mikrobiotos sudėties, anti-α-Gal antikūnų atsako ir maliarijos infekcijos, nustačius α-Gal buvimą trijų paukščių maliarijos parazitų, *Plasmodium ashfordi*, *Plasmodium relictum* ir *Plasmodium homocircumflexum*, baltymų ekstraktuose, gautuose iš eksperimentiniu būdu užkrėstų eurazinių alksninukų (*Spinus spinus)*.
2. Nustatytas didelis mikrobiotos sudėties panašumas tarp dviejų paukščių maliarijos pernešėjų – *Culex pipiens* f. *molestus* ir *Culex quinquefasciatus* – augintų kontroliuojamomis laboratorinėmis sąlygomis. Tačiau bakterijų koegzistavimo tinklo analizė parodė, kad nepaisant šio panašumo, uodų žarnų mikroorganizmų bendrijos, esant imituotiems trikdžiams, pasižymi skirtinga struktūrinės dinamikos reakcija.
3. Pirmą kartą buvo įrodyta, kad paukščiuose susiformavę antikūnai, kaip atsakas į bakterijų išskiriamą α-Gal, keičia uodų žarnos mikrobiotą, taip sukuriant mechanizmą, kuriuo stuburinių imunitetas gali daryti įtaką vektorių mikroorganizmų bendrijoms.
4. Parodyta, kad šeimininko antikūnai, nukreipti prieš specifinius bakterijų antigenus, išlieka funkciškai aktyvūs uodų audiniuose ir gali keisti *Plasmodium* sukeltą vektoriaus mikrobiotos moduliaciją, taip sukeldami žarnyno mikrobiotos restruktūrizavimą ir mažindami parazitų infektyvumą.
5. Paukščių žarnyno mikrobiotos tyrimų metu gauti pirmieji eksperimentiniai įrodymai, kad paukščių maliarijos infekcija sukelia daugiausia laikinus stuburinių šeimininkų žarnyno mkrobiotos pokyčius, paveikdama konkrečių bakterijų taksonų gausumą.
6. Pirmą kartą *Plasmodium* užsikrėtusių paukščių žarnyno mikrobiotos funkcinio profilio anlizė parodė, kad infekcija gali paveikti

mikroorganizmų metabolinius kelius. Kai kurie iš šių kelių galimai prisideda prie mikroorganizmų reakcijos į maliarijos infekciją, o tai rodo, kad ne tik mikrobiotos sudėtis, bet ir jo funkcijos gali turėti įtakos šeimininko, parazito ir mikrobiotos sąveikai.

7. *Plasmodium* infekcija nekeičia bendros stuburinių šeimininkų mikrobiotos įvairovės, tačiau dinamiškai veikia bakterijų rūšių sąveiką, dėl to keičiasi mikroorganizmų tinklo struktūra. *In silico* eksperimentas parodė, kad šie pokyčiai mažina tinklo stabilumą ir atsparumą kolonizacijai, išryškindami anksčiau nepastebėtą šeimininko, parazito ir mikrobiotos sąveikos lygmenį.
8. Pirmą kartą buvo ištirtas eurikseninių parazitų prisitaikymas prie skirtingų rūšių šeimininkų. Rezultatai rodo epigenetinį paveldėjimą, transkripcijos profiliai iš pradžių išlieka panašūs į donoro šeimininko, o vėliau palaipsniui prisitaiko prie kitos rūšies recipiento šeimininko, o atrankos lemiama genetinė divergencija nenustatyta.

TRUMPA LITERATŪROS APŽVALGA

Literatūros apžvalgoje glaustai pristatyta paukščių maliarijos parazitų biologija, jų sąveika su šeimininkais ir uodų pernešėjais, mikrobiotos vaidmuo infekcijos eigai ir parazitų genų raiškos plastiškumas, lemiantis jų ekologinį prisitaikymą.

METODAI IR MEDŽIAGA

Išsamus surinktų medžiagų ir šioje disertacijoje taikomų metodikų aprašymas pateikiamas paskelbtuose straipsniuose (**STRAIPSNIAI I–VI**). Toliau pateikiama trumpa pagrindinių taikomų metodikų apžvalga.

Eksperimentinė imunizacija

Gyvi ir karščiu inaktyvuoti *Escherichia coli* kamienai, kurie, kaip žinoma, turi paplitusius α1,3GT genus, atsakingus už α-Gal išskyrimą, buvo paruošti naminių kanarėlių (*Serinus canaria domestica*) imunizacijai per burną. Bakterijos augintos LB terpėje, nuplautos ir suspenduotos PBS tirpale; karščiu inaktyvuotos 70 °C temperatūroje 1 val. Kiekvienam paukščiui sugirdyta po 50 µL bakterijų suspensijos, pakartotinės dozės – po 1 ir 2 savaičių; kontrolinė grupė gavo PBS. Baltymų koncentracija bakterijų lizatuose nustatyta Bradfordo metodu (**STRAIPSNIS III**).

Eksperimentinis paukščių užkrėtimas inokuliuojant

Eksperimentuose naudoti kanarėlių ir alksninukų (*Spinus spinus*) jaunikliai buvo įsigyti iš komercinių pardavėjų ir laikomi Valstybinio mokslinių tyrimų instituto Gamtos tyrimų centro vivariume (licencijos Nr. LT-61-13-003) standartinėmis paukščių gyvenimo sąlygomis.

Paukščiai buvo eksperimentiniu būdu infekuoti *Plasmodium homocircumflexum* (**STRAIPSNIAI IV**, **VI**) arba *Plasmodium relictum* (**STRAIPSNIAI III, V**) pagal Palinauskas et al. (2008) protokolą. Kiekvienam paukščiui į krūtinės raumenį buvo įšvirkšta 0,10 ml užkrėsto kraujo, sumaišyto su 3,7 % natrio citratu ir 0,9 % fiziologiniu tirpalu (4:1:5), kuriame buvo subrendę merontai.

Eksperimentinis *Plasmodium* pernešimas per uodo įkandimą

Užkrėsti uodams kiekvienas paukštis buvo švelniai įtvirtintas popieriniame vamzdelyje, paliekant tik atviras kojas, kad uodai galėtų maitintis (Kazlauskiene et al., 2013). Vamzdelis buvo įdėtas į narvelį su *Culex quinquefasciatus* uodų patelėmis. Paukščiai buvo laikomi iki 10 minučių arba kol keturi uodai pasisotino. Krauju pasisotinę uodai buvo laikomi mažesniuose narvuose (17,4 × 17,5 × 17,5 cm) 17 dienų standartinėmis sąlygomis, jiems buvo tiekiamas vanduo kiaušinėliams dėti. Po inkubacijos uodams buvo leista maitintis vakcinuotais arba kontroliniais paukščiais (4–5 uodai vienam paukščiui). Tada jie buvo preparuojami, o seilių liaukos buvo tiriamos mikroskopu, ieškant sporozoitų (**STRAIPSNIS III**).

Kraujo surinkimas ir mikroskopija

Kraujo mėginiai buvo surinkti iš eksperimentinių ir laukinių paukščių ir panaudoti kraujo tepinėlių paruošimui, serumo izoliacijai, molekuliniams tyrimams ir RNR analizei (**STRAIPSNIAI III–VI**). Kraujo tepinėliai ir uodų preparatai buvo tirti mikroskopiškai parazitemijai nustatyti, o uodų infekcija ir sporogonija patvirtinta, aptinkant sporozoitus seilių liaukų preparatuose.

Uodų vidurinių žarnų ir seilių liaukų surinkimas

Uodai buvo surinkti ir preparuoti mikroskopiniams ir molekuliniams tyrimams. Iš jų buvo išskirtos žarnos oocistoms skaičiuoti ir mikrobiotai analizuoti, o seilių liaukos – sporozoitams aptikti. Likę audiniai buvo panaudoti papildomai PGR analizei, kiekvieną individą preparuojant atskirai, kad būtų išvengta užteršimo (**STRAIPSNIAI II–V**).

Molekulinė diagnostika

Genominė DNR paukščių kraujo mėginiuose buvo išskirta ir naudojama haemosporidinėms infekcijoms identifikuoti, taikant PGR metodą ir sekoskaitą, o gautos sekos identifikuotos bioinformatiniais metodais (**STRAIPSNIAI III, IV, VI**). DNR taip pat buvo išskirta iš uodų žarnų ir išmatų mėginių ir panaudota 16S rRNR mikrobiomo analizei; amplikonai parengti ir sekoskaita atlikta Illumina MiSeq platformoje, o duomenys paskelbti SRA saugykloje (**STRAIPSNIAI III, IV**).

RNR analizei mėginiai buvo išgryninti ir paruošti transkriptomikai, o sekoskaita atlikta išorinėje laboratorijoje, naudojant Illumina HiSeq platformą; duomenų kokybė patikrinta standartiniais bioinformatikos įrankiais (**STRAIPSNIS VI**).

ELISA

Antikūnų prieš *E. coli* baltymus kiekis paukščių serume buvo nustatytas netiesioginiu ELISA metodu: serumo mėginiai inkubuoti *E. coli* baltymais padengtoje plokštelėje, o prisijungę antikūnai identifikuoti pagal optinio tankio pokytį (**STRAIPSNIS III**).

Bioinformacinė mikrobiomo analizė

Amplikonų sekų variantai buvo nustatyti, remiantis 251 bp ilgio suporuotų sekų duomenimis iš 16S rRNR geno V4 kintamosios srities, naudojant universalius pradmenis (515F/806R). Sekoskaitos duomenys buvo apdoroti, naudojant QIIME2 programinę įrangą, taikant numatytuosius parametrus, išskyrus atvejus, kai parametrai buvo koreguoti, atsižvelgiant į sekų kokybės profilius ir sekoskaitos gylį: sekos demultipleksuotos, filtruotos, apdorotos DADA2, pašalinant chimeras, o gauti ASV suderinti ir panaudoti filogenetiniam medžiui sudaryti. Taksonominė klasifikacija atlikta pagal SILVA duomenų bazę, o taksonominės lentelės sudarytos genčių lygmenyje ir perfiltruotos (**STRAIPSNIAI II–V**).

Funkcinės metagenominės prognozės atliktos PICRUSt2 įrankiu (**STRAIPSNIAI III, IV**).

Bakterijų koegzistavimo tinklai

Bakterijų koegzistavimo tinklai buvo sudaryti, naudojant SparCC metodą, remiantis genties lygmens taksonominiais profiliais, o neklasifikuoti ASV

priskirti aukštesniems taksonominiams lygiams. Juose taksonai vaizduojami kaip mazgai, o reikšmingos teigiamos ir neigiamos sąveikos – kaip jungtys. Tinklai vizualizuoti programoje Gephi 0.9.2-0.9.5, kur buvo apskaičiuoti pagrindiniai topologiniai rodikliai.

Diferencinė genų raiškos analizė

Plasmodium homocircumflexum genų raiškos analizė buvo atlikta, taikant referencinius ir *de novo* metodus: sekos, atitikusios paukščių genomus, buvo pašalintos, o likusios suderintos su *P. relictum* genomu ir paskelbtu *P. homocircumflexum* transkriptomu. Suderinimui naudotas STAR suderinimo įrankis ir Bowtie 2 žemėlapio įrankis, o *de novo* surinkimas atliktas naudojant Trinity transkriptomo surinkimo programą. Remiantis GC kiekiu, atrinkti *Plasmodium* kilmės transkriptai. Genų raiška įvertinta Salmon įrankiu ir normalizuota R aplinkoje, vizualizacijas generuojant su ggplot2 paketu (**STRAIPSNIS VI)**.

Vieno nukleotido polimorfizmų (VNP) analizė atlikta, naudojant RNR sekoskaitos duomenis. Parazitų sekos buvo izoliuotos, nuosekliai šalinant šeimininko sekų duomenis ir naudojant turimus *Plasmodium* etalonus kartu su anksčiau paskelbtu *P. homocircumflexum* transkriptomu, siekiant išsaugoti parazitų sekas. Buvo surinktas *de novo* transkriptomas ir atliktas variantų nustatymas RNR sekose (**STRAIPSNIS VI**).

Statistinė analizė

Statistinė analizė buvo atlikta R, Python ir QIIME2 aplinkose. Infekcijos paplitimo ir intensyvumo skirtumams vertinti naudoti parametriniai ir neparametriniai testai, įskaitant Fisher, Mann-Whitney U, Kruskal–Wallis, Chi-kvadrato ir log-rank testus (**STRAIPSNIAI III, VI**). Imunologiniuose tyrimuose antikūnų lygių pokyčiai analizuoti ANOVA arba atitinkamais neparametriniais testais (**STRAIPSNIS III**). Mikrobiotos analizėms taikyti alfa ir beta įvairovės rodikliai, PERMANOVA, išilginė analizė ir diferencinės gausos metodai (**STRAIPSNIAI II–V**). Skirtingai gausūs taksonai, metaboliniai keliai ir ekspresuojami genai nustatyti DESeq2 arba ALDEx2 metodais, o bendri elementai vizualizuoti Venn diagramomis (**STRAIPSNIAI II–VI**). Mikroorganizmų sąsajų tinklai sudaryti naudojant SparCC ir NetCoMi, jų stabilumas įvertintas NetSwan ir igraph paketais (**STRAIPSNIAI II–V**). Vizualizacijai naudotos R, Python, GraphPad Prism ir Adobe Illustrator programos.

Leidimai, etiniai aspektai ir eksperimentiniai gyvūnai

Visos procedūros buvo atliktos Valstybiniame mokslinių tyrimų institute Gamtos tyrimų centre (Vilnius, Lietuva), laikantis Lietuvos nacionalinių teisės aktų ir Tarptautinių biomedicininių tyrimų su gyvūnais gairių (2012). Etinis leidimas infekcijos eksperimentams ir visiems susijusiems protokolams buvo suteiktas Lietuvos valstybinės maisto ir veterinarijos tarnybos (nuorodos Nr. 2015/05/07-G2-27, 2018/05/03-G2-84) (**STRAIPSNIAI I–VI)**.

Procedūros su gyvūnais buvo atliekamos licencijuotų specialistų (licencijos Nr. 2012/02/06-No-208, 2016/01/29-No-344 ir 2021/02/05-No-527). Kanarėlės ir alksninukai buvo laikomi standartinėmis laikymo sąlygomis (licencija Nr. LT-61-13-003) 21 ± 1 ℃ temperatūroje, turėdami neribotą prieigą prie maisto ir vandens (**STRAIPSNIAI I, III–VI)**.

Eksperimentai su *Culex pipiens* f. *molestus* ir *Culex quinquefasciatus* buvo atliekami laikantis gyvūnų tyrimų etikos standartų, tačiau uodai nėra saugomi pagal Lietuvos teisės aktus (**STRAIPSNIS II**).

REZULTATAI IR JŲ APTARIMAS

Paukščių, malirijos parazitų ir mikrobiotos sistema kaip eksperimentinis modelis

Paukščių, maliarijos parazitų ir mikrobiotos sistema yra perspektyvus eksperimentinis modelis, leidžiantis tirti natūralias kliūtis, ribojančias maliarijos parazitų vystymąsi. Viena iš tokių kliūčių yra imuninis atsakas į oligosacharidą galaktozės-α-1,3-galaktozę (α-Gal), angliavandenių epitopą, sintezuojamą tam tikrų gramneigiamų bakterijų paukščių žarnyne, kuris, kaip manoma, paukščiuose sukelia anti-α-Gal antikūnų gamybą (**STRAIPSNIS I**). Struktūriškai panašūs α-Gal glikanai yra *Plasmodium* sporozoitų paviršiuje (Yilmaz et al., 2014), o tai rodo, kad žarnyno mikrobiota gali netiesiogiai formuoti imunitetą ir riboti parazitų vystymąsi stuburinių šeimininkų organizmuose (**STRAIPSNIS I,** 4 pav.).

Eksperimentiniai tyrimai su žinduolių maliarijos modeliu parodė, kad anti-α-Gal antikūnai gali slopinti *Plasmodium berghei* ANKA sporozoitus pelėse, kurioms trūksta endogeninio α-Gal, tarpininkaujant komplemento priklausomam lizei, kol parazitai pasiekia hepatocitus, ir užkertant kelią infekcijos vystymuisi kraujo stadijoje (Yilmaz et al., 2014). Įdomu tai, kad α-Gal buvo aptiktas užsikrėtusių ir neužsikrėtusių uodų seilių liaukose, kas

leidžia manyti, jog vektoriaus kilmės glikanai gali prisidėti prie anti-α-Gal imuniteto susidarymo stuburiniuose šeimininkuose (Yilmaz et al., 2014).

Preliminarūs eksperimentiniai duomenys patvirtina šią hipotezę. α-Gal buvo aptiktas trijų paukščių *Plasmodium* rūšių – *Plasmodium ashfordi* (GRW2), *Plasmodium relictum* (SGS1) ir *Plasmodium homocircumflexum* (COLL4) – kraujo stadijos baltymų ekstraktuose, gautuose iš eksperimentiniu būdu užkrėstų alksninukų (*Spinus spinus*) (**STRAIPSNIS I,** 1 pav.). Įvairių laukinių ir naminių paukščių rūšių žarnyno mikrobiotos analizė parodė, kad iš daugiau nei 140 bakterijų taksonų *Escherichia-Shigella, Herbaspirillum, Megamonas* ir *Serratia* labiausiai prisidėjo prie α1,3GT geno gausos, patvirtindamos, kad α-Gal gaminančios bakterijos yra paplitusios paukščių žarnyne (**STRAIPSNIS I,** 3 pav.).

Siekiant įvertinti paukščių *Plasmodium* α-Gal imunogeniškumą, buvo matuojamas IgY antikūnų atsakas į du glikano epitopus – Galα1-3Gal ir Galα1-3Galβ1-4GlcNAc – eksperimentiniu būdu užkrėstose naminėse kanarėlėse. *Plasmodium homocircumflexum* užkrėstuose paukščiuose nenustatyti reikšmingi cirkuliuojančio IgY lygio pokyčiai, o *P. relictum* infekcija sukėlė reikšmingą anti-Galα1-3Gal IgY titrų padidėjimą 38 dieną po infekcijos (**STRAIPSNIS I,** 2 pav.). Tai rodo, kad paukščių maliarijos infekcija gali sukelti mikrobiotos formuojamą humoralinį atsaką, analogišką tam, kuris stebimas žinduolių sistemose.

Šie rezultatai pabrėžia paukščių, malirijos parazitų ir mikrobiotos eksperimentinio modelio naudingumą tiriant, kaip žarnyno mikrobiotos sudėtis ir mikrobiotos indukuoti antikūnai veikia kaip natūralus barjeras maliarijos infekcijai. Taip pat tai sudaro pagrindą būsimiems eksperimentiniams ir lauko tyrimams, kuriuose bus nagrinėjami nuo mikrobiotos priklausomi atsparumo mechanizmai ir jų ekologiniai veiksniai paukščių maliarijos dinamikoje (**STRAIPSNIS I**).

Vektorių mikrobiota ir maliarijos parazitų vystymasis

Ankstesni tyrimai parodė, kad simbiontinės bakterijos uodų vidurinėje žarnoje moduliuoja vektoriaus kompetenciją, palengvindamos arba ribodamos patogenų kolonizaciją ir vystymąsi (Hajkazemian et al., 2021; Wang et al., 2021; Bando et al., 2013). Kadangi *Plasmodium* parazitai sporogoniniu būdu vystosi uodų vidurinėje žarnoje (Valkiūnas, 2005), šiame etape gali susidaryti tiesioginės sąveikos tarp parazitų ir vietinės žarnyno mikrobiotos. Siekiant geriau suprasti vektoriaus, mikrobiotos ir patogenų tarpusavio ryšius, buvo ištirta dviejų paukščių maliarijos pernešėjų – *Culex pipiens* f. *molestus* ir *Culex quinquefasciatus* – žarnyno mikrobiota, siekiant nustatyti natūralius šių

rūšių panašumus ir skirtumus bei tai, kaip jų mikrobų bendrijos reaguoja į trikdžius, pavyzdžiui, parazitų infekciją **(STRAIPSNIS II**). Be to, vektorių mikrobiota buvo paveikta specifiniais stuburiniame šeimininke susiformavusiais antikūnais, kurie išlieka funkcionalūs uodų vidurinėje žarnoje po pasimaitinimo krauju (Noden et al., 2011; Maitre et al., 2021), siekiant įvertinti, kaip *Cx. quinquefasciatus* mikrobiota veikia *Plasmodium relictum* vystymąsi (**STRAIPSNIS III**).

Tyrimo metu buvo ištirta dviejų paukščių maliarijos vektorių – *Cx. pipiens* f. *molestus* ir *Cx. quinquefasciatus* – žarnyno mikrobiotos sudėtis ir tinklo dinamika, siekiant įvertinti jų galimą vaidmenį parazitų vystymuisi. Atliekant uodų mikrobiotos 16S rRNR genų sekų analizę nustatyta, kad, nors dauguma taksonų buvo bendri, šių dviejų uodų rūšių mikrobų bendrijų struktūra skyrėsi (**STRAIPSNIS II**, 1 pav.). Tos pačios ekologinės aplinkos sąlygomis panaši mikrobiotos įvairovė yra tikėtina (Muturi et al., 2018), tačiau skirtumai išryškėjo, analizuojant *Wolbachia* endosimbiontų ir *Escherichia-Shigella* komensalinių bakterijų pasiskirstymo dėsningumus. Abiejose rūšyse *Escherichia-Shigella* veikė kaip kertinis taksonas, formuojantis pagrindinius tinklo modulius ir iš esmės prisidedantis prie mikrobų sąveikos (**STRAIPSNIS II,** 2 pav.). Kaip kertinis taksonas, *Escherichia-Shigella* gali vaidinti centrinį vaidmenį, reguliuojant bendrijų struktūrą ir ekologinius santykius, o tai atitinka kitų sistemų tyrimų rezultatus (Banerjee et al., 2018). Priešingai, *Wolbachia* bakterijos parodė rūšiai specifišką modulinę organizaciją. Ji buvo įtraukta į pagrindinį modulį *Cx. pipiens* f. *molestus,* bet sudarė mažą, atskirą modulį *Cx. quinquefasciatus* uodų mikrobiotoje (**STRAIPSNIS II,** 2 pav.). Sumažėjęs *Wolbachia* taksono ryšių gausumas rodo specializuotą ekologinę funkciją uodų mikrobiotoje, galimai susijusią su jos patogenų blokavimo savybėmis ir šeimininko reprodukcinės biologijos moduliacija, kaip aprašyta anksčiau (Moreira et al., 2009; Bian et al., 2010). *In silico* eksperimentas, kuriame buvo pašalinti mazgai, atskleidė skirtingą mikrobų tinklo stabilumą. *Culex pipiens* f. *molestus* rūšyje *Wolbachia* taksono pašalinimas sumažino tinklo ryšių gausumą, o *Cx. quinquefasciatus* rūšyje *Escherichia-Shigella* taksono pašalinimas sumažino tinklo stabilumą (**STRAIPSNIS II,** 4 pav.). Šie rezultatai atskleidžia rūšims būdingus mikroorganizmų tinklo tvirtumo ir atsparumo sisteminiams pokyčiams skirtumus.

Siekiant įvertinti šeimininko antikūnų sukeltų mikrobiotos pokyčių poveikį parazitų vystymuisi, *Cx. quinquefasciatus* uodams buvo leista maitintis kanarėlių krauju, kurios buvo imunizuotos *E. coli* štamais arba užkrėstos *P. relictum*. Cirkuliuojantis anti-*E. coli* IgY išliko aktyvus uodų vidurinėje žarnoje po pasimaitinimo krauju (**STRAIPSNIS III,** 2A pav.).

Bendras mikrobų gausumas ir tolygumas uodų vidurinėje žarnoje tarp eksperimentinių grupių nesiskyrė (**STRAIPSNIS III,** 2B ir 2C pav.). Tačiau buvo nustatyti taksonominės sudėties sirtumai (**STRAIPSNIS III,** 2D pav.). *Plasmodium* užkrėsti uodai, palyginti su kontrolinėmis grupėmis, turėjo skirtingą mikrobų sudėtį, o tie, kurie maitinosi paukščių krauju, turinčiu anti-*E. coli* antikūnų, turėjo pakitusį daugelio bakterijų taksonų gausumą (**STRAIPSNIS III,** 3 ir 4 pav.). Tinklo analizė atskleidė ryškius pokyčius bendrijų struktūroje, įskaitant sumažėjusį *Escherichia-Shigella* ir kitų taksonų bendrą pasiskirstymą bei topologinių parametrų, tokių kaip ryšių gausumas, moduliarumas ir mazgų centriškumas, pokyčius (**STRAIPSNIS III**, 6 ir 7 pav.; 1 lentelė). Panašūs *Escherichia* ryšių gausumo sumažėjimo ir konkrečių bakterijų taksonų gausumo pokyčiai stebėti ir Mateos-Hernández et al. (2021) tirtose erkėse, pasimaitinusiose šeimininko anti-E. *coli* antikūnais. Šie rezultatai rodo, kad šeimininko antikūnai gali keisti vektorių mikrobiotą ir trikdyti mikrobų sąveikas.

Funkciniu požiūriu, šeimininko antikūnų sukelti pokyčiai uodų mikrobiotoje turėjo pastebimą poveikį parazitų vystymuisi. *Plasmodium relictum* oocistų gausumas vidurinėje žarnoje buvo reikšmingai mažesnis uoduose, pasimaitinusiuose paukščių krauju su anti-*E. coli* antikūnais, o sporogoninės stadijos buvo aptinkamos rečiau (**STRAIPSNIS III**, 9 pav.). *Escherichia coli* O86:B7 štamas, kuris pasižymi aukštu α-Gal sintezės lygiu (Yilmaz et al., 2014), turėjo ypač stiprų neigiamą poveikį *P. relictum* vystymuisi *Cx. quinquefasciatus* uoduose. Taip pat buvo pastebėti skirtumai tarp eksperimentinių grupių uodų išgyvenamumo, kur didžiausias mirtingumas buvo tarp uodų, kurie maitinosi paukščiais, imunizuotais *E. coli* BL21 ir užkrėstais *P. relictum* (**STRAIPSNIS III,** 8 pav.). Tai gali rodyti, kad imuninės sistemos sukelti mikrobiotos pokyčiai gali paveikti vektorių tinkamumą pernešti parazitus. Apibendrinant, šie rezultatai rodo, kad šeimininko antikūnai, nukreipti prieš specifines žarnyno bakterijas, gali trukdyti paukščių maliarijos parazitų vystymuisi, atskleidžiant mechanizmą, per kurį stuburinių imunitetas netiesiogiai veikia vektorių kompetenciją ir ligos perdavimą.

Gauti rezultatai rodo, kad natūrali uodų mikrobiotos struktūra ir išoriniai veiksniai, tokie kaip šeimininko antikūnų sukelta moduliacija, daro įtaką paukščių maliarijos vektorių mikrobiotos bendrijų stabilumui. Šios sąveikos taip pat daro įtaką uodų fiziologiniam pajėgumui ir parazitų vystymuisi, pabrėždamos glaudų ryšį tarp šeimininko imuniteto, vektorių mikrobiotos ir maliarijos perdavimo (**STRAIPSNIAI II, III**).

Paukščių šeimininkų, jų žarnyno mikrobiotos ir maliarijos parazitų sąveika vis labiau pripažįstama kaip pagrindinis veiksnys, lemiantis infekcijos baigtį ir turintis įtakos šeimininko sveikatai. Ankstesni tyrimai parodė, kad parazitų infekcijos gali pakeisti šeimininko mikrobiotos bendrijų sudėtį ir struktūrą, sutrikdyti imuninę homeostazę ir paveikti ligos eigą (Videvall et al., 2021; Taniguchi et al., 2015). Tačiau, nepaisant pažangos paukščių mikrobiomo tyrimų srityje, *Plasmodium* infekcijų poveikis paukščių žarnyno mikrobiotai ir šių mikrobų bendrijų ekologiniam stabilumui vis dar menkai žinomas.

Siekiant atsakyti į šį klausimą, naminės kanarėlės buvo eksperimentiniu būdu užkrėstos *Plasmodium homocircumflexum* (**STRAIPSNIS IV**) ir *Plasmodium relictum* (**STRAIPSNIS V**). Tyrimo tikslas buvo įvertinti, kaip infekcija veikia žarnyno mikrobiotos sudėtį, bendrijų formavimąsi ir atsparumą kolonizacijai, analizuojant 16S rRNR amplikono sekas, gautas iš ekskrementų mėginių, surinktų infekcijos eigoje.

Abiejų infekcijų atveju alfa ir beta įvairovės rodikliai tarp užsikrėtusių ir kontrolinių paukščių reikšmingai nesiskyrė, o tai rodo, kad bendras mikrobiotos turtingumas ir tolygumas išliko stabilūs. Šie rezultatai atitinka ankstesnius maliarijos tyrimus, kurie parodė, kad infekcija turi ribotą poveikį bendrai mikrobų įvairovei (Rohrer et al., 2023; Macdonald et al., 2017). Nors bendra mikrobiotos įvairovė išliko nepakitusi, abiejų infekcijų metu nustatyti tam tikrų bakterijų taksonų sudėties pokyčiai. Taksonominė analizė parodė bendrą mikrobiotą ir taksonus, kurių gausumas skyrėsi tarp mėginių ėmimo laikų. *Plasmodium homocircumflexum* eksperimente atlikta funkcinė analizė atskleidė sąsajas tarp konkrečių taksonų ir infekcijos stadijų, parodžiusias laikinus mikrobiotos sudėties pokyčius.

Bakterijų tinklų analizės suteikė papildomų įžvalgų apie infekcijos poveikį bendrijų struktūrai. *Plasmodium. homocircumflexum* ir *P. relictum* infekcijų metu užsikrėtusių paukščių bakterijų tinklai pasižymėjo sumažėjusiu ryšių gausumu ir pakitusiais bakterijų sąveikų modeliais, palyginti su kontrolinėmis grupėmis (**STRAIPSNIAI IV, V**). Užsikrėtę paukščiai turėjo mažiau koreliacijų tarp mazgų ir labiau fragmentuotus tinklo modulius, o kontrolinių paukščių tinklai sudarė didesnius, nuoseklius klasterius su tankiai sąveikaujančiais taksonais, pasižyminčiais dideliu vektoriniu centriškumu (**STRAIPSNIS IV**). Be to, tinklo struktūrinės būsenos, apibrėžiamos kaip santykis tarp taksonų kiekio ir ryšių gausumo (mazgų ir kraštinių skaičiaus), taip pat skyrėsi tarp užsikrėtusių ir kontrolinių paukščių ir rodė bendrą infekcijos poveikį tinklo struktūrai ir organizacijai (**STRAIPSNIS V**). Tinklo

stabilumo analizė patvirtino šiuos rezultatus. Abiejų infekcijų atvejais mazgų pašalinimas sumažino mikrobiotos bakterijų tinklo stabilumą užsikrėtusiuose paukščiuose, o mazgų pridėjimas neturėjo įtakos tinklo stabilumui, o tai rodo mažesnį mikrobiotos bendrijų atsparumą trikdžiams. Šie rezultatai rodo, kad *Plasmodium* infekcija daro įtaką paukščio žarnyno mikrobų sąveikų tinklams ir silpnina kolonizacijos atsparumą, iš esmės nekeisdama bendros mikrobiotos įvairovės.

Atsižvelgiant į abiejų *Plasmodium* rūšių eksperimentų rezultatus, paukščių maliarija sukelia žarnyno mikroorganizmų bendrijų struktūrinę reorganizaciją, o ne plačius taksonominės sudėties pokyčius (**STRAIPSNIAI IV, V**). Nepaisant stabilios alfa ir beta įvairovės, infekcija buvo susijusi su sumažėjusiu tinklo kompleksiškumu ir ryšiais, atspindinčiais laikiną, bet išmatuojamą poveikį bendrijų susidarymui.

Graužikų maliarijos tyrimų (Taniguchi et al., 2015; Mooney et al., 2015) rezultatai taip pat rodo, kad maliarijos infekcija sukelia daugiausia laikinus mikrobiomo pokyčius, turinčius įtakos konkretiems bakterijų taksonams. Tokie sudėties pokyčiai savo ruožtu gali turėti įtakos mikrobų bendrijų organizacijai ir jų sąveikos tinklams (Li et al., 2021). Kaip ir kitų parazitų sistemų tyrimuose (Mammeri et al., 2020), paukščių *Plasmodium* infekcija taip pat buvo susijusi su sumažėjusiu tinklo kompleksiškumu ir ryšių gausumu, o tai rodo, kad mikrobų bendrijų reorganizavimas gali būti dažnas atsakas į parazitų infekciją. Šie pokyčiai gali sumažinti kolonizacijos atsparumą ir paveikti bendrijų atsparumą, o tai gali turėti pasekmių imuniniam atsakui ir imlumui antrinėms infekcijoms.

Apibendrinant, šie rezultatai rodo, kad paukščių *Plasmodium* infekcija keičia žarnyno mikrobiotos organizaciją per bendrijų sudėties ir tinklo struktūros pokyčius, o ne per didelio masto įvairovės praradimą ar padidėjimą. *Plasmodium relictum* ir *P. homocircumflexum* eksperimentų rezultatai rodo bendrą mechanizmą, kuriuo maliarijos parazitai sutrikdo paukščių žarnyno mikrobiotos ekologinę pusiausvyrą. Nors kanarėlių žarnyno mikrobiota išlieka atspari įvairovės požiūriu, laikina mikrobų tinklų reorganizacija rodo funkcinį jautrumą infekcijai ir pabrėžia jų vaidmenį palaikant žarnyno ekosistemos stabilumą ir infekcijos dinamiką.

Parazito transkripcijos atsakas į šeimininko imuninę sistemą

Eurikseniniai maliarijos parazitai turi greitai prisitaikyti prie skirtingų šeimininkų fiziologinės aplinkos, kad užtikrintų išlikimą ir perdavimą (Prati et al., 2022). Šis prisitaikymas gali atsirasti ne tik dėl genetinės variacijos, bet ir dėl transkripcijos plastiškumo, kuris leidžia parazitams moduliuoti genų

raišką, reaguojant į šeimininkui būdingas imunines ir fiziologines sąlygas (Turnbull et al., 2022; Hollin et al., 2023). Siekiant ištirti, kaip *Plasmodium homocircumflexum* reaguoja genetiniu ir transkripciniu lygiais į šeimininko imuninės sistemos variacijas, buvo atlikti eksperimentiniai kryžminiai užkrėtimai, naudojant kanarėles ir alksninukus, dvi paukščių rūšis, kurios skiriasi imunine sistema ir fiziologija (Palinauskas et al., 2020).

Eksperimento tikslas buvo nustatyti, kaip parazito genų raiška prisitaiko prie skirtingų šeimininkų aplinkos ir imuninių reakcijų. Visose eksperimentinėse grupėse parazitemijos pikas pasiektas 8 dieną po infekcijos (dpi) (**STRAIPSNIS VI**, 1 pav.). RNR raiškos analizė parodė, kad ankstyvieji transkripcijos modeliai daugiausia priklausė nuo donoro šeimininko rūšies: iki 8 dpi parazito genų raiška atspindėjo donoro imuninę ir fiziologinę aplinką (**STRAIPSNIS VI**, 2 ir 3 pav.). Šie rezultatai rodo, kad *P. homocircumflexum* gali laikinai išlaikyti donorui būdingus transkripcijos požymius, galimai dėl epigenetiškai paveldėtos būsenos, kuri palengvina spartesnį prisitaikymą naujame šeimininke (Abdrabou et al., 2021). Tolesnė infekcijos eiga rodo, kad recipiento šeimininko imuninė sistema darė selektyvų spaudimą, sukeldama parazito genų raiškos pertvarką: 16 dpi transkripcijos profiliai jau atitiko recipientą šeimininką (**STRAIPSNIS VI**, 2 ir 3 pav.).

Vieno nukleotido polimorfizmo (VNP) analizė neatskleidė aiškių donorų ar recipientų rūšių grupių (**STRAIPSNIS VI**, 5 pav.), o tai rodo, kad nustatyti transkripcijos pokyčiai nebuvo nulemti genetinės diferenciacijos. Nors VNP analizės plačiai taikomos, tiriant šeimininko ir patogeno sąveiką bei atrankos požymius (Maïga-Ascofaré et al., 2010), tik nedidelė VNP dalis skyrėsi tarp grupių, kas rodo silpną atrankos spaudimą šioje infekcijos stadijoje. Todėl tikėtina, kad stebimi transkripcijos pokyčiai atspindi reguliacinį plastiškumą, o ne sekos lygmens evoliucinius pokyčius.

Apibendrinant, rezultatai rodo, kad *P. homocircumflexum* prisitaiko prie naujų paukščių šeimininkų, pirmiausia, per transkripcijos perprogramavimą, o ne per genetinę divergenciją. Toks reguliacinis lankstumas greičiausiai sustiprina parazito gebėjimą išlikti skirtingose šeimininkų aplinkose ir yra svarbi adaptacijos strategija, lemianti maliarijos parazitų generalistų ekologinę sėkmę. Transkripcijos plastiškumas gali būti paplitęs evoliucinis mechanizmas tarp paukščių maliarijos parazitų, leidžiantis jiems užkrėsti šeimininkus su skirtingais imuniniais profiliais, nereikalaujant rūšiai būdingų genetinių pokyčių. Pasikliaudami greitu transkriptominiu atsaku, o ne lėtesne genetine adaptacija, eurikseniniai parazitai gali lanksčiai prisitaikyti prie įvairių šeimininkų fiziologinės aplinkos ir išlaikyti platų šeimininkų spektrą. Šios įžvalgos padeda geriau suprasti, kaip plastiškumas veikia šeimininko ir parazito bendrą evoliuciją, ir

gali paaiškinti, kodėl eurikseniniai *Plasmodium* spp. parazitai yra ekologiškai sėkmingi ir paplitę visame pasaulyje.

Link sisteminio paukščių maliarijos supratimo

Šios disertacijos rezultatai leidžia pateikti struktūrizuotą ekologinę paukščių maliarijos interpretaciją. Jie rodo, kad infekcijos eigą lemia ne atskiros stuburinio šeimininko ir parazito ar vektoriaus ir parazito sąveikos, o tarpusavyje susiję procesai, vienu metu veikiantys stuburinio šeimininko, vektoriaus ir mikrobiotos tinkle.

Šios sistemos pagrindą sudaro mikrobiotos struktūra. Stuburinių ir su uodais susijusios mikroorganizmų bendruomenės sudaro organizuotus ekologinius tinklus, kurių ryšiai, stabilumas ir funkcinė sudėtis formuoja aplinką, kurioje vyksta parazitų vystymasis. Mikroorganizmų bendruomenės veikia kaip ekologiniai filtrai, darantys įtaką parazitų vystymosi sėkmei per imuninės sistemos moduliaciją ir mikroorganizmų tinklų struktūrines savybes. Šie rezultatai rodo, kad parazitų vystymasis ir perdavimas priklauso nuo stuburinio šeimininko ir vektoriaus mikrobiotos struktūros, o ne vyksta neutraliame biologiniame fone.

Tačiau šeimininko ir parazito ar vektoriaus ir parazito sąveika nėra vienakryptė. *Plasmodium* infekcija sukelia išmatuojamus mikroorganizmų bendrijos organizacijos pokyčius, keisdama tinklo topologiją ir atsparumą, nors bendrų mikroorganizmų įvairovės pokyčių gali ir nebūti. Tai rodo, kad infekcija veikia kaip ekologinis trikdis, galintis keisti mikroorganizmų sistemos stabilumą. Todėl mikrobiota ne tik riboja parazitų vystymąsi, bet ir pati kinta jų buvimo sąlygomis, taip susidarant abipusiui grįžtamajam ryšiui stuburinio šeimininko ir vektoriaus sistemoje.

Šiame ekologiniame kontekste svarbų vaidmenį atlieka ir parazitų reguliacinis plastiškumas. Transkriptominės analizės rodo, kad eurikseniniai paukščių maliarijos parazitai keičia genų raišką, reaguodami į skirtingą stuburinių šeimininkų aplinką. Toks transkripcijos perprogramavimas leidžia parazitams prisitaikyti prie šeimininko imuninės aplinkos pokyčių, neįvykstant greitai genetinei diferenciacijai. Ekologiniu požiūriu toks plastiškumas atspindi adaptyvaus atsako mechanizmą, veikiantį nevienalytėje šeimininkų aplinkoje.

Apibendrinus šiuos komponentus, galima išskirti trišalį ekologinį modelį, kuriam būdinga: (i) mikrobiotos lemiama parazitų vystymosi moduliacija, (ii) infekcijos sukeliama mikroorganizmų tinklų struktūros pertvarka ir (iii) parazitų genų raiškos prisitaikymas prie šeimininko aplinkos.

Šie procesai stuburinio šeimininko ir vektoriaus sistemoje veikia vienu metu ir sąveikaudami tarpusavyje, sudarydami dinaminį abipusės moduliacijos tinklą, o ne linijinę priežasčių grandinę. Šioje sistemoje infekcijos baigtį lemia mikroorganizmų bendrijų struktūrinės savybės, imuninių mechanizmų sąveika ir parazitų prisitaikymo geba, veikiantys kartu.

Šis integruotas modelis suteikia nuoseklų ekologinį pagrindą šios disertacijos eksperimentinių rezultatų interpretacijai ir leidžia paukščių maliariją nagrinėti sisteminio lygmens biologiniame kontekste.

IŠVADOS

1. Paukščių, maliarijos parazitų ir mikrobiotos sistema yra naujas eksperimentinis modelis, leidžiantis nustatyti natūralius barjerus, ribojančius maliarijos parazito vystymąsi, kuriuos formuoja *Plasmodium* biologija ir mikrobiotos moduliuojama imuninė apsauga.
2. *Plasmodium relictum* infekcija daro įtaką *Culex pipiens* f. *molestus* ir *Culex quinquefasciatus* žarnos mikrobiotos sudėčiai ir tinklo struktūrai, paveikdama vektoriaus ir parazito sąveiką.
3. Tikslinė paukščių maliarijos vektoriaus *Culex quinquefasciatus* žarnos mikrobiotos moduliacija daro neigiamą įtaką *Plasmodium relictum* parazito sporogoninio vystymosi eigai.
4. *Plasmodium relictum* ir *Plasmodium homocircumflexum* infekcija paveikia stuburinio šeimininko žarnyno mikrobiotą, sutrikdydama mikroorganizmų bendrijų stabilumą ir mažindama atsparumą kolonizacijai.
5. Paukščių maliarijos sukėlėjas *Plasmodium homocircumflexum*, patekęs į naują šeimininką, pasižymi transkriptominiu lankstumu: pradžioje išlaiko donoro rūšiai būdingą genų raiškos profilį, laipsniškai keisdamasis ir prisitaikydamas prie naujo šeimininko aplinkos.

REFERENCES

1. Abdrabou, W., Dieng, M.M., Diawara, A., Sermé, S.S., Almojil, D., Sombié, S., Henry, N.B., Kargougou, D., Manikandan, V., Soulama, I., et al., 2021. Metabolome modulation of the host adaptive immunity in human malaria. *Nature Metabolism* 3(7), 1001–1016. https://doi.org/10.1038/s42255-021-00404-9
2. Agosta, S.J., Janz, N. & Brooks, D.R., 2010. How specialists can be generalists: resolving the "parasite paradox" and implications for emerging infectious disease. *Zoologia* 27(2), 151–162. https://doi.org/10.1590/S1984-46702010000200001
3. Andrews, S., 2010. FastQC: A quality control tool for high throughput sequence data. Unpublished data. Available at: https://www.bioinformatics.babraham.ac.uk/projects/fastqc/
4. Anaconda Software Distribution. 2023. Anaconda Documentation. Anaconda Inc. Retrieved from https://docs.anaconda.com/. (n.d.).
5. Bando, H., Okado, K., Guelbeogo, W., Badolo, A., Aonuma, H., Nelson, B. et al., 2013. Intra-specific diversity of *Serratia marcescens* in *Anopheles* mosquito midgut defines *Plasmodium* transmission capacity. *Scientific Reports* 3, 1641. https://doi.org/10.1038/srep01641
6. Banerjee, S., Schlaeppi, K. & van der Heijden, M.G.A., 2018. Keystone taxa as drivers of microbiome structure and functioning. *Nature Reviews Microbiology* 16(9), 567–576.
7. Bastian, M., Heymann, S., & Jacomy, M. 2009. Gephi: An Open Source Software for Exploring and Manipulating Networks. *Proceedings of the International AAAI Conference on Web and Social Media*, 3(1), 361–362. https://doi.org/10.1609/icwsm.v3i1.13937
8. Belkaid, Y. & Hand, T.W., 2014. Role of the microbiota in immunity and inflammation. *Cell* 157(1), 121–141. https://doi.org/10.1016/j.cell.2014.03.011
9. Bensch, S., Hellgren, O. & Pérez-Tris, J., 2009. MalAvi: A public database of malaria parasites and related haemosporidians in avian hosts based on mitochondrial cytochrome *b* lineages. *Molecular Ecology Resources* 9 (5), 1353–1358. https://doi.org/10.1111/j.1755-0998.2009.02692.x
10. Bensch, S., Stjernman, M., Hasselquist, D., Östman, Ö., Hansson, B., Westerdahl, H. & Pinheiro, R.T., 2000. Host specificity in avian blood parasites: a study of *Plasmodium* and *Haemoproteus* mitochondrial DNA amplified

from birds. *Proceedings of the Royal Society B: Biological Sciences* 267(1452), 1583–1589. https://doi.org/10.1098/rspb.2000.1181

11. Bian, G., Xu, Y., Lu, P., Xie, Y. & Xi, Z., 2010. The endosymbiotic bacterium *Wolbachia* induces resistance to dengue virus in *Aedes aegypti*. *PLoS Pathogens* 6(4), e1000833. https://doi.org/10.1371/journal.ppat.1000833
12. Böhme, U., Otto, T.D., Cotton, J.A., Steinbiss, S., Sanders, M., Oyola, S.O., Nicot, A., Gandon, S., Patra, K.P., Herd, C., et al., 2018. Complete avian malaria parasite genomes reveal features associated with lineage-specific evolution in birds and mammals. *Genome Research* 28(4), 547–560. https://doi.org/10.1101/gr.218123.116
13. Boissière, A., Tchioffo, M.T., Bachar, D., Abate, L., Marie, A., Nsango, S.E., Shahbazkia, H.R., Awono-Ambene, P.H., Levashina, E.A., Christen, R. & Morlais, I., 2012. Midgut microbiota of the malaria mosquito vector *Anopheles gambiae* and interactions with *Plasmodium falciparum* infection. *PLoS Pathogens* 8(5), e1002742. https://doi.org/10.1371/journal.ppat.1002742
14. Bolyen, E., Rideout, J. R., Dillon, M. R., Bokulich, N. A., Abnet, C. C., Al-Ghalith, G. A., Alexander, H., Alm, E. J., Arumugam, M., Asnicar, F., Bai, Y., Bisanz, J. E., Bittinger, K., Brejnrod, A., Brislawn, C. J., Brown, C. T., Callahan, B. J., Caraballo-Rodríguez, A. M., Chase, J., … Caporaso, J. G. 2019. Reproducible, interactive, scalable and extensible microbiome data science using QIIME 2. *Nature Biotechnology*, *37*(8), 852–857. https://doi.org/10.1038/s41587-019-0209-9
15. Cansado-Utrilla, C., Zhao, S.Y., McCall, P.J., Coon, K.L., & Hughes, G.L., 2021. The microbiome and mosquito vectorial capacity: rich potential for discovery and translation. *Microbiome* 9:111. https://doi.org/10.1186/s40168-021-01073-2
16. Cirimotich, C.M., Dong, Y., Clayton, A.M., Sandiford, S.L., Souza-Neto, J.A., Mulenga, M. & Dimopoulos, G., 2011. Natural microbe-mediated refractoriness to *Plasmodium* infection in *Anopheles gambiae*. *Proceedings of the National Academy of Sciences of the United States of America* 108(46), 18020–18025. https://doi.org/10.1073/pnas.1110586108

17. Csárdi, G., & Nepusz, T. 2006. The igraph software package for complex network research. Complex Systems, 1695. https://igraph.org
18. Davies, C. S., Capilla-Lasheras, P., Catelan-Carphio, E., Corregidor-Castro, A., Diez-Méndez, D., Drobniak, S. M., Drzewińska-Chańko, J., Kohl, K., D., Martínez-Renau, E., Ramellini, S., Richardson, D. S., Ruuskanen, S., Sutton, A. O., Szulkin, M., Troisi, C. A., White, J., Worsley, S. F., Bodawatta, K. H., Videvall E., 2026 Bridging the gap: improving methodologies for future avian microbiome research. *J Avian Biol* 2026(2):e03594. https://doi.org/10.1002/jav.03594
19. Dobin, A., Davis, C.A., Schlesinger, F., Drenkow, J., Zaleski, C., Jha, S., Batut, P., Chaisson, M. & Gingeras, T.R., 2013. STAR: ultrafast universal RNA-seq aligner. *Bioinformatics* 29(1), 15–21. https://doi.org/10.1093/bioinformatics/bts635
20. Fernandes, A. D., Reid, J. N., Macklaim, J. M., McMurrough, T. A., Edgell, D. R., & Gloor, G. B. 2014. Unifying the analysis of high-throughput sequencing datasets: Characterizing RNA-seq, 16S rRNA gene sequencing and selective growth experiments by compositional data analysis. *Microbiome*, 2(1), 15. https://doi.org/10.1186/2049-2618-2-15
21. Gabrieli, P., Caccia, S., Varotto-Boccazzi, I., Arnoldi, I., Barbieri, G., Comandatore, F., Epis, S., 2021. Mosquito trilogy: microbiota, immunity and pathogens, and their implications for the control of disease transmission. *Frontiers in Microbiology* 12:630438. https://doi.org/10.3389/fmicb.2021.630438
22. García-Longoria, L., Palinauskas, V., Ilgūnas, M., Valkiūnas, G. & Hellgren, O., 2020. Differential gene expression of *Plasmodium homocircumflexum* (lineage pCOLL4) across two experimentally infected passerine bird species. *Genomics* 112(4), 2857–2865. https://doi.org/10.1016/j.ygeno.2020.03.025
23. Godfrey, R.D., Fedynich, A.M. & Pence, D.B., 1987. Quantification of hematozoa in blood smears. *Journal of Wildlife Diseases* 23, 558–565. https://doi.org/10.7589/0090-3558-23.4.558
24. Grabherr, M., Haas, B.J., Yassour, M., Levin, J.Z., Thompson, D.A., Amit, I., Adiconis, X., Fan, L., Raychowdhury, R., Zeng, Q., et al., 2011. Full-length transcriptome assembly from RNA-Seq data without a reference genome. *Nature Biotechnology* 29(7), 644–652. https://doi.org/10.1038/nbt.1883

25. Grond, K., Sandercock, B.K., Jumpponen, A. & Zeglin, L.H., 2018. The avian gut microbiota: community, physiology and function in wild birds. *Journal of Avian Biology* 49, e01788. https://doi.org/10.1111/jav.01788
26. Grond, K., Santo Domingo, J.W., Lanctot, R.B., Jumpponen, A., Bentzen, R.L., Boldenow, M.L., et al., 2019.Composition and drivers of gut microbial communities in Arctic-breeding shorebirds. *Frontiers in Microbiology* 10, 2258. https://doi.org/10.3389/fmicb.2019.02258
27. Gupta, P., Vishnudas, C.K., Robin, V.V., & Dharmarajan, G., 2020. Host phylogeny matters: examining sources of variation in infection risk by blood parasites across a tropical montane bird community in India. *Parasites & Vectors*13(1), 536. https://doi.org/10.1186/s13071-020-04404-8
28. Gutiérrez-López, R., Bourret, V., & Loiseau, C., 2020. Is host selection by mosquitoes driving vector specificity of parasites? A review on the avian malaria model. *Frontiers in Ecology and Evolution* 8:569230. https://doi.org/10.3389/fevo.2020.569230
29. Hajkazemian, M., Bossé, C., Mozūraitis, R. & Emami, S.N., 2021. Battleground midgut: the cost to the mosquito for hosting the malaria parasite. *Biology of the Cell* 113(2), 79–94. https://doi.org/10.1111/boc.202000039
30. Hall, T.A. 1999. A user-friendly biological sequence alignment editor and analysis program for Windows 98/98/NT. Nucleic Acid Symposium Series 41, 95–98.
31. Hellgren, O., Kutzer, M., Bensch, S., Valkiūnas, G. & Palinauskas, V., 2013. Identification and characterization of the merozoite surface protein 1 (*msp1*) gene in a host-generalist avian malaria parasite, *Plasmodium relictum* (lineages SGS1 and GRW4) using blood transcriptome data. *Malaria Journal* 12, 381. https://doi.org/10.1186/1475-2875-12-381
32. Hellgren, O., Waldenström, J. & Bensch, S., 2004. A new PCR assay for simultaneous studies of *Leucocytozoon*, *Plasmodium*, and *Haemoproteus* from avian blood. *Journal of Parasitology* 90(4), 797–802. https://doi.org/10.1645/GE-184R1
33. Hird, S.M., Sánchez, C., Carstens, B.C. & Brumfield, R.T., 2015. Comparative gut microbiota of 59 Neotropical bird species. *Frontiers in Microbiology* 6, 1403. https://doi.org/10.3389/fmicb.2015.01403

34. Hollin, T., Zeinab, C., Roch, L. & Kafsack, B.F.C., 2023. Epigenetic regulation and chromatin remodeling in malaria parasites. *Annual Review of Microbiology* 77(1), 255–276. https://doi.org/10.1146/annurev-micro-032521-041554
35. Ilgūnas, M., Bukauskaitė, D., Palinauskas, V., Iezhova, T.A., Dinhopl, N., Nedorost, N. & Valkiūnas, G., 2016.Mortality and pathology in birds due to *Plasmodium (Giovannolaia) homocircumflexum* infection, with emphasis on the exoerythrocytic development of avian malaria parasites. *Malaria Journal* 15(1), 1–11. https://doi.org/10.1186/s12936-015-1053-5
36. Ippolito, M.M., Denny, J.E., Langelier, C., Sears, C.L., Schmidt, N.W., 2018. Malaria and the microbiome: A systematic review. *Clinical Infectious Diseases* 67(12), 1831-1839. https://doi.org/10.1093/cid/ciy737
37. Kalbskopf, V., Ahrén, D., Valkiūnas, G., Palinauskas, V., Hellgren, O., 2021. Shifts in Gene Expression Variability in the Blood-Stage of *Plasmodium relictum*. *Gene 792*, 145723. https://doi.org/10.1016/j.gene.2021.145723
38. Kazlauskienė, R., Bernotienė, R., Palinauskas, V., Iezhova, T.A. & Valkiūnas, G., 2013. *Plasmodium relictum* (lineages pSGS1 and pGRW11): complete synchronous sporogony in mosquitoes *Culex pipiens pipiens*. *Experimental Parasitology* 133, 454–461. https://doi.org/10.1016/j.exppara.2013.01.008
39. Kreisinger, J., Čížková, D., Kropáčková, L. & Albrecht, T., 2015. Cloacal microbiome structure in a long-distance migratory bird assessed using deep 16S rRNA pyrosequencing. *PLoS ONE* 10(9), e0137401. https://doi.org/10.1371/journal.pone.0137401
40. Langmead, B. & Salzberg, S.L., 2012. Fast gapped-read alignment with Bowtie 2. *Nature Methods* 9(4), 357–359. https://doi.org/10.1038/nmeth.1923
41. Lhomme, S. (2015). Analyse spatiale de la structure des réseaux techniques dans un contexte de risques. Cybergeo. https://doi.org/10.4000/cybergeo.26763
42. Li, Y., Li, T., Zhao, D., Wang, Z., & Liao, Y. ,2021. Different tillage practices change assembly, composition, and co-occurrence patterns of wheat rhizosphere diazotrophs. *Science of The Total Environment*, 767, 144252. https://doi.org/10.1016/j.scitotenv.2020.144252

43. Llorà-Batlle O., Tintó-Font E., Cortés A., 2019. Transcriptional variation in malaria parasites: why and how. *Brief Funct Genomics*:18(5):329-341. https://doi.org/10.1093/bfgp/elz009
44. Love, M. I., Huber, W., & Anders, S. 2014. Moderated estimation of fold change and dispersion for RNA-seq data with DESeq2. *Genome Biology*, 15(12), 550. https://doi.org/10.1186/s13059-014-0550-8
45. Macdonald, S.E., Nolan, M.J., Harman, K., Boulton, K., Hume, D.A., Tomley, F.M., Stabler, R.A. & Blake, D.P., 2017. Effects of *Eimeria tenella* infection on chicken caecal microbiome diversity, exploring variation associated with severity of pathology. *PLoS ONE* 12, e0184890. https://doi.org/10.1371/journal.pone.0184890
46. Maïga-Ascofaré, O., Le Bras, J., Mazmouz, R., Renard, E., Falcao, S., Broussier, E. & Clain, J., 2010. Adaptive differentiation of *Plasmodium falciparum* populations inferred from single-nucleotide polymorphisms (SNPs) conferring drug resistance and from neutral SNPs. *Journal of Infectious Diseases* 202(7), 1095–1103. https://doi.org/10.1086/656142
47. Maitre, A., Wu-Chuang, A., Aželytė, J., Palinauskas, V., Mateos-Hernández, L., Obregón, D., et al., 2021. Vector microbiota manipulation by host antibodies: the forgotten strategy to develop transmission-blocking vaccines. *Parasites & Vectors* 15, 4. https://doi.org/10.1186/s13071-021-05122-5
48. Mammeri, M., Obregón, D. A., Chevillot, A., Polack, B., Julien, C., Pollet, T., Cabezas-Cruz, A., & Adjou, K. T. , 2020. *Cryptosporidium parvum* Infection Depletes Butyrate Producer Bacteria in Goat Kid Microbiome. *Frontiers in Microbiology*, 11, 548737. https://doi.org/10.3389/fmicb.2020.548737
49. Martínez-de la Puente, J., Santiago-Alarcon, D., Palinauskas, V., Bensch, S., 2021. *Plasmodium relictum*. *Trends in Parasitology* 37(4), 355–356. https://doi.org/10.1016/j.pt.2020.06.004
50. Mateos-Hernández, L., Obregón, D., Wu-Chuang, A., Maye, J., Bornères, J., Versille, N., et al., 2021. Anti-microbiota vaccines modulate the tick microbiome in a taxon-specific manner. *Frontiers in Immunology* 12, 704621. https://doi.org/10.3389/fimmu.2021.704621
51. Mateos-Hernández, L., Risco-Castillo, V., Torres-Maravilla, E., Bermúdez-Humarán, L.G., Alberdi, P., Hernández-Jarguín, A., et al., 2020. Gut microbiota abrogates anti-α-Gal IgA response in lungs and protects against experimental *Aspergillus* infection in

poultry. *Vaccines (Basel)* 8(2), 285. https://doi.org/10.3390/vaccines8020285

52. Mooney, J.P., Lokken, K.L., Byndloss, M.X., George, M.D., Velazquez, E.M., Faber, F., Butler, B.P., Walker, G.T., Ali, M.M., Potts, R., et al., 2015. Inflammation-associated alterations to the intestinal microbiota reduce colonization resistance against non-typhoidal *Salmonella* during concurrent malaria parasite infection. *Scientific Reports* 5, 14603. https://doi.org/10.1038/srep14603
53. Moreira, L.A., Iturbe-Ormaetxe, I., Jeffery, J.A., Lu, G., Pyke, A.T., Hedges, L.M., et al., 2009. A *Wolbachia*symbiont in *Aedes aegypti* limits infection with dengue, chikungunya, and *Plasmodium*. *Cell* 139(7), 1268–1278.
54. Muturi, E. J., Lagos-Kutz, D., Dunlap, C., Ramirez, J. L., Rooney, A. P., Hartman, G. L., Fields, C. J., Rendon, G., & Kim, C.-H., 2018. Mosquito microbiota cluster by host sampling location. *Parasites & Vectors*, 11(1), 468. https://doi.org/10.1186/s13071-018-3036-9
55. Noden, B.H., Vaughan, J.A., Pumpuni, C.B. & Beier, J.C., 2011. Mosquito ingestion of antibodies against mosquito midgut microbiota improves conversion of ookinetes to oocysts for *Plasmodium falciparum*, but not *P. yoelii*. *Parasitology International* 60(4), 440–446. https://doi.org/10.1016/j.parint.2011.07.007
56. Palinauskas, V., Abdelali, S.K., and Cabezas-Cruz, A., 2024. The mosquito microbiota: A key player in vector competence and disease dynamics. *Pathogens* 13(12), 1101. https://doi.org/10.3390/pathogens13121101
57. Palinauskas, V., Martínez-de la Puente, J., Hernández-Soto, S.R. & Marzal, A., 2020. Experimental parasitology and ecoimmunology: concepts and opportunities in avian haemosporidian studies. In: Valkiūnas, G. & Atkinson, C.T. (eds.) *Avian Malaria and Related Parasites in the Tropics*. Springer, Cham, pp. 527–558. https://doi.org/10.1007/978-3-030-51633-8_17
58. Palinauskas, V., Valkiūnas, G., Bolshakov, C.V. & Bensch, S., 2008. *Plasmodium relictum* (lineage P-SGS1): Effects on experimentally infected passerine birds. *Experimental Parasitology* 120, 372–380. https://doi.org/10.1016/j.exppara.2008.09.001

59. Palinauskas, V., Valkiūnas, G., Bolshakov, C.V. & Bensch, S., 2011. *Plasmodium relictum* (lineage SGS1) and *Plasmodium ashfordi* (lineage GRW2): The effects of co-infection on experimentally infected passerine birds. *Experimental Parasitology* 127(2), 527–533. https://doi.org/10.1016/j.exppara.2010.10.007
60. Palinauskas, V., Žiegytė, R., Iezhova, T.A., Ilgūnas, M., Bernotienė, R. & Valkiūnas, G., 2016. Description, molecular characterisation, diagnostics and life cycle of *Plasmodium elongatum* (lineage pERIRUB01), the virulent avian malaria parasite. *International Journal for Parasitology* 46(11), 697–707. https://doi.org/10.1016/j.ijpara.2016.05.009
61. Palinauskas, V., Žiegytė, R., Ilgūnas, M., Iezhova, T.A., Bernotienė, R., Bolshakov, C. & Valkiūnas, G., 2015.Description of the first cryptic avian malaria parasite, *Plasmodium homocircumflexum* n. sp., with experimental data on its virulence and development in avian hosts and mosquitoes. *International Journal for Parasitology* 45(1), 51–62. https://doi.org/10.1016/j.ijpara.2014.08.012
62. Patro, R., Duggal, G., Love, M. I., Irizarry, R. A., & Kingsford, C., 2017. Salmon provides fast and bias-aware quantification of transcript expression. *Nature Methods*, 14(4), 417–419. https://doi.org/10.1038/nmeth.4197
63. Peschel, S., Müller, C. L., von Mutius, E., Boulesteix, A.-L., & Depner, M. 2021. NetCoMi: Network construction and comparison for microbiome data in R. *Briefings in Bioinformatics*, 22(4), bbaa290. https://doi.org/10.1093/bib/bbaa290
64. Prati, S., Grabner, D.S., Pfeifer, S.M., Lorenz, A.W., & Sures, B., 2022. Generalist parasites persist in degraded environments: a lesson learned from microsporidian diversity in amphipods. *Parasitology* 149(7), 973–982. https://doi.org/10.1017/S0031182022000452
65. R Core Team 2021. R: A language and environment for statistical computing. R Foundation for Statistical Computing, Vienna, Austria. URL https://www.R-project.org/. (n.d.).
66. Ramirez, J.L., Short, S.M., Bahia, A.C., Saraiva, R.G., Dong, Y., Kang, S., Tripathi, A., Mlambo, G. & Dimopoulos, G., 2014. Chromobacterium Csp_P reduces malaria and dengue infection in vector mosquitoes and has entomopathogenic and in vitro anti-

pathogen activities. *PLoS Pathogens* 10(10), e1004398. https://doi.org/10.1371/journal.ppat.1004398

67. Rohrer, S.D., Robertson, B.Q., Chubiz, L.M. & Parker, P.G., 2023. Gut microbiome composition associated with *Plasmodium* infection in the Eurasian tree sparrow. *Journal of Avian Biology*, e03027. https://doi.org/10.1111/jav.03027
68. Romoli, O. & Gendrin, M., 2018. *The tripartite interactions between the mosquito, its microbiota and Plasmodium.Parasites & Vectors* 11:200. https://doi.org/10.1186/s13071-018-2784-x
69. Romoli, O., Schönbeck, J.C., Hapfelmeier, S. & Gendrin, M., 2021. Production of germ-free mosquitoes via transient colonisation allows stage-specific investigation of host–microbiota interactions. *Nature Communications* 12:942. https://doi.org/10.1038/s41467-021-21195-3
70. RStudio Team. 2020. RStudio: Integrated Development for R. RStudio, PBC, Boston, MA URL http://www.rstudio.com/. (n.d.).
71. Ruiz-López, M.J., 2020. Mosquito behavior and vertebrate microbiota interaction: implications for pathogen transmission. *Frontiers in Microbiology* 11:573371. https://doi.org/10.3389/fmicb.2020.573371
72. Sambrook, J., Fritsch, E.F. & Maniatis, T., 2001. *Molecular Cloning: A Laboratory Manual*, 3rd ed. New York, NY: Cold Spring Harbor Laboratory Press.
73. Santiago-Alarcon, D. & Marzal, A., 2020. *Avian Malaria and Related Parasites in the Tropics: Ecology, Evolution and Systematics.* Springer, Cham. https://doi.org/10.1007/978-3-030-51633-8
74. Serrano-Durán, L., Vásquez, A.M. & Tobón-Castaño, A., 2022. Epigenetic and epitranscriptomic gene regulation in *Plasmodium falciparum* and how we can use it against malaria. *Genes (Basel)* 13(10), 1734. https://doi.org/10.3390/genes13101734
75. Simberloff, D., & Rejmanek, M. (Eds.), 2019. 100 of the World's Worst Invasive Alien Species: A Selection From The Global Invasive Species Database. In Encyclopedia of Biological Invasions (pp. 715–716). University of California Press. https://doi.org/10.1525/9780520948433-159

76. Sun, F., Chen, J., Liu, K., Tang, M. & Yang, Y., 2022. The avian gut microbiota: Diversity, influencing factors, and future directions. *Frontiers in Microbiology* 13, 934272. https://doi.org/10.3389/fmicb.2022.934272
77. Taniguchi, T., Miyauchi, E., Nakamura, S., Hirai, M., Suzue, K., Imai, T., Nomura, T., Handa, T., Okada, H., Shimokawa, C., Onishi, R., Olia, A., Hirata, J., Tomita, H., Ohno, H., Horii, T. & Hisaeda, H., 2015. *Plasmodium berghei* ANKA causes intestinal malaria associated with dysbiosis. Scientific Reports 5:15699. https://doi.org/10.1038/srep15699
78. Turnbull, L.B., Button-Simons, K.A., Agbayani, N., & Ferdig, M.T., 2022. Sources of transcription variation in *Plasmodium falciparum*. *Journal of Genetics and Genomics* 49(10), 965–974. https://doi.org/10.1016/j.jgg.2022.03.008
79. Valkiūnas G. , 2005. *Avian Malaria Parasites and Other Haemosporidia*. CRC Press
80. Valkiūnas G., Iezhova T.A., 2018. Keys to the Avian Malaria Parasites. *Malar J* 17:212. https://doi.org/10.1186/s12936-018-2359-5
81. Valkiūnas, G., Iezhova, T. A., Križanauskienė, A., Palinauskas, V., Sehgal, R. N. M., & Bensch, S., 2008. A Comparative Analysis of Microscopy and PCR-Based Detection Methods for Blood Parasites. *Journal of Parasitology*, 94(6), 1395–1401. https://doi.org/10.1645/GE-1570.1
82. Videvall, E., Cornwallis, C.K., Ahren, D., Palinauskas, V., Valkiūnas, G. & Hellgren, O., 2017. The transcriptome of the avian malaria parasite *Plasmodium ashfordi* displays host-specific gene expression. *Molecular Ecology* 26(11), 2939–2958. https://doi.org/10.1111/mec.14074
83. Videvall, E., Marzal, A., Magallanes, S., Fleischer, R.C., Espinoza, K. & García-Longoria, L., 2021. The uropygial gland microbiome of house sparrows with malaria infection. *Frontiers in Microbiology* 12, 662383. https://doi.org/10.3389/fmicb.2021.662383
84. Videvall, E., Strandh, M., Engelbrecht, A., Cloete, S. & Cornwallis, C.K., 2018. Measuring the gut microbiome in birds: comparison of faecal and cloacal sampling. *Molecular Ecology Resources* 18(3), 424–434. https://doi.org/10.1111/1755-0998.12744
85. Villarino, N.F., LeCleir, G.R., Denny, J.E., Dearth, S.P., Harding, C.L., Sloan, S.S., et al., 2016. Composition of the gut microbiota

modulates the severity of malaria. *Proceedings of the National Academy of Sciences of the United States of America* 113, 2235–2240. https://doi.org/10.1073/pnas.1504887113

86. Waite, D.W. & Taylor, M.W., 2014. Characterizing the avian gut microbiota: membership, driving influences, and potential function. *Frontiers in Microbiology* 5, 223. https://doi.org/10.3389/fmicb.2014.00223
87. Wang, M., An, Y., Gao, L., Dong, S., Zhou, X., Feng, Y. et al., 2021. Glucose-mediated proliferation of a gut commensal bacterium promotes *Plasmodium* infection by increasing mosquito midgut pH. *Cell Reports* 35(3), 108992. https://doi.org/10.1016/j.celrep.2021.108992
88. Wickham, H., 2016. *ggplot2: Elegant Graphics for Data Analysis.* New York: Springer-Verlag.
89. Yilmaz, B., Portugal, S., Tran, T.M., Gozzelino, R., Ramos, S., Gomes, J., et al., 2014. Gut microbiota elicits a protective immune response against malaria transmission. *Cell* 159(6), 1277–1289. https://doi.org/10.1016/j.cell.2014.10.053

ADDITIONAL SCIENTIFIC PUBLICATIONS NOT ON THE SUBJECT OF THE DISSERTATION

The articles in journals with an impact factor and referred in the Clarivate Analytic Web of Science database:

1. Maitre A, Wu-Chuang A, **Aželytė J**, Palinauskas V, Mateos-Hernández L, Obregon D, Hodžić A, Valiente Moro C, Estrada-Peña A, Paoli JC, Falchi A, Cabezas-Cruz A. Vector microbiota manipulation by host antibodies: the forgotten strategy to develop transmission-blocking vaccines. *Parasites & Vectors* (Q1; IF: 3.20) (2022), 15:4. doi: 10.1186/s13071-021-05122-5

2. Wu-Chuang A, Mateos-Hernandez L, Maitre A, Rego ROM, Šíma R, Porcelli S, Rakotobe S, Foucault-Simonin A, Moutailler S, Palinauskas V, **Aželytė J**, Sĭmo L, Obregon D, Cabezas-Cruz A. Microbiota perturbation by anti-microbiota vaccine reduces the colonization of *Borrelia afzelii* in *Ixodes ricinus*. *Microbiome* (Q1; IF: 13.80) (2023), 11:151. doi: 10.1186/s40168-023-01599-7

3. Kalbskopf V[I], **Aželytė J[I]**, Palinauskas V, Hellgren O. Genomic variation in *Plasmodium relictum* (lineage SGS1) and its implications for avian malaria infection outcomes: insights from experimental infections and genome-wide analysis**.** *Malaria Journal* (Q2; IF: 3.47) (2024), 23:260. doi: 10.1186/s12936-024-05061-3

4. Skičková Š, Svobodová K, Kratou M, Corduneanu A, Cano-Argüelles AL, **Aželytė J**, Tonk-Rügen M, Majláthová V, Obregon D, Piloto-Sardiñas E, Palinauskas V, Cabezas-Cruz A. Holobiont–holobiont interactions across host–ectoparasite systems. *Parasites & Vectors* (Q1; IF: 3.50) (2025), 18:373. doi: 10.1186/s13071-025-07026-0

5. Obregon D, Maitre A, Piloto-Sardiñas E, Wu-Chuang A, Abuin-Denis L, Cano-Argüelles AL, **Aželytė J**, Corona-Guerrero I, Mateos-Hernández L, Kratou M, Skičková Š, Svobodová K, Cabezas-Cruz A. Decoding microbial community assembly: insights on vectors of infectious diseases. *Annual Review of Microbiology* (Q1; IF: 9.90) (2025), 79:547–572. doi: 10.1146/annurev-micro-082024-094943

6. Markakis G, Palinauskas V, **Aželytė J**, Symeonidou I, Krumplevskaja A, Komnenou A, Papadopoulos E. First investigation of haemosporidian species and record of novel genetic lineages in

Eurasian griffon vultures (*Gyps fulvus*) in Greece. *Veterinary Sciences* (Q1; IF: 2.30) (2025), 12:973. doi: 10.3390/vetsci12100973

7. Markakis G, Palinauskas V, **Aželytė J**, Symeonidou I, Sutkaitytė V, Gelasakis AI, Komnenou A, Papadopoulos E. First assessment of the prevalence of haemosporidian infections in Accipitriformes raptors in Greece. *Parasitology Research* (Q3; IF: 2.00) (2025), 124:2. doi: 10.1007/s00436-024-08445-1

The articles in journals with an impact factor and referred in the Clarivate JCR AHCI or ESCI database:

1. Abuin-Denis L, Piloto-Sardiñas E, Maître A, Wu-Chuang A, Mateos-Hernández L, Obregon D, Corona-González B, Fogaça AC, Palinauskas V, **Aželytė J**, Rodríguez-Mallon A, Cabezas-Cruz A. Exploring the impact of Anaplasma phagocytophilum on colonization resistance of Ixodes scapularis microbiota using network node manipulation. Current Research in Parasitology & Vector-Borne Diseases (Q1; IF: 3.10) (2024), 5:100177. doi: 10.1016/j.crpvbd.2024.100177

ACKNOWLEDGEMENTS

Fortune favored me that day when my supervisor, dr. Vaidas Palinauskas, answerd my call to the P. B. Šivickis Laboratory of Parasitology at the State Scientific Research Institute Nature Research Centre. That moment marked the beginning of my journy into parasitology.

Vaidas, my supervisor, I want to express my deepest gratitude for guiding me through numerous projects, starting with my bachelor‘s studies, then my master‘s and finally my PhD. I could hardly list everything I want to thank you for, from teaching me how to recognise a *Plasodium* parasite on a blood slide to giving me many opportunities to grow and meet so many incredible people.

Under Vaidas‘ supervision I always felt that he believed in me more than I believed in myself, and that truly helped me step out of my comfort zone and improve my knowledge and qualifications in the field of science. Thank you for your patience and for sharing your expertise with me.

At the end of my master‘s studies, Vaidas proposed that my PhD would focus not only on avian haemosporidians, but also include microbiota research. My journely into microbiota analysis started even before the official start of my PhD, when I went to Paris and was very warmly welcomed by my second incredible supervisor, dr. Alejandro Cabezas-Cruz.

Alejandro, my supervisor, I would like to scincerely thank you for your guidence. I am fascinated by your knowledge and passion for raising questions that other scientists would not dare to explore because for fear of the unkown. You taught me how to move forward without overanalysing every detail and what to prioritise in order to succeed. I love that our discussions always end with your motivational speeches, because they truly help me to keep going and always bring back my excitment for science. I feel fortunate to have had the opportunity to know you and learn from you. Thank you very much for your patience and believing in me.

I would like to express my gratitude to everyone from the P. B. Šivickis Laboratory of Parasitology: Rita, Dovilė, Melanie D., Carolina, German, Misa, Claudio, Olena, Nathan, Rasa Bi., Tatjana, Romualda, Gražina, Violeta, Mélanie A.T., Mikas, Vaidas, German, Virmantas, Eimantas, James, Andrius, Lena, Gediminas, and to Kristina, Margarita and Rasa Ber. from the Laboratory of Entomology. Although we work on our own projects, we always support each other during laboratory work and fieldwork, while also brightening each other‘s days with our daily conversations.

Special thanks to Lena, who taught me the main laboratory and fieldwork techniques at the very beginning of my journey while completing

her PhD at the P. B. Šivickis Laboratory of Parasitology. You were a wonderful teacher, and it was truly lovely to work with you!

I am also very grateful to Vaidas, Alejandro, and Rita for trusting me and involving me in interesting projects that helped me grow as a scientist.

I would like to thank Vilnius University, which, under ERASMUS+ program, funded one of my two internships at the National Research Institute for Agriculture, Food and Environment in Paris, where I deepend my knowledge in microbiota analysis under supervision of Alejandro.

I would also like to thank the wonderful microbioTick team: Lourdes, Alejandra, Lianet, Apolline, Angelique, Dasiel, Alexandra, Myriam, Elianne, Patrícia, Karolína, Julié, Camille, Ana Laura, Anna, Štefánia, Constance, Salma, Alejandro. To those whom I had the chance to meet in person, thank you very much for making me feel like part of the team, for your support, and for the many fun discussions during lunches and evening gatherings. Although I have not yet met some of you in person, thank you all for the collaborations, and I hope we will meet soon.

Special thanks to Alejandra, who taught me computational analyses from the very basics; to Apolline and Lianet, who helped me deepen my knowledge in microbiota analysis; to Dasiel for the very valuable consultations through Microsoft Teams; and to Lourdes for teaching me immunological assays.

Big thanks to the Swedish team from Lund University for the interesting discussions, support, and for answering the countless questions I had during my stay in Sweden and throughout our later projects.

Special thanks to Stafan and Olof for your support and for sharing your expertise, which contributed to my decision to continue with my PhD after master's studies.

Thank you, Luz and Victor, for sharing your knowledge and wonderful collaborative work.

To the reviewers and everyone who provided feedback, thank you for your valuable comments and questions, which helped me improve and refine my doctoral thesis.

I would also like to thank Ričardas Paškauskas, Gintautas Samuolis, Gediminas Alzbutas, Sigitas Šulčius, and everyone at the Nature Research Centre who initiated and implemented the virtual machine system at our institution. Thanks to this initiative, I was able to introduce and apply new methods from a foreign laboratory that had not previously been used at our institute.

Sincere thanks to Vytautas Eigirdas and Vytautas Jusys for all your help during our fieldwork at the Ventės Ragas Ornithological Station.

Nuoširdi padėka mano šeimai. Mama, ačiū tau, kad mane palaikei morališkai ir finansiškai, kol visą save buvau atidavusi mokslui.

Nuoširdžiai dėkoju savo vyrui, Vaidui, kuris mane palaikė, manimi tikėjo ir bandė įtikinti, kad esu protingiausias žmogus pasaulyje. Tu pasirodei mano gyvenime būtent tada, kai man tavęs labiausiai reikėjo.

Dukrytei Adelei dėkoju už ramias naktis ir už tai, kad džiugina mane kiekvieną dieną.

Ačiū, Jovita, už palaikymą ir už tai, kad skyrei laiko prižiūrėti Adelytę, kad galėčiau nudirbti savo doktorantūros darbus. Esu dėkinga, kad gyvenimas mus suvedė.

Ačiū, Renata, už palaikymą, ir kad galėjau tau išlieti visus doktorantūros sunkumus. Esi nuostabi draugė.

Dėkoju sau, kad sugebėjau užbaigti šį savo gyvenimo skyrių.

Verčiam naują puslapį.

CURRICULUM VITAE

Name, Last name	**Justė Aželytė**
Position	Junior Researcher
Address	Nature Research Centre, Akademijos 2, Vilnius 21, LT-08412, Lithuania
E-mail	juste.azelyte@gamtc.lt
	https://orcid.org/0000-0002-6171-6913

Education and Academic degrees:

Ph.D., Zoology, 2021-2025, Nature Research Centre, Vilnius, Lithuania.
M.Sc., Biodiversity, 2021, Vilnius University, Vilnius, Lithuania.
B. Sc., Biology, 2019, Vilnius University, Vilnius, Lithuania.

Appointments:

2021 – present: Junior Researcher, Nature Research Centre, Vilnius, Lithuania.
2020–2022: Biologist, Nature Research Centre, Vilnius, Lithuania.

Research areas:

Studies concerning the specificity, virulence and identification of avian malaria parasites. Genetic variation and phylogeny of haemosporidians. Application and development of PCR based methods for identification of avian malaria parasites. Microbiota studies, genomic analysis.

Scholarships, awards and recognitions:

Scholarship from Vilnius University, Lithuania (ERASMUS+ programme, 2020).
A grant for (doctoral) academic visits from the Research Council of Lithuania (2022).
A travel grant from organizers to attend the 5th International Conference on Malaria and related Haemosporidian Parasites of Wildlife in Bielefeld (2022).
An award for the best poster at the 5th International Conference on Malaria and Related Haemosporidian Parasites of Wildlife (2022).
An award for the best oral presentation at the 15th Lithuanian Young Scientists' Conference „Biofuture: perspectives of nature and life sciences“ (2022).
A grant from Nature Research Centre for significant scientific activities of 2022 (2022)
Doctoral scholarship from the Research Council of Lithuania (2023).

A travel grant to attend 10th Conference of the Scandinavian-Baltic Society for Parasitology in Tartu, Estonia.
Erasmus+ traineeship grant from Vilnius University, Lithuania (ERASMUS+ programme, 2023).
A grant from Nature Research Centre for significant scientific activities of 2023 (2023).
A travel grant to attend the 2nd WIMANET-COST workshop in Cluj Napoca, Romania (2024).
A grant to attend the Bioinformatics of Microbial Single Cells Workshop at Bigelow Laboratory for Ocean Sciences, East Boothbay, Maine, USA.

Participation in scientific conferences:
The International Online Conference on Blood Parasites of Wildlife, September 14–15, 2020.
The 9th Conference of the Scandinavian – Baltic Society for Parasitology, April 21–23, 2021.
The 15th International Congress of Parasitology (ICOPA 2022), August 21–26, 2022.
The 5th International Conference on Malaria and Related Haemosporidian Parasites of Wildlife, September 05 – 08, 2022.
The National 15th Lithuanian Young Scientists' Conference „Biofuture: perspectives of nature and life sciences“, November 24, 2022.
The COINS 2023: International conference of life sciences, April 24 – 27, 2023.
The 10th International Conference of the Scandinavian – Baltic Society for Parasitology, June 05 – 06, 2023.
The National 16th Lithuanian Young Scientists' Conference „Biofuture: perspectives of nature and life sciences“, November 24, 2023.
The 6th International Conference on Malaria and Related Haemosporidian Parasites of Wildlife, November 26 – 30, 2024.

Languages
Lithuanian (native); English (level C1); Russian (level A2).

Main research grants
1. European Union Structural Funds “Virulence of avian malaria: untangling genetic players for infection severity”. Award No 09.3.3-LMT-K-712-01-0016, (2017–2021). **Investigator**.

2. Research Council of Lithuania. “Investigation of factors limiting the spread of avian haemosporidian infections”. Award No S-MIP-20-25, (2020–2022). **Investigator**.
3. European Research Council (ERC Advanced Grant). “Immunity in Ecology and Evolution: 'Hidden' costs of disease, immune function and their consequences for Darwinian fitness”. Award No 742646, (2017-2021). **Investigator**.
4. Research Council of Lithuania. “Molecular diagnostics and epidemiology of neglected avian blood parasites”. Award No S-MIP-22-50, (2022-2025). **Investigator**.
5. Research Council of Lithuania. “Natural anti-α-Gal antibodies and the protection against avian malaria”. Award No S-MIP-22-52, (2022-2025). **Investigator**.
6. Research Council of Lithuania. “The study of experimental avian malaria co-infections in bloodsucking vectors“. Award No LMT Nr. S-MIP-24-85, (2024-2027). **Investigator**.

Internships and training

2020-01-13 – 2020-07-10. Internship at Lund University (Lund, Sweden) under ERASMUS+ program. A participation of 10 weeks course of Molecular ecology and evolution. The purpose of the internship at Lund University Molecular Ecology and Evolution laboratory was to learn the application and development of qPCR methods for haemosporidian parasite studies.
2021-09-14 – 2021-10-13. Internship at National Research Institute for Agriculture, Food and Environment (Paris, France). The purpose of the internship was to learn new methods used in research: analysis of sequenced genomic data using bioinformatic programs
2023-06-12 – 2023-10-11. Internship at National Research Institute for Agriculture, Food and Environment (Paris, France) under ERASMUS+ program. The purpose of the internship was to learn application of serological methods, improve the skills in bioinformatic analysis.
2023-06-26 – 2023-06-27. Training school on Vector Microbiome of CA21170 Prevention, anticipation and mitigation of tick-borne disease risk applying the DAMA protocol (PRAGMATICK)”. Maisons-Alfort, France.
2024-04-02 – 2024-04-08. The Bioinformatics of Microbial Single Cells Workshop at Bigelow Laboratory for Ocean Sciences, East Boothbay, Maine, USA.

External professional activities:

Member of the Scandinavian – Baltic Society for Parasitology (2019–present).

Justė Aželytė

PAPER I

Exploring the Ecological Implications of Microbiota Diversity in Birds: Natural Barriers Against Avian Malaria

Palinauskas V., Mateos-Hernandez L., Wu-Chuang A., de la Fuente J., **Aželytė J.**, Obregon D., Cabezas-Cruz A.
Frontiers Immunology, 2022, 13:807682
DOI 10.3389/fimmu.2022.807682

frontiers in Immunology

HYPOTHESIS AND THEORY
published: 17 February 2022
doi: 10.3389/fimmu.2022.807682

Exploring the Ecological Implications of Microbiota Diversity in Birds: Natural Barriers Against Avian Malaria

Vaidas Palinauskas[1†], Lourdes Mateos-Hernandez[2†], Alejandra Wu-Chuang[2], José de la Fuente[3,4], Justė Aželytė[1], Dasiel Obregon[5] and Alejandro Cabezas-Cruz[2*]*

[1] Nature Research Centre, Akademijos 2, Vilnius, Lithuania, [2] ANSES, INRAE, Ecole Nationale Vétérinaire d'Alfort, UMR BIPAR, Laboratoire de Santé Animale, Maisons-Alfort, France, [3] SaBio, Instituto de Investigación en Recursos Cinegéticos IREC-CSIC-UCLM-JCCM, Ciudad Real, Spain, [4] Department of Veterinary Pathobiology, Center for Veterinary Health Sciences, Oklahoma State University, Stillwater, OK, United States, [5] School of Environmental Sciences, University of Guelph, Guelph, ON, Canada

OPEN ACCESS

Edited by:
Kézia K. G. Scopel, Juiz de Fora Federal University, Brazil

Reviewed by:
Philippe Christe, University of Lausanne, Switzerland
Erika Martins Braga, Federal University of Minas Gerais, Brazil

***Correspondence:**
Alejandro Cabezas-Cruz
alejandro.cabezas@vet-alfort.fr
Vaidas Palinauskas
palinauskas@gmail.com

†These authors have contributed equally to this work

Specialty section:
This article was submitted to Parasite Immunology, a section of the journal Frontiers in Immunology

Received: *02 November 2021*
Accepted: *28 January 2022*
Published: *17 February 2022*

Citation:
Palinauskas V, Mateos-Hernandez L, Wu-Chuang A, de la Fuente J, Aželytė J, Obregon D and Cabezas-Cruz A (2022) Exploring the Ecological Implications of Microbiota Diversity in Birds: Natural Barriers Against Avian Malaria. Front. Immunol. 13:807682. doi: 10.3389/fimmu.2022.807682

Natural antibodies (Abs), produced in response to bacterial gut microbiota, drive resistance to infection in vertebrates. In natural systems, gut microbiota diversity is expected to shape the spectrum of natural Abs and resistance to parasites. This hypothesis has not been empirically tested. In this 'Hypothesis and Theory' paper, we propose that enteric microbiota diversity shapes the immune response to the carbohydrate α-Gal and resistance to avian malaria. We further propose that anti-α-Gal Abs are transmitted from mother to eggs for early malaria protection in chicks. Microbiota modulation by anti-α-Gal Abs is also proposed as a mechanism favoring the early colonization of bacterial taxa with α1,3-galactosyltransferase (α1,3GT) activity in the bird gut. Our preliminary data shows that bacterial α1,3GT genes are widely distributed in the gut microbiome of wild and domestic birds. We also showed that experimental infection with the avian malaria parasite *P. relictum* induces anti-α-Gal Abs in bird sera. The bird-malaria-microbiota system allows combining field studies with infection and transmission experiments in laboratory animals to test the association between microbiota composition, anti-α-Gal Abs, and malaria infection in natural populations of wild birds. Understanding how the gut microbiome influences resistance to malaria can bring insights on how these mechanisms influence the prevalence of malaria parasites in juvenile birds and shape the host population dynamics.

Keywords: anti-α-Gal antibodies, avian malaria, gut microbiota, transgenerational immunity, protective immunity

INTRODUCTION

Understanding the mechanisms involved in host-microbiota interactions is important as beneficial microbes can influence the health, fitness, and immunity of vertebrate hosts (1), and although less known, host microbiota can also facilitate pathogen infection (2). One important contribution of microbiota to immunity is the induction of natural antibodies (Abs). These Abs can target glycans on the

surface of pathogens, protecting the host from infection. For example, the presence of Gram-negative bacteria expressing the disaccharide Galα1-3Gal (α-Gal) in gut microbiota of animals that do not produce endogenous α-Gal induces the production of natural Abs specific to the glycan (3). Humans, fish and birds lack the enzymatic machinery necessary for α-Gal synthesis (3), which allows for the production of anti-α-Gal Abs (4–8). The broad distribution of bacterial α-1,3-galactosyltransferase (α1,3GT) genes in the human gut microbiome (9), and the high levels of circulating immunoglobulin (Ig) M and IgG directed against the glycan in healthy adults further suggest a link between microbiota and humoral immunity (10).

High levels of natural anti-α-Gal IgM are associated with protection from *Plasmodium falciparum* infection in humans (11, 12). In addition to mosquito-borne *Plasmodium* spp (11)., other vector-borne pathogens such as *Borrelia* spp (13)., transmitted by ticks; *Leishmania* spp (14)., transmitted by sandflies; and *Trypanosoma* spp (15–17)., transmitted by triatomes; express α-Gal on their surface. Induction of high levels of anti-α-Gal Abs by α-Gal immunization protects against experimental infection by these pathogens in mice (8). Oral administration of bacteria expressing high levels of α-Gal recapitulates the etiology of natural anti-α-Gal Ab production in α1,3GT-deficient mice (do not produce endogenous α-Gal) (11), zebrafish (18) and turkeys (7). This microbiota manipulation also induces protective immunity, as gut colonization of α1,3GT-deficient mice by *Escherichia coli* O86: B7 elicited a protective anti-α-Gal IgM response that significantly reduced malaria transmission (11). Furthermore, anti-α-Gal IgM triggered complement-mediated lysis of *Plasmodium* sporozoites associated with sterile protection against murine malaria (11).

The ecological impact of gut microbiota diversity and its association with anti-α-Gal immunity remains to be tested. Birds represent over 30% of known tetrapod diversity with 10 425 described species and more than 20 000 subspecies varieties (19). Their different migratory behaviors, habitats and diets influence microbiota composition diversity (20, 21), which in turn may have large impact on resistance to parasites (22). However, the mechanisms driving bird-parasite-microbiota interactions remain poorly characterized. There are more than 50 avian malaria species and new species are discovered every year (23). Moreover, based on mitochondrial genome analysis of avian *Plasmodium* spp., there might be many more species than previously thought (24). Field and experimental studies reveal that the host specificity of these pathogens varies from strict specialists infecting a single bird species to generalists infecting more than 300 distantly-related bird species (23, 24). Notably, avian malaria infections are common in some bird species, but not in others (25), and the causative factors driving these differences are not clear. In this 'Hypothesis and Theory' paper, we propose to use the bird-malaria-microbiota system to dissect the ecological implications of gut microbiota diversity to anti-α-Gal response, resistance to *Plasmodium* infection and the inter-generational effect of such microbiota-mediated immunity. Within the text, "microbiome" refers to the microorganisms and their metagenome (i.e., when the genes are known and/or are being referred to intentionally) whereas "microbiota" refers only to the microbes themselves (i.e., when the genes are unknown and/or there is no intention to refer to all or any of them in particular).

THE PUZZLING ORIGIN OF THE GLYCAN α-GAL IN *PLASMODIUM* SPP.

Enzymatic glycosylation of proteins and lipids is a common and important biological process in prokaryotic and eukaryotic organisms (26). In general, the identification of genes encoding for enzymes with α1,3GT activity is challenging for several reasons. First, prokaryotic and eukaryotic α1,3GT genes and encoded proteins share little structural homology (26–30). Second, within defined taxonomic groups (i.e., prokaryotic), the α1,3GT diversity is very high with some cases in which single bacterial species have several α1,3GT enzymes translated from different, non-related, genes (9). Third, α1,3GT from different eukaryotic lineages do not share immediate common ancestors. For example, α1,3GT encoded by the gene *ggta1* is responsible for the production of the α-Gal epitope in non-primate mammals, Lemurs and New World monkeys (10). However, no genetic trace of *ggta1* could be found in the genomes of fungi (29), arthropods (e.g., ticks (27) and mosquitoes (31) or Apicomplexan (e.g., *Plasmodium*) (31) organisms expressing α-Gal. This suggests that the capacity for α-Gal synthesis have evolved independently, and multiple times, during prokaryotic and eukaryotic evolution.

Empirical research using *Plasmodium berghei* ANKA and α1,3GT-deficient mice revealed that anti-α-Gal Abs target *Plasmodium* sporozoites for complement-mediated cytotoxicity in the skin after transmission by *Anopheles* mosquitoes (11). This complement-mediated immune reaction prevented sporozoites from reaching host hepatocytes and complete the next step of the parasitic life cycle in the liver. Specific binding of anti-α-Gal Abs requires the presence of α-Gal on the surface of *Plasmodium* sporozoites. However, the origin of *Plasmodium* α-Gal has not been completely elucidated. Particularly, it is not yet clear whether the glycan α-Gal is: (*i*) directly synthesized by the parasite, or (*ii*) synthesized by the vector and metabolically incorporated as a terminal group in glycoproteins and/or glycolipids of the parasite. In the study by Yilmaz et al. (11), the salivary glands of *Plasmodium*-infected *Anopheles* mosquitoes contained α-Gal, but low levels of this glycan were detected also in the salivary glands of uninfected mosquitoes. Furthermore, α-Gal was identified on the surface of sporozoites of the human pathogen *P. falciparum* 3D7, and of the rodent pathogens *P. berghei* ANKA and *Plasmodium yoelii* 17XNL (11). This raised the possibility that both, *Plasmodium* parasites and mosquito vectors, have the enzymatic machinery for endogenous α-Gal synthesis.

A recent study based on protein similarity analysis indicated the presence of homologous to three *Ixodes scapularis* proteins with α1,3GT activity in two mosquito vectors, *Aedes aegypti* and *Anopheles gambiae* (31). However, the genus *Plasmodium* lacked proteins homologous to the three *I. scapularis* proteins with α1,3GT activity (31). Empirical evidences support that the genes

identified in *I. scapularis*, *b4galt7*, *a4galt-1* and *a4galt-2*, have direct α-Gal-synthetizing activity and/or participate in the α-Gal synthesis pathway in ticks (27). First, heterologous expression of these genes in bacterial and human α-Gal-negative cells induced *de novo* synthesis of α-Gal. Second, transcriptional upregulation of the three genes in fed ticks was associated with increased α-Gal levels in tick tissues. Third, RNA interference-mediated silencing of the three genes was associated with reduction of α-Gal levels in tick tissues. Fourth, simultaneous silencing of the three genes reduced the α-Gal levels in the tick cell line IRE/CTVM20 (27). It is important to mention that the α1,3GT activity of mosquito homologous have not been experimentally tested. However, recent studies further suggest that *Plasmodium* and mosquitoes have both the capacity to produce α-Gal epitopes (32). Disruption of α-Gal production in mosquitoes was not associated with significant reduction of α-Gal levels in *Plasmodium* (32).

Our preliminary data shows the presence of α-Gal in protein extracts from three *Plasmodium* species, *P. ashfordi* (genetic lineage GRW2), *P. relictum* (SGS1) and *P. homocircumflexum* (COLL4), obtained from experimentally infected passerine birds, Eurasian siskins (*Carduelis spinus*) (**Figure 1**). Natural anti-α-Gal Abs have variable affinity for different α-Gal-related antigens, including Galα1-3Gal disaccharide and Galα1-3Galβ1-4GlcNAc trisaccharide. To test the immunogenicity of avian *Plasmodium* α-Gal, sera levels of IgY against Galα1-3Gal and Galα1-3Galβ1-4GlcNAc were measured by ELISA in canaries (*Serinus canaria domestica*) experimentally infected with *P. homocircumflexum* or *P. relictum*. The levels of circulating IgY against Galα1-3Gal and Galα1-3Galβ1-4GlcNAc did not change over time in birds infected with *P. homocircumflexum* (**Figure 2A**). In contrast, the levels of circulating IgY against Galα1-3Gal increased significantly at day 38 post infection with *P. relictum*, while the levels of Galα1-3Galβ1-4GlcNAc did not change (**Figure 2B**). These preliminary results showed the presence of α-Gal on avian malaria parasites, and demonstrated the immunogenicity of the *P. relictum* glycan in birds. It is thus plausible that anti-α-Gal IgY induced by blood stages of *P. relictum* mediate the opsonization (i.e., an immune process which uses opsonins such as Abs to tag foreign pathogens for elimination by phagocytes.) of blood parasitic stages. What caused the absence of anti-α-Gal Abs response in *P. homocircumflexum*-infected birds is unclear to us. It can be related with very low levels of the glycan in *P. homocircumflexum*. It is noteworthy that among the three *Plasmodium* species tested, *P. homocircumflexum* has the lowest levels of α-Gal (**Figure 1**).

THE GUT MICROBIOTA AND *PLASMODIUM* INFECTION

Studies on avian gut microbiota are scarce (33). According to Grond et al. (33), from 1980 to 2017 the number of published studies on mammals (including humans), poultry and wild birds microbiota were 16200, 1200 and 32, respectively. The underrepresentation of wild bird microbiota studies in the literature opens a gap in our understanding of the contribution of microbiota to host health, fitness, and immunity in metazoans. Most avian microbiota studies have focused on economically important species such as chicken and turkey (19). In wild birds, the research has focused on the identification of extrinsic and intrinsic factors affecting gut microbiota composition. Next-generation sequence analyses in different bird species have uncovered the diversity of microbial communities in gut microbiota (20). Core microbiota in avian enteric tract included the bacterial taxa Proteobacteria, Firmicutes, Fusobacteria, Actinobacteria and Bacteroidetes (20, 34). The first meta-analysis of the avian gut microbiota revealed that the dominant factor contributing to the composition of gut microbiota in wild birds is host taxonomic category (35). However, Grond et al. (34) showed that local environment has a

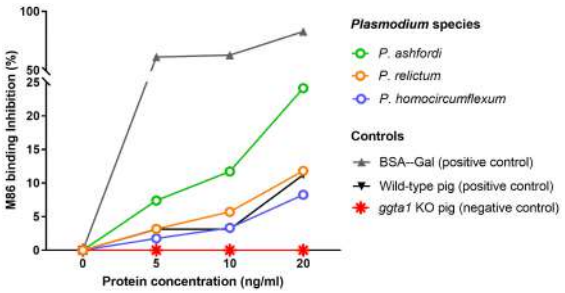

FIGURE 1 | Presence of α-Gal in avian *Plasmodium* species. The levels of α-Gal in protein extracts from different *Plasmodium* species, *P. ashfordi* (GRW2), *P. relictum* (SGS1) and *P. homocircumflexum* (COLL4), are presented. The inhibition of monoclonal mouse anti-α-Gal antibody (mAb) M86 binding to α-Gal-BSA was measured by inhibition ELISA after incubating the mAb M86 with increasing concentrations of total proteins (5, 10 and 20 ng/ml) extracted from each *Plasmodium* species. Proteins extracted from wild-type and *ggta1* (α1,3GT) knockout (KO) *Sus scrofa* (pigs) kidney samples were used as positive and negative controls, respectively. α-Gal-BSA was used as an additional positive control. Results were expressed as percentage of inhibition (%). Experimental procedures are available in **Supplementary Material S1**.

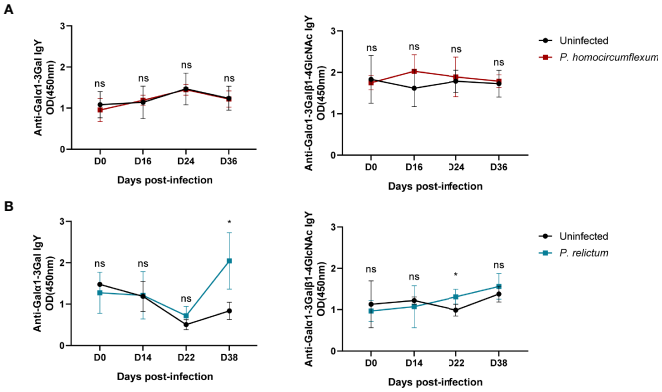

FIGURE 2 | Anti-α-Gal Abs in sera samples of canaries experimentally infected with *Plasmodium* species. The levels of IgY against Galα1-3Gal and Galα1-3Galβ1-4GlcNAc in sera of canaries infected with *P. homocircumflexum* (COLL4) **(A)** or *P. relictum* (SGS1) **(B)** were measured by ELISA. The levels of anti-α-Gal IgY between groups were compared by one-way ANOVA with Dunnett's multiple comparison test applied for individual comparisons (*$p < 0.05$, ns: not significant, 1 experiment for each *Plasmodium* species, n = 3 to 5 per group and three technical replicates per sample). Experimental procedures are available in **Supplementary Material S1**.

large influence on gut microbiota composition of Arctic-breeding shorebirds. Another study on Brown-headed Cowbirds (*Molothrus ater*) showed that environmental factors, rather than genetics, influence passerine gut microbiota composition (36). The impact of other factors such as diet, probiotic treatment, kinship and captive rearing conditions have been assessed in poultry, but these may not be representative of wild life species (19). Ordination analyses of avian microbiota revealed that gastrointestinal tract microbial communities group according to sampling region (i.e., crop, caeca, cloaca, and fecal) (35), as in reptiles (37) and mammals (38). Parasite infection may also influence bird microbiota composition. For example, Coccidiosis, caused by *Eimeria* spp. infection in poultry affects the composition and integrity of gut microbiota, which in turn elevated susceptibility to other diseases (39).

A recent study by Videvall et al. (40) explored the impact of *Plasmodium* infection of the uropygial gland microbiota of house sparrows. Results showed differences in the abundance of certain bacterial genera according to *Plasmodium* infection status. These results suggest a possible interaction between infection and microbiota. Some microorganisms have been identified as potential symbionts in the uropygial gland (41). Based on functional predictions using 16S rRNA sequences, uropygial gland bacteria were suggested to produce metabolites with antimicrobial properties, such as terpenes (41). Whether microbes within the uropygial gland or intestinal tract play protective roles against avian malaria infection in birds is currently unknown.

However, strong evidence suggests a link between mammalian gut microbiota and human and murine malaria infection. Villarino et al. (42) found that differences in the gut microbiota determined severity of malaria caused by *P. yoelii* infection in mice. Further microbiota composition analysis revealed increased abundance of *Lactobacillus* and *Bifidobacterium* in resistant mice (42). In a follow up study, the authors tested whether synthesis of short-chain fatty acids (SCFAs), a well-studied mechanism by which the intestinal microbiota exerts an effect on host health explained the differences in susceptibility to malaria (43). However, the presence of fecal SCFAs did not explain differential susceptibility to *P. yoelli* infection (43). Microbial metabolites could influence the immune response to infection or alter parasite growth, as demonstrated by the impairment of *Salmonella* growth by the presence of propionate produce by Bacteroides (44). To gain further insight into the mechanism of resistance, another group determined the combined host and microflora metabolome and metatranscriptome (45). Differences in metabolite pools were associated with malaria resistance or susceptibility in mice (45). However, the relevance of identified metabolites for malaria infection, microbial community activity, or host response remains elusive (45). Another study demonstrated that both malaria infection severity and pregnancy outcome can by influenced by modulating the composition of the gut microbiota in an outbred mouse model for malaria in pregnancy (46).

Although the mechanism of microbiota-mediated resistance to murine malaria has not been elucidated, additional evidence further supports a protective role of host microbiota against malaria infection. For example, gut microbiota composition is very different between malaria endemic and non-endemic countries (47). Microbiota composition differences can be due to variation in diet, but also to host–pathogen adaptations, in

which individual from endemic countries acquired, maintain and develop a gut microbiota that may influence protection to malaria transmission and/or tolerance to severe malaria (48). In agreement with this idea, observational studies from malaria-endemic regions show correlations between the composition of gut microbiota and lower risk of malaria infection (26).

It is important to mention that in the studies mentioned above by Villarino et al. (42), Chakravarty et al. (43) and Stough et al. (45), a mechanism mediated by anti-α-Gal Abs was rule out, as the experiments were carried out in wild-type mice that express α-Gal and cannot produce anti-α-Gal Abs. This suggests that different mechanisms may account for malaria resistance in animals that produce endogenous α-Gal (e.g., wild-type mice) and those that do not produce α-Gal (e.g., humans and birds). An interesting observation is that bacteria of the family Enterobacteriaceae (e.g., *Escherichia-Shigella*) and the genus *Bifidobacterium* were found in the microbiota of Malian children with lower risk of *P. falciparum* infection (49). The protective mechanism mediated by *Bifidobacterium* might be activated in animals that produce (e.g., wild-type mice), or not (e.g., humans), endogenous α-Gal. However, the presence of Enterobacteriaceae expressing α-Gal may be an additional protective barrier against malaria infection in humans and birds.

ENTEROBACTERIACEAE, A RICH SOURCE OF α1,3GT GENES IN HUMAN AND BIRD MICROBIOTA

A recent study found 193 species and strains of bacteria containing α1,3GT genes in the human gut microbiota (9). Bacteria of the families Enterobacteriaceae (genus *Escherichia-Shigella*), Pasteurellaceae (genus *Haemophilus*), Lactobacillaceae (genera *Pediococcus, Lactobacillus*) are among those containing α1,3GT genes in the human gut microbiota. Among the α1,3GT genes identified in the human microbiome are the *gspA*-general secretion pathway protein A (accession K02450), *waaL*, *rfaL*-O-antigen ligase (K02847); *waaO*, *rfaI*-UDP-glucose: (glucosyl) LPS alpha-1,3-glucosyltransferase (K03275); *waaJ*, *rfaJ*, UDP-glucose: (galactosyl) LPS alpha-1,2-glucosyltransferase (K03279); *waaR*, *waaT*, *rfaJ*-UDP-glucose/galactose: (glucosyl) LPS alpha-1,2-glucosyl/galactosyltransferase (K03276) and *waaI*, *rfaI*-UDP-D-galactose: (glucosyl) LPS alpha-1,3-D-galactosyltransferase (K03278).

We hypothesize that different migratory behaviors (i.e., non-migrating and short or long-distance migrants), diets (i.e., insectivorous and seedeaters) and ecology conditions might influence gut microbiota composition, as well as the distribution of α1,3GT genes in bacterial microbiota of birds. Here we predicted the presence of α1,3GT genes (i.e., K02450, K02847, K03275, K03279, K03276, K03278) in the microbiomes from various wild bird species representing diverse diets and habitats. These included the Japanese quail (*Coturnix coturnix*), fairy prion (*Pachyptila turtur*), common diving petrel (*Pelecanoides urinatrix*), barn swallow (*Hirundo rustica*), gulls (*Larus delawarensis*), black vulture (*Coragyps atratus*), turkey vulture (*Cathartes aura*), and two breed of poultry (*Gallus gallus domesticus*), white leghorn and brown chicken. The results showed that α1,3GT genes were distributed in more than 140 bacterial taxa in the microbiome of the analyzed birds. Not all taxa contributed equally to the distribution of α1,3GT genes, as various of these taxa had very low abundance in the microbiomes and thus contributed only marginally to α1,3GT genes. The set of taxa with the highest abundance and contribution (~ 20% of the total number of taxa) was selected for further analysis. All the α1,3GT genes were present in all the bird species under study, except for *P. turtur* and *P. urinatrix* in which only the genes K03278 and K02450 were found, respectively (**Figure 3**). Among these genes, the most frequent were K03275 and K02847. Notably, the taxa with the highest contribution to α1,3GT genes in these birds was Enterobacteriaceae (genus *Escherichia-Shigella*, **Figure 3**), as in the human microbiome (9). Other bacterial genera such as *Herbaspirillum, Megamonas* and *Serratia* also contain α1,3GT genes (**Figure 3**). This preliminary data suggests that birds are an ideal model to test the relation between gut microbiota, *Plasmodium* infection and anti-α-Gal immunity. Based on the above evidence, a malaria blocking mechanism mediated by anti-α-Gal IgM in birds is proposed (**Figure 4**).

HOST GUT MICROBIOTA MANIPULATION AND ANTI-α-GAL IMMUNE RESPONSE

A recent study demonstrated for the first time that modulation of anti-α-Gal immunity using gut microbiota manipulation protects birds against avian aspergillosis, caused by experimental infection with *Aspergillus fumigatus*, a pathogen expressing α-Gal (7). Specifically, oral administration of *E. coli* O86:B7 increased the levels of IgY against the disaccharide Galα1-3Gal, along with a decrease in the levels of IgY against the trisaccharide Galα1-3Galβ1-4GlcNAc in sera of treated turkeys. Oral administration of *E. coli* O86:B7 was also associated with decreased anti-α-Gal IgA in lungs compared with non-treated turkeys. Interestingly, decreased levels of anti-α-Gal IgA were accompanied by a reduction in the occurrence of lung granulomas, which is associated with acute aspergillosis in turkeys. These results suggest a crosstalk mechanism in birds by which the gut microbiota modulates the immune response in the lungs (50). In this infection model (i.e., intratracheal infectious challenge with *A. fumigatus*) (7), the mechanism of protection against avian aspergillosis does not seem mediated by increased anti-Galα1-3Gal IgY in sera. However, increased sera levels of anti-Galα1-3Gal IgY induced by oral administration of *E. coli* O86:B7 may be relevant to prevent avian malaria transmission by mosquitoes.

Other bacterial species such as *Aeromonas veronii* and *Pseudomonas entomophila* have been used to modulate the microbiota and induced anti-α-Gal immunity (18). Recently, Pacheco et al. (18) reported that native *A. veronii* and *P. entomophila* bacteria isolated from the zebrafish gut have high content of α-Gal. Fish fed with commercial feed coated with *A. veronii* or *P. entomophila* showed increased anti-α-Gal IgM levels. Anti-α-Gal IgM response in the *P. entomophila* group was

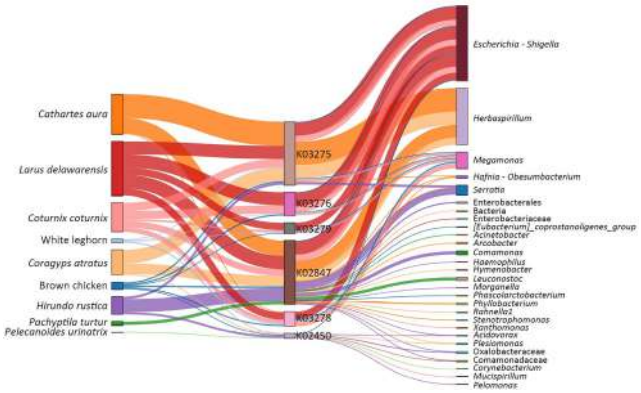

FIGURE 3 | Contribution of commensal bacteria to α1,3GT genes in the microbiome of wild birds and poultry. Alluvial plot showing the presence α1,3GT genes (i.e. K02450, K02847, K03275, K03279, K03276, K03278) in the microbiome from various avian host. The bacterial genera harboring these genes in each host are also displayed. The presence and abundance of α1,3GT genes was inferred from the 16S rRNA data using the bioinformatics pipeline PICRUSt2 for metagenome prediction. The *α1,3GT* genes were annotated based on KEGG orthologs (KO) database as reference. K02450: *gspA*, general secretion pathway protein A; K02847: waaL, rfaL, O-antigen ligase [EC:2.4.1.-]; K03275: *waaO*, *rfaI*, UDP-glucose:(glucosyl)LPS alpha-1,3-glucosyltransferase [EC:2.4.1.-]; K03279: waaJ, rfaJ, UDP-glucose:(galactosyl)LPS alpha-1,2-glucosyltransferase [EC:2.4.1.58]; K03276: *waaR*, *waaT*, *rfaJ*, UDP-glucose/galactose:(glucosyl)LPS alpha-1,2-glucosyl/galactosyltransferase [EC:2.4.1.-]; K03278: *waaI*, *rfaI*, UDP-D-galactose:(glucosyl)LPS alpha-1,3-D-galactosyltransferase [EC:2.4.1.44]. Node segments by columns represent host (First column), functional genes (Second column) and bacterial taxa (Third column), respectively. Node size is proportional to the abundance of contributing host or bacterial taxa or genes. The cords indicate the connections between host, the α1,3GT genes and taxa. The contribution of each taxon to different α1,3GT genes is represented proportionally by the size of cords. Experimental procedures are available in **Supplementary Material S1**.

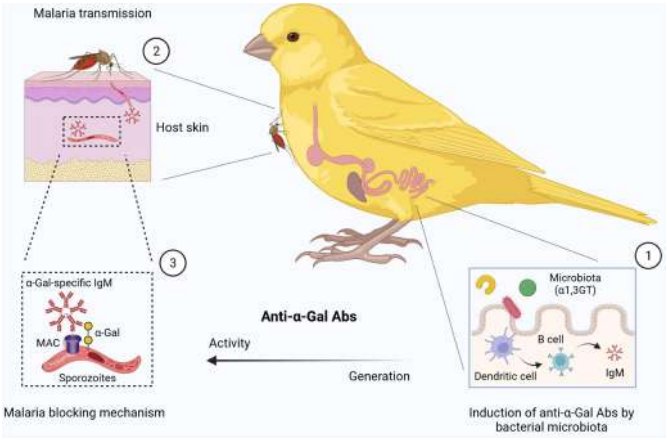

FIGURE 4 | Proposed malaria blocking mechanism mediated by gut microbiota in birds (1). The α-Gal-expressing microbes cause the stimulation of B cells to produce anti-α-gal IgM. The structure of the α-Gal glycan is similar in microbiota and *Plasmodium* sporozoite surface. (2) *Plasmodium* sporozoite transmission by mosquitoes, (3) can be blocked *via* a complement-mediated lysis of sporozoites in the skin. MAC, Membrane Attack Complex. Figure created with BioRender.com.

associated with a significant reduction in mycobacterial infection, caused by *Mycobacterium marinum* (18). These results provide evidence that various bacteria species with high α-Gal content can be identified in the gut microbiota of animals lacking endogenous α-Gal. Probiotic treatment in zebrafish was also associated with significant changes in the beta diversity and taxa abundance in fish microbiota (18). Furthermore, the abundance of some taxa was negatively correlated with the anti-α-Gal IgM levels, suggesting a role of anti-α-Gal Abs in modulating fish gut microbiota, as reported for mammalian gut microbiota (51). Another interesting insight of the zebrafish study is that gene expression analysis in probiotic-treated fish challenged with *M. marinum* suggests that protective mechanism associated with anti-α-Gal immunity can go beyond anti-α-Gal Abs-mediated control of mycobacteria (18). Protection was also associated with B-cell maturation, induced innate immune responses and beneficial effects on nutrient metabolism and oxidative stress (18). The results of this trial in fish support immune and metabolic implications of α-Gal-mediated immunity, beyond induction of anti-α-Gal Abs. It remains to be tested whether α-Gal-mediated immunity induced by oral administration of *E. coli* O86:B7, or other bacteria expressing α-Gal, produce malaria resistance associated with broad metabolic and immune effects in birds.

CROSSTALK BETWEEN HOST AND VECTOR GUT MICROBIOTA

The presence and distribution of α1,3GT genes in bacterial microbiota suggests the production of natural anti-α-Gal Abs in wild birds. Can the anti-α-Gal Abs bind and/or lyse bacteria expressing α-Gal in the mosquito microbiota? What impact would mosquito microbiota modulation by anti-α-Gal Abs have on mosquito fitness and/or malaria transmission? Host antibodies taken in the blood meal can target pathogens and bacterial microbiota within hematophagous arthropods (52). Functional host antibodies have been shown to interact with symbionts in *Rhodnius prolixus* (53) and *Glossina morsitans* (54) as well as with bacterial microbiota in mosquitoes (55) and ticks (56, 57). Recent research showed that α1,3GT genes are broadly distributed in tick bacterial microbiota (56). Immunization with a tick microbiota Enterobacteriaceae, caused significant mortality of engorging ticks (56). Anti-α-Gal IgM and IgG were associated with a mean mortality of approximately 45% in ticks fed on α1,3GT-deficient mice (56). Anti-microbiota vaccine directed at Enterobacteriaceae in the microbiota of *I. scapularis* disrupted both the makeup and functions of the microbiome and decreased pathways central to lysine degradation (57). Interestingly, Enterobacteriaceae (i.e., *Escherichia-Shigella*) is shared by the microbiota of ticks and mosquitoes, but not of sandflies (58). Anti-microbiota vaccines are a microbiome manipulation tool for the induction of infection-refractory states in the vector microbiome (52). The evidence suggests that ingestion of avian anti-α-Gal Abs with the blood meal could target mosquito microbiota expressing α-Gal (e.g., Enterobacteriaceae) with a potential impact on *Plasmodium* colonization of mosquito tissues.

FROM MOTHER TO OFFSPRING: TRANSGENERATIONAL *VS.* INTER-GENERATIONAL IMMUNE MECHANISMS

Evolution of complex traits such as host resistance to pathogen infection can be linked to phenotypic variation due to 'transgenerational' or 'inter-generational' immune mechanisms (59, 60). 'Transgenerational' here is defined as transmission across generations (i.e., from grandparents to a grandchild), without involving direct exposure to the environmental stimulus that triggered the primal host response (60, 61). Unequivocal transgenerational transmission of an adult phenotype through the germ-line requires assessment of the F3 generation for embryonic exposure, and F2 generation for postnatal exposure (60). 'Inter-generational' represents the transmission of traits from one generation to the next (i.e., from mother to offspring). Phenotypic traits acquired by parents can be transmitted by transgenerational or inter-generational epigenetic inheritance (59, 61).

Epigenetic inheritance involves stimuli-triggered changes in gene expression due to processes that arise independent of changes in the underlying DNA sequence. Some of these processes include DNA methylation (62), histone modifications and/or chromatin-remodeling proteins (63). Epigenetic inheritance remains poorly explored in birds (64). However, some transgenerational epigenetic mechanisms have been described in birds (64, 65). For example, the regulation of immunoglobulin gene expression in the offspring of broiler hens under different environmental stimulus (i.e., unpredictable or predictable light regimens) was linked to epigenetic mechanisms (65, 66). These genes are involved in both neural development (67) and immunity, and their regulation suggests that immune parameters can be epigenetically transferred to the next generation (66). Although the epigenetic markers associated with this trait in birds remain to be identified. In addition to epigenetic inheritance, maternal antibodies have also been described as non-genetic, information-bearing molecules that transfer information about the immunologically relevant environment (e.g., exposure to pathogens) gathered by the mother to her offspring (65). The hypothesis of transfer of anti-α-Gal IgY with anti-malaria effect in birds can be tested without accounting for transgenerational epigenetic mechanisms.

INTER-GENERATIONAL TRANSMISSION AND AVIAN MICROBIOTA REPROGRAMMING BY ANTI-α-GAL ABS

Several studies show that the inter-generational transfer of maternal Abs provides humoral immune defense against pathogens in eggs and early-life offspring. This mechanism is crucial as endogenous production of Abs in chicks occur only 10-14 days post-hatching (68). For example, Grindstaff et al. (69) reported that the offspring from female pied flycatchers

(*Ficedula hypoleuca*) injected with *Salmonella typhimurium* lipopolysaccharide (LPS) had higher Abs levels compared to offspring from pied flycatchers not injected to this bacterial antigen. Kittiwakes (*Rissa tridactyla*) mothers naturally exposed to the tick-borne bacteria *Borrelia burgdorferi* transfer anti-*Borrelia* Abs to their eggs and offspring (70, 71). In addition, the levels of anti-*Borrelia* Abs of kittiwake chicks at 10 and 20 days of age were higher when 5 days old had significantly higher anti-*Borrelia* Ab titres (72). High anti-*Borrelia* Ab levels in 5-day-old chicks were presumably transferred from the mother (72). These results suggest that maternal exposure to pathogens, including vector-borne pathogens such as *Borrelia* or *Plasmodium*, can enhance the humoral immunity of early-life offspring.

The levels of anti-α-Gal IgY in eggs are variable (73, 74, **Figure 5A**), and they are more abundant in egg yolks than in egg whites (73, 74, **Figure 5B**). Anti-α-Gal IgY isolated from birds are able to bind α-Gal antigens in mammal tissues. Particularly, binding of avian anti-α-Gal Abs block the binding of human anti-α-Gal to xenograft endothelial cells (75, 76). Avian anti-α-Gal also block human blood complement activation and antibody-dependent cell-mediated lysis mechanisms that are responsible of hyperacute rejections in xenografts (75, 76). This shows the functionality of avian anti-α-Gal Abs. Whether anti-α-Gal Abs transmitted from the mother to egg to chick, have protective functions against malaria or other infectious diseases remains an open question.

Besides the preferential presence of IgY in egg yolks, IgM and IgA are predominantly found in egg whites (77). Difference on the distribution of Abs in different egg compartments could be associated to their immunity role in different part of bird's body. While IgY is transported to the embryonic circulation, IgM and IgA are transferred to the gastrointestinal gut of developing chick, where they exert an important role in local immunity (77–80). IgA recognize bacteria in the gut microbiota (81–83) shaping the microbiota composition, and ecology, by limiting bacterial growth (84), or promoting bacterial interactions with the host, favoring bacterial retention, fitness, and colonization (85, 86). Removal of α1,3GT activity shaped the composition of the gut microbiota in mice (51). This occurred *via* an IgA-dependent mechanism, associated with targeting of α-Gal-expressing bacteria by IgA in mice (51). *Ggta1* deletion enhances microbiota-specific IgA responses without interfering with total IgA (51). Interestingly, the microbiota composition diverged between *ggta1*$^{+/+}$ and *ggta1*$^{-/-}$ mice in F3, F4 and F5 generations, suggesting that the α1,3GT-negative genotype per se alters microbiota composition (51), which suggest a transgenerational effect. Differences in avian anti-α-Gal IgA levels in eggs may be associated with variations in the gut microbiota of chicks, with reduced or increased abundance of defined subsets of species within bacterial families expressing α-Gal such as Enterobacteriaceae. IgA-mediated selection of commensal Enterobacteriaceae within the avian enteric microbiota would provide α1,3GT activity, high levels of circulating anti-α-Gal IgY and IgM with potential malarial resistance effects.

EXPLORING THE ECOLOGY OF THE BIRD-MALARIA-MICROBIOTA SYSTEM

To test our hypothesis, we propose firstly to perform an observational field study and sample wild bird species with different migratory behaviors, habitats and diets. Then, to measure the levels of natural anti-α-Gal Abs in different bird species and the presence of α-Gal in different *Plasmodium* spp. which can help elucidating whether an association exists between microbiome composition, the levels of anti-α-Gal Abs and *Plasmodium* infection within and between habitats and diets. The immunological analysis of samples obtained from wild birds

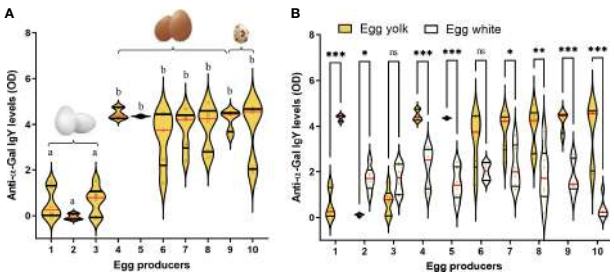

FIGURE 5 | Anti-α-Gal Abs in bird eggs. **(A)** Anti-α-Gal IgY levels were measured by indirect ELISA in egg yolks of ten individual eggs. **(B)** The anti-α-Gal IgY levels in egg yolks are shown together and those in egg whites from the same eggs. The eggs were purchased from three (1-3, Leghorn hens), six (4-9, ISA brown hens) and one (10, quails) different commercial vendors in France. The levels of anti-α-Gal IgY between groups were compared by one-way ANOVA with Dunnett's multiple comparison test applied for individual comparisons. Different letters in panel **(A)** indicate statistically significant differences ($p < 0.05$). In panel **(B)**, significant differences were denoted as $^{*}p < 0.05$, $^{**}p < 0.001$, $^{***}p < 0.0001$, ns: not significant. In both panels (n = 3 eggs per vendors and two technical replicates per sample). Experimental procedures are available in **Supplementary Material S1**.

will provide valuable information about the changes in anti-α-Gal Abs in infected birds within the same habitat and the impact of haemosporidian parasites on the immune system of different host species.

Our preliminary results from three different *Plasmodium* species gives a hint that different malarial parasites exhibit different levels of α-Gal in protein extracts. We expect that the α-Gal levels vary in *Plasmodium* species, especially from different, distantly related, subgenera, as these parasites would have some developmental differences during the life cycle and different life history traits (87). For instance, *P. ashfordi* (GRW2), a tropical generalist parasite infecting 21 different bird species (24) from *Novyella* subgenus, showed the highest level of α-Gal (**Figure 1**), while other two parasites exhibited relatively lower levels. Further analysis of different parasites with various specializations can help untangling the questions related to infectivity of avian malarial parasites.

FROM OBSERVATION TO ECOLOGY-INFORMED EXPERIMENTATION

To test the impact of anti-α-Gal Abs on the infectivity of malarial parasites, experimental studies with canaries, malarial parasites, gut bacteria and mosquitoes can be performed. We will use avian malarial parasite *P. relictum*, which is listed among the most invasive organisms in the world, infecting more than 300 bird species and is prevalent all around the world (88). *Culex pipiens* mosquitoes, the natural vector of *P. relictum*, will be used as a vector. *Escherichia coli* O86:B7 will be used as a bacterial source of α-Gal. This system will give us a unique possibility to experimentally test whether the gut microbiota bacteria expressing α-Gal increases anti-α-Gal Abs with an impact on the infectivity of malarial parasites (**Figure 6**). We predict that avian malaria can be affected by increased anti-α-Gal Abs when small numbers of sporozoites are inoculated. Partial infections of hosts with avian malarial parasites were reported in previous experimental studies (89, 90), where only some *Plasmodium* parasites developed parasitemia after mosquito bite. Factors which could influence the survival of sporozoites and therefore infectivity of the host were studied in many previous studies (91–94), however, none of them evaluated possible impact of the microbiota.

Experimental study with mothers having different α-Gal immunity status and comparison of offspring resistance to malarial pathogen, will allow assessment of the importance of the microbiome and anti-α-Gal Abs on infectivity of early life offspring with vector-borne pathogens. According to ecological studies, nestlings are less infected with haemosporidian parasites (25, 95, 96). However, in some species of diurnal raptors and owls, nestlings can be infected with *Leucocytozoon* spp. (species closely related to *Plasmodium*) up to 30% or even 70% (25). Apparently, some differences of nestling infectivity could be explained by the prolonged time stay of hatched nestlings in the nest (25). Experimental study with chaffinches showed that nestlings up to 12 days of age usually do not get infected with haemosporidian parasites, while birds of the same species of approximately one-month age exhibit up to 36% prevalence of haemosporidian infection (25). These differences probably could also be explained by inter-generational defense against pathogens, which is formed in offspring after immunization of mother before lying eggs (69). Our experimental system will enable to answer if the protective effect mediated by anti-α-Gal Abs against malaria can be passed from parents to offspring as a mechanism of inter-generational immunity and will help understanding the level of protective shield against infection diseases in birds.

DISCUSSION

The maintenance and functionality across time and space of the complex populations of microbes present in the animal intestine is poorly understood. Birds have a global distribution, being in every continent and exhibiting an extreme morphological (97) and ecological diversity (98). They have different diets, from strictly carrion to nectar feeders, with corresponding variation in intestinal morphology. Among other factors (20), bird microbiota composition can be influenced by host genetics (99), host phylogeny, location within the gut (35), diet (19, 35), and association with humans (35). Little is known, however, about how microbiota diversity under these factors influence susceptibility or resistance to avian diseases, or whether certain microbiota assemblies are under selective pressures by parasites in natural systems. The unparalleled genetic and rich phenotypic diversity of avian malaria pathogens, together with variations in infectivity of avian malarial parasites provides endless opportunities for exploring how bird microbiota contributes to the selective pressures under which hosts and parasites evolve. This makes bird-malaria-microbiota interactions a unique system to understand the impact of microbiota on animal ecology.

Evidence shows that bacterial communities in birds are inherited (19, 99), which suggest that microbiota composition can be under selection. The spread of highly virulent avian malaria infections across a bird population (100) could select for individuals carrying a protective microbiome. This is, if some microbiome composition decreases the susceptibility to malaria infection in birds, as in human and rodent malaria (see above 'The gut microbiota and *Plasmodium* infection'). The research results revised and summarized here, together with our preliminary data, supports the hypothesis that avian resistance to malaria is influenced by variations in α1,3GT activity in bird gut microbiota which in turn elicits anti-α-Gal Abs with anti-malaria activity. The evidence presented and discussed here further supports that gut microbiota triggers anti-α-Gal IgM and/or IgA, while blood stages of some *Plasmodium* species can triggered anti-α-Gal Abs IgY in birds (**Figure 7A**). These three isotypes of anti-α-Gal Abs can be transfer from mother to offspring (**Figure 7B**), providing malaria resistance mechanisms in a tissue-specific manner (**Figure 7C**).

The field and experimental studies proposed here can be used to test specific questions to demonstrate this hypothesis such as: (*i*) does the enteric microbiome of birds influences the resistance

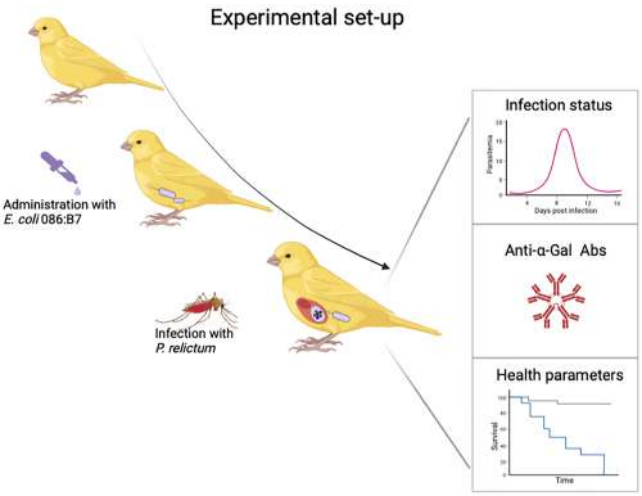

FIGURE 6 | Experimental set-up to test whether orally administered bacteria expressing high levels of α-Gal lead to increase of anti-α-Gal Abs and blocks transmission of *P. relictum*. Figure created with BioRender.com.

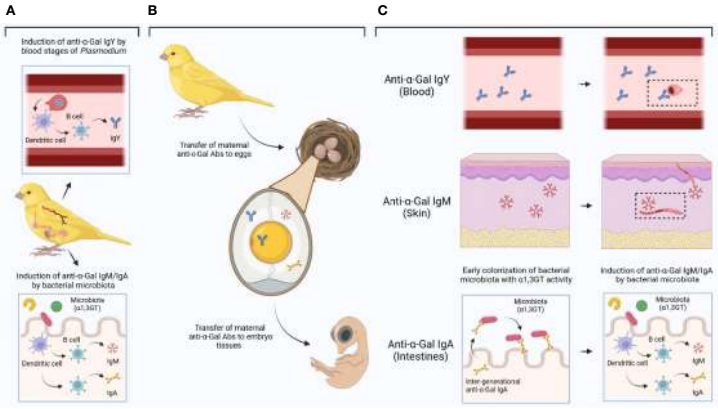

FIGURE 7 | Induction of anti-α-Gal Abs in birds and tissue-specific mechanisms of protection. **(A)** Blood stages of some malaria parasites induces anti-α-Gal IgY, while bacterial microbiota with α1,3GT activity could induce anti-α-Gal IgM/IgA. **(B)** Anti-α-Gal IgY, IgM and/or IgA can be transferred from mother to eggs and from there to the embryo and subsequently to the chick. **(C)** Different isotypes of anti-α-Gal Abs could be located in different embryo/chick tissues (tissue blocks to the left) with tissue-specific functions (tissue blocks to the right). Anti-α-Gal IgY could mediate opsonization of blood stages of malaria parasites (the insert represents an anti-α-Gal IgY-*Plasmodium* complex). Anti-α-Gal IgM could target sporozoites in the skin (the insert represents complement-mediated lysis of *Plasmodium* upon anti-α-Gal IgM binding on the surface of the parasite). Anti-α-Gal IgA could be involved in the early colonization of bacterial microbiota with α1,3GT activity with the subsequent activation of anti-α-Gal IgM/IgA production mechanisms. Figure created with BioRender.com.

to malaria *via* anti-α-Gal IgM and/or IgY? (*ii*) are anti-α-Gal IgM and IgY in the eggs associated with early resistance to malaria in chicks? and (*iii*) do anti-α-Gal IgA in eggs can favors the colonization of bacteria with α1,3GT activity such as Enterobacteriaceae in the gut microbiome of newly hatched chicks? Avian malaria is the oldest experimental system for investigating the biology and transmission of *Plasmodium* parasites (101). In the light of the new hypothesis and theories presented here, this 'old model' can shed light on the ecological impact of microbiota diversity and the role of anti-α-Gal Abs in malaria resistance.

DATA AVAILABILITY STATEMENT

Publicly available datasets were analyzed in this study. This data can be found here: Published and publicly available 16S datasets were used for the prediction of functional traits of the microbiome of wild birds and poultry. Datasets of eleven untreated wild birds were included in this study: Japanese quail from Kohl et al., 2008 (accession PRJNA244306), fairy prion and common diving petrel from Dewar et al., 2014 (PRJEB1549), barn swallow from Kreisinger et al., 2015 (PRJEB7057), gulls from Koskey et al., 2013 (PRJNA229760), black and turkey vultures from Roggenbuck et al., 2014 (PRJNA243051). Finally, two datasets from two breeds of poultry were also included: untreated brown chicken (Hy-line brown) from Xu et al., 2019 (PRJNA510025) and white leghorn (Hy-Line W36) and brown chicken (Hy-line brown) reared in conventional cages from Adhikari et al., 2020 (PRJNA627663).

ETHICS STATEMENT

All procedures were performed at the Nature Research Centre in Vilnius, Lithuania, according to Lithuanian and International Guiding Principles for Biomedical Research Involving Animals (2012). Infection experiments and other procedures were reviewed and approved by the Lithuanian State Food and Veterinary Service, Ref. No. 2020/07/24-G2-84 and International Research Cooperation Agreement between the Biological Station "Rybachy" and the Nature Research Centre (25/05/2010, 04/09/2015). The assessment of the animal health and all described procedures were implemented by trained professionals (under licenses 2012/02/06-No-208, and 2016/01.29-No-344).

AUTHOR CONTRIBUTIONS

AC-C and VP conceived the study. LM-H, AW-C, VP, and JA performed the experiments and acquired the data. DO, AW-C, LM-H, and AC-C analyzed the data. DO, AW-C, and AC-C prepared figures. AC-C, VP, and JF contributed reagents and other resources. AC-C, VP, and DO supervised the work. AC-C, LM-H, and VP drafted the first version of the manuscript. All the authors made editorial contributions and revised and accepted the final version of the manuscript.

FUNDING

UMR BIPAR is supported by the French Government's Investissement d'Avenir program, Laboratoire d'Excellence "Integrative Biology of Emerging Infectious Diseases" (grant no. ANR-10-LABX-62-IBEID). AW-C is supported by Programa Nacional de Becas de Postgrado en el Exterior "Don Carlos Antonio López" (grant no. 205/2018).

SUPPLEMENTARY MATERIAL

The Supplementary Material for this article can be found online at: https://www.frontiersin.org/articles/10.3389/fimmu.2022.807682/full#supplementary-material

REFERENCES

1. Belkaid Y, Hand TW. Role of the Microbiota in Immunity and Inflammation. *Cell* (2014) 157:121–41. doi: 10.1016/j.cell.2014.03.011
2. Stevens EJ, Bates KA, King KC. Host Microbiota can Facilitate Pathogen Infection. *PloS Pathog* (2021) 17:e1009514. doi: 10.1371/journal.ppat.1009514
3. Galili U, Mandrell RE, Hamadeh RM, Shohet SB, Griffiss JM. Interaction Between Human Natural Anti-Alpha-Galactosyl Immunoglobulin G and Bacteria of the Human Flora. *Infect Immun* (1988) 56:1730–7. doi: 10.1128/iai.56.7.1730-1737.1988
4. Contreras M, Pacheco I, Alberdi P, Diaz-Sánchez S, Artigas-Jerónimo S, Mateos-Hernández L, et al. Allergic Reactions and Immunity in Response to Tick Salivary Biogenic Substances and Red Meat Consumption in the Zebrafish Model. *Front Cell Infect Microbiol* (2020) 10:78. doi: 10.3389/fcimb.2020.00078
5. Pacheco I, Contreras M, Villar M, Risalde MA, Alberdi P, Cabezas-Cruz A, et al. Vaccination With Alpha-Gal Protects Against Mycobacterial Infection in the Zebrafish Model of Tuberculosis. *Vaccines (Basel)* (2020) 8:195. doi: 10.3390/vaccines8020195
6. Posekany KJ, Pittman HK, Bradfield JF, Haisch CE, Verbanac KM. Induction of Cytolytic Anti-Gal Antibodies in Alpha-1,3-Galactosyltransferase Gene Knockout Mice by Oral Inoculation With *Escherichia Coli* O86:B7 Bacteria. *Infect Immun* (2002) 70:6215–22. doi: 10.1128/IAI.70.11.6215-6222.2002
7. Mateos-Hernández L, Risco-Castillo V, Torres-Maravilla E, Bermúdez-Humarán LG, Alberdi P, Hernández-Jarguin A, et al. Gut Microbiota Abrogates Anti-α-Gal IgA Response in Lungs and Protects Against Experimental Aspergillus Infection in Poultry. *Vaccines (Basel)* (2020) 8:285. doi: 10.3390/vaccines8020285
8. Hodžić A, Mateos-Hernández L, de la Fuente J, Cabezas-Cruz A. α-Gal-Based Vaccines: Advances, Opportunities, and Perspectives. *Trends Parasitol* (2020) 36:992–1001. doi: 10.1016/j.pt.2020.08.001
9. Montassier E, Al-Ghalith GA, Mathé C, Le Bastard Q, Douillard V, Garnier A, et al. Distribution of Bacterial α1,3-Galactosyltransferase Genes in the Human Gut Microbiome. *Front Immunol* (2020) 10:3000. doi: 10.3389/fimmu.2019.03000
10. Macher BA, Galili U. The Galα1,3galβ1,4glcnac-R (α-Gal) Epitope: A Carbohydrate of Unique Evolution and Clinical Relevance. *Biochim Biophys Acta* (2008) 1780:75–88. doi: 10.1016/j.bbagen.2007.11.003

11. Yilmaz B, Portugal S, Tran TM, Gozzelino R, Ramos S, Gomes J, et al. Gut Microbiota Elicits a Protective Immune Response Against Malaria Transmission. *Cell* (2014) 159:1277–89. doi: 10.1016/j.cell.2014.10.053
12. Cabezas-Cruz A, Mateos-Hernández L, Alberdi P, Villar M, Riveau G, Hermann E, et al. Effect of Blood Type on Anti-α-Gal Immunity and the Incidence of Infectious Diseases. *Exp Mol Med* (2017) 49:e301. doi: 10.1038/emm.2016.164
13. Hodžić A, Mateos-Hernández L, Leschnik M, Alberdi P, Rego ROM, Contreras M, et al. Tick Bites Induce Anti-α-Gal Antibodies in Dogs. *Vaccines (Basel)* (2019) 7:114. doi: 10.3390/vaccines7030114
14. Moura APV, Santos LCB, Brito CRN, Valencia E, Junqueira C, Filho AAP, et al. Virus-Like Particle Display of the α-Gal Carbohydrate for Vaccination Against *Leishmania* Infection. *ACS Cent Sci* (2017) 3:1026–31. doi: 10.1021/acscentsci.7b00311
15. Couto AS, Gonçalves MF, Colli W, de Lederkremer RM. The N-Linked Carbohydrate Chain of the 85-Kilodalton Glycoprotein From *Trypanosoma Cruzi* Trypomastigotes Contains Sialyl, Fucosyl and Galactosyl (Alpha 1-3) Galactose Units. *Mol Biochem Parasitol* (1990) 39:101–7. doi: 10.1016/0166-6851(90)90012-b
16. Almeida IC, Milani SR, Gorin PA, Travassos LR. Complement-Mediated Lysis of *Trypanosoma Cruzi* Trypomastigotes by Human Anti-Alpha-Galactosyl Antibodies. *J Immunol* (1991) 146:2394–400.
17. Portillo S, Zepeda BG, Iniguez E, Olivas JJ, Karimi NH, Moreira OC, et al. A Prophylactic α-Gal-Based Glycovaccine Effectively Protects Against Murine Acute Chagas Disease. *NPJ Vaccines* (2019) 4:13. doi: 10.1038/s41541-019-0107-7
18. Pacheco I, Diaz-Sánchez S, Contreras M, Villar M, Cabezas-Cruz A, Gortázar C, et al. Probiotic Bacteria With High Alpha-Gal Content Protect Zebrafish Against Mycobacteriosis. *Pharmaceut (Basel)* (2021) 14:635. doi: 10.3390/ph14070635
19. Colston TJ, Jackson CR. Microbiome Evolution Along Divergent Branches of the Vertebrate Tree of Life: What Is Known and Unknown. *Mol Ecol* (2016) 25:3776–800. doi: 10.1111/mec.13730
20. Hird SM, Sánchez C, Carstens BC, Brumfield RT. Comparative Gut Microbiota of 59 Neotropical Bird Species. *Front Microbiol* (2015) 6:1403. doi: 10.3389/fmicb.2015.01403
21. Hird SM. Evolutionary Biology Needs Wild Microbiomes. *Front Microbiol* (2017) 8:725. doi: 10.3389/fmicb.2017.00725
22. Knutie SA. Food Supplementation Affects Gut Microbiota and Immunological Resistance to Parasites in a Wild Bird Species. *J Appl Ecol* (2020) 57:536–47. doi: 10.1111/1365-2664.13567
23. Valkiūnas G, Iezhova TA. Keys to the Avian Malaria Parasites. *Malar J* (2018) 17:212. doi: 10.1186/s12936-018-2359-5
24. Bensch S, Hellgren O, Pérez-Tris J. MalAvi: A Public Database of Malaria Parasites and Related Haemosporidians in Avian Hosts Based on Mitochondrial Cytochrome B Lineages. *Mol Eco Resour* (2009) 9:1353–8. doi: 10.1111/j.1755-0998.2009.02692.x
25. Valkiūnas G. *Avian Malaria Parasites and Other Haemosporidia*. Florida: CRC Press (2004). p. 946.
26. Hennet T. The Galactosyltransferase Family. *Cell Mol Life Sci* (2002) 59:1081–95. doi: 10.1007/s00018-002-8489-4
27. Cabezas-Cruz A, Espinosa PJ, Alberdi P, Šimo L, Valdés JJ, Mateos-Hernández L, et al. Tick Galactosyltransferases Are Involved in α-Gal Synthesis and Play a Role During *Anaplasma Phagocytophilum* Infection and *Ixodes Scapularis* Tick Vector Development. *Sci Rep* (2018) 8:14224. doi: 10.1038/s41598-018-32664-z
28. Jennings MP, Virji M, Evans D, Foster V, Srikhanta YN, Steeghs L, et al. Identification of a Novel Gene Involved in Pilin Glycosylation in Neisseria Meningitidis. *Mol Microbiol* (1998) 29:975–84. doi: 10.1046/j.1365-2958.1998.00962.x
29. Ohashi T, Fujiyama K, Takegawa K. Identification of Novel α1,3-Galactosyltransferase and Elimination of α-Galactose-Containing Glycans by Disruption of Multiple α-Galactosyltransferase Genes in Schizosaccharomyces Pombe. *J Biol Chem* (2012) 287:38866–75. doi: 10.1074/jbc.M112.347351
30. Chen C, Liu B, Xu Y, Utkina N, Zhou D, Danilov L, et al. Biochemical Characterization of the Novel α-1, 3-Galactosyltransferase WclR From *Escherichia Coli* O3. *Carbohydr Res* (2016) 430:36–43. doi: 10.1016/j.carres.2016.04.012
31. Ramasamy R. Mosquito Vector Proteins Homologous to α1-3 Galactosyl Transferases of Tick Vectors in the Context of Protective Immunity Against Malaria and Hypersensitivity to Vector Bites. *Parasit Vectors* (2021) 14:303. doi: 10.1186/s13071-021-04801-7
32. Ribero Rocha HD. *The Role of α-Gal (Galα1-3galβ1-4glcnac-R) on Plasmodium Spp. Sporozoites in Anopheles Spp. Mosquito Salivary Glands Invasion. [Dissertation Thesis]*. Portugal (Lisbon): Universidade Nova de Lisboa (2021).
33. Grond K, Sandercock BK, Jumpponen A, Zeglin LH. The Avian Gut Microbiota: Community, Physiology and Function in Wild Birds. *J Avian Biol* (2018) 49:e01788. doi: 10.1111/jav.01788
34. Grond K, Santo Domingo JW, Lanctot RB, Jumpponen A, Bentzen RL, Boldenow ML, et al. Composition and Drivers of Gut Microbial Communities in Arctic-Breeding Shorebirds. *Front Microbiol* (2019) 10:2258. doi: 10.3389/fmicb.2019.02258
35. Waite DW, Taylor MW. Characterizing the Avian Gut Microbiota: Membership, Driving Influences, and Potential Function. *Front Microbiol* (2014) 5:223. doi: 10.3389/fmicb.2014.00223
36. Hird SM, Carstens BC, Cardiff SW, Dittmann DL, Brumfield RT. Sampling Locality Is More Detectable Than Taxonomy or Ecology in the Gut Microbiota of the Brood-Parasitic Brown-Headed Cowbird (*Molothrus Ater*). *PeerJ* (2014) 2:e321. doi: 10.7717/peerj.321
37. Colston TJ, Noonan BP, Jackson CR. Phylogenetic Analysis of Bacterial Communities in Different Regions of the Gastrointestinal Tract of Agkistrodon Piscivorus, the Cottonmouth Snake. *PloS One* (2015) 10: e0128793. doi: 10.1371/journal.pone.0128793
38. Ley RE, Hamady M, Lozupone C, Turnbaugh PJ, Ramey RR, Bircher JS, et al. Evolution of Mammals and Their Gut Microbes. *Science* (2008) 320:1647–51. doi: 10.1126/science.1155725
39. Madlala T, Okpeku M, Adeleke MA. Understanding the Interactions Between Eimeria Infection and Gut Microbiota, Towards the Control of Chicken Coccidiosis: A Review. *Parasite* (2021) 28:48. doi: 10.1051/parasite/2021047
40. Videvall E, Paxton KL, Campana MG, Cassin-Sackett L, Atkinson CT, Fleischer RC. Transcriptome Assembly and Differential Gene Expression of the Invasive Avian Malaria Parasite *Plasmodium Relictum* in Hawai'i. *Ecol Evol* (2021) 11:4935–44. doi: 10.1002/ece3.7401
41. Bodawatta KH, Schierbech SK, Petersen NR, Sam K, Bos N, Jønsson KA, et al. Great Tit (*Parus Major*) Uropygial Gland Microbiomes and Their Potential Defensive Roles. *Front Microbiol* (2020) 11:1735. doi: 10.3389/fmicb.2020.01735
42. Villarino NF, LeCleir GR, Denny JE, Dearth SP, Harding CL, Sloan SS, et al. Composition of the Gut Microbiota Modulates the Severity of Malaria. *Proc Natl Acad Sci USA* (2016) 113:2235–40. doi: 10.1073/pnas.1504887113
43. Chakravarty S, Mandal RK, Duff ML, Schmidt NW. Intestinal Short-Chain Fatty Acid Composition Does Not Explain Gut Microbiota-Mediated Effects on Malaria Severity. *PloS One* (2019) 14:e0214449. doi: 10.1371/journal.pone.0214449
44. Jacobson A, Lam L, Rajendram M, Tamburini F, Honeycutt J, Pham T, et al. A Gut Commensal-Produced Metabolite Mediates Colonization Resistance to *Salmonella* Infection. *Cell Host Microbe* (2018) 24:296–307.e7. doi: 10.1016/j.chom.2018.07.002
45. Stough JMA, Dearth SP, Denny JE, LeCleir GR, Schmidt NW, Campagna SR, et al. Functional Characteristics of the Gut Microbiome in C57BL/6 Mice Differentially Susceptible to Plasmodium Yoelii. *Front Microbiol* (2016) 7:1520. doi: 10.3389/fmicb.2016.01520
46. Morffy Smith CD, Gong M, Andrew AK, Russ BN, Ge Y, Zadeh M, et al. Composition of the Gut Microbiota Transcends Genetic Determinants of Malaria Infection Severity and Influences Pregnancy Outcome. *EBioMedicine* (2019) 44:639–55. doi: 10.1016/j.ebiom.2019.05.052
47. Aakko J, Endo A, Mangani C, Maleta K, Ashorn P, Isolauri E, et al. Distinctive Intestinal Lactobacillus Communities in 6-Month-Old Infants From Rural Malawi and Southwestern Finland. *J Pediatr Gastroenterol Nutr* (2015) 61:641–8. doi: 10.1097/MPG.0000000000000878
48. Cabezas-Cruz A, de la Fuente J. Immunity to α-Gal: The Opportunity for Malaria and Tuberculosis Control. *Front Immunol* (2017) 8:1733. doi: 10.3389/fimmu.2017.01733
49. Yooseph S, Kirkness EF, Tran TM, Harkins DM, Jones MB, Torralba MG, et al. Stool Microbiota Composition Is Associated With the Prospective Risk

of *Plasmodium Falciparum* Infection. *BMC Genomics* (2015) 16:631. doi: 10.1186/s12864-015-1819-3
50. Mach N, Baranowski E, Nouvel LX, Citti C. The Airway Pathobiome in Complex Respiratory Diseases: A Perspective in Domestic Animals. *Front Cell Infect Microbiol* (2021) 11:583600. doi: 10.3389/fcimb.2021.583600
51. Singh S, Bastos-Amador P, Thompson JA, Truglio M, Yilmaz B, Cardoso S, et al. Glycan-Based Shaping of the Microbiota During Primate Evolution. *Elife* (2021) 10:e67450. doi: 10.7554/eLife.67450
52. Maitre A, Wu-Chuang A, Aželytė J, Palinauskas V, Mateos-Hernández L, Obregon D, et al. Vector Microbiota Manipulation by Host Antibodies: The Forgotten Strategy to Develop Transmission-Blocking Vaccines. *Parasit Vectors* (2022) 15:4. doi: 10.1186/s13071-021-05122-5
53. Ben-Yakir D. Growth Retardation of *Rhodnius Prolixus* Symbionts by Immunizing Host Against *Nocardia* (*Rhodococcus*) Rhodnii. *J Insect Physiol* (1987) 33:379–83. doi: 10.1016/0022-1910(87)90015-1
54. Nogge G. Aposymbiotic Tsetse Flies, *Glossina Morsitans Morsitans* Obtained by Feeding on Rabbits Immunized Specifically With Symbionts. *J Insect Physiol* (1978) 24:299–304. doi: 10.1016/0022-1910(78)90026-4
55. Noden BH, Vaughan JA, Pumpuni CB, Beier JC. Mosquito Ingestion of Antibodies Against Mosquito Midgut Microbiota Improves Conversion of Ookinetes to Oocysts for *Plasmodium Falciparum*, But Not P. Yoelii. *Parasitol Int* (2011) 60:440–6. doi: 10.1016/j.parint.2011.07.007
56. Mateos-Hernández L, Obregón D, Maye J, Borneres J, Versille N, de la Fuente J, et al. Anti-Tick Microbiota Vaccine Impacts *Ixodes Ricinus* Performance During Feeding. *Vaccines (Basel)* (2020) 8:702. doi: 10.3390/vaccines8040702
57. Mateos-Hernández L, Obregón D, Wu-Chuang A, Maye J, Bornères J, Versillé N, et al. Anti-Microbiota Vaccines Modulate the Tick Microbiome in a Taxon-Specific Manner. *Front Immunol* (2021) 12:704621. doi: 10.3389/fimmu.2021.704621
58. Sonenshine DE, Stewart PE. Microbiomes of Blood-Feeding Arthropods: Genes Coding for Essential Nutrients and Relation to Vector Fitness and Pathogenic Infections. A Review. *Microorganisms* (2021) 9:2433. doi: 10.3390/microorganisms9122433
59. Gómez-Díaz E, Jordà M, Peinado MA, Rivero A. Epigenetics of Host-Pathogen Interactions: The Road Ahead and the Road Behind. *PloS Pathog* (2012) 8:e1003007. doi: 10.1371/journal.ppat.1003007
60. Skinner MK. What Is an Epigenetic Transgenerational Phenotype? F3 or F2. *Reprod Toxicol* (2008) 25:2–6. doi: 10.1016/j.reprotox.2007.09.001
61. Lacal I, Ventura R. Epigenetic Inheritance: Concepts, Mechanisms and Perspectives. *Front Mol Neurosci* (2018) 11:292:292. doi: 10.3389/fnmol.2018.00292
62. Suzuki MM, Bird A. DNA Methylation Landscapes: Provocative Insights From Epigenomics. *Nat Rev Genet* (2008) 9:465–76. doi: 10.1038/nrg2341
63. Bannister AJ, Kouzarides T. Regulation of Chromatin by Histone Modifications. *Cell Res* (2011) 21:381–95. doi: 10.1038/cr.2011.22
64. Guerrero-Bosagna C, Morisson M, Liaubet L, Rodenburg TB, de Haas EN, Košťál L, et al. Transgenerational Epigenetic Inheritance in Birds. *Environ Epigenet* (2018) 4:dvy008. doi: 10.1093/eep/dvy008
65. Berghof TVL, Parmentier HK, Lammers A. Transgenerational Epigenetic Effects on Innate Immunity in Broilers: An Underestimated Field to be Explored? *Poult Sci* (2013) 92:2904–13. doi: 10.3382/ps.2013-03177
66. Nätt D, Lindqvist N, Stranneheim H, Lundeberg J, Torjesen PA, Jensen P. Inheritance of Acquired Behaviour Adaptations and Brain Gene Expression in Chickens. *PloS One* (2009) 4:e6405. doi: 10.1371/journal.pone.0006405
67. Huh GS, Boulanger LM, Du H, Riquelme PA, Brotz TM, et al. Functional Requirement for Class I MHC in CNS Development and Plasticity. *Science* (2000) 290:2155–9. doi: 10.1126/science.290.5499.2155
68. Hasselquist D, Nilsson JA. Maternal Transfer of Antibodies in Vertebrates: Trans-Generational Effects on Offspring Immunity. *Philos Trans R Soc Lond B Biol Sci* (2009) 364:51–60. doi: 10.1098/rstb.2008.0137
69. Grindstaff JL, Hasselquist D, Nilsson JK, Sandell M, Smith HG, Stjernman M, et al. Transgenerational Priming of Immunity: Maternal Exposure to a Bacterial Antigen Enhances Offspring Humoral Immunity. *Proc Biol Sci* (2006) 273:2551–7. doi: 10.1098/rspb.2006.3608
70. Gasparini J, McCoy KD, Haussy C, Tveraa T, Boulinier T. Induced Maternal Response to the Lyme Disease Spirochaete *Borrelia Burgdorferi Sensu Lato* in a Colonial Seabird, the Kittiwake Rissa Tridactyla. *Proc Biol Sci* (2001) 268:647–50. doi: 10.1098/rspb.2000.1411
71. Gasparini J, McCoy KD, Tveraa T, Boulinier T. Related Concentrations of Specific Immunoglobulins Against the Lyme Disease Agent *Borrelia Burgdorferi Sensu Lato* in Eggs, Young and Adults of the Kittiwake (*Rissa Tridactyla*). *Ecol Lett* (2002) 5:519–24. doi: 10.1046/j.1461-0248.2002.00345.x
72. Gasparini J, McCoy KD, Staszewski V, Haussy C, Boulinier T. Dynamics of Anti-*Borrelia* Antibodies in Black-Legged Kittiwake (*Rissa Tridactyla*) Chicks Suggest a Maternal Educational Effect. *Can J Zool* (2006) 84:623–7. doi: 10.1139/z06-024
73. Cook CL, Pao W, Firca JR, Anderson BE, Fryer JP. Simple Purification Methods for an Alphagalactose-Specific Antibody From Chicken Eggs. *J Biosci Bioeng* (2001) 91:305–10. doi: 10.1263/jbb.91.305
74. Bouhours JF, Richard C, Ruvoen N, Barreau N, Naulet J, Bouhours D, et al. Characterization of a Polyclonal Anti-Galalpha1-3gal Antibody From Chicken. *Glycoconj J* (1998) 15:93–9. doi: 10.1023/a:1006903919461
75. Walsh W, Anderson BE, Ivancic D, Zhang Z, Piccini JP, Rodgers TG, et al. Distribution of, and Immune Response to, Chicken Anti-Alpha Gal Immunoglobulin Y Antibodies in Wild-Type and Alpha Gal Knockout Mice. *Immunology* (2000) 101:467–73. doi: 10.1046/j.1365-2567.2000.00136.x
76. Fryer J, Firca J, Leventhal J, Blondin B, Malcolm A, Ivancic D, et al. IgY Antiporcine Endothelial Cell Antibodies Effectively Block Human Antiporcine Xenoantibody Binding. *Xenotransplantation* (1999) 6:98–109. doi: 10.1034/j.1399-3089.1999.00015.x
77. Hamal KR, Burgess SC, Pevzner IY, Erf GF. Maternal Antibody Transfer From Dams to Their Egg Yolks, Egg Whites, and Chicks in Meat Lines of Chickens. *Poult Sci* (2006) 85:1364–72. doi: 10.1093/ps/85.8.1364
78. Rose ME, Orlans E. Immunoglobulins in the Egg, Embryo, and Young Chick. *Dev Comp Immunol* (1981) 5:15–20. doi: 10.1016/S0145-305X(81)80003-1
79. Kaspers B, Bondl H, Göbel TW. Transfer of IgA From Albumen Into the Yolk Sac During Embryonic Development in the Chicken. *Zentralbl Veterinarmed A* (1996) 43:225–31. doi: 10.1111/j.1439-0442.1996.tb00448.x
80. Kowalczyk K, Daiss J, Helpern I, Roth ITF. Quantitation of Maternal-Fetal IgG Transport in the Chicken. *Immunology* (1985) 54:755–62.
81. Bunker JJ, Flynn TM, Koval JC, Shaw DG, Meisel M, McDonald BD, et al. Innate and Adaptive Humoral Responses Coat Distinct Commensal Bacteria With Immunoglobulin a. *Immunity* (2015) 43:541–53. doi: 10.1016/j.immuni.2015.08.007
82. Bunker JJ, Erickson SA, Flynn TM, Henry C, Koval JC, Meisel M, et al. Natural Polyreactive IgA Antibodies Coat the Intestinal Microbiota. *Science* (2017) 358:eaan6619. doi: 10.1126/science.aan6619
83. Macpherson AJ, Gatto D, Sainsbury E, Harriman GR, Hengartner H, et al. A Primitive T Cell-Independent Mechanism of Intestinal Mucosal IgA Responses to Commensal Bacteria. *Science* (2000) 288:2222–6. doi: 10.1126/science.288.5474.2222
84. Moor K, Diard M, Sellin ME, Felmy B, Wotzka SY, Toska A, et al. High-Avidity IgA Protects the Intestine by Enchaining Growing Bacteria. *Nature* (2017) 544:498–502. doi: 10.1038/nature22058
85. Donaldson GP, Ladinsky MS, Yu KB, Sanders JG, Yoo BB, Chou W-C, et al. Gut Microbiota Utilize Immunoglobulin A for Mucosal Colonization. *Science* (2018) 360:795–800. doi: 10.1126/science.aaq0926
86. McLoughlin K, Schluter J, Rakoff-Nahoum S, Foster KR. Host Selection of Microbiota *via* Differential Adhesion. *Cell Host Microbe* (2016) 19:550–9. doi: 10.1016/j.chom.2016.02.021
87. Palinauskas V, Žiegytė R, Ilgūnas M, Iezhova TA, Bernotienė A, Bolshakov C, et al. Description of the First Cryptic Avian Malaria Parasite, Plasmodium Homocircumflexum N. Sp. With Experimental Data on Its Virulence and Development in Avian Hosts and Mosquitoes. *Int J Parasitol* (2015) 45:51–62. doi: 10.1016/j.ijpara.2014.08.012
88. Martinez-de la Puente J, Santiago-Alarcon D, Palinauskas V, Bensch S. *Plasmodium relictum*. *Trends Parasitol* (2020) 37:355–6. doi: 10.1016/j.pt.2020.06.004
89. Palinauskas V, Platonova E, Žiegytė R, Mukhin A. Dynamics of Blood Stage and Sporozoite-Induced Malarial Infections in Experimentally Infected Passerines. *Int J Parasitol* (2020) 50:1057–65. doi: 10.1016/j.ijpara.2020.05.015
90. Fink E. Experimentelle Infektion Von Kanarien Mit *Plasmodium Cathemerium* Hartman, 1927, Durch Den Stich Infizierter MCken (*Culex*

Pipiens L.) Und Durch Inokulation Isolierter Sporozoiten. *Z Ĭfr Parasitenkd* (1968) 31:232–53. doi: 10.1007/BF00259704
91. Rozeboom LE, Shah KS. Preliminary Studies on the Production of Bird Malaria Infections by the Injection of Sporozoites. *J Parasitol* (1934) 20:198. doi: 10.2307/3272140
92. Tonkin IM. The Influence of the Suspending Fluid on the Survival of Sporozoites In Vitro. *Trans R Soc Trop Med Hyg* (1947) 41:259–62. doi: 10.1016/S0035-9203(47)80010-0
93. Porter RJ, Laird RL, Dusseau EM. Studies on Malarial Sporozoites. I. Effect of Various Environmental Conditions. *Exp Parasitol* (1952) 1:229–44. doi: 10.1016/0014-4894(52)90013-1
94. Porter RJ, Laird RL, Dusseau EM. Studies on Malarial Sporozoites. II. Effect of Age and Dosage of Sporozoites on Their Infectiousness. *Exp Parasitol* (1954) 3:267–74. doi: 10.1016/0014-4894(54)90026-0
95. Cosgrove CL, Knowles SCL, Day KP, Sheldon BC. No Evidence for Avian Malaria Infection During the Nestling Phase in a Passerine Bird. *J Parasitol* (2006) 92:1302–4. doi: 10.1645/GE-878R.1
96. Zehtindjiev P, Križanauskienė A, Scebba S, Dimitrov D, Valkiūnas G, Hegemann A, et al. Haemosporidian Infections in Skylarks (*Alauda Arvensis*): A Comparative PCR-Based and Microscopy Study on the Parasite Diversity and Prevalence in Southern Italy and the Netherlands. *Eur J Wildl* (2011) 58:335–44. doi: 10.1007/s10344-011-0586-y
97. Ricklefs RE. Species Richness and Morphological Diversity of Passerine Birds. *Proc Natl Acad Sci U.S.A.* (2012) 109:14482–7. doi: 10.1073/pnas.1212079109
98. Jenkins CN, Pimm SL, Joppa LN. Global Patterns of Terrestrial Vertebrate Diversity and Conservation. *Proc Natl Acad Sci USA* (2013) 110:e2602–10. doi: 10.1073/pnas.1302251110
99. Banks JC, Cary SC, Hogg ID. The Phylogeography of Adelie Penguin Faecal Flora. *Environ Microbiol* (2009) 11:577–88. doi: 10.1111/j.1462-2920.2008.01816.x
100. Ilgūnas M, Bukauskaitė D, Palinauskas V, Iezhova T, Fragner K, Platonova E, et al. Patterns of *Plasmodium Homocircumflexum* Virulence in Experimentally Infected Passerine Birds. *Malar J* (2019) 18:174. doi: 10.1186/s12936-019-2810-2
101. Rivero A, Gandon S. Evolutionary Ecology of Avian Malaria: Past to Present. *Trends Parasitol* (2018) 34:712–26. doi: 10.1016/j.pt.2018.06.002

Conflict of Interest: The authors declare that the research was conducted in the absence of any commercial or financial relationships that could be construed as a potential conflict of interest.

Publisher's Note: All claims expressed in this article are solely those of the authors and do not necessarily represent those of their affiliated organizations, or those of the publisher, the editors and the reviewers. Any product that may be evaluated in this article, or claim that may be made by its manufacturer, is not guaranteed or endorsed by the publisher.

PAPER II

Nested patterns of commensals and endocymbionts in microbial communities of mosquito vectors

Aželytė J., Maitre A., Abuin-Denis L., Wu-Chuang A., Žiegytė R., Mateos-Hernández L., Obregón D., Palinauskas V., Cabezas-Cruz A.

BMC Microbiology, 2024, 24(1), 1-13

DOI 10.1186/s12žžž0i866-024-03593-x

Aželytė *et al. BMC Microbiology* (2024) 24:434
https://doi.org/10.1186/s12866-024-03593-x

BMC Microbiology

RESEARCH Open Access

Nested patterns of commensals and endosymbionts in microbial communities of mosquito vectors

Justė Aželytė[1], Apolline Maitre[2,3,4], Lianet Abuin-Denis[2,5], Alejandra Wu-Chuang[2], Rita Žiegytė[1], Lourdes Mateos-Hernandez[2], Dasiel Obregon[6], Vaidas Palinauskas[1*] and Alejandro Cabezas-Cruz[2*]

Abstract

Background Mosquitoes serve as vectors for numerous pathogens, posing significant health risks to humans and animals. Understanding the complex interactions within mosquito microbiota is crucial for deciphering vector-pathogen dynamics and developing effective disease management strategies. Here, we investigated the nested patterns of *Wolbachia* endosymbionts and *Escherichia-Shigella* within the microbiota of laboratory-reared *Culex pipiens* f. *molestus* and *Culex quinquefasciatus* mosquitoes. We hypothesized that *Wolbachia* would exhibit a structured pattern reflective of its co-evolved relationship with both mosquito species, while *Escherichia-Shigella* would display a more dynamic pattern influenced by environmental factors.

Results Our analysis revealed different microbial compositions between the two mosquito species, although some microorganisms were common to both. Network analysis revealed distinct community structures and interaction patterns for these bacteria in the microbiota of each mosquito species. *Escherichia-Shigella* appeared prominently within major network modules in both mosquito species, particularly in module P4 of *Cx. pipiens* f. *molestus*, interacting with 93 nodes, and in module Q3 of *Cx. quinquefasciatus*, interacting with 161 nodes, sharing 55 nodes across both species. On the other hand, *Wolbachia* appeared in disparate modules: module P3 in *Cx. pipiens* f. *molestus* and a distinct module with a single additional taxon in *Cx. quinquefasciatus*, showing species-specific interactions and no shared taxa. Through computer simulations, we evaluated how the removal of *Wolbachia* or *Escherichia-Shigella* affects network robustness. In *Cx. pipiens* f. *molestus*, removal of *Wolbachia* led to a decrease in network connectivity, while *Escherichia-Shigella* removal had a minimal impact. Conversely, in *Cx. quinquefasciatus*, removal of *Escherichia-Shigella* resulted in decreased network stability, whereas *Wolbachia* removal had minimal effect.

Conclusions Contrary to our hypothesis, the findings indicate that *Wolbachia* displays a more dynamic pattern of associations within the microbiota of *Culex pipiens* f. *molestus* and *Culex quinquefasciatus* mosquitoes, than *Escherichia-Shigella*. The differential effects on network robustness upon *Wolbachia* or *Escherichia-Shigella* removal suggest that

*Correspondence:
Vaidas Palinauskas
palinauskas@gmail.com
Alejandro Cabezas-Cruz
alejandro.cabezas@vet-alfort.fr

Full list of author information is available at the end of the article

these bacteria play distinct roles in maintaining community stability within the microbiota of the two mosquito species.

Keywords Mosquitoes, *Escherichia-Shigella*, *Wolbachia*, Nestedness theory, Community assembly

Background

Mosquitoes, as obligate hematophagous insects, are significant vectors for various pathogens, posing substantial health threats to humans and animals alike [1]. Among mosquito species, *Culex pipiens* f. *molestus* and *Culex quinquefasciatus* are of particular importance due to their role in transmitting diseases such as avian malaria, West Nile virus [2] and filariasis [3], among others [4]. In addition to pathogens, mosquitoes harbor diverse microbial communities, including commensals and endosymbionts, collectively termed the microbiota [5]. These microbes play crucial roles in vector survival, fitness, and vector competence [6]. Understanding the assembly and dynamics of mosquito microbial communities is essential for elucidating vector-pathogen interactions and developing novel disease management strategies [7].

Nestedness theory [8] provides a valuable framework for understanding the diverse patterns of interactions between symbionts, commensals, and pathogens within the mosquito microbiota [9]. Nested patterns, characterized by structured interactions among species or taxa subsets, have been extensively studied in various ecological systems [10, 11]. Analyzing nestedness in mosquito microbiota networks can provide insights into the ecological relationships among different taxa and their implications for vector biology [9].

In this study, we investigate the differential nested patterns of *Wolbachia* endosymbionts and the commensal bacterial taxon *Escherichia-Shigella* within the microbial communities of laboratory-reared *Cx. pipiens* f. *molestus* and *Cx. quinquefasciatus*. *Wolbachia*, being an endosymbiont [12], is known to manipulate host reproduction and influence pathogen transmission [13, 14]. It is also known to modulate microbiome structure of insects [15–17]. In laboratory-reared mosquitoes, where environmental conditions are controlled and stable, *Wolbachia* may exhibit a more consistent and structured pattern within the microbiota. Its presence and abundance may be tightly linked to the mosquito host's physiological state and reproductive biology, leading to a nested pattern within the microbial community. On the other hand, *Escherichia-Shigella* is of interest due to its ability to modulate the mosquito microbiota and influence malaria transmission [7]. Bacteria from the Enterobacteriaceae family are associated with natural microbial communities of mosquito vectors [18]. *Escherichia-Shigella*, as a commensal bacterium [19], may display a different pattern within the microbiota. Its abundance and occurrence could be influenced by various factors such as diet, environmental conditions, and interactions with other microbial taxa [20]. In laboratory-reared mosquitoes, where environmental factors are controlled, *Escherichia-Shigella* may still exhibit dynamic patterns within the microbiota due to its versatile ecological roles and interactions with the host.

Therefore, here we hypothesized that *Wolbachia* endosymbionts would form a nested pattern, reflecting its stable and co-evolved relationship within the host, while *Escherichia-Shigella* may exhibit a less consistent pattern within the microbial community, influenced by environmental and ecological factors. By examining the differential nested patterns of *Wolbachia* endosymbionts and *Escherichia-Shigella* within the mosquito microbiota, we aim to gain insights into the complex interactions shaping vector microbiota assembly. This research may contribute to our understanding of vector-microbiota dynamics and inform the development of novel strategies for controlling mosquito-borne diseases in both public health and veterinary settings.

Methods

Ethical statement

The study utilizes two species of laboratory-reared mosquitoes, *Culex pipiens* f. *molestus* and *Culex quinquefasciatus*. While conducted in accordance with ethical standards for animal use in scientific research, it is noted that mosquitoes are not protected under current laws of Lithuania.

Maintenance of mosquitoes

We analysed P. B. Šivickis parasitology laboratory-reared *Culex quinquefasciatus* and *Cx. pipiens* f. *molestus* mosquitoes. The colonies were maintained as described in Žiegytė et al. study [21]. Briefly, two species of mosquitoes were kept in separate rooms in a nylon netted cage (45×45×120 cm) under controlled conditions (room temperature 23±1° C; humidity 50–60%; photoperiod 14:10 light: dark). Adult insects were provided with cotton wools saturated with 5% saccharose solution. Larvae were fed with aquarium fish food flakes ("JBL NovoRed", JBL GmbH & Co. KG, Germany).

Mosquitoes' dissection

Mosquito females of *Cx. quinquefasciatus* and *Cx. pipiens* f. *molestus* were haphazardly collected with an insect aspirator from the colonies (n=39 of each species). Before dissection, mosquitoes were euthanised by shaking vigorously to stun them in an insect aspirator. The

mosquito wings and legs were removed. The dissection was performed under the binocular stereoscopic microscope. Each mosquito was carefully separated into two segments, the thorax with head and abdomen. The abdomen was placed in a drop of saline, and the midgut of the mosquito was extracted. The midguts were pooled up to 3–4 in sterile microtubes and frozen at -20 °C for microbiota analysis. To prevent contamination of samples, new dissecting needles were used for each pool of dissected insects.

DNA extraction and 16 S rRNA sequencing

The DNA was extracted from frozen midguts using a Pure Link Microbiome DNA Purification Kit (Invitrogen, Thermo Fisher Scientific, CA, USA). Bound DNA was eluted in 70 µL of elution buffer. Genomic DNA quality (OD260/280 between 1.8 −2.0) was measured with NanoDrop™ One (Thermo Scientific, Waltham, MA, USA). Sequencing of the 16 S rRNA gene amplicons utilized over 200 ng of DNA at a concentration of 20 ng/µL. The procedure was outsourced to Novogene Bioinformatics Technology Co. (London, UK). DNA libraries were prepared using the NEBNext® Ultra™ II DNA Library Prep Kit from New England Biolabs (MA, USA). Illumina MiSeq sequencing was performed on a single lane, generating 251-base paired-end reads targeting the V4 variable region of the 16 S rRNA gene. Barcoded universal primers (515 F/806R) were employed in the sequencing of mosquito midgut samples, *Cx. quinquefasciatus* ($n=13$) and *Cx. pipiens* f. *molestus* ($n=13$). The raw 16 S rRNA sequences obtained from mosquito midguts were deposited at the SRA repository (Bioproject No. PRJNA1114695).

Identification and removal of contaminants from the sequencing data

Extraction reagent controls were set in which the DNA extraction processes were followed using the same conditions as for the samples but using water as template. DNA amplification was subsequently carried out on the extraction controls under the same conditions applied to the other samples. To statistically identify potential contaminant DNA in the samples intended for 16S rRNA gene sequencing, the 'decontam' package [22] was utilized, employing the 'prevalence' method. This method defines prevalence as the presence or absence of sequence features across samples and compares the prevalence in actual samples to that in negative controls to detect contaminants. Identified contaminants were then excluded from the dataset prior to further microbiome analysis [22].

16 S rRNA sequences processing

The analysis of 16 S rRNA sequences was conducted through the QIIME 2 pipeline (v. 2023.5) [23]. Initial processing involved denoising and merging of sequences within the fastq files, utilizing the DADA2 software [24] as integrated into QIIME 2. Subsequently, amplicon sequence variants (ASVs) were aligned using MAFFT via q2-alignment plugin [25] and employed to construct a phylogeny with FastTree2 via q2-phylogeny [26]. Taxonomic classification of ASVs was performed using a pretrained classify-sklearn naïve Bayes classifier [27]. This classifier was trained on the SILVA database (release 138) [28], specifically for the V4 region bound by the 515 F/806R primer pair. Taxonomic data tables were then collapsed at the genus level and subjected to filtration to exclude taxa with fewer than 10 total reads and presence in less than 3 samples within each dataset.

Statistical analysis of microbial diversity and abundance

Alpha and beta diversity metrics were computed through the q2-diversity plugin in QIIME 2 [23]. Shannon diversity index [29], Pielou's evenness index [30], Faith's phylogenetic diversity index [31] and observed features [32] were compared between the mosquito using the Kruskal–Wallis test ($p<.05$) within QIIME 2 [23]. Beta diversity was evaluated using the Bray-Curtis dissimilarity index [33] and compared between groups using the PERMANOVA test ($p<.05$) also implemented in QIIME 2 [23]. Bacterial variability within the population, known as dispersion, was computed using the 'betadisper' function in the Vegan package [34] within R ver. 4.2 [35]. The dispersion between the species was further analyzed using the ANOVA test ($p<0.05$).

The disparities in taxa abundance between the mosquito species were evaluated using the ANOVA-like differential expression package 'ALDEx2' [36] within the R program (ver. 4.2.) [35]. This approach employs a centered log ratio (clr) transformation, utilizing the geometric mean of read counts in each sample to assess relative abundance [37]. Statistical comparisons were conducted using a t-test ($p\leq0.05$). Visual representation of shared taxa between different conditions was generated using Venn diagrams, facilitated by an online tool (http://bioinformatics.psb.ugent.be/webtools/Venn/; accessed on 17 April 2023).

Comparative network analysis of microbiota assembly in mosquitoes

Co-occurrence networks were derived for each experimental condition based on taxonomic profiles, employing the Sparse Correlations for Compositional data (SparCC) approach for correlation matrix calculation [38], in the R ver 4.2 [35]. The analysis included only significant positive correlations (weight>0.7) or negative

correlations (weight < -0.7). Network analysis and visualization were performed using Gephi 0.9.2 software [39]. Topological parameters, encompassing node and edge counts, network diameter, average and weighted degrees, average path length, modularity, number of modules, and average clustering coefficient, were computed to characterize each network.

The Core Association Network (CAN) was utilized to examine common nodes and edges across different networks. The core structures of networks from two mosquito species were identified using the Anuran toolbox [40] with default configurations. This analysis was carried out within the Anaconda Python environment [41].

Microbial networks underwent comparison between conditions using the Network Construction and Comparison for microbiome data (NetCoMi) package [42] in R ver 4.2 [35]. A differential network was generated finding the correlations that vary between identical taxa in two bacterial networks. An association analysis gauged similarities between networks via shared nodes and edges using the same network layout in both groups. Two p-values, $P(J \leq j)$ and $P(J \geq j)$, were computed for each Jaccard index, indicating the probability of observing the Jaccard index value equal to or less than, or greater than or equal to, the expected value at random (significance at $p < 0.05$). The similarity between networks was further explored using the Jaccard index, considering various centrality measures, including degree, betweenness, closeness, eigenvector centrality, and hub taxa. This index measures the similarity between nodes with centrality scores above the 75% quartile, ranging from 0 (completely dissimilar) to 1 (identical).

To assess clustering dissimilarity in networks, the adjusted Rand index (ARI) was calculated, with values ranging from −1 to 1. Positive or negative ARI values indicate higher or lower clustering than random, respectively, with identical clustering having an ARI value of 1 and dissimilar clustering having an ARI value of 0 [42].

To assess the network's robustness to node removal, the Network Strengths and Weaknesses Analysis (NetSwan) package was utilized [43]. Various node removal strategies, including random, betweenness centrality, degree, and cascading, were executed to gauge network tolerance in terms of connectivity loss. The standard error for connectivity loss was computed, accounting for variability, using a threshold of 0.975. The proportion of nodes removal required to achieve connectivity loss of 80% for each network was evaluated. Bacterial co-occurrence network analysis and visualization were conducted using the igraph package [44].

Furthermore, the robustness of microbial networks to node addition was evaluated by employing the Network analysis and visualization igraph package [44]. Nodes were systematically added in increments ranging from 1 to 1000, and network connectivity was quantified based on the degree metric of the largest connected component (LCC) and average path length. Statistical significance for LCC and average path length was determined using a Wilcoxon signed-rank test, with p-values adjusted using the Benjamini-Hochberg (BH) method to control the false discovery rate. Additionally, bootstrapping was performed to derive confidence intervals for the variables, with significance established at a threshold of $p < 0.05$.

Local connectivity of Escherichia-Shigella and Wolbachia in the microbial communities of Cx. Quinquefasciatus and cx. Pipiens f. molestus and in silico removal of target taxa

In order to explore the relationship between *Escherichia-Shigella/Wolbachia* and other bacterial members of the microbiota, the *Escherichia-Shigella/Wolbachia* was depicted in connection with all taxa it exhibited positive or negative correlations with, creating *Escherichia-Shigella/Wolbachia* sub-networks. These sub-networks were exported and analysed by comparing interacting partners between the conditions. The analyses were conducted using Gephi software [39] and the online tool of Venn diagrams (http://bioinformatics.psb.ugent.be/webtools/Venn/; accessed on 17 April 2023).

To further investigate the nestedness of *Escherichia-Shigella/Wolbachia* in the networks, we conducted an in-silico experiment where *Escherichia-Shigella/Wolbachia* was removed from the networks to observe its effect on node centrality distribution and network robustness. The comparisons of the networks with and without *Escherichia-Shigella/Wolbachia* in *Cx. quinquefasciatus* and *Cx. pipiens* f. *molestus* were performed following the procedures as described above.

Keystone taxa identification

The keystone taxa were identified based on three established criteria, as outlined in previous studies [45, 46]: (i) ubiquitous presence, (ii) high eigenvector centrality (≥0.75), and (iii) high relative abundance (clr value exceeding the average).

Results

Differential structure of bacterial microbiota in Culex pipiens f. molestus and Culex quinquefasciatus

After statistically identifying and removing DNA features classified as contaminants (Table S1), the bacterial community composition and diversity of mosquito microbiota were analyzed using 16 S rRNA gene profiling, followed by a comparative network analysis to assess microbial sample similarity between two mosquito species and identify species-specific patterns of *Escherichia-Shigella* and *Wolbachia* nestedness. The comparison of microbial composition between *Culex pipiens* f. *molestus* and *Culex quinquefasciatus* species showed differences

in alpha (i.e., Shannon diversity index, Pielou's evenness index, Faith's phylogenetic diversity index, and observed features) and beta diversity (Bray Curtis index and beta dispersion) metrics. Significantly higher Shannon and Pielou's indices were observed ($p<0.05$; Fig. 1A, B) in the *Cx. quinquefasciatus* group compared to *Cx. pipiens* f. *molestus*, while the differences in Faith's phylogenetic diversity and observed features did not have statistical significance between the groups. However, the compositional analysis revealed that two mosquito species shared most of the existing bacteria in the microbiota (97% in total of 820 taxa; Fig. 1C), while 7 and 15 were unique to *Cx. pipiens* f. *molestus* and *Cx. quinquefasciatus*, respectively (Table S2). Comparison of Bray-Curtis dissimilarity indices and beta dispersion between the species showed significant differences (PERMANOVA, F=19.36, $p=0.001$; ANOVA, F=10.023, $p=0.001$, respectively; Fig. 1D). Differential relative abundance analysis identified 10 taxa, which had significantly higher abundance in the microbiota of *Cx. pipiens* f. *molestus*, and 16 taxa

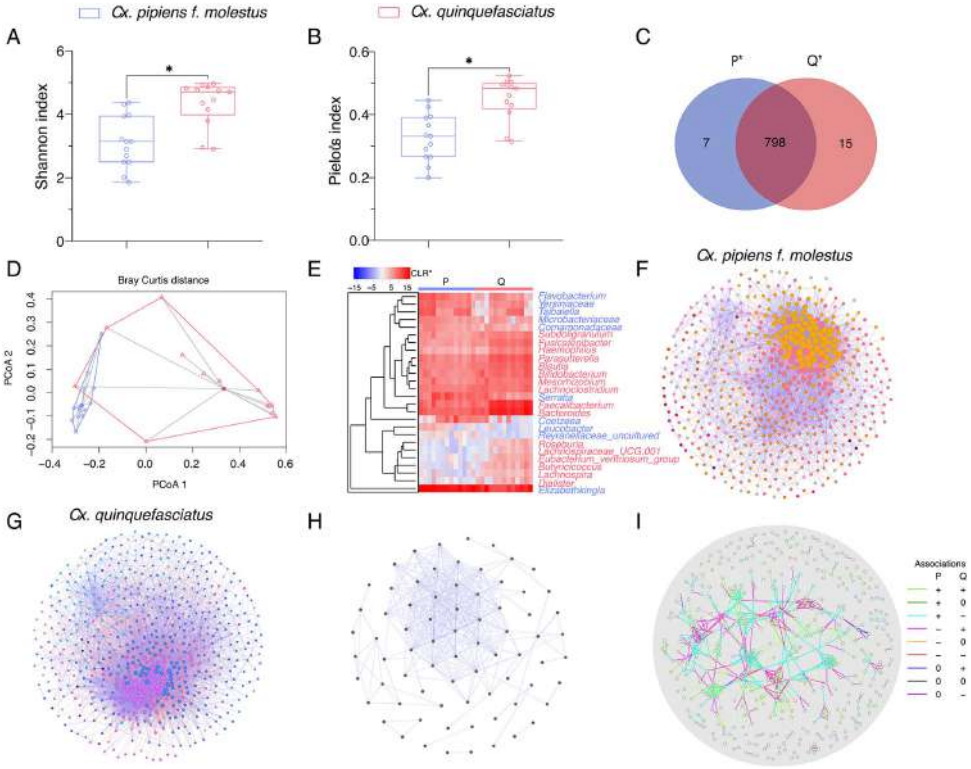

Fig. 1 Differences in mosquito microbiota diversity and community assembly between *Culex pipiens* f. *molestus* and *Culex quinquefasciatus*. (**A**) Shannon diversity and (**B**) Pielou's evenness indices showed significant differences between microbiota of *Cx. pipiens* f. *molestus* and *Cx. quinquefasciatus*. (**C**) Venn diagram showing the number of bacterial taxa that are shared or unique among the networks of two mosquito species. *$p<0.05$ (**D**) Beta diversity of mosquito microbiota of two species represented in PCoA plot obtained by Betadisper function. There are significant differences in dispersions (variances) (ANOVA, $p<0.01$). (**E**) Heatmap representing the abundance (expressed as *Centered Log-Ratio) of the 10 taxa whose abundance was higher *in Cx. pipiens* f. *molestus* group and 16 taxa whose abundance was higher in *Cx. quinquefasciatus*. (**F**, **G**) Bacterial co-occurrence networks were inferred from 16SrRNA sequences obtained from laboratory reared mosquitoes of two species (**F**) *Cx. pipiens* f. *molestus* and (**G**) *Cx. quinquefasciatus* (SparCC > 0.5 or < -0.5). Nodes correspond to taxa (family or genus level). The colours of nodes specify modules in which taxa occur. The size of nodes is related to their eigenvector centrality, the bigger the node, the higher eigenvector centrality value it has. Positive (purple) and negative (coral) correlations are shown by the colour of the edges. (**H**) Core Association Network (CAN) (SparCC > 0.75 or < -0.75). Positive correlations are shown by purple edges. Nodes correspond to taxa. (**I**) Differential network between *Cx. pipiens* f. *molestus* and *Cx. quinquefasciatus* natural networks illustrating the correlations that vary between identical taxa in two bacterial networks. Grey nodes represent taxa, and edges represent differential associations between taxa. P* - *Cx. pipiens* f. *molestus*; Q* - *Cx. quinquefasciatus*; CLR* - Centered log ratio

Table 1 Network features

Network features	Cx. pipiens f. molestus	Cx. quinquefsciatus
Nodes	592 (805)	642 (813)
Edges	6577	10,514
Positive	4185 (64%)	5783 (55%)
Negative	2392 (36%)	4731 (45%)
Network diameter	9	7
Average degree	22.22	32.754
Weighted degree	4.219	2.571
Average path length	3.14	2.871
Modularity	1.392	2.89
Number of modules	45	40
Average clustering coefficient	0.454	0.489

Table 2 Jaccard index for *Cx. Pipiens* f. *molestus* and *cx. Quinquefasciatus* networks

Local centrality measures	Cx. pipiens f. molestus vs. Cx. quinquefasciatus		
	Jacc[a]	*P*(<=Jacc)	*P*(>=Jacc)
Degree	0.458	0.999994	0.000010*
Betweenness centr.	0.459	0.999995	0.000008*
Closeness centr.	0.470	0.999999	0.000002*
Eigenvec. centr.	0.419	0.998997	0.001495*
Hub taxa	0.507	1.000000	0.000000*

[a]Jaccard index

*$p<0.05$

more abundant in *Cx. quinquefasciatus* (Welch t-test, $p<0.05$; Fig. 1E).

Bacteria co-occurrence networks were inferred to compare microbiota assembly between two mosquito species (Fig. 1F, G). Visual inspection of the networks and their features revealed some differences between the species (Fig. 1F, G; Table 1). The network of *Cx. quinquefasciatus* consists of a higher number of edges compared to the *Cx. pipiens* f. *molestus*, while the number of nodes is similar between the species (Fig. 1F, G; Table 1). This relates to a higher value of average degree in *Cx. quinquefasciatus* group compared to the other mosquito species as this topological parameter indicates an average number of edges connected to a node (Table 1). However, the weighted degree value is greater on *Cx. pipiens* f. *molestus* species referring to stronger correlations in the network. Although the number of modules is similar in both groups, the lower value of modularity suggests higher interconnectedness between modules in *Cx. pipiens* f. *molestus* network compared to *Cx. quinquefasciatus* (Table 1). Core Association Network (CAN) analysis revealed 74 core associated nodes and 337 positive edges between the groups of *Cx. pipiens* f. *molestus* and *Cx. quinquefasciatus* (Fig. 1H). Furthermore, network dissimilarity analysis revealed differential associations between taxa in the groups (Fig. 1I).

A statistical network comparison analysis was performed to evaluate the differences in local centrality measures between the groups (Table 2). Jaccard index values for a degree, hub taxa, betweenness, closeness, and eigenvector centrality between the two mosquito species varied from 0.4 to 0.5, which were significantly higher than expected by random ($P(\geq Jacc)<0.05$) suggesting a moderate degree of similarity.

Placement of Escherichia-Shigella *and* Wolbachia *across equivalent modules in* Culex pipiens f. molestus *and* Culex quinquefasciatus *Microbiota networks*

The networks of *Cx. pipiens* f. *molestus* and *Cx. quinquefasciatus* group to 4 major modules composed of 89% and 91% of nodes of a whole network, respectively. The biggest modules of *Cx. pipiens* f. *molestus* (P4 – the total of 208 nodes; Fig. 2A) and *Cx. quinquefasciatus* (Q3 – the total of 294 nodes; Fig. 2B) consists of the highest number of unique nodes, 19% and 21%, respectively. The comparison of taxa in these modules showed that 93 (22.7%; Table 3) nodes are shared between the *Cx. pipiens* f. *molestus* and *Cx. quinquefasciatus*. Based on the percentage of taxa shared between the modules, Q3 and P4 exhibit a moderate level of equivalence. In addition, the modules Q3 and P4 accommodate the commensal bacterial taxon *Escherichia-Shigella* (Fig. 2A, B). However, the module Q3 (294 nodes) of *Cx. quinquefasciatus* could be considered more equivalent to P3 (105 nodes) module of *Cx. pipiens* f. *molestus* based on the percentage of shared taxa of 24.3% (Table 3).

Notably, in *Cx. pipiens* f. *molestus*, *Wolbachia* was found in module P3 (Fig. 2A), while it formed a distinctive module in *Cx. quinquefasciatus* (Fig. 2B). The highest equivalence between the species was estimated between the second major modules consisting of 143 (P1) and 191 (Q1) nodes. Between the modules, 92 nodes are shared (38%; Table 3). Modules P2 (71 nodes) and Q2 (76 nodes) are similar in size and share 34 nodes (30.1%) (Table 3). The network of *Cx. quinquefasciatus* has a smaller module Q4 of 28 nodes, which does not have an equivalent in the network of *Cx. pipiens* f. *molestus*, however, 14 nodes are shared with P4 module (6.3%) (Table 3). Visual inspection of interactions inside modules shows that positive edges are dominant in both species. The same pattern of interactions was seen in the networks of *Cx. pipiens* f. *molestus* and *Cx. quinquefasciatus* where the two biggest modules of a network had mostly negative edges between each other (Fig. 2A, B). An estimated association analysis was performed to further analyse microbial associations in the networks (Fig. 2C, D). In the networks of the same layout the clusters and modules are seen to be different between the species. However, one cluster is similar between the networks (Fig. 2C, D, red cluster), consisting of mostly shared taxa with higher

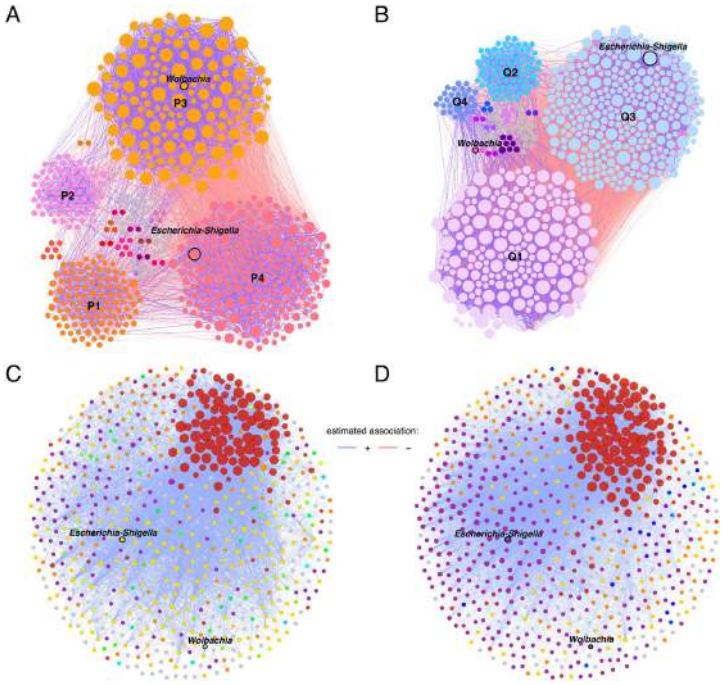

Fig. 2 Differences in mosquito bacterial modules between *Culex pipiens* f. *molestus* and *Culex quinquefasciatus*. (**A**, **B**) Bacterial co-occurrence networks of (**A**) *Cx. pipiens* f. *molestus* and (**B**) *Cx. quinquefasciatus* divided by modules. Node colours are based on modularity class metric, each module is represented by a different colour. Grey colored nodes represents single node modules. The size of nodes is related to their eigenvector centrality, the bigger the node, the higher eigenvector centrality value it has. Positive (purple) or negative (coral) correlations are shown by the colour of the edges. Bacterial taxa (family or genus level) with at least one connection are symbolized by nodes, whilst connected edges represent correlations between them (SparCC ≥ 0.5 or ≤ -0.5). (**C**, **D**) Co-occurrence networks in the same layout were extrapolated from the microbiota of (**C**) *Cx. pipiens* f. *molestus* and (**D**) *Cx. quinquefasciatus*. Bacterial taxa (family or genus level) with at least one connection are symbolized by nodes, whilst connected edges represent a significant correlation between them (SparCC ≥ 0.75 or ≤ -0.75). Node colours are based on determined clusters and sized according to the node's eigenvector centrality. Positive (purple) or negative (red) correlations are shown by the colour of the edges

Table 3 The percentage of taxa shared between different modules

	P1	P2	P3	P4
Q1	38%	1.9%	4.2%	9.9%
Q2	0.9%	30.1%	2.3%	8.0%
Q3	5.8%	10.3%	24.3%	22.7%
Q4	1.2%	2.1%	2.3%	6.3%

eigenvector centrality values. The adjusted Rand index (ARI) was 0.151 (p=0.000), showing some clustering similarities between the networks.

Based on taxa ubiquitousness, relative abundance and eigenvector centrality (>0.7), keystone taxa were identified in the networks of *Cx. pipiens* f. *molestus* and *Cx. quinquefasciatus*. One keystone taxon, *Escherichia-Shigella*, was identified in the microbiota of *Cx. pipiens* f. *molestus* (P4 module; Fig. 2A). This taxon has positive correlations with other taxa from the P4 module (Figs. 2A and 3A). However, only negative correlations are formed with taxa of the P3 module (Fig. 3A). Bacteria *Escherichia-Shigella*, as a keystone taxon, was also identified in the microbiota of *Cx. quinquefasciatus* alongside *Lachnoclostridium*, *Robinsoniella*, *Desulfovibrio*, *Muribaculum*. All keystones except *Muribaculum* are part of the Q3 module (Fig. 2B). The keystones have positive correlations between each other and with other taxa from the Q3 modules; negative correlations are formed with taxa from the Q1 module (Figs. 2B and 3B). The placement of the taxon *Escherichia-Shigella* could be considered equivalent inside the networks of two mosquito species. It has correlations with 93 (Fig. 3A) and 161 (Fig. 3B) nodes in the networks of *Cx. pipiens* f. *molestus* and *Cx. quinquefasciatus*, respectively. The comparison

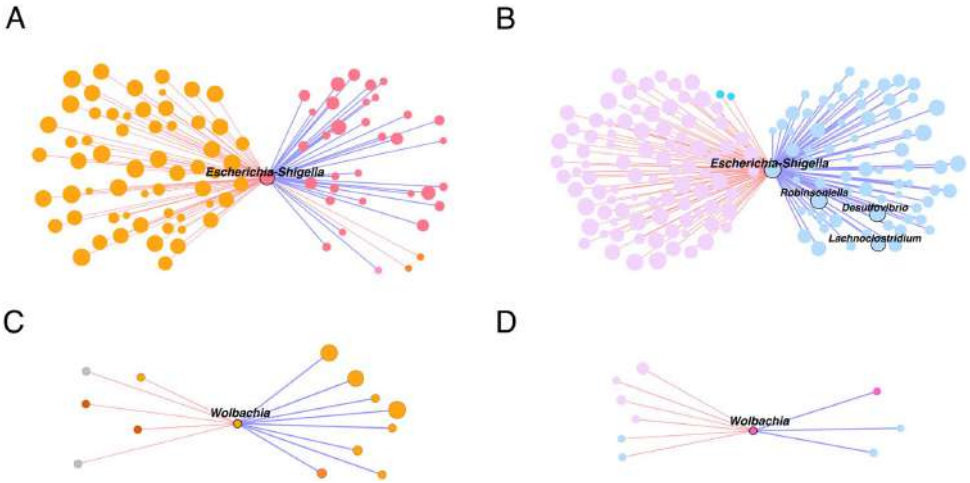

Fig. 3 Differences in the local connectivity of *Escherichia-Shigella* and *Wolbachia* between *Culex pipiens* f. *molestus* and *Culex quinquefasciatus* microbiota. (**A**, **B**) Sub-networks of the local connectivity of *Escherichia-Shigella* and (**C**, **D**) *Wolbachia* were extracted from (**A**, **C**) *Cx. pipiens* f. *molestus* and (**B**, **D**) *Cx. quinquefasciatus* natural networks. The size of nodes is related to their eigenvector centrality, the bigger the node, the higher eigenvector centrality value it has. Positive (purple) or negative (coral) correlations are shown by the colour of the edges. Bacterial taxa (family or genus level) with at least one connection are symbolized by nodes, whilst connected edges represent correlations between them (SparCC ≥ 0.5 or ≤ -0.5)

of interacting bacteria showed 55 shared taxa between the species.

We determined the associations of common symbiont *Wolbachia* in the networks of both groups. The symbiont was prevalent in all samples of the study, which abundance did not differ significantly between the mosquito species. The number of ASVs classified as *Wolbachia* ranged from 3 to 512 in *Cx. pipiens* f. *molestus* samples and from 31 to 892 in *Cx. quinquefasciatus* samples. *Wolbachia* belonging to the P3 module of *Cx. pipiens* f. *molestus* has positive interactions within the P3 module and mostly negative interactions with nodes from other modules (Figs. 2A and 3C). *Wolbachia* in the network of *Cx. quinquefasciatus* forms a distinctive module together with bacteria SB-5 belonging to phylum Bacteroidota. It forms mostly negative interactions within the network with nodes from modules Q3 and Q1. The placement of *Wolbachia* inside the networks is not equivalent. The symbiont has 13 (Fig. 3C) and 9 (Fig. 3D) correlating nodes within the networks of *Cx. pipiens* f. *molestus* and *Cx. quinquefasciatus*, respectively. None of the interacting taxa are shared between the species.

While *Escherichia-Shigella* and *Wolbachia* do not cluster together in the network of *Cx. pipiens* f. *molestus* (Fig. 2C), in the network of *Cx. quinquefasciatus* (Fig. 2D) mentioned bacteria belong to the same cluster.

Effect of Escherichia-Shigella *and* Wolbachia *on network robustness in* Culex pipiens f. molestus *and* Culex quinquefasciatus

An in-silico experiment was carried out to assess the potential influence of *Escherichia-Shigella* and *Wolbachia* on the microbial assembly and structure of *Cx. pipiens* f. *molestus* and *Cx. quinquefasciatus.* Only minor changes were recorded in the networks' features after removing either *Escherichia-Shigella* or *Wolbachia* (Table S3). After the removal of target taxa, an increase in the number of modules was recorded in all networks (Table S3). The clusters with which *Wolbachia* associated changed after the removal of *Escherichia-Shigella* in the networks of *Cx. pipiens* f. *molestus* (Figure S1A) and *Cx. quinquefasciatus* (Figure S1B). However, the removal of *Wolbachia* from the networks did not change the clusters of *Escherichia-Shigella* (Fig. 2C, D; Figure S1C, D). Local centrality measures of natural networks were compared to the ones with removed taxon *Escherichia-Shigella* or *Wolbachia* using the Jaccard index (Table S4). All measures were significantly higher than expected by random with high Jaccard index values (Table S4). Differential network analysis did not detect any differentially associated taxa. These findings suggest that target taxa removal did not greatly affect the node centrality traits of a network.

To further analyse the differences between the species and how target taxa removal or addition affects the network, we performed multiple comparisons of

network robustness after node removal and addition (Fig. 4, Figure S2, and Figure S3). Node removal by cascading attack had the most significant impact on connectivity in all networks (Figure S2). The difference in network resistance to node removal was evaluated by calculating the delta value of the percentage of nodes removed. The highest delta value between the networks of *Cx. pipiens* f. *molestus* and *Cx. quinquefasciatus* was recorded at 80% of connectivity loss (Fig. 4A, D, G). The delta between the natural networks was 5% (Fig. 4A). The target taxa removal from the networks caused a slight increase in the delta value of robustness to 7% and 6% of networks without *Escherichia-Shigella* (Fig. 4D) and *Wolbachia* (Fig. 4G), respectively. Node addition did not greatly affect the network robustness based on the largest connected component ((LCC); Fig. 4B, E, H) and the average path length (Fig. 4C, F, I) of neither of the species (Figure S3). However, the network of *Cx. quinquefasciatus* initially has a bigger LCC and shorter average path length compared to *Cx. pipiens* f. *molestus* in all comparisons (Fig. 4). The difference in the size of the LCC between the species has increased between the networks without *Escherichia-Shigella* (Fig. 4E) and decreased between the networks without *Wolbachia* (Fig. 4H) compared to the natural network (Figure S3). No change in average path length was recorded between *Cx. pipiens* f. *molestus* and *Cx. quinquefasciatus* after removing target taxa from the networks (Fig. 4C, F, I).

The robustness of natural networks was compared to that of the ones without the target taxa. In silico removal

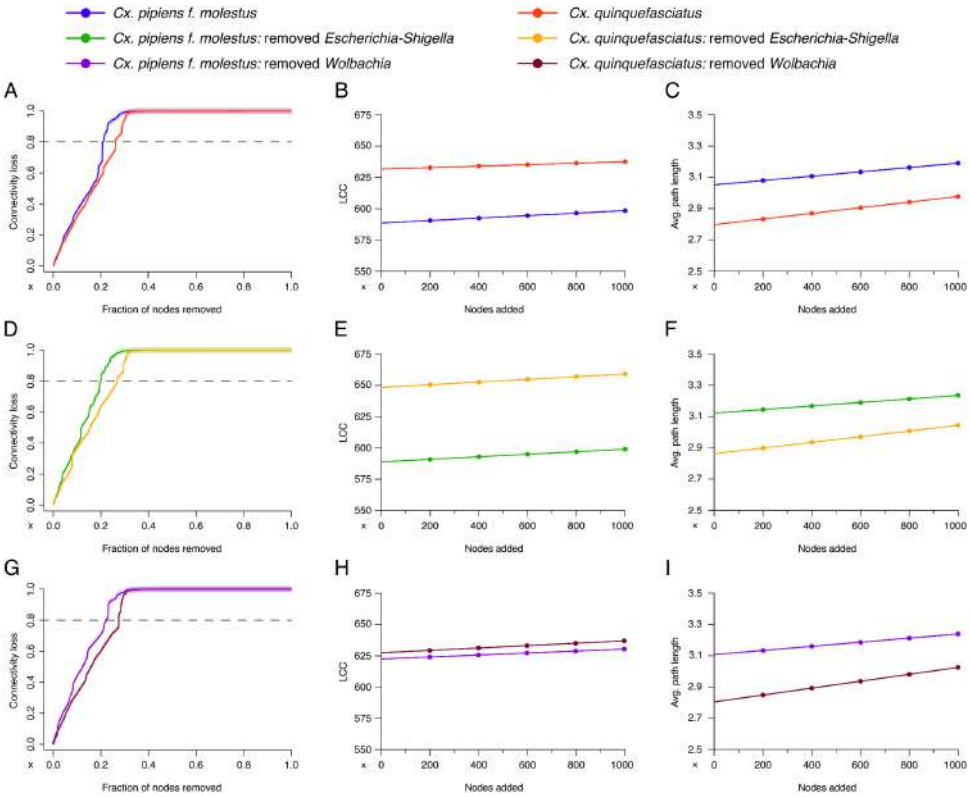

Fig. 4 Differences in the microbial network response to node removal and addition between *Culex pipiens* f. *molestus* and *Culex quinquefasciatus*. (**A**, **D**, **G**) The resistance to cascading attack was measured and compared between *Cx. pipiens* f. *molestus* and *Cx. quinquefasciatus* (**A**) natural networks, (**D**) networks without *Escherichia-Shigella* or (**G**) *Wolbachia*. The robustness to nodes addition (from 0 to 1000) based on the size of the largest connected component (LCC) (**B**, **E**, **H**) and average path length (avg. path length) (**C**, **F**, **I**) was measured and compared between *Cx. pipiens* f. *molestus* and *Cx. quinquefasciatus* natural networks (**B**, **C**), networks without *Escherichia-Shigella* (**E**, **F**) and *Wolbachia* (**H**, **I**). Different curve colours represent different groups

of *Escherichia-Shigella* and *Wolbachia* did not have the same effects on the network robustness of *Cx. pipiens* f. *molestus* and *Cx. quinquefasciatus* (Figure S3). The difference in connectivity loss between the natural networks and without the target taxa was only noticed in *Cx. pipiens* f. *molestus* group (Figure S3A; S3D; S3G; S3J). Cascading removal of nodes showed deltas of -4% for the network without *Escherichia-Shigella* and −2% for the network without *Wolbachia* (Figure S3A, D). There was no change in the size of LCC in the network of *Cx. pipiens* f. *molestus* without *Escherichia-Shigella* (Figure S3B) and *Cx. quinquefasciatus* without *Wolbachia* (Figure S3K). However, LCC has increased in the network of *Cx. pipiens* f. *molestus* without *Wolbachia* (Figure S3E). and *Cx. quinquefasciatus* without *Escherichia-Shigella* (Figure S3H). The average path length has slightly increased after taxa removal in all the networks (Figure S3C, F, I, L).

Discussion

Our research uncovers complex ecological interactions and patterns among commensal and endosymbiotic microbes. These microbes are crucial for synthesizing essential nutrients and significantly influence mosquito health and ability to transmit diseases, aligning with findings from Minard et al. [47] and Douglas [48] that highlight the essential role of microbial communities in insect nutritional ecology and overall fitness.

There is limited published literature on the specific microbiota network complexity of *Cx. pipiens* f. *molestus* and *Cx. quinquefasciatus*. Our results revealed a moderate degree of similarity between the microbiota of the two mosquito species. This similarity may be attributed to their taxonomic closeness and shared ecological niches, echoing the results of other studies, showing that closely related mosquito species tend to harbor similar microbial communities due to ecological and evolutionary constraints [20]. These findings suggest that a stable nested pattern of *Wolbachia* endosymbionts might be observed in both species, while some differences might appear in the structure surrounding the commensal bacteria *Escherichia-Shigella*.

First, we compared the microbial diversity between the species, which showed a high number of shared taxa between *Culex pipiens* f. *molestus* and *Culex quinquefasciatus*, highlighting the influence of the ecological setting on microbiota composition and diversity. The environment in which both mosquito species were raised was controlled and stable, which likely led to the high similarity in their microbiota diversity. This observation aligns with the findings of Muturi et al. [49], who reported that environmental factors play a pivotal role in shaping the mosquito microbiota, thereby affecting the host's vectorial capacity. The shared microbiota between these species suggests common ecological pressures and evolutionary histories that influence their microbial community structures [50]. Our results show that variability of microbial composition is different between the species, *Cx. quinquefasciatus* having more heterogenous communities compared to *Cx. pipiens* f. *molestus*. Lower beta dispersion in *Cx. pipiens* f. *molestus* could imply that the community structure is more stable and less influenced by disturbances. These findings are supported by the robustness analysis showing *Cx. pipiens* f. *molestus* network being more resilient compared to *Cx. quinquefasciatus* (Fig. 4).

While both networks exhibit a degree of complexity, *Cx. quinquefasciatus* has a network characterized by a higher number of edges, suggesting more interactions among microbial taxa (Fig. 2A, B; Table 1). Despite being reared in similar settings, the networks still retain some distinct characteristics influenced by host-specific factors and microbial dynamics. The structural similarities in their microbial networks underscore the potential for common microbial interaction patterns across different mosquito species [20, 51].

Bacterial co-occurrence networks revealed a structured pattern of interactions between commensal bacteria *Escherichia-Shigella* and 55 taxa present in the microbiota of *Cx. pipiens* f. *molestus* and *Cx. quinquefasciatus*. The commensal was identified as a keystone taxon in both species, which points to its critical role within the microbial community (Fig. 3A, B). The keystones likely facilitate essential ecological functions and interactions within their networks, similar to findings in other systems where keystone species contribute disproportionately to community structure and function [52]. Enterobacteriaceae is an important contributor to normal mosquito microbiota, commonly found in larval and adult mosquitoes of different genera such as *Culex*, *Aedes*, *Anopheles* etc [53, 54]. The nature of commensals' assembly is driven by nutrient (carbon source) availability, with Enterobacteriaceae being one of the fastest growing bacteria [55].

We did not observe a consistent nested pattern of *Wolbachia*, which goes against our hypothesis. *Wolbachia*'s position in the network appears less central, with fewer interactions compared to *Escherichia* (Fig. 3). *Wolbachia*, present in over 60% of insect species, is considered highly important due to its significant effects on mosquito lifespan and immune response. It enhances the mosquito's defense mechanisms and may outcompete pathogens for cellular resources, inhibiting the transmission of various pathogens [2]. Rasgon and Scott [56] demonstrated that a single *Wolbachia* strain infects *Cx. pipiens*, with infection frequencies near fixation across all populations sampled over two years. Their findings suggest that *Wolbachia* has the potential to invade vector populations and could be leveraged in strategies to reduce vector-borne diseases. There is limited information on how *Wolbachia* impacts

the microbiota structure of mosquitoes. Lee et al. [57] demonstrated that *Wolbachia* tends to have antagonistic relationships with other bacteria in the host's microbial community. A similar pattern has been observed in other insect species, where *Wolbachia*-infected individuals exhibit reduced overall microbial diversity compared to non-infected counterparts [15–17]. The nuanced role of *Wolbachia* as a less interconnected taxon in our study within *Culex* mosquitoes suggests a specialized function within the mosquito microbiota, potentially related to its pathogen-blocking capabilities and influence on host reproductive biology, as documented in previous studies [2, 58]. Although we did not perform strain-specific analyses to determine if the two mosquito species carry identical *Wolbachia* strains, both species were reared under the same controlled laboratory conditions, making it unlikely that they harbor different *Wolbachia* strains. Nonetheless, future studies should incorporate strain typing methods to definitively confirm the similarity of *Wolbachia* strains between the mosquito species.

An in-silico experiment was conducted in this study to understand the impact of removing *Escherichia-Shigella* and *Wolbachia* on the microbial community structure of *Cx. pipiens* f. *molestus* and *Cx. quinquefasciatus*. The results showed only minor changes in network features upon removing these taxa. However, an increase in network modules was observed, suggesting a certain role in microbial network assembly. An increase in the number of modules, with a mostly consistent number of nodes and edges in the network representing associations within the community, indicates an abundance of weaker, interchangeable interactions. This suggests that the network is more resilient and capable of withstanding disturbances in both mosquito species. Such behavior in the interactions within the network was noted in the study by the Coyte et al. (2021) [59]. The centrality measures, indicative of network connectivity and importance, remained significantly high even after taxa removal, indicating the robustness of the microbial communities against the loss of these specific taxa. This finding suggests that certain taxa may have broader ecological roles or competitive advantages within the microbiota, impacting network robustness and resilience [52, 60].

Conclusions

This study provides a comprehensive analysis of the microbial communities within two mosquito species, *Culex pipiens* f. *molestus* and *Culex quinquefasciatus*, with a specific focus on the differential nested patterns of *Wolbachia* endosymbionts and the commensal bacterial taxon *Escherichia-Shigella*. The high similarity in microbiota composition between *Cx. pipiens* f. *molestus* and *Cx. quinquefasciatus* can be attributed to the controlled and stable laboratory conditions under which they were reared. This environmental consistency likely facilitated the development of similar microbial communities, reflecting common ecological pressures and evolutionary histories. However, despite this overall similarity, the beta diversity metrics and network analyses indicated distinct patterns of microbial interactions within each species.

Escherichia-Shigella was identified as a keystone taxon in both mosquito species, highlighting its critical role within the microbial community. Its interactions with a substantial number of taxa suggest it plays a significant role in shaping the microbial network structure. Conversely, *Wolbachia* did not exhibit the expected stable nested pattern and showed fewer interactions within the microbial networks. This nuanced role of *Wolbachia* suggests it may function more as a specialized entity within the microbiota, influencing specific aspects of mosquito physiology and pathogen transmission.

The differential nested patterns of *Escherichia-Shigella* and *Wolbachia* provide valuable insights into the assembly and dynamics of mosquito microbial communities. Understanding these interactions is crucial for developing innovative strategies to control mosquito-borne diseases. Future studies should explore the mechanisms driving these interactions and their implications for vector competence and disease transmission, particularly in natural environments where mosquito-microbiota interactions are influenced by more variable and complex ecological factors.

Abbreviations

Avg	Average
ARI	Adjusted Rand Index
CAN	The Core Association Network
F	Form
LCC	Largest Connected Component
SparCC	The Sparse Correlations for Compositional data

Supplementary Information

The online version contains supplementary material available at https://doi.org/10.1186/s12866-024-03593-x.

Supplementary Material 1
Supplementary Material 2
Supplementary Material 3
Supplementary Material 4
Supplementary Material 5
Supplementary Material 6
Supplementary Material 7
Supplementary Material 8

Author contributions

A.C.-C. and V.P. conceived the study and supervised the work. J.A., A.M., L.A.-D., D.O., A.W.-C., L.M.-H., V.P. and R.Ž. performed the analyses. J.A. and A.M. prepared the figures. J.A., A.M. and A.C.-C. drafted the manuscript. All authors revised and accepted the last version of the manuscript.

Funding
This work was supported by the French Government's Investissement d'Avenir program, Laboratoire d'Excellence "Integrative Biology of Emerging Infectious Diseases" (Grant ANR–10–LABX–62–IBEID). VP was supported by the Research Council of Lithuania (LMTLT) (Project No. S-MIP-22-52). AM was supported by the 'Collectivité de Corse', grant: 'Formations superieures' (SGCE-RAPPORT No. 0300).

Data availability
The datasets generated and analysed during the current study are available in the SRA repository (Bioproject No. PRJNA1114695), https://www.ncbi.nlm.nih.gov/sra.

Declarations

Ethical approval
The study utilizes two species of laboratory-reared mosquitoes, *Culex pipiens* f. *molestus* and *Culex quinquefasciatus*. While conducted in accordance with ethical standards for animal use in scientific research, it is noted that mosquitoes are not protected under current laws of Lithuania.

Consent for publication
Not applicable.

Competing interests
The authors declare no competing interests.

Author details
[1]Nature Research Centre, Akademijos 2, Vilnius LT-08412, Lithuania
[2]Laboratoire de Santé Animale, ANSES, INRAE, Ecole Nationale Vétérinaire d'Alfort, UMR BIPAR, Maisons-Alfort F-94700, France
[3]Laboratoire de Recherches Sur Le Développement de L'Elevage (SELMET-LRDE), INRAE, UR 0045, Corte 20250, France
[4]Laboratoire de Virologie, Université de Corse, EA 7310, Corte, France
[5]Animal Biotechnology Department, Center for Genetic Engineering and Biotechnology, Avenue 31 between 158 and 190, P.O. Box 6162, Havana 10600, Cuba
[6]School of Environmental Sciences, University of Guelph, Guelph, ON N1G 2W1, Canada

Received: 19 July 2024 / Accepted: 21 October 2024
Published online: 26 October 2024

References

1. Caminade C, McIntyre KM, Jones AE. Impact of recent and future climate change on vector-borne diseases. Ann N Y Acad Sci janv. 2019;1436(1):157–73.
2. Moreira LA, Iturbe-Ormaetxe I, Jeffery JA, Lu G, Pyke AT, Hedges LM, et al. A Wolbachia symbiont in Aedes aegypti limits infection with dengue, Chikungunya, and Plasmodium. Cell 24 déc. 2009;139(7):1268–78.
3. Simón F, González-Miguel J, Diosdado A, Gómez PJ, Morchón R, Kartashev V. The complexity of zoonotic Filariasis Episystem and its consequences: a multidisciplinary view. Biomed Res Int. 2017;2017:6436130.
4. Huang Y-JS, Higgs S, Vanlandingham DL. Emergence and re-emergence of mosquito-borne arboviruses. Curr Opin Virol févr. 2019;34:104–9.
5. El-Sayed A, Aleya L, Kamel M. Microbiota's role in health and diseases. Environ Sci Pollut Res Int Juill. 2021;28(28):36967–83.
6. Romoli O, Schönbeck JC, Hapfelmeier S, Gendrin M. Production of germ-free mosquitoes via transient colonisation allows stage-specific investigation of host-microbiota interactions. Nat Commun. 11 févr. 2021;12(1):942.
7. Aželytė J, Wu-Chuang A, Žiegytė R, Platonova E, Mateos-Hernandez L, Maye J, et al. Anti-microbiota vaccine reduces avian malaria infection within mosquito vectors. Front Immunol. 2022;13:841835.
8. Ren Z, Li H, Luo W. Unraveling the mystery of antibiotic resistance genes in green and red Antarctic snow. Sci Total Environ 10 mars. 2024;915:170148.
9. Seabourn PS, Weber DE, Spafford H, Medeiros MCI. Aedes albopictus microbiome derives from environmental sources and partitions across distinct host tissues. Microbiologyopen juin. 2023;12(3):e1364.
10. Cobo-López S, Gupta VK, Sung J, Guimerà R, Sales-Pardo M. Stochastic block models reveal a robust nested pattern in healthy human gut microbiomes. PNAS Nexus Juill. 2022;1(3):pgac055.
11. Song C, Rohr RP, Saavedra S. Why are some plant-pollinator networks more nested than others? J Anim Ecol Oct. 2017;86(6):1417–24.
12. Werren JH, Baldo L, Clark ME. Wolbachia: master manipulators of invertebrate biology. Nat Rev Microbiol oct. 2008;6(10):741–51.
13. Johnson KN. The impact of Wolbachia on Virus infection in mosquitoes. Viruses 4 nov. 2015;7(11):5705–17.
14. Torres R, Hernandez E, Flores V, Ramirez JL, Joyce AL. Wolbachia in mosquitoes from the Central Valley of California, USA. Parasit Vectors 10 nov. 2020;13(1):558.
15. Simhadri RK, Fast EM, Guo R, Schultz MJ, Vaisman N, Ortiz L, et al. The gut commensal microbiome of Drosophila melanogaster is modified by the Endosymbiont *Wolbachia*. mSphere. 2017;2:e00287–17.
16. Detcharoen M, Jiggins FM, Schlick-Steiner BC, Steiner FM. Wolbachia endosymbiotic bacteria alter the gut microbiome in the fly Drosophila Nigrosparsa. J Invertebr Pathol. 2023;198:107915.
17. Duan X-Z, Sun J-T, Wang L-T, Shu X-H, Guo Y, Keiichiro M, et al. Recent infection by Wolbachia alters microbial communities in wild Laodelphax striatellus populations. Microbiome. 2020;8:104.
18. Thongsripong P, Chandler JA, Green AB, Kittayapong P, Wilcox BA, Kapan DD, et al. Mosquito vector-associated microbiota: metabarcoding bacteria and eukaryotic symbionts across habitat types in Thailand endemic for dengue and other arthropod-borne diseases. Ecol Evol. 2018;8:1352–68.
19. Chandler JA, Liu RM, Bennett SN. RNA shotgun metagenomic sequencing of northern California (USA) mosquitoes uncovers viruses, bacteria, and fungi. Front Microbiol. 2015;6:185.
20. Hegde S, Khanipov K, Albayrak L, Golovko G, Pimenova M, Saldaña MA, et al. Microbiome Interaction Networks and Community structure from Laboratory-Reared and Field-Collected Aedes aegypti, Aedes albopictus, and Culex quinquefasciatus Mosquito vectors. Front Microbiol. 2018;9:2160.
21. Žiegytė R, Bernotienė R, Bukauskaitė D, Palinauskas V, Iezhova T, Valkiūnas G. Complete sporogony of *Plasmodium relictum* (lineages pSGS1 and pGRW11) in mosquito *Culex pipiens pipiens* form molestus, with implications to avian malaria epidemiology. J Parasitol déc. 2014;100(6):878–82.
22. Davis NM, Proctor DM, Holmes SP, Relman DA, Callahan BJ. Simple statistical identification and removal of contaminant sequences in marker-gene and metagenomics data. Microbiome. 2018;6:226.
23. Bolyen E, Rideout JR, Dillon MR, Bokulich NA, Abnet CC, Al-Ghalith GA, et al. Reproducible, interactive, scalable and extensible microbiome data science using QIIME 2. Nat Biotechnol août. 2019;37(8):852–7.
24. Callahan BJ, McMurdie PJ, Rosen MJ, Han AW, Johnson AJA, Holmes SP. DADA2: high-resolution sample inference from Illumina amplicon data. Nat Methods Juill. 2016;13(7):581–3.
25. Katoh K, Misawa K, Kuma K, Miyata T. MAFFT: a novel method for rapid multiple sequence alignment based on fast Fourier transform. Nucleic Acids Res 15 Juill. 2002;30(14):3059–66.
26. Price MN, Dehal PS, Arkin AP. FastTree 2–approximately maximum-likelihood trees for large alignments. PLoS One 10 mars. 2010;5(3):e9490.
27. Bokulich NA, Kaehler BD, Rideout JR, Dillon M, Bolyen E, Knight R, et al. Optimizing taxonomic classification of marker-gene amplicon sequences with QIIME 2's q2-feature-classifier plugin. Microbiome 17 mai. 2018;6(1):90.
28. Yarza P, Yilmaz P, Pruesse E, Glöckner FO, Ludwig W, Schleifer K-H, et al. Uniting the classification of cultured and uncultured bacteria and archaea using 16S rRNA gene sequences. Nat Rev Microbiol Sept. 2014;12(9):635–45.
29. Shannon CE. A Mathematical Theory of Communication. Bell Syst Tech J. 1948;27:379–423.
30. Pielou EC. The measurement of diversity in different types of biological collections. J Theoretical Biology J Theoretical Biology. 1966;13:131–44.
31. Faith DP. Conservation evaluation and phylogenetic diversity. Biol Conserv. 1992;61(1):1–10.
32. DeSantis TZ, Hugenholtz P, Larsen N, Rojas M, Brodie EL, Keller K, et al. Greengenes, a chimera-checked 16S rRNA gene database and workbench compatible with ARB. Appl Environ Microbiol Juill. 2006;72(7):5069–72.
33. Bray JR, Curtis JT. An ordination of the upland forest communities of Southern Wisconsin. Ecol Monogr. 1957;27(4):325–49.
34. Oksanen J, Blanchet FG, Friendly M, Kindt R, Legendre P, McGlinn D et al. vegan: Community Ecology Package. R package version 25 – 7 [Internet]. 2020; https://CRAN.R-project.org/package=vegan

35. R Core Team. R: A language and environment for statistical computing. 2022;R Foundation for Statistical Computing, Vienna, Austria. https://www.R-project.org/
36. Fernandes AD, Reid JN, Macklaim JM, McMurrough TA, Edgell DR, Gloor GB. Unifying the analysis of high-throughput sequencing datasets: characterizing RNA-seq, 16S rRNA gene sequencing and selective growth experiments by compositional data analysis. Microbiome. 2014;2:15.
37. Aitchison J, Methodological B.). 1982.
38. Friedman J, Alm EJ. Inferring correlation networks from genomic survey data. PLoS Comput Biol. 2012;8(9):e1002687.
39. Bastian M, Heymann S, Jacomy M. Gephi: An open source software for exploring and manipulating networks. WebAtlas. 2009.
40. Röttjers L, Vandeputte D, Raes J, Faust K. Null-model-based network comparison reveals core associations. ISME Commun 16 Juill. 2021;1(1):36.
41. Anaconda Inc. Anaconda Software Distribution. Anaconda Documentation [Internet]. 2020; https://docs.anaconda.com/
42. Peschel S, Müller CL, von Mutius E, Boulesteix A-L, Depner M. NetCoMi: network construction and comparison for microbiome data in R. Brief Bioinform 20 Juill. 2021;22(4):bbaa290.
43. Lhomme S. Analyse spatiale de la structure des reseaux techniques dans un contexte de risques. Cybergeo: European Journal of Geography. 2015.
44. Csárdi G, Nepusz T, Csárdi. Gábor and Tamás Nepusz. The igraph software package for complex network research. (2006). InterJournal Complex Syst. 2006;1695(5):1–9.
45. Mateos-Hernández L, Obregón D, Maye J, Borneres J, Versille N, de la Fuente J, et al. Anti-tick Microbiota Vaccine impacts Ixodes ricinus performance during feeding. Vaccines (Basel) 21 nov. 2020;8(4):702.
46. Mateos-Hernández L, Obregón D, Wu-Chuang A, Maye J, Bornères J, Versillé N, et al. Anti-microbiota vaccines modulate the Tick Microbiome in a taxon-specific manner. Front Immunol. 2021;12:704621.
47. Minard G, Mavingui P, Moro CV. Diversity and function of bacterial microbiota in the mosquito holobiont. Parasit Vectors 20 mai. 2013;6:146.
48. Douglas AE. The microbial dimension in insect nutritional ecology. Funct Ecol. 2009;23(1):38–47.
49. Muturi EJ, Lagos-Kutz D, Dunlap C, Ramirez JL, Rooney AP, Hartman GL et al. Mosquito microbiota cluster by host sampling location. Parasit Vectors. 14 août. 2018;11(1):468.
50. Dickson LB, Jiolle D, Minard G, Moltini-Conclois I, Volant S, Ghozlane A, et al. Carryover effects of larval exposure to different environmental bacteria drive adult trait variation in a mosquito vector. Sci Adv août. 2017;3(8):e1700585.
51. da Silva H, Oliveira TMP, Sallum MAM. nov. Bacterial Community Diversity and Bacterial Interaction Network in Eight Mosquito Species. Genes (Basel). 2022 Nov 7;13(11):2052. https://doi.org/10.3390/genes13112052. PMID: 36360289; PMCID: PMC9690548.
52. Banerjee S, Schlaeppi K, van der Heijden MGA. Keystone taxa as drivers of microbiome structure and functioning. Nat Rev Microbiol Sept. 2018;16(9):567–76.
53. Tchioffo MT, Abate L, Boissière A, Nsango SE, Gimonneau G, Berry A, et al. An epidemiologically successful Escherichia coli sequence type modulates Plasmodium falciparum infection in the mosquito midgut. Infect Genet Evol Sept. 2016;43:22–30.
54. Boissière A, Tchioffo MT, Bachar D, Abate L, Marie A, Nsango SE, et al. Midgut microbiota of the malaria mosquito vector Anopheles gambiae and interactions with Plasmodium falciparum infection. PLoS Pathog. 2012;8(5):e1002742.
55. Aranda-Díaz A, Willis L, Nguyen TH, Ho P-Y, Vila J, Thomsen T et al. Assembly of gut-derived bacterial communities follows « early-bird » resource utilization dynamics. bioRxiv. 14 janv 2023;2023.01.13.523996.
56. Rasgon JL, Scott TW. Wolbachia and cytoplasmic incompatibility in the California Culex pipiens mosquito species complex: parameter estimates and infection dynamics in natural populations. Genet déc. 2003;165(4):2029–38.
57. Lee JM, Yek SH, Wilson RF, Rahman S. Characterization of the Aedes albopictus (Diptera: Culicidae) holobiome: bacterial composition across land use type and mosquito sex in Malaysia. Acta Trop. 2020;212:105683.
58. Bian G, Xu Y, Lu P, Xie Y, Xi Z. The endosymbiotic bacterium Wolbachia induces resistance to dengue virus in Aedes aegypti. PLoS Pathog 1 avr. 2010;6(4):e1000833.
59. Coyte KZ, Rao C, Rakoff-Nahoum S, Foster KR. Ecological rules for the assembly of microbiome communities. PLoS Biol févr. 2021;19(2):e3001116.
60. Coyte KZ, Schluter J, Foster KR. The ecology of the microbiome: networks, competition, and stability. Sci 6 nov. 2015;350(6261):663–6.

Publisher's note

PAPER III

Anti-Microbiota Vaccine Reduces Avian Malaria Infection Within Mosquito Vectors

Aželytė J., Wu-Chuang A., Žiegytė R., Platonova E., Mateos-Hernandez L., Maye J., Obregon D., Palinauskas V., Cabezas-Cruz A.

Frontiers Immunology, 2022, 13:841835
DOI 10.3389/fimmu.2022.841835

frontiers in Immunology

ORIGINAL RESEARCH
published: 03 March 2022
doi: 10.3389/fimmu.2022.841835

Anti-Microbiota Vaccine Reduces Avian Malaria Infection Within Mosquito Vectors

Justė Aželytė[1†], Alejandra Wu-Chuang[2†], Rita Žiegytė[1], Elena Platonova[1], Lourdes Mateos-Hernandez[2], Jennifer Maye[3], Dasiel Obregon[4], Vaidas Palinauskas[1] and Alejandro Cabezas-Cruz[2*]*

[1] Nature Research Centre, Akademijos 2, Vilnius, Lithuania, [2] ANSES, INRAE, Ecole Nationale Vétérinaire d'Alfort, UMR BIPAR, Laboratoire de Santé Animale, Maisons-Alfort, France, [3] SEPPIC Paris La Défense, La Garenne Colombes, France, [4] School of Environmental Sciences, University of Guelph, Guelph, ON, Canada

Animal and human pathogens that are transmitted by arthropods are a global concern, particularly those vectored by mosquitoes (e.g., *Plasmodium* spp. and dengue virus). Vector microbiota may hold the key to vector-borne pathogen control, as mounting evidence suggests that the contributions of the vector microbiota to vector physiology and pathogen life cycle are so relevant that vectorial capacity cannot be understood without considering microbial communities within the vectors. Anti-tick microbiota vaccines targeting commensal bacteria of the vector microbiota alter vector feeding and modulate the taxonomic and functional profiles of vector microbiome, but their impact on vector-borne pathogen development within the vector has not been tested. In this study, we tested whether anti-microbiota vaccination in birds targeting Enterobacteriaceae within mosquito midguts modulates the mosquito microbiota and disrupt *Plasmodium relictum* development in its natural vector *Culex quinquefasciatus*. Domestic canaries (*Serinus canaria domestica*) were experimentally infected with *P. relictum* and/or immunized with live vaccines containing different strains of *Escherichia coli*. Immunization of birds induced *E. coli*-specific antibodies. The midgut microbial communities of mosquitoes fed on *Plasmodium*-infected and/or *E. coli*-immunized birds were different from those of mosquitoes fed on control birds. Notably, mosquito midgut microbiota modulation was associated with a significant decrease in the occurrence of *P. relictum* oocysts and sporozoites in the midguts and salivary glands of *C. quinquefasciatus*, respectively. A significant reduction in the number of oocysts was also observed. These findings suggest that anti-microbiota vaccines can be used as a novel tool to control malaria transmission and potentially other vector-borne pathogens.

Keywords: anti-microbiota vaccines, avian malaria, mosquitoes, networks, microbiota

Edited by:
Kézia K.G. Scopel,
Juiz de Fora Federal University, Brazil

Reviewed by:
Yukita Sato,
Nihon University, Japan
Krishnendu Mukherjee,
University Hospital Münster, Germany

***Correspondence:**
Vaidas Palinauskas
palinauskas@gmail.com
Alejandro Cabezas-Cruz
alejandro.cabezas@vet-alfort.fr

†These authors have contributed equally to this work

Specialty section:
This article was submitted to Vaccines and Molecular Therapeutics, a section of the journal Frontiers in Immunology

Received: *22 December 2021*
Accepted: *11 February 2022*
Published: *03 March 2022*

Citation:
Aželytė J, Wu-Chuang A, Žiegytė R, Platonova E, Mateos-Hernandez L, Maye J, Obregon D, Palinauskas V and Cabezas-Cruz A (2022) Anti-Microbiota Vaccine Reduces Avian Malaria Infection Within Mosquito Vectors. Front. Immunol. 13:841835. doi: 10.3389/fimmu.2022.841835

INTRODUCTION

Mosquitoes are vectors of major human diseases such as dengue (caused by dengue virus), and malaria (caused by *Plasmodium* spp.) (1). According to literature, there are more than 50 avian *Plasmodium* species and new species are discovered every year (2) and infection by these parasites is common in some bird species (3). Among the *Plasmodium* species affecting birds, *P. relictum* is listed among the most invasive organisms in the world, infecting more than 300 bird species and is prevalent all around the world (4). *Plasmodium relictum* is transmitted mostly by *Culex* mosquitoes, including *Culex pipiens* and *Culex quinquefasciatus* (5). The midgut is the first organ in which *P. relictum* ingested with the host blood can survive (3). From the midgut lumen, the parasite traverses the peritrophic membrane and epithelial layer of the midgut and develops to oocysts (3). The oocysts invade other vector tissues such as salivary glands to complete the sporogonic development (3). In general, the susceptibility of mosquitoes to *Plasmodium* parasites infection is under genetic control (6–8), but the large variability in oocyst number among closely related mosquitoes indicates that environmental factors also play a role. Of special interest are the interactions between the vector, its microbiota and transmitted pathogens, since commensal bacteria interact with mosquito-borne pathogens (9) and can facilitate (10) or compete (11) with pathogen colonization and development within the vector midguts, prompting research into microbiota manipulation and transmission-blocking strategies (12). Depleting vector microbiota from bacteria that facilitates pathogen development could be exploited as a mean for blocking transmission. For example, the bacterium *Asaia bogorensis* increases midgut pH promoting *Plasmodium berghei* gametogenesis within *Anopheles stephensi* (10), and high abundance of Enterobacteriaceae increases *Plasmodium falciparum* infection in *Anopheles gambiae* midgut (13), making the reduction of these bacterial species a sound strategy to reduce pathogen infection in the vector and potentially block transmission to the host.

Although targeting specific commensal bacteria could block pathogen transmission, the lack of tools for the precise manipulation of the vector microbiota is currently a major limitation to developing novel transmission-blocking strategies. Specific host antibodies (Abs) are easily induced by vaccination, and once taken with the blood meal, they remain functional within the vector tissues and can bind symbionts (14) and other bacterial microbiota (15) within hematophagous arthropods (16). Surprisingly, host Abs specific to bacterial microbiota had never been used for microbiota manipulation and transmission blocking strategies (16). It was recently shown that anti-microbiota vaccines modulate the tick microbiota in a taxon-specific manner (17). Firstly, combining next-generation sequencing (NGS) and network analysis, Enterobacteriaceae was identified as a keystone taxon (i.e., highly connected taxa driving community composition and function) in the microbiota of *Ixodes ricinus* ticks (17, 18). Secondly, the abundance of vector-associated Enterobacteriaceae decreased in ticks fed on mice immunized with a live bacteria vaccine containing *Escherichia coli* (17). Thirdly, vaccination against Enterobacteriaceae had cascading ecological impacts on the whole tick microbiome by reducing bacterial diversity and modulating the functional profiles of the microbiome (17). Fourthly, decreased Enterobacteriaceae abundance was correlated with high levels of *E. coli*-specific Abs (17). Last but not least, no mortality or sign of pain were observed after the vaccination in the mice (17, 18) and the fecal microbiota of immunized mice showed no significant alterations (17). Here we tested whether modulation of mosquito microbiota by anti-microbiota vaccination of host birds against commensal Enterobacteriaceae disrupts *P. relictum* development within midguts and salivary glands of the vector *C. quinquefasciatus*.

RESULTS

Anti-Microbiota Vaccination in Birds Interferes With Plasmodium-Induced Modulation of Mosquito Midgut Microbiota

Immunization was followed by experimental malaria infection and mosquito infestation (**Figure 1**). Anti-microbiota vaccination of birds with *E. coli* O86:B7 or *E. coli* BL21 increased the levels of IgY specific to *E. coli* (**Figure 2A**). Anti-*E. coli* IgY also increased in the sera of birds that received both anti-microbiota vaccines and infection with *P. relictum* (**Figure 2A**). No significant change was observed in the levels of anti-*E. coli* Abs in birds that received the mock vaccination (PBS) or those only infected with *Plasmodium* (**Figure 2A**). Following the bacterial immunization and *P. relictum* infection in birds, *C. quinquefasciatus* mosquitoes were allowed to feed on the birds to acquire the parasites and/or anti-*E. coli* Abs. The midguts of fed mosquitoes were dissected and used for microbiota analysis.

Bacterial community composition and diversity were compared between groups to assess the impact of anti-microbiota vaccines and *P. relictum* infection on the mosquito midgut microbiota. Analysis of alpha diversity indexes showed that overall, the phylogenetic richness (**Figure 2B**) and evenness (**Figure 2C**) did not differ between experimental groups (Kruskal-Wallis, $p > 0.05$). However, pairwise comparisons between groups revealed a reduced taxonomic richness in mosquitoes from *E. coli* O86:B7 + *P. relictum* group compared to *P. relictum*-infected mosquitoes (Kruskal-Wallis, $p = 0.036$, **Figure 2B**). Beta diversity analysis revealed a significant difference in Bray Curtis dissimilarity index between the groups (PERMANOVA, $F = 2.40$, $p = 0.001$). Specifically, *Plasmodium*-infected mosquito microbiota shows a tendency to separate from the other groups. Furthermore, dispersion analysis of Bray Curtis dissimilarity index did not show significant differences between groups (BetaDisper $F= 1.01$, $p = 0.426$, **Figure 2D**).

Further characterization of the impact of anti-*E. coli* O86:B7 immunization and *Plasmodium* infection on mosquito midgut microbiota was achieved using differential abundance analysis. Significant changes in the abundance of 20 and 7 bacterial genera were detected in the midgut microbiota of mosquitoes fed on *P. relictum*-infected (**Figures 3A, B**) or *E. coli* O86:B7-immunized canaries (**Figures 3C, D**), respectively, compared to those fed on mock-immunized canaries. This suggests that *P. relictum* infection and the anti-microbiota vaccine disturb the mosquito

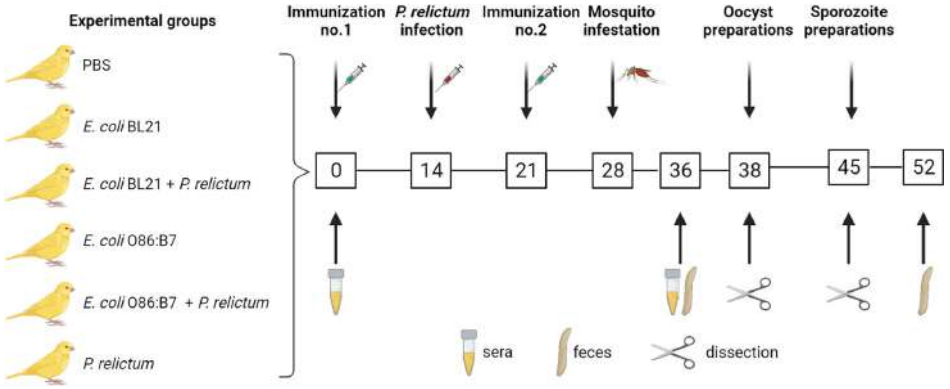

FIGURE 1 | Experimental design and sample collection. Canaries were immunized twice (at day 0 and day 21) with a live vaccine containing *E. coli* BL21 (n = 7) or *E. coli* O86:B7 (n =7) or with a mock vaccine (PBS) (n = 3). A group of canaries (n = 5) and part of the birds vaccinated with *E. coli* BL21 (n = 4) or *E. coli* O86:B7 (n = 4) were infected with *P. relictum* at day 14. The birds were used as donors to feed *C. quinquefasciatus* (n = 20-50 mosquitoes per bird). The midgut of mosquitoes was dissected for microbiota (day 38 and day 45) and oocyst (day 38) analysis and salivary glands for sporozoite (day 45) analysis. Bird sera (used for ELISA and immunofluorescence) and fecal (used for bird gut microbiota analysis) samples were collected at different time points as indicated.

microbiota. We next asked whether anti-microbiota vaccination could interfere with pathogen-induced modulation of the mosquito microbiota. The midgut microbiota of mosquito exposed to both *P. relictum* infection and anti-*E. coli* O86:B7 Abs had 23 and four taxa with significant changes in abundance compared to mosquitoes fed on *Plasmodium*-infected (**Figures 3E, F**), and *E. coli* O86:B7-immunized canaries (**Figures 3G, H**), respectively. Vaccination with *E. coli* BL21 was also associated with changes in the abundance of several bacterial taxa, compared with the control mock-vaccinated and with *Plasmodium* infection groups (**Figure 4**). Notably, compared with the mock-vaccinated group, the bacterial taxa affected by infection or vaccination alone were different between them and from those affected simultaneously by vaccination and infection (**Figure 5**). These results suggest that *P. relictum* infection and the anti-microbiota vaccines modulate the mosquito midgut microbiota in different ways and that the anti-microbiota vaccines interfere with the *Plasmodium*-induced modulation of the mosquito microbiota.

To rule out a negative effect of anti-microbiota vaccine on host microbiota, we collected bird feces after mosquitoes infestation (d36) and at the end of the experiment (d52). We compared fecal microbiota of mock-immunized, *E. coli* BL21-immunized and *E. coli* O86:B7-immunized birds. The results showed non-significant differences in the microbial richness (Kruskal-Wallis, $p > 0.05$), as measured by Faith's phylogenetic index (**Supplementary Figure S1A**). Similarly, species evenness did not differ between the different experimental groups (Kruskal-Wallis, $p > 0.05$, **Supplementary Figure S1B**). Regarding the beta diversity of the microbial communities in bird guts, Bray Curtis dissimilarity index did not show significant differences among mock-immunized, *E. coli* BL21-immunized and *E. coli* O86:B7-immunized birds (PERMANOVA, F = 1.35, $p = 0.25$).

Anti-Microbiota Vaccination Re-Structures the Microbial Communities in Midgut of Plasmodium-Infected Mosquitoes

Bacteria co-occurrence networks were used to further characterize the impact of *Plasmodium* infection and anti-microbiota vaccines on the mosquito microbiota. Visual inspection of the taxonomic networks revealed that anti-microbiota vaccines and malaria infection, together and separately, changes network topology, compared with the control mock vaccine group (**Figure 6** and **Table 1**). Jaccard index was used to test for similarities (Jacc = 0, lowest similarity and Jacc = 1, highest similarity) in selected local network centrality measures (i.e., hub taxa, degree, betweenness centrality, closeness centrality, and eigenvector centrality) of the different networks. The observed Jaccard index for the betweenness centrality was higher than expected by random for the comparison between *E. coli* BL21 and *E. coli* O86:B7 networks (Jacc = 0,418, $p = 0.01$) (**Supplementary Table S1**). In addition, except for the Jaccard index of betweenness centrality in the PBS - *P. relictum* (Jacc = 0,432, $p = 0.004$), PBS - *E. coli* BL21 (Jacc = 0,512, $p = 0.000002$) and PBS - *E. coli* O86:B7 (Jacc = 0,522, $p = 0.000001$) network comparisons, the observed Jaccard indexes of the other centrality measures were lower than expected by random in most networks (**Supplementary Table S1**). This suggests low similarity between compared networks. Topological differences, together with dissimilarity in local network centrality measures, indicate a major shift in the

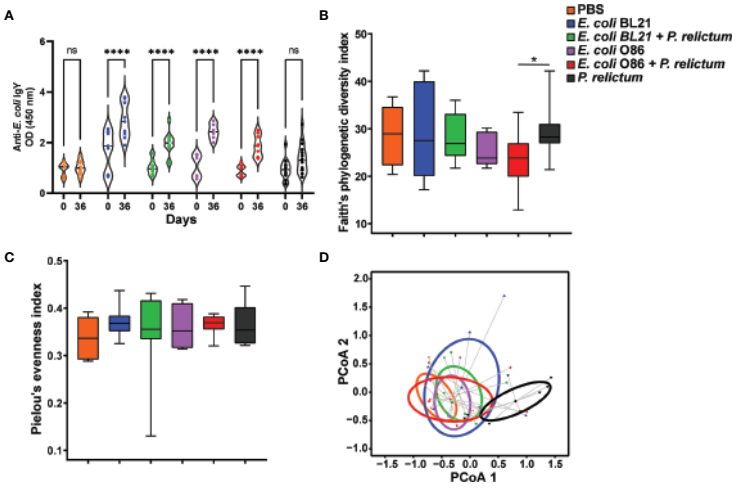

FIGURE 2 | Impact of anti-microbiota vaccine and P. relictum infection on bird antibody response and mosquitoes' microbial diversity. **(A)** Levels of IgY specific to *E. coli* proteins were measured by semiquantitative ELISA in sera of canaries before immunization (day 0) and in sera of canaries immunized with a mock vaccine, *E. coli* BL21 and E. coli O86:B7 alone or challenged with *P. relictum* (day 36 after first vaccination) (****p < 0.00001; ns, not significant). **(B)** Faith's phylogenetic diversity and **(C)** Pielou's evenness indexes were used to measure the richness and evenness, respectively, of microbiota of mosquitoes fed on canaries immunized with a mock vaccine, *E. coli* BL21 and *E. coli* O86:B7 alone or challenged with *P. relictum*. The asterisk indicates significative differences between groups (pairwise Kruskal-wallis, $p = 0.03$). **(D)** Beta diversity of mosquito microbiota in the different experimental conditions represented in PCoA plot obtained by Betadisper function. There were no differences in the intragroup dispersions (variances) (ANOVA, $p = 0.426$), whereas differences were found in the community composition between groups (PERMANOVA, $p = 0.001$), specifically the group infected with *P. relictum* alone was different from the other groups. Taxonomic profiles at the level of ASVs, used to measure the alpha and beta diversity, were obtained from 16S rRNA sequences from midgut of mosquitoes fed on mock-immunized (n = 5 mosquitoes midgut pool), *E. coli* O86:B7-immunized (n = 5 mosquitoes midgut pool), *E. coli* O86:B7-immunized and challenged with *P. relictum* (n = 8 mosquitoes midgut pool) and challenged only with *P. relictum* (n = 8 mosquitoes midgut pool).

community structure induced by anti-microbiota vaccines and malaria infection.

High variation of local connectedness of *Escherichia-Shigella* was observed in co-occurrence sub-networks of experimental groups (**Figure 7**). Specifically, the number of direct neighbors co-occurring with *Escherichia-Shigella* in the microbiota of mosquitoes fed on birds of the different experimental groups decreased in comparison to the sub-network of the microbiota of mosquitoes fed on mock-vaccinated birds. Although the number of edges directly connected to *Escherichia-Shigella* was similar in the sub-networks of the microbiota of mosquitoes fed on mock-immunized (47 co-occurring taxa) and *E. coli* O86:B7-immunized birds (45 co-occurring taxa), an increase of negative co-occurrence correlation was observed in the latter compared to the former group. A detailed analysis of the nodes connected to *Escherichia-Shigella* revealed the inexistence of shared taxa among the different sub-networks (**Supplementary Figure S2**). In addition, we used the eigenvector centrality metric to evaluate the "keystoneness" (importance of a node within the network) of *Escherichia-Shigella* in the different microbial networks. Eigenvector centrality value of *Escherichia-Shigella* in the sub-network of mosquitoes fed on *E. coli* BL21-immunized (eigenvector 0.03) and *E. coli* O86:B7-immunized birds (eigenvector 1) decreased and increased, respectively, compared to that in the control sub-network (i.e., mock vaccine group, eigenvector 0.29). Interestingly, eigenvector centrality values of *Escherichia-Shigella* decreased dramatically in the groups *E. coli* BL21+*P. relictum* (eigenvector 0.07), *E. coli* O86:B7+*P. relictum* (eigenvector 0), compared with the *P. relictum* infected mosquito group (eigenvector 0.16). Variable local interactions and "keystoneness" of *Escherichia-Shigella* between networks suggest that this taxon is affected by anti-microbiota vaccines and *Plasmodium* infection. More importantly, *Escherichia-Shigella* losses importance in the microbiota of mosquito exposed simultaneously to anti-*E. coli* Abs and *P. relictum*.

Anti-Microbiota Vaccination Reduces Plasmodium Infection Within Mosquito Tissues

Mosquito survival was recorded and compared between groups. Results showed a significant difference in survival rate between the groups (Fisher's exact test, $p = 0.013$). However, pairwise comparison of individual groups revealed significant differences

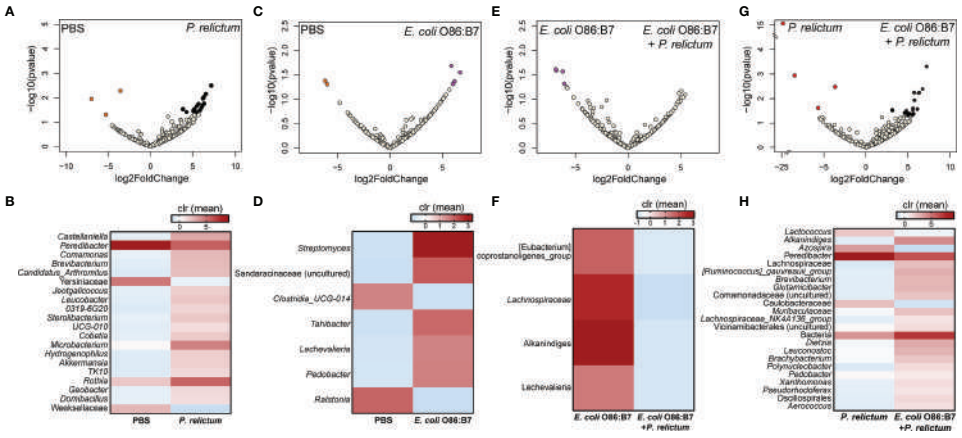

FIGURE 3 | Impact of *E. coli* O86:B7 vaccine and *P. relictum* infection on the taxonomic profiles of mosquito microbiota. Volcano plot showing the differential bacterial abundance in mosquito microbiota between different experimental groups **(A)** PBS *vs*. *P. relictum*, **(C)** PBS *vs*. *E. coli* O86:B7, **(E)** *E. coli* O86:B7 *vs*. *E. coli* O86:B7+*P. relictum* and **(G)** *P. relictum vs*. *E. coli* O86:B7+*P. relictum*. Taxa with significant differences (Wald test, $p < 0.05$) between the groups are represented with colored dots (i.e., orange, purple, red and black). The gray dots represent taxa with no significant differences between groups. Heatmaps representing the relative abundance (expressed as clr) of taxa with significant differences between **(B)** PBS *vs*. *P. relictum*, **(D)** PBS *vs*. *E. coli* O86:B7, **(F)** *E. coli* O86:B7 *vs*. *E. coli* O86:B7+*P. relictum* and **(H)** *P. relictum vs*. *E. coli* O86:B7+*P. relictum*. Taxa with significant differences in their abundance were identified using DeSeq2 algorithm. The taxonomic profiles were obtained from 16S rRNA sequences from midgut of mosquitoes fed on mock-immunized (n = 5 mosquitoes midgut pool), *E. coli* O86: B7-immunized (n = 5 mosquitoes midgut pool), *E. coli* O86:B7-immunized and challenged with *P. relictum* (n = 8 mosquitoes midgut pool) and challenged only with *P. relictum* (n = 8 mosquitoes midgut pool).

only in the survival of mosquitoes fed on birds of the *E. coli* BL21 and *E. coli* BL21-*P. relictum* groups between them ($p = 0.02$) and with the others (**Figure 8**). Mosquitoes in the *E. coli* BL21 and *E. coli* BL21+*P. relictum* groups had the highest and lowest survival rates.

The occurrence (i.e., number of mosquitoes in which at least one oocyst was found) and number of *P. relictum* oocysts in midguts and occurrence of sporozoites in salivary glands of mosquitoes were measured. The results showed a significant overall difference in the occurrence of oocysts between the groups (Fisher's exact test, $p = 0.03$). Pairwise comparisons revealed that the occurrence of *Plasmodium* oocysts was significantly lower in the midguts of mosquitoes fed on birds vaccinated with *E. coli* O86:B7 ($p = 0.01$), but not with *E. coli* BL21 ($p > 0.05$), compared with mosquitoes infected with *P. relictum* and not exposed to anti-*E. coli* Abs (**Figure 9A**). The number of oocysts was significantly lower in midguts of mosquitoes fed on birds vaccinated with both *E. coli* O86:B7 ($p = 0.01$) and *E. coli* BL21 ($p = 0.001$), compared with control mosquitoes (**Figure 9B**). We then hypothesized that decreased oocysts load in midguts might be associated with lower sporozoite infection in salivary glands. Results showed a significant difference between sporozoite occurrence between the groups (Fisher's exact test, $p < 0.001$). The occurrence of sporozoites in salivary glands of mosquitoes fed on *E. coli* O86: B7-immunized, but not *E. coli* BL21-immunized ($p > 0.05$), birds was significantly lower ($p = 0.001$) than the control group (i.e., *P. relictum* infection alone) (**Figure 9C**).

DISCUSSION

In this study, we showed that anti-microbiota vaccination of birds with two strains of *E. coli* O86:B7 and BL21 modulate *C. quinquefasciatus* midgut microbiota. These results concur with a previous report in which live bacteria vaccine were used as a tool for the manipulation of tick microbiome (17, 18). During feeding, hematophagous ectoparasites ingest blood from the vertebrate host, along with host immune molecules. Host Abs and/or complement proteins have been detected in the guts of ticks (19–24), mosquitoes (25, 26), sandflies (27, 28), and tsetse flies (29). Once ingested, host immune components can remain active from a few hours to months depending on the species of blood-sucking arthropod, raising the possibility that vertebrate Abs could interact with pathogens and microbiota (16). Empirical work shows that host Abs can target vector-borne pathogens within ticks (30) and mosquitoes (31–33). Targeting pathogen proteins expressed within the arthropod vectors is the rationale behind transmission-blocking vaccines (32–34). Functional host Abs have also been shown to interact with symbionts in *Rhodnius prolixus* (14) and *Glossina morsitans* (35), as well as with bacterial microbiota in mosquitoes (15) and

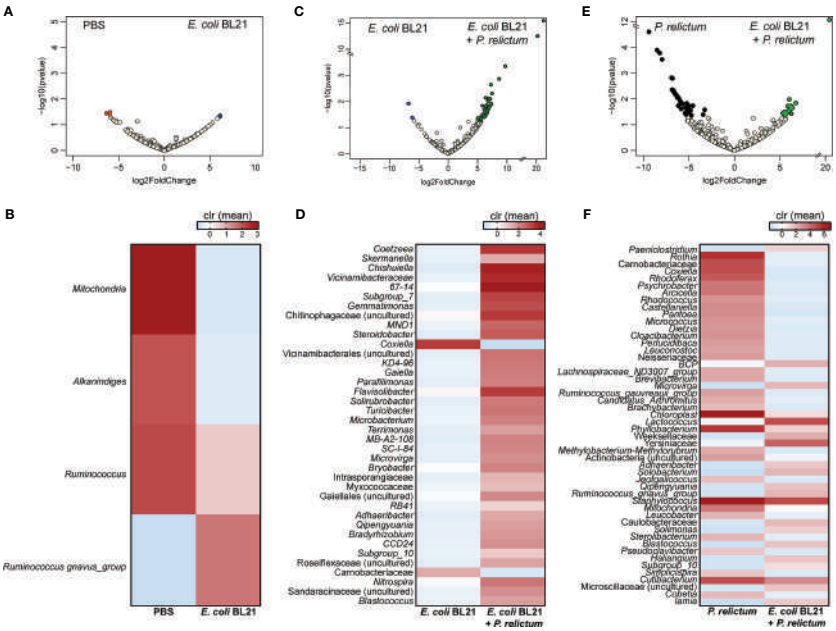

FIGURE 4 | Impact of *E. coli* BL21 vaccine and *P. relictum* infection on the taxonomic profiles of mosquito microbiota. Volcano plot showing the differential bacterial abundance in microbiota of mosquitoes from different experimental groups **(A)** PBS *vs*. *E. coli* BL21, **(C)** *E. coli* BL21 *vs*. *E. coli* BL21+*P. relictum*, **(E)** *P. relictum vs*. *E. coli* BL21+*P. relictum*. Taxa with significant differences (Wald test, $p < 0.05$) between the groups are represented with colored dots (i.e., orange, blue, green and black). The gray dots represent taxa with no significant differences between groups. Heatmaps represent the relative abundance (expressed as clr) of taxa with significant differences in the comparisons **(B)** PBS *vs*. *E. coli* BL21, **(D)** *E. coli* BL21 *vs*. *E. coli* BL21+*P. relictum*, and **(F)** *P. relictum* vs. *E. coli* BL21+*P. relictum*. Taxa with significant differences in their abundance were identified using DeSeq2 algorithm. The taxonomic profiles were obtained from 16S rRNA sequences from midgut of mosquitoes fed on mock-immunized (n = 5 mosquitoes midgut pool), *E. coli* BL21-immunized (n = 7 mosquitoes midgut pool), *E. coli* BL21-immunized and challenged with *P. relictum* (n = 7 mosquitoes midgut pool) and challenged only with *P. relictum* (n = 8 mosquitoes midgut pool).

ticks (17, 18). Vaccination of mice with *E. coli* BL21 induced anti-*E. coli* Abs that when ingested with the blood decreased Enterobacteriaceae abundance within the tick microbiota (17). Targeting commensal *Escherichia* in ticks with anti-*E. coli* Abs reduced the connectivity of this taxon in the co-occurring networks (17). Similarly, in this study we observed reduced connectivity of *Escherichia* in the co-occurring networks of mosquitoes fed on birds vaccinated with *E. coli* BL21, but not in those vaccinated against *E. coli* O86:B7. However, we did observe a switch in the bacterial connectivity pattern of mosquitoes fed on *E. coli* O86:B7 compared to the control group PBS. In the control group, the majority of *Escherichia* correlations with its direct neighbor nodes were positive, while in the *E. coli* O86:B7 group most correlations were negative. These results show that antibody-mediated disturbance of the microbiome had cascading ecological impacts on the whole tick microbiome with strong impact on the structure of the microbial community of the vectors.

Recent research on vector-pathogen-microbiota interactions shows that microbial communities within vectors strongly influence pathogen colonization and transmission (36). Despite recent advances in vector microbiota research, the lack of tools for the precise and selective manipulation of the vector microbiome is currently a major limitation to disrupt pathogen-microbiome interactions in a taxon-specific manner (12, 37). Here we showed that mosquitoes fed on birds immunized with the Enterobacteriaceae bacteria *E. coli* O86:B7 and *E. coli* BL21 had reduced numbers of *P. relictum* oocysts in the midguts. The results support the potential role of commensal Enterobacteriaceae as a key player in the early development of *Plasmodium* within the vector. In agreement with this, high abundance of Enterobacteriaceae was previously associated with increase *P. falciparum* infection in *A. gambiae* midgut (13), and several studies showed that the ookinete–oocyst transition of *Plasmodium* spp. is strongly influenced by resident midgut microbiota in different mosquito species (38–41). However, the directionality (facilitation *vs*. competition) of midgut

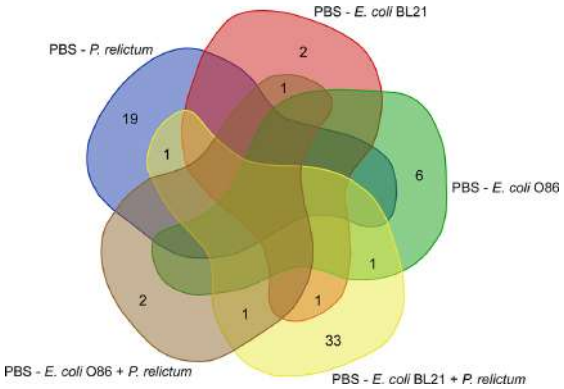

FIGURE 5 | Comparison of unique and shared taxa across different experimental groups. Venn diagram showing the common and different taxa with significant changes in their abundance between vaccinated and infected groups, compared to the mock-vaccinated group (PBS).

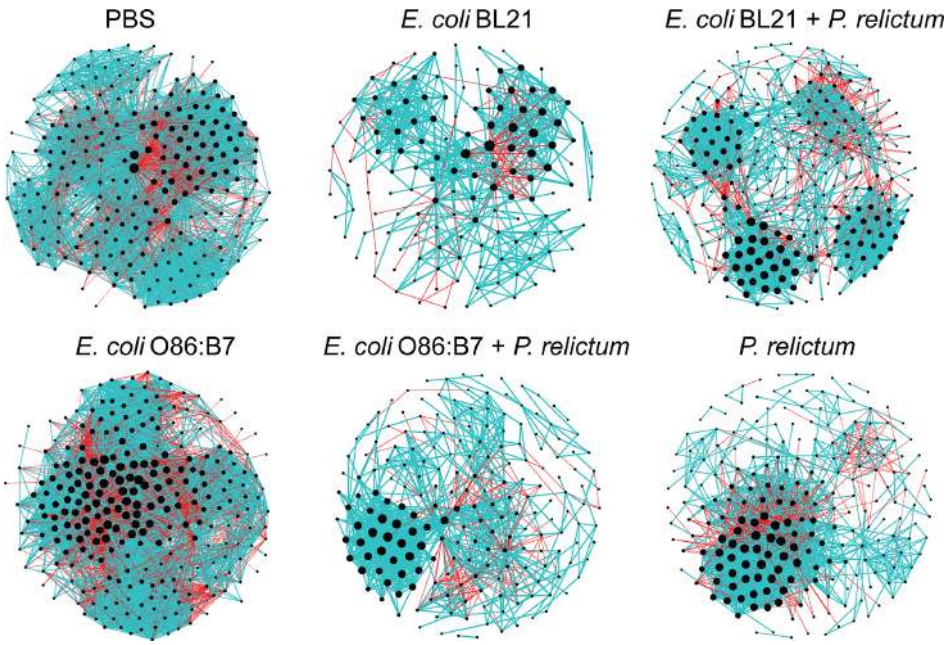

FIGURE 6 | Co-occurrence networks of *C. quinquefasciatus* microbiota in the different experimental groups. Bacterial co-occurrence networks were inferred from the microbiota of mosquitoes fed on control (PBS), vaccinated and/or infected birds. Nodes represent bacterial taxa and connecting edges stand for a co-occurrence correlation (SparCC > 0.75). Node sizes are proportional to the eigenvector centrality value. Edges representing positive or negative correlations were colored in blue and red, respectively. Only nodes with at least one connection are displayed.

TABLE 1 | Topological parameters of co-occurrence networks.

Network features	PBS	*E. coli* BL21	*E. coli* BL21 + *P. relictum*	*E. coli* O86:B7	*E. coli* O86:B7 + *P. relictum*	*P. relictum*
Nodes	231	137	267	261	199	221
Edges	4417	591	1787	6629	991	1709
Positive	3,041 (68.9%)	476 (80.5%)	1,386 (77.6%)	3,827 (57.7%)	822 (82.9%)	1,232 (72.1%)
Negative	1,376 (31.2%)	115 (19.5%)	401 (22.4%)	2,802 (42.3%)	169 (17.1%)	477 (27.9%)
Network diameter	3	10	13	4	10	12
Average degree	38.242	8.628	13.386	50.797	9.96	15.466
Weighted degree	12.07	4.265	6.113	7.018	5.287	5.83
Average path length	1.909	3.47	3.871	1.993	3.609	3.716
Modularity	1.459	0.974	1.105	2.996	0.785	0.872
Number of modules	6	18	27	13	20	32
Average clustering coefficient	0.719	0.556	0.621	0.658	0.538	0.623

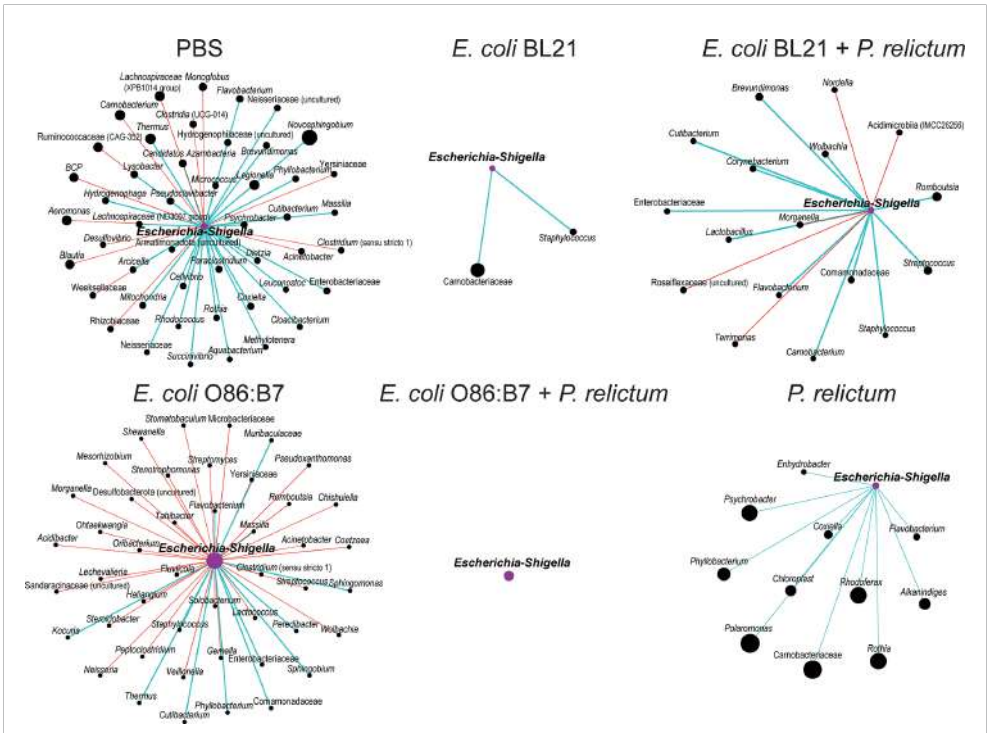

FIGURE 7 | Local connectivity of *Escherichia-Shigella* in the co-occurrence networks of *C. quinquefasciatus* microbiota in the different experimental groups. The nodes/taxa linked to *Escherichia-Shigella* (purple node) were identified in the bacterial co-occurrence networks of mosquitoes fed on mock-immunized (PBS), *E. coli*-immunized and infected birds. Node sizes are proportional to the eigenvector centrality value. Only nodes with at least one connection are displayed. Connecting edges stand for a co-occurrence correlation (SparCC > 0.75), representing positive (blue edges) and negative (red edges) interactions between bacteria. BCP – *Burkholderia Caballeronia Paraburkholderia*.

microbiota contribution to infection cannot be simplified to the abundance of a single taxon, while neglecting global changes of the microbial community as a whole. For example, experimental exposure of mosquitoes to a cocktail of penicillin and streptomycin (PS) reduced the proportion of microbiota-resident Enterobacteriaceae 92-fold, while simultaneous exposure to PS and *Plasmodium* infection increased the prevalence and intensity of *P. berghei* oocyst in *A. gambiae* midguts (42). This is not expected if

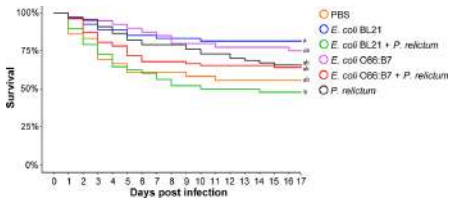

FIGURE 8 | Survival of blood-fed mosquitoes throughout the experiment. The highest mortality was observed in the mosquito group fed on donors vaccinated with *E. coli* BL21 and infected with *P. relictum*, which significantly differed from the group fed on the birds vaccinated with *E. coli* BL21 ($p = 0.02$). Survival of mosquitoes between other groups did not differ significantly. Survival of mosquitoes was estimated by Fisher's exact test with Bonferroni correction. Different letters at the end of the curves indicate statistically significant differences in survival rate ($p < 0.05$).

Enterobacteriaceae facilitates *Plasmodium* infection (13). However, regardless that the impact of Enterobacteriaceae on parasite infectivity may differ between *Plasmodium* species (e.g., *P. berghei vs. P. falciparum*), the decreased of Enterobacteriaceae has been associated with a 19-fold increase of *Asaia* sp. in PS-exposed *A. gambiae* (42). Commensal *Asaia bogorensis* remodels glucose metabolism and increases midgut pH which in turn induces *P. berghei* gametogenesis and facilitates parasite infection of *A. stephensi* (10). Thus, the decrease of Enterobacteriaceae abundance may be balanced by the increase of another taxon (e.g., *Asaia* sp.) that also facilitates infection with a net effect of increased *Plasmodium* infectivity. Our results showed that anti-microbiota vaccines altered the *Plasmodium*-induced modulation of the mosquito microbiota, resulting in a global microbial community transformation and the reduction of *Plasmodium* infectivity.

We also found a significant reduction of sporozoites occurrence in the salivary glands of mosquitoes fed on *E. coli* O86:B7-immunized birds, but no in those fed on *E. coli* BL21-immunized birds. This could be explained by differences in the levels of the glycan Galα1-3Gal (α-Gal) in these two *E. coli* strains. The strain *E. coli* O86:B7 expresses high levels of α-Gal (43), which is not the case for *E. coli* BL21 (44, 45). Even when *E. coli* BL21 produces low levels of α-Gal, immunization with this bacterium induces anti-α-Gal (18), as low-abundant antigens could also induce immune responses. However, immunization with *E. coli* O86:B7 may induce anti-α-Gal Abs at levels even higher than *E. coli* BL21. This is relevant because as previously shown in ticks (18), α-1,3-galactosyltransferase genes, and possibly α-Gal, may be widely distributed in mosquito bacterial microbiota, increasing the number of bacterial taxa targeted by Abs induced by *E. coli*-vaccination. Another point to consider is that α-Gal has been detected on the surface of *P. falciparum*, *P. berghei* and *Plasmodium yoelii* sporozoites (43). Whether *P. relictum* sporozoites express α-Gal within *C. quinquefasciatus* salivary glands and whether anti-α-Gal Abs could target this *Plasmodium* stage within mosquito salivary glands remain to be tested.

Interestingly, mosquitoes fed on birds immunized with *E. coli* BL21 or *E. coli* O86:B7 had the highest survival rates, although the differences were significant only for mosquitoes in the *E. coli* BL21 group, compared with the *P. relictum*+*E. coli* BL21 group. Similar impact on survival was observed on mosquitoes fed on blood supplemented with PS (42). Exposure of *A. gambiae* to PS

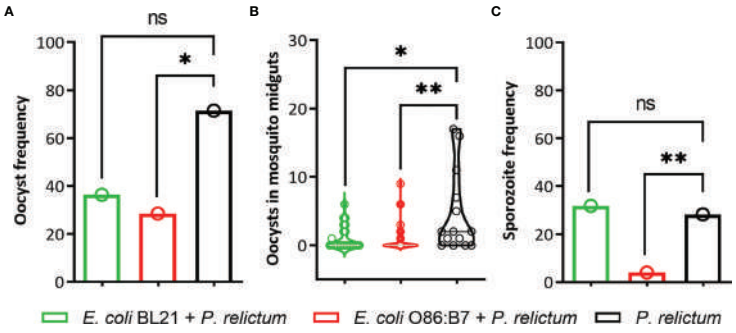

FIGURE 9 | Impact of anti-microbiota vaccines on P. relictum development in infected mosquitoes. Three groups of P. relictum-infected birds were used as infection donors for mosquitoes. One of the groups was vaccinated with *E. coli* BL21, the other with *E. coli* O86:B7, and a third group was a control (only infection). **(A)** The percentage of mosquitoes in which at least one oocyst was found in the midgut by microscopy and compared between the groups was measured. **(B)** The number of oocysts in the midgut of P. relictum-infected mosquitoes was calculated and compared between the groups. **(C)** The percentage of mosquitoes in which sporozoites were detected in salivary glands by microscopy or PCR was measured and compared between the groups. The parameters were compared between groups by Fisher's exact test with Bonferroni correction (oocyst and sporozoite frequency) and the Mann-Whitney U test (number of oocyst). (*p <0.05; **p <0.001; ns, not significant; n = 14-53 mosquitoes per group).

increased survival and fecundity, which are known to augment vectoral capacity (42). Our results can be interpreted as if microbiota modulation by *E. coli* BL21 vaccination: (i) increases *C. quinquefasciatus* fitness, and/or as if microbiota modulation by *E. coli* BL21 vaccination together with *Plasmodium* infection (ii) increases *P. relictum* virulence on mosquitoes and/or (iii) induces changes in the microbiome that impose a high cost on mosquito midguts homeostasis.

CONCLUSIONS

The vector microbiome can be assembled in different possible states, some of which may be incompatible with pathogen infection and/or transmission, while others increase vector competence or could increase or reduce vector fitness. Unraveling how to modulate these different states in a precise manner offers a powerful tool to develop novel transmission-blocking vaccines (16). Our results support the use of anti-microbiota vaccines to target vector commensal bacteria that facilitate pathogen infection (16, 46). In addition to taxon-specific effects, the community-level effects and cascading ecological impact of anti-microbiota vaccines on vector microbiota might induce infection-refractory states in the vector microbiome. Effective infection by vector-borne pathogens involves competent vectors, infective pathogens, and an infection-compatible microbiome (16). Mismatch of at least one of these components can result in an impaired ability of the vector to support the pathogen life cycle. For example, one strategy used to reduce the vector competence for pathogens is the genetic modification of insects that no longer transmit pathogens (47). Our results provide strong evidence that alterations in the vector midgut microbiomes, without the need to altering vector and/or pathogen genetics, affect pathogen infection in the vector. Therefore, deviations from infection-compatible microbiomes could block transmission and disease development. Anti-microbiota vaccines can be used as a microbiome manipulation tool for the induction of infection-refractory states in the vector microbiome for the control of major vector-borne pathogens such as malaria.

MATERIAL AND METHODS

Ethical Statement

All procedures were performed at the Nature Research Centre in Vilnius, Lithuania, according to Lithuanian and International Guiding Principles for Biomedical Research Involving Animals (2012). Infection experiments and other procedures were reviewed and approved by the Lithuanian State Food and Veterinary Service, Ref. No. 2020/07/24-G2-84. The assessment of the animal health and all described procedures were implemented by trained professionals (under licenses 2012/02/06-No-208, and 2016/01.29-No-344).

Birds and Housing Conditions

Seven-months-old domestic canaries were purchased commercially and kept for adaptation for one-month before experimental procedures. Birds were kept at the Nature Research Centre vivarium (License No. LT-61-13-003) under standard living conditions for birds. Experimental animals were housed in cages, up to three birds per cage. The facilities were under a controlled temperature of 21°C, which was maintained throughout the time that the experimentation lasted. Animals were supplied with a standard food for canaries and water *ad libitum*.

Experimental Design

Domestic canaries (*Serinus canaria domestica*) were used as a model for avian malaria infection, anti-microbiota vaccination and as donors of *P. relictum* to mosquitoes. Before the experimental procedures began, birds were randomly separated into six groups as displayed in **Figure 1**. Birds in one group received a mock vaccination containing PBS and adjuvant. Another group of birds was only infected with *P. relictum*. All birds in the other four groups received anti-microbiota vaccines and in two of these groups, birds were additionally infected with *P. relictum*. After *Plasmodium* infection and antibody titers to anti-microbiota vaccines were confirmed, *C. quinquefasciatus* mosquito females were fed on the birds for pathogen acquisition experiment. In total, 22 experimental birds from all groups were exposed to mosquito bites as described in the sections below. Engorged mosquitoes (n = 663) were used for midgut and/or salivary glands preparations. Mosquito tissues were used for oocyst (midguts) and sporoites (salivary glands) counting. Mosquito midguts were also used for DNA extraction and microbiota analysis using bacterial 16S rRNA amplicon sequencing. Bird feces were collected to test for an impact of anti-microbiota vaccines on bird gut microbiota. Experimental procedures are described below.

Bacterial Cultures and Live Bacteria Immunization

Representative bacteria of the genus *Escherichia-Shigella* were selected to be included in live bacteria vaccine formulations as previously reported (17, 18). Anti-microbiota vaccinations were used to test the impact of host immune response against targeted bacteria on mosquito microbiota composition and structure, mosquito survival and *Plasmodium* infection. The *Escherichia coli* strains BL21 (DE3, Invitrogen, Carlsbad, CA, USA), and O86:B7 (ATCC® 12701TM) were selected. The two bacterial strains were prepared as previously described (17, 18). Briefly, *E. coli* was grown on Luria Broth (LB, Sigma-Aldrich, St. Louis, MO, USA) at 37°C under vigorous agitation, washed with phosphate buffer saline (PBS) 10 mM NaH2PO4, 2.68 mM KCl, 140 mM NaCl, pH 7.2 (Thermo Scientific, Waltham, MA, USA), resuspended at 3.6×10^4 colony-forming unit (CFU)/mL, and homogenized using a glass homogenizer. Eight-month-old, canaries were immunized subcutaneously with *Escherichia* sp. in 50 µL (4, 1×10^6 CFU per bird) of a water-in-oil emulsion containing 70% (w/w) Montanide™ ISA 71 VG adjuvant (Seppic, Paris, France), with a booster dose two weeks after the first dose. Control birds received a mock vaccine containing PBS and adjuvant. All reagents used for bacterial preparation were apyrogenic.

Bacterial Protein Extraction

Escherichia coli strains were washed twice with PBS, centrifuged at 1,000× g for 5 min at 4°C, resuspended in 1% Trion-PBS lysis buffer (Sigma-Aldrich, St. Louis, MO, USA) and homogenized with 20 strokes using a glass balls homogenizer. The homogenate was then centrifuged at 300× g for 5 min at 4°C and the supernatant was collected. Protein concentration was determined using the Bradford Protein Assay (Thermo Scientific, San Jose, CA, USA) with Bovine Serum Albumin (BSA) as standard. Bacterial protein extracts were used in the indirect ELISA to measure anti-*E. coli* Abs in bird sera.

Thawing the Cryopreserved Avian Malaria Sample

The cryopreserved *P. relictum* strain SGS1 was thawed and used to infect donor canaries. Tubes containing *Plasmodium*-infected avian blood, conserved frozen in liquid nitrogen, were thawed as described by Dimitrov et al. (48). Briefly, thawed samples were mixed with 12% NaCl (1/3 of thawed sample amount). After 5 min equilibration, one volume of 1.6% of NaCl was added followed by centrifugation at 10,000 rpm for 5 min. After centrifugation, the supernatant was removed and 1.6% NaCl (1/3 of original sample) was added and centrifuged again. The same procedure was repeated three times with 0.9% NaCl solution. The final mixture was diluted with 0.9% NaCl and sub-inoculated into two canaries.

Experimental Infection of Birds

All birds from the mock-immunized group and birds randomly selected (n = 4) from *E. coli* BL21-immunized and *E. coli* O86:B7-immunized groups were experimentally infected with *P. relictum* (SGS1) using the protocol described by Palinauskas et al. (49). Each experimental bird was sub-inoculated with a mixture (0.10 mL) of infected blood, 3.7% sodium citrate and 0.9% saline in proportion 4:1:5 into the pectoral muscles. Each bird received approximately 1 x 10^5 of mature *P. relictum* meronts. The duration of experimental time before exposure to the mosquitoes was 13 days post inoculation (dpi). This time was sufficient to develop higher parasitemia in the blood for malaria parasites. Birds with suitable infection levels were exposed to feed mosquitoes. Parasitemia was examined every 4 days by taking blood from the brachial vein as described in the section below.

Maintenance of Mosquitoes

For experimental infection of *P. relictum* in mosquitoes, we used the P. B. Šivickis parasitology laboratory-reared *C. quinquefasciatus* mosquitoes. The colony was maintained as described in Žiegytė et al. (50). Mosquitoes were kept in a nylon netted cage (65×65×65 cm) under controlled conditions (room temperature 23 ± 1°C; humidity 75-80%; photoperiod 17:7 light:dark). Adult insects were provided with cotton wools saturated with 5% saccharose solution. Mosquito females were randomly separated from the main colony into smaller cages (about 300 mosquitoes) for each experimental group. For experimental infection we used insects of the same age, approximately one week after hatching.

Mosquito Exposure to Vaccinated Birds and Infection With Plasmodium

We evaluated gametocytemia in all donor birds immediately after mosquito exposure. The gametocytemia of *P. relictum*-infected donor birds varied between 0.005% – 1.5%, *E. coli* BL21-immunized birds – 0.02% – 2% and *E. coli* O86:B7-immunized birds – 0.01% – 3.5%. For experimental exposure to mosquito bites, the donor bird was carefully immobilized and fixed in a paper tube, leaving only the legs exposed for the mosquitoes (51). The tube was placed into a separate mosquito cage with separated female mosquitoes taken from the main colony. The bird was kept up to one hour, or when approximately 40 fully saturated mosquitoes were counted. Engorged insects were separated into small cages (17.4 × 17.5 × 17.5 cm) and kept there up to 17 days post exposure (dpe) under the same rearing conditions as described above. All cages were additionally provided with cups containing water for oviposition. Mosquitoes were exposed to donor birds immunized with *E. coli* BL21, *E. coli* O86:B7 and mock vaccine 28 days post first vaccination (dpvI). *Plasmodium*-infected donor birds were used for mosquito infestation 28 dpvI (i.e., 14 dpi). Exposed mosquitoes were dissected gradually for preparations of different sporogonic stages and sampling for microbiota analysis.

Blood Sample and Bird Feces Collection

Blood samples were taken from birds by puncturing brachial vein using microcapillaries. A small drop of blood was used to make smears for microscopy to estimate the development of parasites in the blood. Smears were air-dried, fixed with absolute methanol and stained as described by Valkiūnas et al. (52). A fraction of blood (20-30 µL) was placed in SET-buffer for molecular analysis (PCR, see below) to confirm the lineage in recipient birds. The rest of the blood (100 µL) was used to obtain serum for immunological analysis. Before centrifugation the blood was incubated for 2 h at room temperature, allowing it to coagulate. Then samples were centrifuged at 5,000x g for 5 min and serum separated in microtube and kept in a freezer at -15°C until processing. The blood for smears and SET-buffer was collected on days 0, 4, 8, 12, after inoculation of parasites. The blood for serum was taken on days 0 and 36 after the first vaccine inoculation. Fresh feces were collected from each bird in sterile tubes on days 36 and 52 and were stored at -20°C before genomic DNA extraction.

Microscopic Examination

We used an Olympus BX61 light microscope (Olympus, Japan) to examine blood smears and preparations of mosquito tissues. Parasitemia was calculated as a percentage by actual counting of the number of parasites per 10,000 erythrocytes as described by Godfrey et al. (53). The infection intensity in the mosquito was evaluated by counting the oocysts in the midgut. Successful sporogony was determined by examining salivary glands preparations and confirming sporozoite development.

Indirect ELISA

The levels of Abs reactive to bacterial proteins were measured in bird sera as previously reported (17, 18), with small modifications. The 96-well ELISA plates (Thermo Scientific, Waltham, MA, USA)

were coated with 50 ng/mL (100 µL/well) of *E. coli* BL21 protein extracts in carbonate/bicarbonate buffer (0.05 M, pH 9.6) and incubated for 2 h with 100 rpm shaking at RT. Subsequently, plates were incubated overnight at 4°C. Wells were washed three times with 100 µL of PBS containing 0.05% (vol/vol) Tween 20 (PBST), and then blocked by adding 100 µL of 1% Human Serum Albumin (HSA)/PBS for 1 h at RT and 100 rpm shaking. After three washes, sera samples, diluted at 1:200 in 0.5% HSA/PBS, were added to the wells and incubated for 1 h at 37°C and 100 rpm shaking. The plates were washed three times and HRP-conjugated Abs (goat anti-turkey IgG) (MyBioSource, San Diego, CA, USA) were added at 1:1,000 dilution in 0.5% HSA/PBST (100 µL/well) and incubated for 1 h at RT with shaking. The plates were washed three times and the reaction was developed with 100 µL ready-to-use TMB solution (Promega, Madison, WI, USA) at RT for 20 min in the dark, and then stopped with 50 µL of 4% H_2SO_4. Optimal antigen concentration and dilutions of sera and conjugate were defined using titration assays. The optical density (OD) was measured at 450 nm using an ELISA plate reader (Filter-Max F5, Molecular Devices, San Jose, CA, USA). All samples were tested in triplicate and the average value of three blanks (no Abs) was subtracted from the reads. The cut-off was determined as two times the mean OD value of the blank controls.

Evaluation of Mosquito Survival and Collection of Midguts and Salivary Glands for Testing *P. relictum* Development and Midgut Microbiota Analyses

The survival of mosquitoes was estimated by daily checking the mosquito cages at 10 am and counting dead insects until 17 dpe. On 10 dpe, mosquito midguts were dissected for estimation of developed oocysts and microbiota analysis. Before dissection, mosquitoes were euthanized by shaking vigorously to stun them in insect aspirator. Wings and legs of the insects were removed before dissection, which was performed under the binocular stereoscopic microscope. Each mosquito was carefully separated in two segments, the thorax with head and abdomen. The abdomen was placed in the drop of saline and the midgut of the mosquito was extracted. The midgut was stained according to Kazlauskienė et al. (51) for counting oocysts of *Plasmodium* parasite. For microbiota analysis, unstained midguts were pooled up to 10 in sterile microtubes and frozen at -20C. To eliminate contamination of samples, new dissecting needles were used for each dissected insect. On 17 dpe, each mosquito was carefully separated in two segments, the thorax with head and abdomen. Salivary glands were extracted from the thorax, placed in a separate sterile drop of saline and grinded to make a smear to record the presence of sporozoites (51). The remnants of salivary gland preparations and thorax were fixed in SET-buffer for PCR analysis. The abdomen, the same as on day 10, was placed in a drop of saline to prepare the samples for the midgut microbiota analysis.

DNA Extraction and PCR for *P. relictum* Identification

Total DNA for PCR analysis was extracted from the blood remnants of mosquitoes using an ammonium acetate extraction protocol by Sambrook & Russel (54). A nested PCR protocol described by Hellgren et al. (55) was used to confirm *P. relictum* infection in the donor birds and test mosquitoes for positive parasite sporozoite development. For the first PCR we used the primers HaemNFI [5'-CATATATTAAGAGAAITATGGAG-3'] and HaemNR3 [5'-ATAGAAAGATAAGAAATACCATTC-3'] (55). In the second PCR a mitochondrial *cyt b* gene (478 bp) was amplified using the primers HaemF [5'-ATGGTGCTTTCGATATATGCATG-3'] and HaemR2 [5'-GCATTATCTGGATGTGATAATGGT-3'] (56). For PCR mix we used 12.5 µl of DreamTaq Master Mix (Thermo Fisher Scientific, Lithuania), 8.5 µl of nuclease-free water, 1 µl of each primer and 2 µl of template DNA (extracted DNA or products of first PCR). *P. relictum*-positive samples were determined by running 2 µl of second PCR product on 2% agarose gel. For parasite lineage confirmation, samples containing parasite DNA were sequenced from the 5` end using the HAEMF primer on an ABI PRISM TM 3100 capillary sequencing robot (Applied Biosystems, USA) as described by Bensch et al. (56). The BLAST search tool (National Centre for Biotechnology Information website: http://www.ncbi.nlm.nih.gov/BLAST) was used to determine SGS1 lineage.

DNA Extraction and 16S rRNA Sequencing for Microbiota Analysis

Genomic DNA for microbiota analysis was extracted from frozen midguts of engorged mosquitoes and from fecal samples of birds using a Pure Link Microbiome DNA Purification Kit (Invitrogen, Thermo Fisher Scientific, CA, USA). Each DNA sample was eluted in 100 µl of elution buffer. Genomic DNA quality (OD260/280 between 1.8 –2.0) was measured with NanoDrop™ One (Thermo Scientific, Waltham, MA, USA). More than 850ng of DNA at ≥ 8.5 ng/µL concentration were sent for amplicon sequencing of the bacterial 16S rRNA gene, which was commissioned to Novogene Bioinformatics Technology Co. (London, UK). Libraries were prepared with NEBNext® Ultra™ IIDNA Library Prep Kit (New England Biolabs, MA, USA). A single lane of Illumina MiSeq system was used to generate 251-base paired-end reads from the V4 variable region of the 16S rRNA gene using barcoded universal primers (515F/806R) in samples from mosquitoes engorged on *E. coli* BL21-immunized (n = 7 midgut pools), *E. coli* BL21-immunized and *Plasmodium*-infected (n = 7), *E. coli* O86:B7-immunized (n = 5), *E. coli* O86:B7-immunized and *Plasmodium*-infected (n = 8), *Plasmodium*-infected (n = 8) or mock-immunized (n = 5) birds. The raw 16S rRNA sequences obtained from mosquito samples were deposited in the SRA repository, Bioproject No. PRJNA778616. One extraction reagent control was set in which the different DNA extraction and amplification steps were performed using the same conditions as for the samples but using water as template.

16S rRNA Sequences Processing

The analysis of 16S rRNA sequences was performed using QIIME 2 pipeline (v. 2021.4) (57). The sequences in the fastq files were denoised and merged using the DADA2 software (58) as implemented in QIIME 2. The amplicon sequence variants (ASVs) were aligned with q2-alignment of MAFFT (59) and used

to construct a phylogeny (60). Taxonomy was assigned to ASVs using a classify-sklearn naïve Bayes taxonomic classifier (61) based on SILVA database (release 132) (62). The taxonomic data tables were collapsed at genus level and filtered excluding taxa with less than 10 total reads and present in less than 30% of samples of each dataset.

Bacterial Co-Occurrence Networks

Co-occurrence networks were inferred for each experimental condition based on taxonomic profiles. Correlation matrices were calculated using the Sparse Correlations for Compositional data (SparCC) method (63), implemented in the R Studio (64). Network visualization and calculation of topological features and taxa connectedness (i.e., the number of nodes and edges, network diameter, average degree, weighted degree, average path length, modularity, number of modules, average clustering coefficient) was performed using the software Gephi 0.9.2 (65).

Statistical Analysis

Statistical analysis was performed using R program (version 4.0.4) (66). Differences in oocyst and sporozoite frequency between the groups of infected mosquitoes were compared using Fisher's exact test with Bonferroni comparison tests. The numbers of oocysts formed in mosquito midguts were compared between infected groups by the Mann-Whitney U test. Differences in relative Ab levels (i.e., OD) among groups of immunized birds in the different time points were compared using two-way ANOVA with Bonferroni multiple comparison tests applied for individual comparisons. Microbial diversity analyses were carried out on rarefied ASV tables, calculated using the q2-diversity plugins. The alpha diversity (richness and evenness) was explored using Faith's phylogenetic alpha diversity index (67) and Pielou's evenness index (68). Differences in α-diversity metric between groups were assessed using Kruskal-Wallis test (alpha= 0.05). Bacterial β-diversity was assessed using the Bray Curtis dissimilarity (69) and compared between groups using the PERMANOVA test. Betadisper function was used for the construction of PCoA plot, and an ANOVA test was used to compare the dispersion of the samples by groups. The differential features were detected by comparing the log2 fold change (LFC) using the Wald test as implemented in the compositional data analysis method DESeq2 (70). The number of shared co-occurring taxa among different experimental groups was done in R studio using the package "Venn".

Differential Network Analysis

Comparison of the similarity of the most central nodes between two networks was done with the package "NetCoMi" (71) in R studio using the read count taxonomic tables. "Most central" nodes are defined as those nodes with a centrality value above the empirical 75% quartile. The comparison returns Jaccard's indexes for each of four local measures (i.e., degree, betweenness centrality, closeness centrality, eigenvector centrality) of the sets of most central nodes as well as for the sets of hub taxa between the two networks compared. Thus, the Jaccard's index express the similarity of the sets of most central nodes as well as the sets of hub taxa between the two networks. Jaccard index of 0 indicates completely different sets while a value of 1 indicates equal sets of most central nodes or hub taxa between the compared networks. The two *p*-values $P(J \leq j)$ and $P(J \geq j)$ for each Jaccard's index are the probability that the observed value of Jaccard's index is 'less than or equal' or 'higher than or equal', respectively, to the Jaccard value expected at random, which is calculated taking into account the present total number of taxa in both sets [based on Real and Vargas (72)].

DATA AVAILABILITY STATEMENT

The datasets presented in this study can be found in online repositories. The names of the repository/repositories and accession number(s) can be found below: https://www.ncbi.nlm.nih.gov/sra, PRJNA778616.

ETHICS STATEMENT

All procedures were performed at the Nature Research Centre in Vilnius, Lithuania, according to Lithuanian and International Guiding Principles for Biomedical Research Involving Animals (2012). Infection experiments and other procedures were reviewed and approved by the Lithuanian State Food and Veterinary Service, Ref. No. 2020/07/24-G2-84. The assessment of the animal health and all described procedures were implemented by trained professionals (under licenses 2012/02/06-No-208, and 2016/01.29-No-344).

AUTHOR CONTRIBUTIONS

AC-C and VP conceived the study. JA, RŽ, JM, EP, LM-H, and VP performed the experiments and acquired the data. JA, AW-C, and DO analyzed the data. JA, AW-C, and AC-C prepared the figures. AC-C, VP, and JM contributed reagents and other resources. AC-C, VP, and DO supervised the work. JA, AW-C, AC-C, and VP drafted the first version of the manuscript. All authors contributed to the article and approved the submitted version.

FUNDING

This research was funded by the French Government's Investissement d'Avenir program, Laboratoire d'Excellence "Integrative Biology of Emerging Infectious Diseases" (grant no. ANR-10-LABX-62-IBEID). Funding for VP from European Social Fund (project No 09.3.3-LMT-K-712-01-0016) under grant agreement with the Research Council of Lithuania (LMTLT). AW-C was supported by Programa Nacional de Becas de Postgrado en el Exterior "Don Carlos Antonio López" (Grant No. 205/2018).

SUPPLEMENTARY MATERIAL

The Supplementary Material for this article can be found online at: https://www.frontiersin.org/articles/10.3389/fimmu.2022.841835/full#supplementary-material.

Supplementary Figure S1 | Impact of anti-microbiota vaccines on fecal microbiota of birds. Comparison of ASV richness and evenness, measured with **(A)** Faith's phylogenetic diversity index and **(B)** Pielou's evenness index, respectively, among the microbiota of mock-immunized, *E. coli* BL21-immunized and *E. coli* O86:B7-immunized birds.

Supplementary Figure S2 | Number of shared co-occurring taxa of *Escherichia-Shigella* among the sub-networks of different experimental group. Venn diagram showing the number of bacteria that are common or unique among the taxa that co-occur directly to *Escherichia-Shigella* in the different experimental group.

Supplementary Table S1 | Jaccard indexes of local centrality measures. Jaccard's indexes for each of local centrality measures (i.e., degree, betweenness centrality, closeness centrality, eigenvector centrality and hub taxa) of the sets of most central nodes for pairwise network comparisons. The two *p*-values, $P(J \leq j)$ and $P(J \geq j)$, for each Jaccard's index were added.

REFERENCES

1. Lee H, Halverson S, Ezinwa N. Mosquito-Borne Diseases. *Prim Care* (2018) 45(3):393–407. doi: 10.1016/j.pop.2018.05.001
2. Valkiūnas G, Iezhova TA. Keys to the Avian Malaria Parasites. *Malar J* (2018) 17:212. doi: 10.1186/s12936-018-2359-5
3. Valkiunas G. *Avian Malaria Parasites and Other Haemosporidia. 1st*. Boca Raton, FL: CRC Press (2004).
4. Martínez-de la Puente J, Santiago-Alarcon D, Palinauskas V, Bensch S. Plasmodium Relictum. *Trends Parasitol* (2021) 37(4):355–6. doi: 10.1016/j.pt.2020.06.004
5. Santiago-Alarcon D, Palinauskas V, Schaefer HM. Diptera Vectors of Avian Haemosporidian Parasites: Untangling Parasite Life Cycles and Their Taxonomy. *Biol Rev Camb Philos Soc* (2012) 87(4):928–64. doi: 10.1111/j.1469-185X.2012.00234.x
6. Blandin SA, Wang-Sattler R, Lamacchia M, Gagneur J, Lycett G, Ning Y, et al. Dissecting the Genetic Basis of Resistance to Malaria Parasites in Anopheles Gambiae. *Science* (2009) 326:147–50. doi: 10.1126/science.1175241
7. Collins FH, Sakai RK, Vernick KD, Paskewitz S, Seeley DC, Miller LH, et al. Genetic Selection of a *Plasmodium*-Refractory Strain of the Malaria Vector Anopheles Gambiae. *Science* (1986) 234:607–10. doi: 10.1126/science.3532325
8. Vernick KD, Oduol F, Lazzaro BP, Glazebrook J, Xu J, Riehle M, et al. Molecular Genetics of Mosquito Resistance to Malaria Parasites. *Curr Top Microbiol Immunol* (2005) 295:383–415. doi: 10.1007/3-540-29088-5_15
9. Hajkazemian M, Bossé C, Mozūraitis R, Emami SN. Battleground Midgut: The Cost to the Mosquito for Hosting the Malaria Parasite. *Biol Cell* (2021) 113(2):79–94. doi: 10.1111/boc.202000039
10. Wang M, An Y, Gao L, Dong S, Zhou X, Feng Y, et al. Glucose-Mediated Proliferation of a Gut Commensal Bacterium Promotes *Plasmodium* Infection by Increasing Mosquito Midgut Ph. *Cell Rep* (2021) 35(3):108992. doi: 10.1016/j.celrep.2021.108992
11. Bando H, Okado K, Guelbeogo W, Badolo A, Aonuma H, Nelson B, et al. Intra-Specific Diversity of *Serratia Marcescens* in *Anopheles* Mosquito Midgut Defines *Plasmodium* Transmission Capacity. *Sci Rep* (2013) 3:1641. doi: 10.1038/srep01641
12. Shaw WR, Catteruccia F. Vector Biology Meets Disease Control: Using Basic Research to Fight Vector-Borne Diseases. *Nat Microbiol* (2019) 4:20–34. doi: 10.1038/s41564-018-0214-7
13. Boissière A, Tchioffo MT, Bachar D, Abate L, Marie A, Nsango SE, et al. Midgut Microbiota of the Malaria Mosquito Vector *Anopheles Gambiae* and Interactions With *Plasmodium Falciparum* Infection. *PloS Pathog* (2012) 8(5):e1002742. doi: 10.1371/journal.ppat.1002742
14. Ben-Yakir D. Growth Retardation of *Rhodnius Prolixus* Symbionts by Immunizing Host Against *Nocardia* (*Rhodococcus*) Rhodnii. *J Insect Physiol* (1987) 33:379–83. doi: 10.1016/0022-1910(87)90015-1
15. Noden BH, Vaughan JA, Pumpuni CB, Beier JC. Mosquito Ingestion of Antibodies Against Mosquito Midgut Microbiota Improves Conversion of Ookinetes to Oocysts for *Plasmodium Falciparum*, But Not P. *yoelii Parasitol Int* (2011) 60(4):440–6. doi: 10.1016/j.parint.2011.07.007
16. Maitre A, Wu-Chuang A, Aželytė J, Palinauskas V, Mateos-Hernández L, Obregon D, et al. Vector Microbiota Manipulation by Host Antibodies: The Forgotten Strategy to Develop Transmission-Blocking Vaccines. *Parasit Vectors* (2021) 15:4. doi: 10.1186/s13071-021-05122-5
17. Mateos-Hernández L, Obregón D, Wu-Chuang A, Maye J, Bornères J, Versille N, et al. Anti-Microbiota Vaccines Modulate the Tick Microbiome in a Taxon-Specific Manner. *Front Immunol* (2021) 12:704621. doi: 10.3389/fimmu.2021.704621
18. Mateos-Hernández L, Obregón D, Maye J, Borneres J, Versille N, de la Fuente J, et al. Anti-Tick Microbiota Vaccine Impacts *Ixodes Ricinus* Performance During Feeding. *Vaccines (Basel)* (2020) 8(4):702. doi: 10.3390/vaccines8040702
19. Ackerman S, Clare FB, McGill TW, Sonenshine DE. Passage of Host Serum Components, Including Antibody, Across the Digestive Tract of *Dermacentor Variabilis* (Say). *J Parasitol* (1981) 67(5):737–40. doi: 10.2307/3280459
20. Ben-Yakir D, Fox CJ, Homer JT, Barker RW. Quantification of Host Immunoglobulin in the Hemolymph of Ticks. *J Parasitol* (1987) 73(3):669–71. doi: 10.2307/3282157
21. Wang H, Nuttall PA. Excretion of Host Immunoglobulin in Tick Saliva and Detection of IgG-Binding Proteins in Tick Haemolymph and Salivary Glands Parasitology. *Parasitology* (1994) 109(4):525–30. doi: 10.1017/s0031182000080781
22. Willadsen P. Novel Vaccines for Ectoparasites. *Vet Parasitol* (1997) 71(2-3):209–22. doi: 10.1016/s0304-4017(97)00028-9
23. Rathinavelu S, Broadwater A, de Silva AM. Does Host Complement Kill *Borrelia Burgdorferi* Within Ticks? *Infect Immun* (2003) 71(2):822–9. doi: 10.1128/IAI.71.2.822-829.2003
24. Galay RL, Matsuo T, Hernandez EP, Talactac MR, Kusakisako K, Umemiya-Shirafuji R, et al. Immunofluorescent Detection in the Ovary of Host Antibodies Against a Secretory Ferritin Injected Into Female *Haemaphysalis Longicornis* Ticks. *Parasitol Int* (2018) 67(2):119–22. doi: 10.1016/j.parint.2017.10.006
25. Hatfield PR. Detection and Localization of Antibody Ingested With a Mosquito Bloodmeal. *Med Vet Entomol* (1988) 2(4):339–45. doi: 10.1111/j.1365-2915.1988.tb00206.x
26. Lackie AM, Gavin S. Uptake and Persistence of Ingested Antibody in the Mosquito Anopheles Stephensi. *Med Vet Entomol* (1989) 3(3):225–30. doi: 10.1111/j.1365-2915.1989.tb00220.x
27. Tesh RB, Chen WR, Catuccio D. Survival of Albumin, IgG, IgM, and Complement (C3) in Human Blood After Ingestion by *Aedes Albopictus* and Phlebotomus Papatasi. *Am J Trop Med Hyg* (1988) 39(1):127–30. doi: 10.4269/ajtmh.1988.39.127
28. Saab NAA, Nascimento AAS, Queiroz DC, da Cunha IGM, Pereira AA, D'Ávila Pessoa GC, et al. How *Lutzomyia Longipalpis* Deals With the Complement System Present in the Ingested Blood: The Role of Soluble Inhibitors and the Adsorption of Factor H by Midgut. *J Insect Physiol* (2020) 120:103992. doi: 10.1016/j.jinsphys.2019.103992
29. Nogge G, Giannetti M. Specific Antibodies: A Potential Insecticide. *Science* (1980) 209(4460):1028–9. doi: 10.1126/science.7403865
30. Kumar M, Kaur S, Kariu T, Yang X, Bossis I, Anderson JF, et al. *Borrelia Burgdorferi* BBA52 is a Potential Target for Transmission Blocking Lyme Disease Vaccine. *Vaccine* (2011) 29(48):9012–9. doi: 10.1016/j.vaccine.2011.09.035
31. Tachibana M, Wu Y, Iriko H, Muratova O, MacDonald NJ, Sattabongkot J, et al. N-Terminal Prodomain of Pfs230 Synthesized Using a Cell-Free System

is Sufficient to Induce Complement-Dependent Malaria Transmission-Blocking Activity. *Clin Vaccine Immunol* (2011) 18(8):1343–50. doi: 10.1128/CVI.05104-11
32. Chowdhury DR, Angov E, Kariuki T, Kumar N. A Potent Malaria Transmission Blocking Vaccine Based on Codon Harmonized Full Length Pfs48/45 Expressed in Escherichia Coli. *PloS One* (2009) 4(7):e6352. doi: 10.1371/journal.pone.0006352
33. Kapulu MC, Da DF, Miura K, Li Y, Blagborough AM, Churcher TS, et al. Comparative Assessment of Transmission-Blocking Vaccine Candidates Against Plasmodium Falciparum. *Sci Rep* (2015) 5:11193. doi: 10.1038/srep11193
34. de Silva AM, Telford SR3rd, Brunet LR, Barthold SW, Fikrig E. *Borrelia Burgdorferi* OspA is an Arthropod-Specific Transmission-Blocking Lyme Disease Vaccine. *J Exp Med* (1996) 183(1):271–5. doi: 10.1084/jem.183.1.271
35. Nogge G. Aposymbiotic Tsetse Flies, *Glossina Morsitans Morsitans* Obtained by Feeding on Rabbits Immunized Specifically With Symbionts. *J Insect Physiol* (1978) 24(4):299–304. doi: 10.1016/0022-1910(78)90026-4
36. Wu-Chuang A, Hodzic A, Mateos-Hernandez L, Estrada-Peña A, Obregon D, Cabezas-Cruz A, et al. Current Debates and Advances in Tick Microbiome Research. *CRPVBD* (2021) 1:100036. doi: 10.1016/j.crpvbd.2021.100036
37. Narasimhan S, Swei A, Abouneameh S, Pal U, Pedra JHF, Fikrig E. Grappling With the Tick Microbiome. *Trends Parasitol* (2021) 37(8):722–33. doi: 10.1016/j.pt.2021.04.004
38. Pumpuni CB, Beier MS, Nataro JP, Guers LD, Davis JR. *Plasmodium Falciparum*: Inhibition of Sporogonic Development in *Anopheles Stephensi* by Gram-Negative Bacteria. *Exp Parasitol* (1993) 77(2):195–9. doi: 10.1006/expr.1993.1076
39. Pumpuni CB, Demaio J, Kent M, Davis JR, Beier JC. Bacterial Population Dynamics in Three Anopheline Species: The Impact on *Plasmodium* Sporogonic Development. *Am J Trop Med Hyg* (1996) 54(2):214–8. doi: 10.4269/ajtmh.1996.54.214
40. Straif SC, Mbogo CN, Toure AM, Walker ED, Kaufman M, Toure YT, et al. Midgut Bacteria in *Anopheles Gambiae* and An. Funestus (Diptera: Culicidae) From Kenya and Mali. *J Med Entomol* (1998) 35(3):222–6. doi: 10.1093/jmedent/35.3.222
41. Dong Y, Manfredini F, Dimopoulos G. Implication of the Mosquito Midgut Microbiota in the Defense Against Malaria Parasites. *PloS Pathog* (2009) 5(5):e1000423. doi: 10.1371/journal.ppat.1000423
42. Gendrin M, Rodgers F, Yerbanga R, Bosco J, Basañez MG, Cohuet A, et al. Antibiotics in Ingested Human Blood Affect the Mosquito Microbiota and Capacity to Transmit Malaria. *Nat Commun* (2015) 6:5921. doi: 10.1038/ncomms6921
43. Yilmaz B, Portugal S, Tran TM, Gozzelino R, Ramos S, Gomes J, et al. Gut Microbiota Elicits a Protective Immune Response Against Malaria Transmission. *Cell* (2014) 159(6):1277–89. doi: 10.1016/j.cell.2014.10.053
44. Mateos-Hernández L, Risco-Castillo V, Torres-Maravilla E, Bermúdez-Humarán LG, Alberdi P, Hodzic A, et al. Gut Microbiota Abrogates Anti-α-Gal IgA Response in Lungs and Protects Against Experimental *Aspergillus* Infection in Poultry. *Vaccines (Basel)* (2020) 8(2):285. doi: 10.3390/vaccines8020285
45. Cabezas-Cruz A, Mateos-Hernández L, Alberdi P, Villar M, Riveau G, Hermann E, et al. Effect of Blood Type on Anti-α-Gal Immunity and the Incidence of Infectious Diseases. *Exp Mol Med* (2017) 49(3):e301. doi: 10.1038/emm.2016.164
46. Wu-Chuang A, Obregon D, Mateos-Hernández L, Cabezas-Cruz A. Anti-Tick Microbiota Vaccines: How can This Actually Work? *Biologia* (2021). doi: 10.1007/s11756-021-00818-6
47. Burt A. Site-Specific Selfish Genes as Tools for the Control and Genetic Engineering of Natural Populations. *Proc Biol Sci* (2003) 270(1518):921–8. doi: 10.1098/rspb.2002.2319
48. Dimitrov D, Palinauskas V, Iezhova TA, Bernotiene R, Ilgunas M, Bukauskaite D, et al. *Plasmodium* Spp.: An Experimental Study on Vertebrate Host Susceptibility to Avian Malaria. *Exp Parasitol* (2015) 148:1–16. doi: 10.1016/j.exppara.2014.11.005
49. Palinauskas V, Valkiunas G, Bolshakov CV, Bensch S. *Plasmodium Relictum* (Lineage P-SGS1): Effects on Experimentally Infected Passerine Birds. *Exp Parasitol* (2008) 120:372–80. doi: 10.1016/j.exppara.2008.09.001
50. Žiegytė R, Bernotienė R, Bukauskaitė D, Palinauskas V, Iezhova T, Valkiūnas G. Complete Sporogony of *Plasmodium Relictum* (Lineages Psgs1 and Pgrw11) in Mosquito *Culex Pipiens Pipiens* Form *Molestus*, With Implications to Avian Malaria Epidemiology. *J Parasitol* (2014) 100:878–82. doi: 10.1645/13-469.1
51. Kazlauskiene R, Bernotiene R, Palinauskas V, Iezhova TA, Valkiunas G. *Plasmodium Relictum* (Lineages Psgs1 and Pgrw11): Complete Synchronous Sporogony in Mosquitoes Culex Pipiens Pipiens. *Exp Parasitol* (2013) 133:454–61. doi: 10.1016/j.exppara.2013.01.008
52. Valkiūnas G, Iezhova TA, Križanauskienė A, Palinauskas V, Sehgal RNM, Bensch S. A Comparative Analysis of Microscopy and PCR-Based Detection Methods for Blood Parasites. *J Parasitol* (2008) 94:1395–401. doi: 10.1645/GE-1570.1
53. Godfrey RD, Fedynich AM, Pence DB. Quantification of Hematozoa in Blood Smears. *J Wildl Dis* (1987) 23:558–65. doi: 10.7589/0090-3558-23.4.558
54. Sambrook J, Fritsch EF, Mamiatis T. *Molecular Cloning: A Laboratory Manual. 3rd*. New York, NY: Cold Spring Harbor Laboratory Press (2001).
55. Hellgren O, Waldenström J, Bensch S. A New PCR Assay for Simultaneous Studies of *Leucocytozoon, Plasmodium*, and *Haemoproteus* From Avian Blood. *J Parasitol* (2004) 90:797–802. doi: 10.1645/GE-184R1
56. Bensch S, Stjernman M, Hasselquist D, Orjan O, Hannson B, Westerdahl H, et al. Host Specificity in Avian Blood Parasites: A Study of *Plasmodium* and *Haemoproteus* Mitochondrial DNA Amplified From Birds. *Proc R Soc B Biol Sci* (2000) 267:1583–9. doi: 10.1098/rspb.2000.1181
57. Bolyen E, Rideout JR, Dillon MR, Bokulich NA, Abnet CC, Al-Ghalith GA, et al. Reproducible, Interactive, Scalable and Extensible Microbiome Data Science Using QIIME 2. *Nat Biotechnol* (2019) 37(8):852–57. doi: 10.1038/s41587-019-0209-9
58. Callahan BJ, McMurdie PJ, Rosen MJ, Han AW, Johnson AJA, Holmes SP. DADA2: High-Resolution Sample Inference From Illumina Amplicon Data. *Nat Methods* (2016) 13:581–3. doi: 10.1038/nmeth.3869
59. Katoh K. MAFFT: A Novel Method for Rapid Multiple Sequence Alignment Based on Fast Fourier Transform. *Nucleic Acids Res* (2002) 30:3059–66. doi: 10.1093/nar/gkf436
60. Price MN, Dehal PS, Arkin AP. FastTree 2 – Approximately Maximum-Likelihood Trees for Large Alignments. *PloS One* (2010) 5:e9490. doi: 10.1371/journal.pone.0009490
61. Bokulich NA, Kaehler BD, Rideout JR, Dillon M, Bolyen E, Knight R, et al. Optimizing Taxonomic Classification of Marker-Gene Amplicon Sequences With QIIME 2's Q2-Feature-Classifier Plugin. *Microbiome* (2018) 6:90. doi: 10.1186/s40168-018-0470-z
62. Yarza P, Yilmaz P, Pruesse E, Glöckner FO, Ludwig W, Schleifer K-H, et al. Uniting the Classification of Cultured and Uncultured Bacteria and Archaea Using 16S rRNA Gene Sequences. *Nat Rev Microbiol* (2014) 12:635–45. doi: 10.1038/nrmicro3330
63. Friedman J, Alm EJ. Inferring Correlation Networks From Genomic Survey Data. *PloS Comput Biol* (2012) 8:1–11. doi: 10.1371/journal.pcbi.1002687
64. RStudio Team. *RStudio: Integrated Development for R RStudio*. Boston: PBC (2020).
65. Bastian M, Heymann S, Jacomy M. Gephi: An Open Source Software for Exploring and Manipulating Networks. In: *Proc Int AAAI Conf Weblogs Soc Media* (2009) 3:1. doi: 10.13140/2.1.1341.1520
66. Wickham H, Grolemund G. *R for Data Science: Import, Tidy, Transform, Visualize, and Model Data. 1st*. Canada: O'Reilly (2016). Available at: http://r4ds.had.co.nz/.
67. Faith DP. Conservation Evaluation and Phylogenetic Diversity. *Biol Conserv* (1992) 61:1–10. doi: 10.1016/0006-3207(92)91201-3
68. Pielou EC. The Measurement of Diversity in Different Types of Biological Collections. *J Theor Biol* (1966) 13:131–44. doi: 10.1016/0022-5193(66)90013-0
69. Bray JR, Curtis JT. An Ordination of the Upland Forest Communities of Southern Wisconsin. *Ecol Monogr* (1957) 27:325–49. doi: 10.2307/1942268
70. Love MI, Huber W, Anders S. Moderated Estimation of Fold Change and Dispersion for RNA-Seq Data With Deseq2. *Genome Biol* (2014) 15:550. doi: 10.1186/s13059-014-0550-8
71. Peschel S, Müller CL, von Mutius E, Boulesteix AL, Depner M. NetCoMi: Network Construction and Comparison for Microbiome Data in R. *Brief Bioinf* (2021) 22:bbaa290. doi: 10.1093/bib/bbaa290

72. Real R, Vargas JM. The Probabilistic Basis of Jaccard's Index of Similarity. *Syst Biol* (1996) 45:380–5. doi: 10.1093/sysbio/45.3.380

Conflict of Interest: The authors declare that the research was conducted in the absence of any commercial or financial relationships that could be construed as a potential conflict of interest.

Publisher's Note: All claims expressed in this article are solely those of the authors and do not necessarily represent those of their affiliated organizations, or those of the publisher, the editors and the reviewers. Any product that may be evaluated in this article, or claim that may be made by its manufacturer, is not guaranteed or endorsed by the publisher.

PAPER IV

Avian Malaria Parasites Modulate Gut Microbiome Assembly in Canaries

Aželytė J., Wu-Chuang A., Maitre A., Žiegytė R., Mateos-Hernández L., Obregón D., Palinauskas V., Cabezas-Cruz A.

Microorganisms, 2023, 11:563
DOI 10.3390/microorganisms11030563

microorganisms

MDPI

Article

Avian Malaria Parasites Modulate Gut Microbiome Assembly in Canaries

Justė Aželytė [1,†], Alejandra Wu-Chuang [2,†], Apolline Maitre [2,3,4], Rita Žiegytė [1], Lourdes Mateos-Hernández [2], Dasiel Obregón [5], Vaidas Palinauskas [1,*] and Alejandro Cabezas-Cruz [2,*]

[1] Nature Research Centre, Akademijos 2, LT-09412 Vilnius, Lithuania
[2] ANSES, INRAE, Ecole Nationale Vétérinaire d'Alfort, UMR BIPAR, Laboratoire de Santé Animale, F-94700 Maisons-Alfort, France
[3] INRAE, UR 0045 Laboratoire de Recherches Sur Le Développement de L'Elevage (SELMET-LRDE), F-20250 Corte, France
[4] EA 7310, Laboratoire de Virologie, Université de Corse, F-20250 Corte, France
[5] School of Environmental Sciences, University of Guelph, Guelph, ON N1G 2W1, Canada
* Correspondence: vaidas.palinauskas@gamtc.lt (V.P.); alejandro.cabezas@vet-alfort.fr (A.C.-C.)
† These authors contributed equally to this work.

Abstract: Rodent and human malaria parasites cause dysbiosis in the host gut microbiome, but whether *Plasmodium* species affecting birds cause dysbiosis in their hosts is currently unknown. Here we used a model of avian malaria infection to test whether parasite infection modulates the bird microbiome. To this aim, bird fecal microbiomes were characterized at different time points after infection of canaries with the avian malaria parasite *Plasmodium homocircumflexum*. Avian malaria caused no significant changes in the alpha and beta diversity of the microbiome in infected birds. In contrast, we discovered changes in the composition and abundance of several taxa. Co-occurrence networks were used to characterize the assembly of the microbiome and trajectories of microbiome structural states progression were found to be different between infected and uninfected birds. Prediction of functional profiles in bacterial communities using PICRUSt2 showed infection by *P. homocircumflexum* to be associated with the presence of specific degradation and biosynthesis metabolic pathways, which were not found in healthy birds. Some of the metabolic pathways with decreased abundance in the infected group had significant increase in the later stage of infection. The results showed that avian malaria parasites affect bacterial community assembly in the host gut microbiome. Microbiome modulation by malaria parasites could have deleterious consequences for the host bird. Knowing the intricacies of bird-malaria-microbiota interactions may prove helpful in determining key microbial players and informing interventions to improve animal health.

Keywords: avian malaria; microbiome; parasite-microbiota interactions

Citation: Aželytė, J.; Wu-Chuang, A.; Maitre, A.; Žiegytė, R.; Mateos-Hernández, L.; Obregón, D.; Palinauskas, V.; Cabezas-Cruz, A. Avian Malaria Parasites Modulate Gut Microbiome Assembly in Canaries. *Microorganisms* **2023**, *11*, 563. https://doi.org/10.3390/microorganisms11030563

Academic Editor: Marie-France Cesbron-Delauw

Received: 18 December 2022
Revised: 17 February 2023
Accepted: 21 February 2023
Published: 23 February 2023

1. Introduction

The scarcity of gut microbiome studies compared with other taxonomic groups underscores a gap in our understanding of host-microbiota interactions in metazoans [1]. Next-generation sequencing and microbiome analyses in different bird species [2] provide a significant contribution to our understanding of the diversity of microbial communities in the gut microbiota of metazoans and a first insight into the functional contribution of bird microbiome to host physiology [3]. Studies on the identification of extrinsic and intrinsic factors affecting gut microbiome composition revealed that host genetics is among the most important factors accounting for differences in the composition of gut microbiome in wild birds [4]. The local habitat of the birds was also shown to have a large influence on gut microbiome composition in Arctic-breeding shorebirds [5],

and Brown-headed Cowbirds [6]. The ecological implications of microbiota diversity in wild birds remain to be explored [7].

In addition to host genetics and environmental factors, empirical evidence shows that parasite infection triggers changes in host microbiome [8–10]. For example, a recent study by Videvall et al. [11] showed differential bacterial abundance in the microbiome of uropygial gland of *Plasmodium*-infected house sparrows compared to uninfected birds. These results suggest that *Plasmodium* infection may affect the abundance, but also the composition and/or diversity of commensal bacteria associated with the host. This has been shown experimentally for murine malaria parasites [12–14]. By disrupting the microbiota-immune system homeostasis, malaria alters the profiles of mouse gut microbiome [12–14]. Two independent studies provided evidence that infection with rodent malaria parasites *Plasmodium yoelii* [15] and *Plasmodium berghei* [16] resulted in alterations in the gut microbiome profile. Similar results were reported for other apicomplexan parasites such as *Eimeria* spp. in chicken [10] and *Cryptosporidium parvum* in goat kids [8]. Mechanistically, deviation from immune homeostasis due to malaria infections may impact the host microbiome composition, and malaria-related changes in the composition of the microbiome may further alter the host immunity [14], which may result in different patterns of disease susceptibility and/or severity.

Based on morphological and mitochondrial genome features, more than 55 species of avian malaria parasites have been described [17,18]. Host specificity of malaria parasites varies from specialists infecting a single bird species to generalists infecting more than 300 distantly-related bird species [17–19]. *Plasmodium homocircumflexum* (COLL4) is known to infect around 19 different bird species belonging to 11 families (MalAvi v. 2.5.5) [18]. The distribution of this parasite in wildlife populations is not well known, however, the detection of *P. homocircumfelxum* in the European migratory birds, wintering in Africa, and resident birds of Africa and South America regions indicates its natural occurrence (MalAvi v. 2.5.5) [18]. Experimental infections of several bird species showed that this parasite can be highly virulent [20–22], however, the pathologies caused by *P. homocircumflexum* varies in different bird species, which might appear due to the adaptation of parasite gene expression in the avian hosts of different species [23]. The pathogenicity of *P. homocircumfelxum* is manifested by the development of severe parasitemia and/or exoerythrocytic stages in various organs leading to death of the host [21,22].

In this study, we tested whether experimental infection of canaries (*Serinus canaria domestica*) by the generalist avian malaria parasite *P. homocircumflexum* modulate the bird host gut microbiome from acute and chronic stages of the primary infection to the beginning of the latent stage. The results support that, as with murine and human malaria, avian malaria parasites influence the composition and structure of commensal bacteria populations in the host gut.

2. Material and Methods

2.1. Ethical Statement

All procedures were performed at Nature Research Centre in Vilnius, Lithuania, according to Lithuanian and International Guiding Principles for Biomedical Research Involving Animals (2012). Infection experiments were reviewed and approved by the Lithuanian State Food and Veterinary Service, Ref. No 2020/07/24-G2-84. The assessment of the animal health and all described procedures were implemented by trained professionals (under licenses 2012/02/06-No-208, 2016/01/29-No-344, and 2021/02/05-No-527).

2.2. Birds and Housing Conditions

One-year-old domestic canaries (*Serinus canaria domestica*) were kept in the same room of Nature Research Centre vivarium (License No. LT-61-13-003) under standard living conditions for birds. Experimental birds were housed in cages individually. The

facilities were under a controlled temperature of 21 °C throughout the duration of the experiment. Standard food for canaries and water were provided *ad libitum*.

2.3. Experimental Design

Canaries were used as a model for avian malaria infection with *P. homocircumflexum* parasite. Before the experimental procedures began, birds were randomly separated in 'infected' and 'control' groups (Figure 1). Birds in the control group received blood from uninfected bird donors. The infected group of birds received an inoculation of infectious blood with *P. homocircumflexum* parasites. Every four days post-infection (DPI) blood samples were collected and parasitemia was measured. Bird feces were collected and used for DNA extraction and microbiome analysis using bacterial 16S rRNA amplicon sequencing to test for an impact of malaria infection on bird gut microbiome. Experimental procedures are described below.

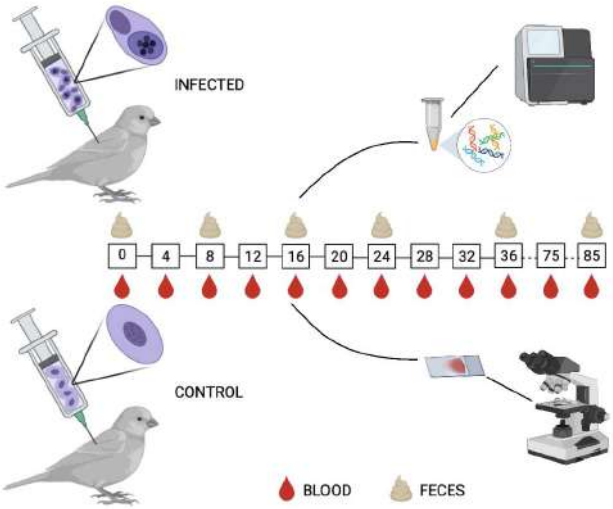

Figure 1. Experimental design. Canaries were inoculated with *P. homocircumflexum*-infected (n = 8) or uninfected (n = 8) donor blood. Blood and fecal samples were collected at different time points as indicated. Created with BioRender.com.

2.4. Thawing the Cryopreserved Avian Malaria Sample

The cryopreserved *P. homocircumflexum* strain COLL4 was thawed and used to infect donor canaries. Samples containing *P. homocircumflexum*-infected avian blood, cryopreserved in liquid nitrogen, were thawed as described by Dimitrov et al. [24]. Briefly, thawed samples were mixed with 12% NaCl (1/3 of thawed sample amount). After 5 min equilibration, one volume of 1.6% of NaCl was added followed by centrifugation at 1400 rpm for 5 min. After centrifugation, the supernatant was removed and 1.6% NaCl (1/3 of original sample) was added and centrifuged again. The same procedure was repeated three times with 0.9% NaCl solution. The final mixture was diluted with 0.9% NaCl and sub-inoculated into two donor canaries.

2.5. Experimental Infection of Birds

Birds from one group (n = 8) were experimentally infected with *P. homocircumflexum* using the protocol described by Palinauskas et al. [25]. Each experimental bird was sub-inoculated with a mixture (0.10 mL) of infected blood, 3.7% sodium citrate and 0.9% saline in proportion 4:1:5 into the pectoral muscles. Each bird received approximately 3×10^5 of mature *P. homocircumflexum* meronts. The duration of experiment was 85 DPI. Parasitemia was examined every 4 DPI until 36 DPI by taking blood from the brachial vein as described in the section below. After 36 DPI, parasitemia was measured two more times at 75 and 85 DPI (Figure 1).

2.6. Blood Sample and Bird Feces Collection

Blood samples were taken from birds by puncturing brachial vein using heparinized microcapillaries. A small drop of blood was used to make two smears for microscopy to count erythrocytic stages in the blood (see below). Smears were air-dried, fixed with absolute methanol and stained as described by Valkiūnas et al. [26]. A fraction of blood (20–30 μL) was placed in SET-buffer for molecular analysis (PCR, see below) to confirm the lineage in recipient birds. The blood for smears and SET-buffer was collected at 0 DPI prior to the inoculation of infected and non-infected blood and every 4 DPI until 36 DPI, and on 75 and 85 DPI (Figure 1). Fresh feces were collected from each bird in sterile tubes at the same time as blood taking on 0, 8, 16, 24, 36, and 85 DPI. Samples were stored at −20 °C before genomic DNA extraction.

2.7. Microscopic Examination

We used an Olympus BX61 light microscope (Olympus, Tokyo, Japan) to examine blood smears and calculated the parasitemia as a percentage by actual counting of the number of parasites per 10,000 erythrocytes as described by Godfrey et al. [27].

2.8. DNA Extraction and PCR for P. homocircumflexum Identification

Total DNA for PCR analysis was extracted from the blood stored in SET-buffer using an ammonium acetate extraction protocol by Sambrook and Russel [28]. We performed a nested PCR following a protocol described by Hellgren et al. [29] to confirm *P. homocircumflexum* infection. For the first PCR we used the primers HaemNFI [5′-CATATATTAAGAGAAITATGGAG-3′] and HaemNR3 [5′-ATAGAAAGATAAGAAATACCATTC-3′] [29]. In the second PCR a fragmentt of mitochondrial *cyt b* gene (478 bp) was amplified using the primers HaemF [5′-ATGGTGCTTTCGATATATGCATG-3′] and HaemR2 [5′-GCATTATCTGGATGTGATAATGGT-3′] [30]. For PCR mix we used 12.5 μL of DreamTaq Master Mix (Thermo Fisher Scientific, Vilnius, Lithuania), 8.5 μL of nuclease-free water, 1 μL of each primer and 2 μL of template DNA (extracted DNA or products of first PCR). *Plasmodium homocircumflexum*-positive samples were determined by running 2 μL of second PCR product on 2% agarose gel. For parasite lineage confirmation, samples containing parasite DNA were sequenced from the 5′end using the HAEMF primer on an ABI PRISM TM 3100 capillary sequencing robot (Applied Biosystems, Waltham, MA, USA) as described by Bensch et al. [30]. The BLAST search tool (National Centre for Biotechnology Information website: http://www.ncbi.nlm.nih.gov/BLAST, accessed on 12 October 2022) was used to determine COLL4 lineage.

2.9. DNA Extraction and 16S rRNA Sequencing for Microbiome Analysis

Genomic DNA was isolated from fecal samples of uninfected or *Plasmodium*-infected canaries using a Pure Link Microbiome DNA Purification Kit (Invitrogen, Waltham, MA, USA; Thermo Fisher Scientific, Vallejo St. Emeryville, CA, USA). Final DNA samples were eluted in 70 μL of elution buffer. Genomic DNA quality (OD260/280 between 1.8–2.0) was measured with NanoDrop™ One (Thermo Scientific, Waltham, MA, USA). More

than 200 ng of DNA at 20 ng/μL concentration were used for amplicon sequencing of the 16S rRNA gene, which was commissioned to Novogene Bioinformatics Technology Co., (London, UK). Libraries were prepared with NEBNext® Ultra™ IIDNA Library Prep Kit (New England Biolabs, Ipswich, MA, USA). A single lane of Illumina MiSeq system was used to generate 251-base paired-end reads from the V4 variable region of the 16S rRNA gene using barcoded universal primers (515F/806R) in samples from uninfected (n = 8) or *P. homocircumflexum*-infected (n = 8) canaries. The raw 16S rRNA sequences obtained from bird fecal samples were deposited at the SRA repository (Bioproject No. PRJNA904724).

2.10. 16S rRNA Sequences Processing

The software package Quantitative Into Microbial Ecology (QIIME) 2 pipeline (v. 2021.4) [31] was used for the analysis of sequencing data. First, 16S rRNA gene sequences were first demultiplexed and then quality trimmed based on the average quality per base of the forward and reverse reads using DADA2 software [32] implemented in QIIME2. Reads were then merged and chimeric variants were removed. The resulting representative sequences were taxonomically assigned using a pre-trained naïve Bayes taxonomic classifier [33] based on SILVA database version 132 [34] and the 515F/806R primer set. The resulting taxonomic data tables were collapsed at genus level and low abundant taxa were removed by filtering taxa with less than 10 total reads and present in less than 30% of samples. The taxonomic data tables were used for network analysis and keystone taxa identification.

2.11. Statistical Analysis

Alpha and beta diversity analyses of taxonomic and functional profiles were performed using rarefied amplicon sequence variants (ASVs) and pathway tables, respectively. Differences in alpha diversity metrics (i.e., Faith's phylogenetic diversity, observed features and Pielou's evenness index) within and between different groups were tested using a pairwise Kruskal–Wallis test. Beta diversity was explored using the Bray–Curtis dissimilarity index and compared among the groups using a PERMANOVA test. To test whether factors such as 'time' or 'infection status' have an impact on beta diversity, an Adonis PERMANOVA test was used. Longitudinal analyses, including comparisons of first differences in alpha diversity metric (i.e., Shannon entropy differences in an individual between different samplings days (DPI)) and first distances (i.e., Bray–Curtis dissimilarity between an individual's microbiome composition at two separate sampling days), were used to compare the individual's variation rate over time; specifically, we compared the temporal variations for both metrics in all DPI intervals, using 0 DPI as reference (e.g., form 0 to 8 DPI, from 0 to 16 DPI, and so on). Consequently, the variation rates were compared between uninfected and infected birds using Kruskal–Wallis test and Mann–Whitney U test, respectively. Longitudinal analyses were also performed on the taxonomic profile, detecting and ranking the bacterial genera with the strongest temporal signal (i.e., changes in abundance across time). The longitudinal analyses were performed using the Qiime2 plugin q2-longitudinal pipeline, using the "feature-volatility" function, which detects only features of importance in terms of temporal variations and includes descriptive statistics for all important features. This pipeline mostly uses the random forests ensemble learning as a supervised regression method [35].

Differential abundance of taxa and pathway analyses were performed using the R package 'DeSeq2' [36], which applies data normalization based on negative binomial distribution and links variance and mean by local regression, and compares the magnitude of the changes, expressing it as log ratio (log fold change). The comparisons were performed with the Wald test. The number of shared taxa or predicted pathways in the different experimental conditions were visualized using Venn diagrams implemented in

the online tool (http://bioinformatics.psb.ugent.be/webtools/Venn/, accessed on 12 October 2022). Differences were considered significant when $p < 0.05$.

For differential network analysis Jaccards index (Jacc) was calculated with Network Construction and Comparison for Microbiome Data (NetComi) script [37] on R studio [38]. This index test for dissimilarities between the "most central nodes" in the networks for degree, betweenness centrality, closeness centrality, eigenvector centrality and for the hub taxa. The "most central nodes" are defined as nodes with a centrality value higher than the empirical 75% quartile. For testing the similarity of most central nodes, two *p*-values $p(J \leq j)$ and $p(J \geq j)$ for each Jacc, which represent the probability that the observed Jacc value is "lower than or equal" or "higher than or equal", respectively, to the Jacc value expected by random, were calculated taking into account the total number of taxa in both sets [39]. The Jacc ranges from 0 (completely different sets) to 1 (sets equal).

2.12. Bacterial Co-Occurrence Networks and Attack Tolerance Test

Co-occurrence microbial networks were built for each condition using the taxonomic profiles at genera level. Microbial networks were used for the graphical representation and visualization of the microbial community assemblies and the quantification of the importance of bacterial taxa in the network community. In the networks, bacterial taxa are represented by nodes and the significant positive (weight > 0.75) or negative (weight < −0.75) co-occurrence interaction between the nodes are represented by edges. The network analysis and construction were performed using Sparse Correlations for Compositional data (SparCC) method [40], implemented in R studio environment [38]. The software Gephi 0.9.5 [41], was used to visualize the microbial networks and to measure the topological features of networks (i.e., number of nodes and edges, network diameter, average degree, weighted degree, average path length, modularity and number of modules). The progression of the 'microbiome structural state' was presented using the alpha diversity metric of observed feature [42], measured with QIIME2 pipeline [31], and the number of edges and nodes collected from Gephi [41]. To test the network tolerance to attacks, the Network Strengths and Weaknesses Analysis (NetSwan) script [43] was conducted in R studio [38]. This script simulates a network attack by removing first the nodes with the highest betweenness centrality value, and measures decreases on network connectivity. Connectivity values ranged between 0 (maximum of connectivity between nodes) and 1 (total disconnection between nodes).

2.13. Prediction of Functional Traits in the Bird Microbiome

For the metabolic profiling of each sample, PICRUSt2 software [44] was used for the prediction of functional gene abundances based on 16S rRNA gene amplicon sequences. Briefly, the ASVs were aligned and placed into a reference tree (NSTI cut-off value of 2), which was then used to infer gene family copy numbers of each ASVs and finally determine gene family abundance per sample. Kyoto Encyclopedia of Genes and Genomes (KEGG) orthologs (KO) [45], Enzyme Classification numbers (EC) and Cluster of Orthologous Genes (COGs) [46] were used as gene family catalogs for the predictions. Pathway profiles were inferred from structured pathway mapping based on MetaCyc database [47].

3. Results

3.1. Experimental Infection of Plasmodium homocircumflexum in Birds

To test how malaria infection modulates the microbiome of vertebrate hosts, we followed an experimental model of avian malaria (Figure 1). All canaries experimentally infected with *P. homocircumflexum* were susceptible to the infection and developed parasitemia (Figure 2). As expected, the control group composed of uninfected birds remained negative to *Plasmodium* infection throughout the experiment. One bird from each group died during the experiment. Based on microscopic examination, the prepatent pe-

riod, before the parasite appeared in the peripheral blood for the first time, was less than 4 days post-infection (DPI). The dynamics of infection varied individually. The peak of parasitemia was recorded at 8 DPI in six infected birds, and in two canaries the peak was reached at 12 DPI. The parasitemia at the peak varied between 6.5–15.6% of infected erythrocytes. The parasitemia decreased four days after the peak at which point parasitemia was under 0.5% in all infected birds. From 24 DPI onwards the infection fluctuated between disappearance from peripheral blood and very low parasitemia. The parasite was detected in the peripheral blood in two infected birds at 85 DPI.

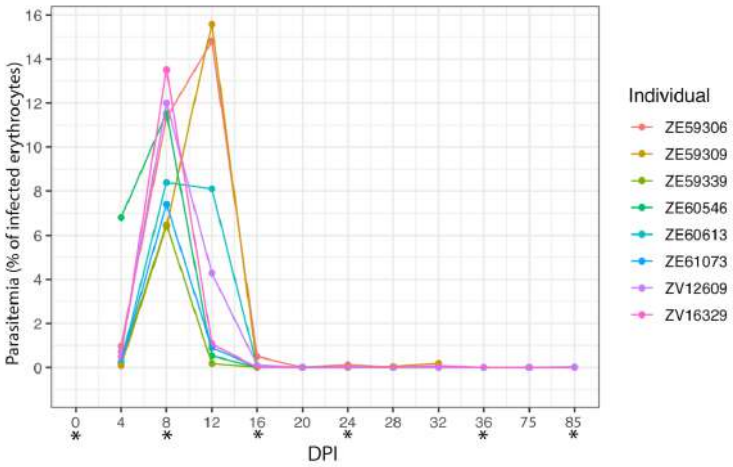

Figure 2. Temporal dynamics of *P. homocircumflexum* parasitemia. Individual parasitemia values (% of infected erythrocytes) of *P. homocircumflexum* based on microscopy are presented. * DPI selected for fecal sample collection and microbiome analysis.

3.2. Changes in the Taxonomic Profiles of Bird Gut Microbiome in Response to P. homocircumflexum Infection

To assess the impact of *P. homocircumflexum* infection on the gut microbiome of canaries, the diversity and composition of amplicon sequence variants (ASVs) of uninfected and *Plasmodium*-infected birds were analyzed in fecal samples collected at different DPI (Figure 1) with variation in parasitemia (Figure 2). Comparison of alpha diversity indexes within groups revealed significant differences in the Faith's index and observed features (Kruskal–Wallis test: Faith's index, $p < 0.001$; Observed features, $p < 0.001$), but no in the species evenness (Kruskal–Wallis test, $p = 0.113$). In addition, pairwise comparisons of these alpha diversity indexes between the groups at each sampling day show no significant differences between infected and uninfected birds (Kruskal–Wallis test, $p > 0.05$) (Figure S1). Similarly, beta diversity (Bray–Curtis dissimilarity index) comparisons showed no difference between groups (PERMANOVA, $p > 0.05$), or within groups across time (PERMANOVA, $F = 1.44$; $p = 0.147$) (Figure S2). Further statistical comparison of Bray–Curtis dissimilarity index using multifactorial PERMANOVA (Adonis function), detected significant compositional changes in time, but not associated with the infection state of the birds (Adonis: time, $p = 0.002$; infection, $p = 0.135$, interaction, $p = 0.285$). To further confirm these results, we used the longitudinal statistical approach "q2-longitudinal", which, by means of machine learning algorithms, analyzes temporal changes in the microbiome. Shannon's entropy, which combines richness and evenness

into one index, showed no significant difference between infected and uninfected birds, regardless of time intervals (Figure 3A). Likewise, no differences in Bray–Curtis's distance were found for any of the time intervals (Figure 3B). Altogether, these results showed that *P. homocircumflexum* infection does not modify the alpha or beta diversity of bird microbiome.

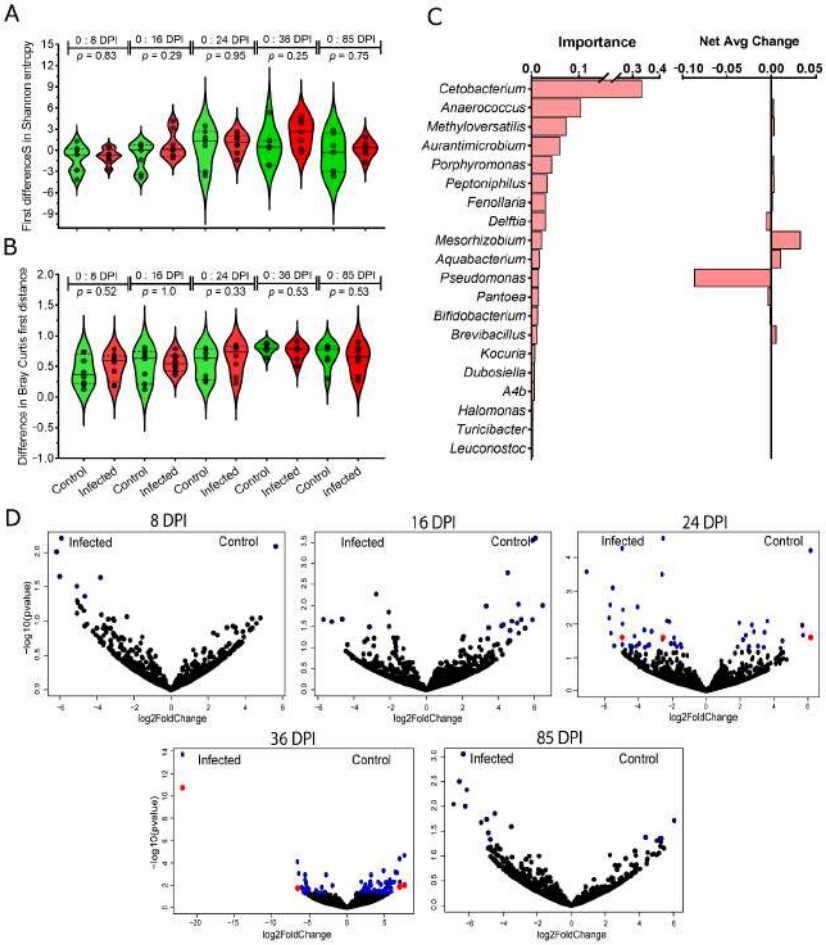

Figure 3. Effect of *P. homocircumflexum* infection on host microbial diversity and taxonomic profiles of bird microbiome. (**A**) Shannon entropy was used in the longitudinal analysis to compare the differences in alpha diversity between infected and uninfected birds at different time intervals (i.e., from 0 to 8 DPI, from 0 to 16 DPI, from 0 to 24 DPI, from 0 to 36 DPI, and from 0 to 85 DPI). Kruskal–Wallis was used to compare the differences (alpha = 0.05). (**B**) Similar longitudinal analysis was performed for beta diversity, based on Bray–Curtis distance. Between-groups comparisons were performed using Mann–Whitney U test (alpha = 0.05). (**C**) Longitudinal feature-volatility analysis of bacterial genera among infected and uninfected birds. The top 20 important features (i.e., from

100 taxa detected by random forest modeling exhibiting important temporal variations in abundance) are shown, including their temporal signal (importance) and net average change. (**D**) Volcano plot showing the differential bacterial abundance in bird microbiome between control and infected groups throughout the duration of experiment. Taxa with significant differences between the groups are represented with blue (Wald test, $p < 0.05$) and red (Wald test, p (corrected with Benjamin and Hochberg method) < 0.05) dots. The gray dots represent taxa with no significant differences between groups. Taxa with significant differences in their abundance were identified using DeSeq2 algorithm.

Taxonomic profiling of microbiome in uninfected and infected birds revealed the presence of a taxonomic core (i.e., taxa identified in all DPI, in either infected or uninfected birds) in both groups, as well as unique taxa associated to different sampling days (Figure S3A). A higher number of unique taxa (125) was found in the taxonomic core of the control group compared to that of the infected group (79), while 268 bacterial genera were present in the taxonomic core of both groups (Figure S3B). The unique taxa found at each sampling day were mostly specific to each group (Figure S3B), and those found only in infected birds were listed (Table S1). This suggested that infection is associated with modulation of the bird microbiome composition.

The longitudinal analysis on the taxonomical profiles revealed a total of 100 "important" taxa in terms of their temporal signal (i.e., their abundance changes gradually over time or are strongly predictive of specific timepoints), considering both infected and uninfected birds (Table S2). The top 20 important taxa included *Cetobacterium* (phylum Fusobacteriota), *Anaerococcus* (Firmicutes), *Methyloversatilis* (Proteobacteria), *Aurantimicrobium* (Actinobacteriota), *Porphyromonas* (Bacteroidota), among others (Figure 3C). Differential analysis of taxa abundance between infected and uninfected birds revealed significant differences only at 24 and 36 DPI in 3 and 4 bacterial genera, respectively, belonging to Proteobacteria (*Escherichia-Shigella*, *Undibacterium*, *Pseudahrensia*, and *Croceicoccus*), Chloroflexi (*Anaerolinea*), Verrucomicrobia (*Opitutaceae*) and Firmicutes (*Lachnospiraceae*) (Wald test, $p < 0.05$; Figure 3D; Table S3). The taxa abundance per phylum shows that the most abundant bacteria in the gut microbiome of birds belongs to Chloroflexi, Proteobacteria, Firmicutes, and Actinobacteriota (Figure S3C).

3.3. Changes in Microbial Community Assembly in Response to P. homocircumflexum Infection

Bacteria co-occurrence networks were inferred and used to assess the impact of *P. homocircumflexum* infection on the assembly of microbial communities in bird guts at different DPI. Visual inspection revealed that malaria infection changes network topology (Figure 4), and its parameters (Table 1). The difference of topological parameters between *Plasmodium*-infected and control group varied at each sampling day, however more noteworthy differences in topology were recorded at 8 and 24 DPI (Table 1).

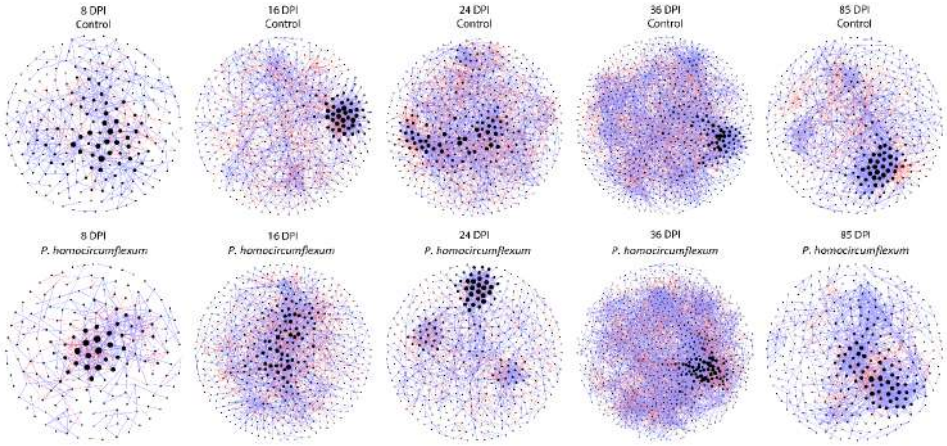

Figure 4. Co-occurrence networks of bird microbiome in the different experimental groups at 8, 16, 24, 36 and 85 DPI. Bacterial co-occurrence networks were inferred from the microbiome of *P. homocircumflexum*-infected birds and control. Nodes represent bacterial taxa and connecting edges stand for a co-occurrence correlation (SparCC > 0.75). Node sizes are proportional to the eigenvector centrality value. Edges representing positive or negative correlations were colored in lilac and red, respectively. Only nodes with at least one connection are displayed.

Table 1. Topological parameters of co-occurrence networks.

Network Features	8 DPI *		16 DPI		24 DPI		36 DPI		85 DPI	
	Control	*Plasmodium*-Infected	Control	*Plasmodium*-Infected	Control	*Plasmodium*-Infected	Control	*Plasmodium*-Infected	Control	*Plasmodium*-Infected
Nodes	242 (688) **	180 (641)	482 (938)	571 (1100)	534 (938)	473 (1023)	771 (1059)	926 (1267)	463 (926)	364 (666)
Edges	617	399	1929	2354	2673	1597	4375	6299	1934	1736
Positive	453 (73.4%)	245 (61.4%)	1130 (58.6%)	1467 (62.3%)	1597 (59.8%)	1079 (67.6%)	2877 (65.8%)	4169 (66.2%)	1423 (73.6%)	1403 (80.8%)
Negative	164 (26.6%)	154 (38.6%)	799 (41.4%)	887 (37.7%)	1076 (40.2%)	518 (32.4%)	1498 (34.2%)	2130 (33.8%)	511 (26.4%)	333 (19.2%)
Network diameter	15	16	11	13	9	12	8	13	12	17
Average degree	5.099	4.433	8.004	8.245	10.011	6.753	11.349	13.605	8.354	9.538
Weighted degree	1.928	0.827	1.124	1.67	1.651	1.946	2.897	3.649	3.254	4.84
Average path length	4.434	5.367	4.551	4.279	3.914	5.046	3.72	3.985	4.321	4.944
Modularity	1.13	2.118	2.85	2.001	2.345	1.474	1.657	1.543	1.013	0.939
Number of modules	55	49	75	106	59	84	63	61	73	45
Average clustering coefficient	0.43	0.422	0.529	0.459	0.466	0.448	0.475	0.446	0.458	0.473

* DPI—days post-infection. ** a number of nodes with at least one connection (a total number of nodes).

To assess the progression of microbiome structural states, we plotted observed features (as a measured of taxa inventory) against connected nodes (as a measure of connectivity), or edges (as a measure of degree) for each DPI in infected and uninfected birds. Thus, 'observed features-connected nodes' (Figure 5A) and 'observed features-edges' (Figure 5B) plots were referred as 'microbiome structural states', from state 1 (8 DPI) to 5 (85 DPI), and the temporal succession of plots (from one DPI to the next) was referred as progression of structural states. The progression of structural states was dif-

ferent in control and *Plasmodium*-infected birds. Notably, transitions from state 2 to state 3 and from state 3 to state 4 were different in infected and control groups. In the microbiome of uninfected birds, the transition from state 2 to state 3 was characterized by an increase in 'observed features' with a decrease in 'connected nodes' (Figure 5A) and an increase in 'edges' (Figure 5B), while in infected birds this transition was characterized by a decrease in 'observed features' with an increase in 'connected nodes' (Figure 5A) and a decrease in 'edges' (Figure 5B). In the control group, the transition from state 3 to state 4 was characterized by no change in 'observed features', while in the infected group we observed an increase in 'observed features'. In both infected and control, transitions from state 3 to state 4 were associated with higher number of 'connected nodes' and 'edges'.

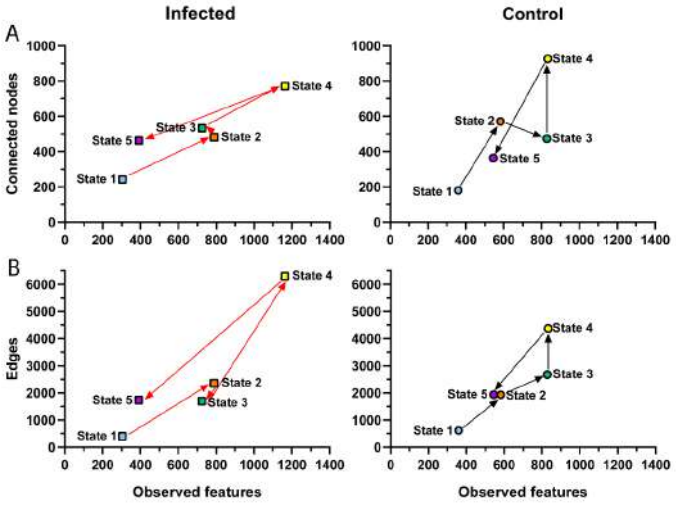

Figure 5. Changes in microbiome structural states of *P. homocircumflexum*-infected and control groups. Scatter plot showing the mean of observed features versus number of (**A**) connected nodes and (**B**) edges found in the microbial co-occurrence networks of infected (left) and control (right) birds throughout the course of experiment, from state 1 (8 DPI) to 5 (85 DPI) connected by arrows.

3.4. Impact of P. homocircumflexum Infection on Network Centrality Distribution and Robustness

The observed Jacc values for comparisons between networks of infected and uninfected groups were higher than expected by random at 16, 24 and 85 DPI (Table S4). At 8 DPI, the observed Jacc of all centrality measures comparisons was also higher than expected by random, except for betweenness centrality which followed a random distribution (Table S4). At 36 DPI, the observed Jacc of the centrality measures comparisons was higher than expected by random, except for eigenvector centrality and hub taxa, which followed a random distribution (Table S4). It is noteworthy that despite observed Jacc values were higher than expected by random for most centrality measures, these values were lower than 0.5 suggesting low similarity between centrality measures distribution in the microbiome of *Plasmodium*-infected and uninfected birds.

To test whether changes in network structure, and centrality measures impacted the network robustness, we assessed losses in connectivity after directed taxa removal (removing first the nodes with higher betweenness centrality). A major deviation from normal microbiome robustness was observed at 24 DPI in the microbiome of infected birds, while microbiome robustness in the other sampling days was very similar between

groups (Figure 6). Particularly, removal of 0.11 and 0.23 fraction of the taxa was enough to reach 90% loss in connectivity in the infected and uninfected groups at 24 DPI, respectively. The results suggest that microbiome modulation due to *Plasmodium* infection reduces network robustness significantly at 24 DPI.

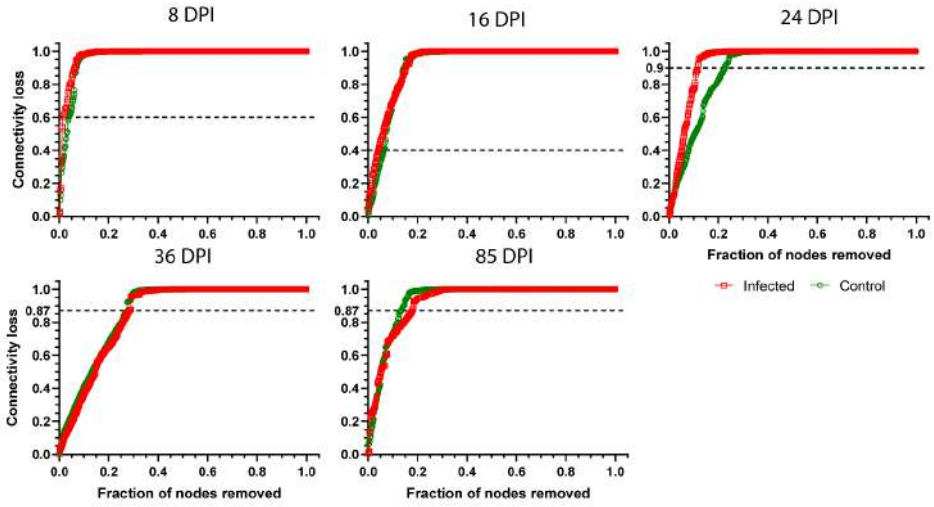

Figure 6. Network tolerance to directed attack. Values of connectivity loss in *P. homocircumflexum*-infected (red squares) and control (green circles) birds at different days of experiment were compared. At each sampling day a threshold (dashed lines) for connectivity loss was determined where the difference of removed nodes between the infected and control group was the largest.

3.5. Impact of P. homocircumflexum Infection on the Functional Profiles of Bird Guts Microbiome

To assess the impact of avian microbiome taxonomic modulation by *P. homocircumflexum* infection on the functional profiles of birds' microbiome, we performed pathway profiling based on predicted metagenomic functions using PICRUSt2 [44]. The comparison of predicted functional profiles revealed core (i.e., pathways identified in all DPI) and unique pathways in both groups. The functional cores in uninfected and infected birds consisted of 420 (total: 455, 92%) and 415 (total: 455, 91%) pathways, respectively (Figure 7A). Most of the core pathways were shared between the groups (413; total: 455, 91%), with 2 and 7 pathways specific to infected and control group, respectively (Figure S4). Pathways unique to infected birds on 16, 36 and 85 DPI were listed (Table S5).

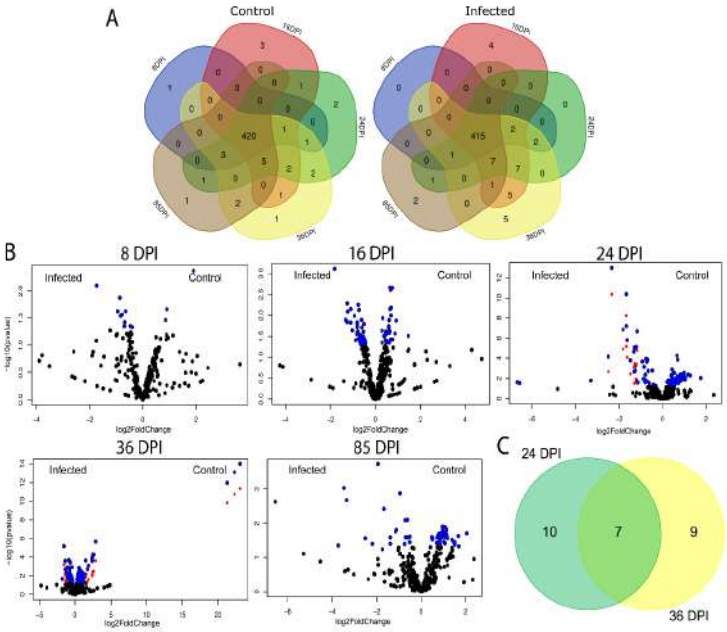

Figure 7. Impact of *P. homocircumflexum* infection on the predicted functional profiles of bird gut microbiome. (**A**) Venn diagram showing the common and different predicted bacterial pathways found in the microbiome of birds infected with *P. homocircumflexum* and uninfected birds at different sampling days. (**B**) Volcano plot showing differential pathway abundance in *Plasmodium*-infected and uninfected birds detected by DESeq2 analysis at 8, 16, 24, 35 and 85 DPI. The blued dots indicate all statistically significant (p(un-adjusted) < 0.05) pathways, red dots indicate pathways with statistically significant (p(adjusted) < 0.05) log2 fold changes in the absolute value (cut-off of 1); the black dots are not significant (p > 0.05). Detailed information on pathway identity is presented in Table S6. (**C**) Venn diagram. Comparison of unique and shared pathways with significant changes in abundance (p(adjusted) < 0.05) between the *Plasmodium*-infected and uninfected groups at 24 and 36 DPI. Only pathways with statistically significant log2 fold changes in the absolute value (cut-off of 1) were considered.

The comparison of predicted pathway abundance between infected and control birds showed significant fold changes in relative abundance of 17 and 16 pathways at 24 and 36 DPI, respectively (Log2fold change > 1, p(adjusted) < 0.05, Figure 7B, Table S6). Seven of these were shared between 24 and 36 DPI (Figure 7C). No significant change in predicted pathway abundance was found between groups at 8 DPI, 16 and 85 DPI.

We then tested a possible association between the taxonomic composition and unique pathways present in infected birds at 16, 36 and 85 DPI. The number of taxa contributing to the unique pathways at 16 DPI (33 taxa) and 36 DPI (30 taxa) were similar to each other, but higher to that at 85 DPI (4 taxa) (Figure S5). Most of the contributing taxa were found to be specific to each sampling day. The decreased number of taxa contributing to unique pathways at 85 DPI could be associated with latent stage of *P. homocircumflexum* infection when the parasite impact on bird microbiome is not as prominent as during acute phase.

4. Discussion

Natural infection with malaria parasites was associated with changes in the human gut microbiome [48], and the uropygial gland microbiome of house sparrows [11], and experimental infection with murine malaria parasites modulated the gut microbiome of mice [15,16]. We hypothesized that infection with avian malaria would impact bird gut microbiome diversity and structure. To test this hypothesis, we examined microbiome changes caused by experimental infection of *P. homocircumflexum* in canaries. As most available studies on the relation between avian microbiome composition and pathogen encounter focused on economically important species such as chicken and turkey [49], this study is a significant contribution to our understanding of wild bird microbiome in response to infection.

Parasite infection can have synergistic or antagonistic effects on commensal bacteria, effectively shifting microbiome taxonomic [8,50,51] and functional [8] profiles in mammalian [8,15,16] and avian [50,52] hosts. Our results show that microbiome modulation in *Plasmodium*-infected birds was most prominent during the chronic stage of primary infection (from 16 DPI) with a recovered microbiome state by the beginning of the latent stage (85 DPI), although changes of microbiome network topology were observed as early as 8 DPI, at the peak parasitemia. Although here we did not aim at testing the relation between microbiome changes and host health, it is noteworthy that small changes in microbiome composition could affect greatly the health of birds, as fluctuations in microbial functions could have a large impact on microbial-mediated processes such as degradation, detoxification and host defensive mechanisms [3].

We found that alpha diversity of the canary gut microbiome was not greatly affected by *Plasmodium* infection within the tested time points; however, some changes were found in the bacterial composition of *Plasmodium*-infected birds compared with uninfected birds. Similarly, a microbiome study of wild Eurasian tree sparrows by Rohrer et al. [53], found no significant differences in the alpha and beta diversity of birds infected or not with *Plasmodium*. Similarly, Macdonald et al. [52] showed that infection with *Eimeria tenella*, another avian apicomplexan parasite, did not affect microbial alpha diversity of caecal microbiome in chicken within the analyzed time point (i.e., 4 ½ DPI). In contrast, Zhou et al. [50] reported that *E. tenella* infection increased the caecal microbial alpha diversity at 7 DPI. Differences in the tissue tropism of *Plasmodium* (a blood parasite) and *Eimeria* (a prominent gut parasite) in birds may explain differences in their impact on the gut bacterial diversity. Interestingly, infection with murine malaria parasite *P. yoelii* decreased the alpha diversity of the fecal microbiome at 10 DPI, just before a secondary peak of parasitemia, with a gradual recovery by 30 DPI, when the peak parasitemia of *P. yoelii* decreases [15]. Similarly, alpha diversity metrics analysis revealed that infection with *P. berghei* transiently (day 5 to 7) increased richness and evenness, but then these parameters decreased at 9 DPI during acute stage of parasitemia [16]. The results of the latter two studies suggest that murine malaria reduces alpha diversity during acute stage of infection, regardless of parasite species (i.e., *P. yoelii* or *P. berghei*). The results suggest that avian malaria parasites, unlike other apicomplexan pathogens, cause no impact in the bacterial diversity of infected birds.

In this study, avian *Plasmodium* infection had the highest impact on the abundance of genera of the phyla Proteobacteria (*Escherichia-Shigella*, *Undibacterium*, *Pseudahrensia*, and *Croceicoccus*), followed by Chloroflexi (*Anaerolinea*), Verrucomicrobia (*Opitutaceae*) and Firmicutes (*Lachnospiraceae*). Specifically, infection increased and decreased the abundance of Proteobacteria taxa in the infected birds at 24 and 36 days, respectively. *Plasmodium berghei* infection reduced Firmicutes in two lines of laboratory mouse, C57BL/6 and BALB/c, and increased Proteobacteria and Verrucomicrobia in C57BL/6 mice over a period of 9 days during acute stage of infection [16]. Fecal microbiome of *P. yoelii*-infected C57BL/6 mice showed a decreased abundance of Firmicutes and a relative increase in the abundance of Bacteroidetes at the peak stage of infection, which reverted to baseline by 30 days when parasitenia decreased [15]. Similarly, *P. yoelii* infection in-

duced a reduction in the abundance of Firmicutes and an increase in the abundance of Bacteroidetes in the gut microbiome of BALB/c mice [54]. In addition, changes to the intestinal milieu caused by *P. yoelii* infection promote colonization of the intestine with both *Salmonella enterica* serotype Typhimurium and *Escherichia coli* [15]. In case of avian malaria, the changes in bacteria abundance appeared at a chronic stage of infection concurring with low parasitemia, while rodent malaria effects were detected when the parasite was still at the primary stage of development. Our results together with previously published studies on murine malaria [15,55] suggest that the impact of malaria infection on microbiome is mainly transient and can affect different bacterial taxa.

Bacterial communities are dynamic systems with high intra-individual compositional variability across time [55,56], and infection causes deviations from normal microbiome dynamics across biological systems, from animals [57] to plants [58,59]. Similarly, infection of mice with the pathogen *Citrobacter rodentium* revealed unique, time-dependent microbial signatures associated with host response to infection [57]. Compositional changes may impact community assembly and co-occurrence networks [60]. We found that network topology and progression of microbiome structural states were affected by infection. Particularly, we found that arrival to, and departure from, state three (24 DPI) was different in infected birds compared with the control group.

Notably, network of infected birds in state three were less robust than the control network. These results suggest that 'state three' plays a key role on the temporal dynamics of bird microbiome. Network robustness, measured here as tolerance to sequential removal of highly-central nodes [61], is a lower-order connectivity feature investigated at the level of individual nodes and edges [62–64]. There is a possibility that the accumulation of some taxa facilitated by infection and/or removal of other taxa excluded by infection within the first 24 DPI change microbe-microbe interactions affecting the hierarchical organization (who influences who) of the community. Resulting redistribution of betweenness centrality values in the network could in turn affect network robustness; with networks having higher betweenness centrality nodes tending to be more vulnerable to directed attacks [64]. Although the Jacc for betweenness centrality at 24 DPI was higher than expected by random, the Jacc value was lower than 0.50 suggesting low similarity in the distribution of betweenness centrality values among nodes in infected and uninfected networks. The combination of Jacc and robustness analysis supports that redistribution of betweenness centrality values induced by infection at 24 DPI reduces network robustness at 24 DPI. In addition to lower-order connectivity features, higher-order network features (i.e., patterns of interconnections or network motifs [65]), play a fundamental role in understanding the organization of many complex systems [65], and affect network robustness [64,66,67]. Occurrence of motifs in complex networks is not random, as motifs tend to perform important functions [68,69]. Thus, robustness reduction in state three networks of infected birds could be associated not only with redistribution of betweenness centrality across nodes, but also with modifications in patterns of network motifs. Further studies should address whether there is an association between network motifs and network robustness in the avian malaria system presented here.

Despite it is not clear how malaria parasites interact with intestinal microbiota to induce dysbiosis [13,14], several mechanisms can potentially account for changes in bacterial abundance and composition caused by *Plasmodium* infection [12,14]. The host-parasite relationships during malarial infections include immune response of the host that may directly, or indirectly, impact the host microbiome composition during malaria infections [14]. For example, activation and degranulation of mast cells during human and murine malaria damage the gastrointestinal barrier resulting in release of intestinal bacteria into the bloodstream [70]. Concomitantly, hemolysis caused by *Plasmodium* infection of red blood cells decreases reactive oxygen species (ROS) production by neutrophils increasing the growth of intestinal invading bacteria within these polymorphonuclear leukocytes [71]. The occurrence of some of these potential mechanisms is yet to be tested in birds.

Beyond changes in taxonomic profiles, the metabolites produced by specific bacterial species in the gut exert systemic effects on the host [72], as well as influence malaria infection and disease severity [73]. According to our study, most of the unique pathways identified in the microbiome of *Plasmodium*-infected birds could not be directly associated with avian malaria infection, however a PWY5F9-12 (biphenyl degradation) and PWY-3081 (L-lysine biosynthesis V) could be involved in anti-malarial response [74,75]. The presence of pathways of toluene degradation in the *Plasmodium*-infected birds could also be as response to the infection due to the production of toluene by the parasite [76,77].

5. Conclusions

Microbiota diversity in wild birds is highly influenced by the host ecology. As a consequence, microbiome composition and assembly may be under selective pressures by parasites in natural systems. We found that infection with the avian malaria parasite *P. homocircumflexum* modulated the fecal microbiome of canary hosts causing deviation from normal development, while no significant change in bacterial diversity was observed. The results showed changes in community assembly as early as 8 DPI, followed by more prominent fluctuations in bacterial composition with the emergence of infection-specific taxa and pathways at the later stages of infection. Although the microbiome of *Plasmodium*-infected birds has mainly recovered by 85 DPI, latent malaria infection could have long-lasting effect in the host microbiome with impact on bird health [3], and potentially host evolution. In addition, the spread of low virulent avian malaria parasites across a bird population could select for individuals carrying an infection-permissive microbiome. Parasite infection may select against the occurrence or high abundance of bacteria associated with anti-malarial mechanisms. For example, bacteria within the family Enterobacteriaceae are a rich source of α1,3-galactosyltransferase (α1,3GT) activity. Immune response to the carbohydrate α-Gal on the surface of microbiota bacteria in birds could trigger anti-α-Gal antibodies [7], with malaria killing activity [78]. Interestingly, the abundance of *Escherichia-Shigella* was significantly reduced in *P. homocircumflecxum*-infected birds at 24 DPI. By reducing the occurrence of Enterobacteriaceae across the bird population the parasite may reduce anti-malarial immunity at the population level.

Supplementary Materials: The following supporting information can be downloaded at: https://www.mdpi.com/article/10.3390/microorganisms11030563/s1, Figure S1: Alpha diversity indexes of infected and control bird microbiome. (A) Faith's phylogenetic diversity index, (B) observed features, (C) Pielou's evenness index, were calculated at the level of ASVs and compared between infected and control groups for each DPI. Control birds, n = 8; infected birds, n = 8. Days post-infection (DPI); Figure S2: Beta diversity of infected and control bird microbiome. (A) Bray–Curtis distance from each time point is represented in PCoA plot obtained by Betadisper function. (B) Bray–Curtis volatility plot, indicating how the microbiome composition changed in each group over time. The lines represent the mean and the standard error mean from each group. Control birds, n = 8; infected birds, n = 8. Days post-infection (DPI); Figure S3: Shared and unique bacterial genera found in the microbiome of infected and uninfected birds. (A) Venn diagrams displaying the number of shared and unique taxa detected within groups at different time points. (B) Unique taxa detected at the different time points in uninfected and infected birds were compared and displayed in Venn diagrams; the percentage at the sides of the core, shows proportional size of shared taxa in infected and control groups. (C) Taxa abundance per phylum in the microbiome of infected and control birds at different time points of experiment. Control birds, n = 8; infected birds, n = 8. Days post-infection (DPI); Figure S4: Shared and unique metabolic pathways found in the microbiome of infected and uninfected birds. Unique pathways of infected/control groups at different experimental days were selected and compared. The functional profiles of microbiome were predicted from 16S rRNA amplicon sequences using PICRUSt2. Control birds, n = 8; infected birds, n = 8. Days post-infection (DPI); Figure S5: Taxa contribution to metabolic pathways. Bacterial taxa contribution to unique pathways in the gut microbiome of infected and control birds at 16, 36 and 85 DPI is displayed as Sankey diagrams. Taxonomic contribution was assessed using PICRUSt2.

Node size is proportional to the abundance of contributing taxa or pathways. The contribution of each taxon to different pathways is represented proportionally by the size of cords. Days post-infection (DPI); Table S1: List of unique bacterial taxa in *P. homocircumflexum*-infected birds at different DPI and taxonomic core (i.e., taxa identified in all DPI) are listed; Table S2: List of taxa with important changes in abundance across time; Table S3: List of differentially abundant taxa identified by the DESeq2 method between the gut microbiome of *P. homocircumflexum*-infected and uninfected birds at 24 and 36 DPI. Only taxa with statistically significant log2 fold changes in the absolute value (cut-off of 1) are presented (p(adjusted) < 0.05); Table S4: Jaccard indexes of local centrality measures. Jaccard's indexes for each of local centrality measures (i.e., degree, betweenness centrality, closeness centrality, eigenvector centrality and hub taxa) of the sets of most central nodes for pairwise network comparisons. The two p-values, $p(J \leq j)$ and $p(J \geq j)$, for each Jaccard's index were added. *$p < 0.05$, ** $p < 0.01$; *** $p < 0.001$; Table S5: List of pathways unique to *P. homocircumflexum*-infected birds on 16, 36 and 85 DPI; Table S6: List of differential pathways identified by the DESeq2 method between the gut microbiome of *P. homocircumflexum*-infected and uninfected birds at 24 and 36 DPI. Only pathways with statistically significant (p(adjusted) < 0.05) log2 fold changes in the absolute value (cut-off of one) are listed.

Author Contributions: V.P. and A.C.-C. conceived the study. J.A., R.Ž. and V.P. performed the experiments and acquired the data. J.A., A.W.-C., D.O., A.M. and L.M.-H. analyzed the data. J.A., D.O. and A.C.-C. prepared figures and Supplementary Materials. V.P. and A.C.-C. contributed reagents and other resources. V.P., A.C.-C. and D.O. supervised the work. J.A., A.W.-C., A.M. and A.C.-C. drafted the first version of the manuscript. All authors contributed to the revision and edition of the article. All authors have read and agreed to the published version of the manuscript.

Funding: UMR BIPAR is supported by the French Government's Investissement d'Avenir program, Laboratoire d'Excellence "Integrative Biology of Emerging Infectious Diseases" (grant no. ANR-10-LABX-62-IBEID). V.P. obtained funding from the Research Council of Lithuania (project No S-MIP-22-52). A.W.-C. was supported by Programa Nacional de Becas de Postgrado en el Exterior "Don Carlos Antonio López" (Grant No. 205/2018). A.M. is supported by the 'Collectivité de Corse', grant: 'Formations superieures' (SGCE–RAPPORT N° 0300).

Institutional Review Board Statement: All procedures were performed at Nature Research Centre in Vilnius, Lithuania, according to Lithuanian and International Guiding Principles for Biomedical Research Involving Animals (2012). Infection experiments were reviewed and approved by the Lithuanian State Food and Veterinary Service, Ref. No 2020/07/24-G2-84. The assessment of the animal health and all described procedures were implemented by trained professionals (under licenses 2012/02/06-No-208, 2016/01/29-No-344, and 2021/02/05-No-527).

Informed Consent Statement: Not applicable.

Data Availability Statement: The datasets presented in this study can be found in SRA repository (Bioproject No. PRJNA904724).

Conflicts of Interest: The authors declare no conflict of interest.

References

1. Grond, K.; Sandercock, B.K.; Jumpponen, A.; Zeglin, L.H. The Avian Gut Microbiota: Community, Physiology and Function in Wild Birds. *J. Avian Biol.* **2018**, *49*, e01788. https://doi.org/10.1111/jav.01788.
2. Hird, S.M.; Sánchez, C.; Carstens, B.C.; Brumfield, R.T. Comparative Gut Microbiota of 59 Neotropical Bird Species. *Front. Microbiol.* **2015**, *6*, 1403. https://doi.org/10.3389/fmicb.2015.01403.
3. Bodawatta, K.H.; Hird, S.M.; Grond, K.; Poulsen, M.; Jønsson, K.A. Avian Gut Microbiomes Taking Flight. *Trends Microbiol.* **2022**, *30*, 268–280. https://doi.org/10.1016/j.tim.2021.07.003.
4. Waite, D.W.; Taylor, M.W. Characterizing the Avian Gut Microbiota: Membership, Driving Influences, and Potential Function. *Front. Microbiol.* **2014**, *5*, 223. https://doi.org/10.3389/fmicb.2014.00223.
5. Grond, K.; Santo Domingo, J.W.; Lanctot, R.B.; Jumpponen, A.; Bentzen, R.L.; Boldenow, M.L.; Brown, S.C.; Casler, B.; Cunningham, J.A.; Doll, A.C.; et al. Composition and Drivers of Gut Microbial Communities in Arctic-Breeding Shorebirds. *Front. Microbiol.* **2019**, *10*, 2258. https://doi.org/10.3389/fmicb.2019.02258.
6. Hird, S.M.; Carstens, B.C.; Cardiff, S.W.; Dittmann, D.L.; Brumfield, R.T. Sampling Locality Is More Detectable than Taxonomy or Ecology in the Gut Microbiota of the Brood-Parasitic Brown-Headed Cowbird (*Molothrus ater*). *PeerJ* **2014**, *2*, e321. https://doi.org/10.7717/peerj.321.

7. Palinauskas, V.; Mateos-Hernandez, L.; Wu-Chuang, A.; de la Fuente, J.; Aželytė, J.; Obregon, D.; Cabezas-Cruz, A. Exploring the Ecological Implications of Microbiota Diversity in Birds: Natural Barriers Against Avian Malaria. *Front. Immunol.* **2022**, *13*, 807682. https://doi.org/10.3389/fimmu.2022.807682.
8. Mammeri, M.; Obregón, D.A.; Chevillot, A.; Polack, B.; Julien, C.; Pollet, T.; Cabezas-Cruz, A.; Adjou, K.T. Cryptosporidium Parvum Infection Depletes Butyrate Producer Bacteria in Goat Kid Microbiome. *Front. Microbiol.* **2020**, *11*, 548737. https://doi.org/10.3389/fmicb.2020.548737.
9. Madlala, T.; Okpeku, M.; Adeleke, M.A. Understanding the Interactions between *Eimeria* Infection and Gut Microbiota, towards the Control of Chicken Coccidiosis: A Review. *Parasite* **2021**, *28*, 48. https://doi.org/10.1051/parasite/2021047.
10. Videvall, E.; Paxton, K.L.; Campana, M.G.; Cassin-Sackett, L.; Atkinson, C.T.; Fleischer, R.C. Transcriptome Assembly and Differential Gene Expression of the Invasive Avian Malaria Parasite *Plasmodium Relictum* in Hawai'i. *Ecol. Evol.* **2021**, *11*, 4935–4944. https://doi.org/10.1002/ece3.7401.
11. Videvall, E.; Marzal, A.; Magallanes, S.; Fleischer, R.C.; Espinoza, K.; García-Longoria, L. The Uropygial Gland Microbiome of House Sparrows with Malaria Infection. *J. Avian Biol.* **2021**, *52*, jav.02686. https://doi.org/10.1111/jav.02686.
12. Bamgbose, T.; Anvikar, A.R.; Alberdi, P.; Abdullahi, I.O.; Inabo, H.I.; Bello, M.; Cabezas-Cruz, A.; de la Fuente, J. Functional Food for the Stimulation of the Immune System Against Malaria. *Probiotics Antimicro. Prot.* **2021**, *13*, 1254–1266. https://doi.org/10.1007/s12602-021-09780-w.
13. Ippolito, M.M.; Denny, J.E.; Langelier, C.; Sears, C.L.; Schmidt, N.W. Malaria and the Microbiome: A Systematic Review. *Clin. Infect. Dis.* **2018**, *67*, 1831–1839. https://doi.org/10.1093/cid/ciy374.
14. Mukherjee, D.; Chora, Â.F.; Mota, M.M. Microbiota, a Third Player in the Host–Plasmodium Affair. *Trends Parasitol.* **2020**, *36*, 11–18. https://doi.org/10.1016/j.pt.2019.11.001.
15. Mooney, J.P.; Lokken, K.L.; Byndloss, M.X.; George, M.D.; Velazquez, E.M.; Faber, F.; Butler, B.P.; Walker, G.T.; Ali, M.M.; Potts, R.; et al. Inflammation-Associated Alterations to the Intestinal Microbiota Reduce Colonization Resistance against Non-Typhoidal Salmonella during Concurrent Malaria Parasite Infection. *Sci. Rep.* **2015**, *5*, 14603. https://doi.org/10.1038/srep14603.
16. Taniguchi, T.; Miyauchi, E.; Nakamura, S.; Hirai, M.; Suzue, K.; Imai, T.; Nomura, T.; Handa, T.; Okada, H.; Shimokawa, C.; et al. Plasmodium Berghei ANKA Causes Intestinal Malaria Associated with Dysbiosis. *Sci. Rep.* **2015**, *5*, 15699. https://doi.org/10.1038/srep15699.
17. Valkiūnas, G.; Iezhova, T.A. Keys to the Avian Malaria Parasites. *Malar. J.* **2018**, *17*, 212. https://doi.org/10.1186/s12936-018-2359-5.
18. Bensch, S.; Hellgren, O.; Pérez-Tris, J. MalAvi: A Public Database of Malaria Parasites and Related Haemosporidians in Avian Hosts Based on Mitochondrial Cytochrome *b* Lineages. *Mol. Ecol. Resour.* **2009**, *9*, 1353–1358. https://doi.org/10.1111/j.1755-0998.2009.02692.x.
19. Valkiūnas, G. *Avian Malaria Parasites and Other Haemosporidia*; CRC Press: Boca Raton, FL, USA, 2005; ISBN 978-0-415-30097-1.
20. Palinauskas, V.; Žiegytė, R.; Ilgūnas, M.; Iezhova, T.A.; Bernotienė, R.; Bolshakov, C.; Valkiūnas, G. Description of the First Cryptic Avian Malaria Parasite, *Plasmodium Homocircumflexum* n. Sp., with Experimental Data on Its Virulence and Development in Avian Hosts and Mosquitoes. *Int. J. Parasitol.* **2015**, *45*, 51–62. https://doi.org/10.1016/j.ijpara.2014.08.012.
21. Ilgūnas, M.; Bukauskaitė, D.; Palinauskas, V.; Iezhova, T.A.; Dinhopl, N.; Nedorost, N.; Weissenbacher-Lang, C.; Weissenböck, H.; Valkiūnas, G. Mortality and Pathology in Birds due to *Plasmodium* (*Giovannolaia*) *Homocircumflexum* Infection, with Emphasis on the Exoerythrocytic Development of Avian Malaria Parasites. *Malar. J.* **2016**, *15*, 256. https://doi.org/10.1186/s12936-016-1310-x.
22. Ilgūnas, M.; Bukauskaitė, D.; Palinauskas, V.; Iezhova, T.; Fragner, K.; Platonova, E.; Weissenböck, H.; Valkiūnas, G. Patterns of *Plasmodium Homocircumflexum* Virulence in Experimentally Infected Passerine Birds. *Malar. J.* **2019**, *18*, 174. https://doi.org/10.1186/s12936-019-2810-2.
23. Garcia-Longoria, L.; Palinauskas, V.; Ilgūnas, M.; Valkiūnas, G.; Hellgren, O. Differential Gene Expression of *Plasmodium Homocircumflexum* (Lineage PCOLL4) across Two Experimentally Infected Passerine Bird Species. *Genomics* **2020**, *112*, 2857–2865. https://doi.org/10.1016/j.ygeno.2020.03.025.
24. Dimitrov, D.; Palinauskas, V.; Iezhova, T.A.; Bernotienė, R.; Ilgūnas, M.; Bukauskaitė, D.; Zehtindjiev, P.; Ilieva, M.; Shapoval, A.P.; Bolshakov, C.V.; et al. Plasmodium Spp.: An Experimental Study on Vertebrate Host Susceptibility to Avian Malaria. *Exp. Parasitol.* **2015**, *148*, 1–16. https://doi.org/10.1016/j.exppara.2014.11.005.
25. Palinauskas, V.; Valkiūnas, G.; Bolshakov, C.V.; Bensch, S. *Plasmodium Relictum* (Lineage P-SGS1): Effects on Experimentally Infected Passerine Birds. *Exp. Parasitol.* **2008**, *120*, 372–380. https://doi.org/10.1016/j.exppara.2008.09.001.
26. Valkiūnas, G.; Iezhova, T.A.; Križanauskienė, A.; Palinauskas, V.; Sehgal, R.N.M.; Bensch, S. A Comparative Analysis of Microscopy and PCR-Based Detection Methods for Blood Parasites. *J. Parasitol.* **2008**, *94*, 1395–1401. https://doi.org/10.1645/GE-1570.1.
27. Godfrey, R.D.; Fedynich, A.M.; Pence, D.B. Quantification of hematozoa in blood smears. *J. Wildl. Dis.* **1987**, *23*, 558–565. https://doi.org/10.7589/0090-3558-23.4.558.
28. Sambrook, J.; Russell, D.W. *Molecular Cloning: A Laboratory Manual*, 3rd ed.; Cold Spring Harbor Laboratory Press: Cold Spring Harbor, NY, USA, 2001; ISBN 978-0-87969-577-4.
29. Hellgren, O.; Waldenström, J.; Bensch, S. A new PCR assay for simultaneous studies of *Leucocytozoon*, *Plasmodium*, and *Haemoproteus* from avian blood. *J. Parasitol.* **2004**, *90*, 797–802. https://doi.org/10.1645/GE-184R1.

30. Bensch, S.; Stjernman, M.; Hasselquist, D.; Örjan, Ö.; Hannson, B.; Westerdahl, H.; Pinheiro, R.T. Host Specificity in Avian Blood Parasites: A Study of *Plasmodium* and *Haemoproteus* Mitochondrial DNA Amplified from Birds. *Proc. R. Soc. Lond. B* **2000**, *267*, 1583–1589. https://doi.org/10.1098/rspb.2000.1181.
31. Bolyen, E.; Rideout, J.R.; Dillon, M.R.; Bokulich, N.A.; Abnet, C.C.; Al-Ghalith, G.A.; Alexander, H.; Alm, E.J.; Arumugam, M.; Asnicar, F.; et al. Reproducible, Interactive, Scalable and Extensible Microbiome Data Science Using QIIME 2. *Nat. Biotechnol.* **2019**, *37*, 852–857. https://doi.org/10.1038/s41587-019-0209-9.
32. Callahan, B.J.; McMurdie, P.J.; Rosen, M.J.; Han, A.W.; Johnson, A.J.A.; Holmes, S.P. DADA2: High-Resolution Sample Inference from Illumina Amplicon Data. *Nat. Methods* **2016**, *13*, 581–583. https://doi.org/10.1038/nmeth.3869.
33. Bokulich, N.A.; Kaehler, B.D.; Rideout, J.R.; Dillon, M.; Bolyen, E.; Knight, R.; Huttley, G.A.; Gregory Caporaso, J. Optimizing Taxonomic Classification of Marker-Gene Amplicon Sequences with QIIME 2's Q2-Feature-Classifier Plugin. *Microbiome* **2018**, *6*, 90. https://doi.org/10.1186/s40168-018-0470-z.
34. Yarza, P.; Yilmaz, P.; Pruesse, E.; Glöckner, F.O.; Ludwig, W.; Schleifer, K.-H.; Whitman, W.B.; Euzéby, J.; Amann, R.; Rosselló-Móra, R. Uniting the Classification of Cultured and Uncultured Bacteria and Archaea Using 16S RRNA Gene Sequences. *Nat. Rev. Microbiol.* **2014**, *12*, 635–645. https://doi.org/10.1038/nrmicro3330.
35. Bokulich, N.A.; Dillon, M.R.; Zhang, Y.; Rideout, J.R.; Bolyen, E.; Li, H.; Albert, P.S.; Caporaso, J.G. Q2-Longitudinal: Longitudinal and Paired-Sample Analyses of Microbiome Data. *mSystems* **2018**, *3*, e00219-18. https://doi.org/10.1128/mSystems.00219-18.
36. Love, M.I.; Huber, W.; Anders, S. Moderated Estimation of Fold Change and Dispersion for RNA-Seq Data with DESeq2. *Genome Biol.* **2014**, *15*, 550. https://doi.org/10.1186/s13059-014-0550-8.
37. Peschel, S.; Müller, C.L.; von Mutius, E.; Boulesteix, A.-L.; Depner, M. NetCoMi: Network Construction and Comparison for Microbiome Data in R. *Brief. Bioinform.* **2021**, *22*, bbaa290. https://doi.org/10.1093/bib/bbaa290.
38. RStudio Team (2020). RStudio: Integrated Development for R. RStudio, PBC, Boston, MA URL Http://Www.Rstudio.Com/.
39. Real, R.; Vargas, J.M. The Probabilistic Basis of Jaccard's Index of Similarity. *Syst. Biol.* **1996**, *45*, 380–385. https://doi.org/10.1093/sysbio/45.3.380.
40. Friedman, J.; Alm, E.J. Inferring Correlation Networks from Genomic Survey Data. *PLoS Comput. Biol.* **2012**, *8*, e1002687. https://doi.org/10.1371/journal.pcbi.1002687.
41. Bastian, M.; Heymann, S.; Jacomy, M. Gephi: An Open Source Software for Exploring and Manipulating Networks. *ICWSM* **2009**, *3*, 361–362. https://doi.org/10.1609/icwsm.v3i1.13937.
42. DeSantis, T.Z.; Hugenholtz, P.; Larsen, N.; Rojas, M.; Brodie, E.L.; Keller, K.; Huber, T.; Dalevi, D.; Hu, P.; Andersen, G.L. Greengenes, a Chimera-Checked 16S RRNA Gene Database and Workbench Compatible with ARB. *Appl. Environ. Microbiol.* **2006**, *72*, 5069–5072. https://doi.org/10.1128/AEM.03006-05.
43. Lhomme, S. Analyse Spatiale de La Structure Des Réseaux Techniques Dans Un Contexte de Risques. *Cybergeo* **2015**. https://doi.org/10.4000/cybergeo.26763.
44. Douglas, G.M.; Maffei, V.J.; Zaneveld, J.R.; Yurgel, S.N.; Brown, J.R.; Taylor, C.M.; Huttenhower, C.; Langille, M.G.I. PICRUSt2 for Prediction of Metagenome Functions. *Nat. Biotechnol* **2020**, *38*, 685–688. https://doi.org/10.1038/s41587-020-0548-6.
45. Kanehisa, M. KEGG: Kyoto Encyclopedia of Genes and Genomes. *Nucleic Acids Res.* **2000**, *28*, 27–30. https://doi.org/10.1093/nar/28.1.27.
46. Tatusov, R.L. The COG Database: A Tool for Genome-Scale Analysis of Protein Functions and Evolution. *Nucleic Acids Res.* **2000**, *28*, 33–36. https://doi.org/10.1093/nar/28.1.33.
47. Caspi, R.; Billington, R.; Fulcher, C.A.; Keseler, I.M.; Kothari, A.; Krummenacker, M.; Latendresse, M.; Midford, P.E.; Ong, Q.; Ong, W.K.; et al. The MetaCyc Database of Metabolic Pathways and Enzymes. *Nucleic Acids Res.* **2018**, *46*, D633–D639. https://doi.org/10.1093/nar/gkx935.
48. Yooseph, S.; Kirkness, E.F.; Tran, T.M.; Harkins, D.M.; Jones, M.B.; Torralba, M.G.; O'Connell, E.; Nutman, T.B.; Doumbo, S.; Doumbo, O.K.; et al. Stool Microbiota Composition Is Associated with the Prospective Risk of Plasmodium Falciparum Infection. *BMC Genom.* **2015**, *16*, 631. https://doi.org/10.1186/s12864-015-1819-3.
49. Colston, T.J.; Jackson, C.R. Microbiome Evolution along Divergent Branches of the Vertebrate Tree of Life: What Is Known and Unknown. *Mol. Ecol.* **2016**, *25*, 3776–3800. https://doi.org/10.1111/mec.13730.
50. Zhou, B.; Jia, L.; Wei, S.; Ding, H.; Yang, J.; Wang, H. Effects of *Eimeria Tenella* Infection on the Barrier Damage and Microbiota Diversity of Chicken Cecum. *Poult. Sci.* **2020**, *99*, 1297–1305. https://doi.org/10.1016/j.psj.2019.10.073.
51. Macdonald, S.E.; van Diemen, P.M.; Martineau, H.; Stevens, M.P.; Tomley, F.M.; Stabler, R.A.; Blake, D.P. Impact of *Eimeria Tenella* Coinfection on *Campylobacter Jejuni* Colonization of the Chicken. *Infect. Immun.* **2019**, *87*, e00772-18. https://doi.org/10.1128/IAI.00772-18.
52. Macdonald, S.E.; Nolan, M.J.; Harman, K.; Boulton, K.; Hume, D.A.; Tomley, F.M.; Stabler, R.A.; Blake, D.P. Effects of *Eimeria Tenella* Infection on Chicken Caecal Microbiome Diversity, Exploring Variation Associated with Severity of Pathology. *PLoS ONE* **2017**, *12*, e0184890. https://doi.org/10.1371/journal.pone.0184890.
53. Rohrer, S.D.; Robertson, B.Q.; Chubiz, L.M.; Parker, P.G. Gut Microbiome Composition Associated with *Plasmodium* Infection in the Eurasian Tree Sparrow. *J. Avian Biol.* **2023**, *2023*, e03027. https://doi.org/10.1111/jav.03027.
54. Guan, W.; Song, X.; Yang, S.; Zhu, H.; Li, F.; Li, J. Observation of the Gut Microbiota Profile in BALB/c Mice Induced by *Plasmodium Yoelii* 17XL Infection. *Front. Microbiol.* **2022**, *13*, 858897. https://doi.org/10.3389/fmicb.2022.858897.

55. Olsson, L.M.; Boulund, F.; Nilsson, S.; Khan, M.T.; Gummesson, A.; Fagerberg, L.; Engstrand, L.; Perkins, R.; Uhlén, M.; Bergström, G.; et al. Dynamics of the Normal Gut Microbiota: A Longitudinal One-Year Population Study in Sweden. *Cell Host Microbe* **2022**, *30*, 726–739.e3. https://doi.org/10.1016/j.chom.2022.03.002.
56. Priya, S.; Blekhman, R. Population Dynamics of the Human Gut Microbiome: Change Is the Only Constant. *Genome Biol.* **2019**, *20*, 150. https://doi.org/10.1186/s13059-019-1775-3.
57. Belzer, C.; Gerber, G.K.; Roeselers, G.; Delaney, M.; DuBois, A.; Liu, Q.; Belavusava, V.; Yeliseyev, V.; Houseman, A.; Onderdonk, A.; et al. Dynamics of the Microbiota in Response to Host Infection. *PLoS ONE* **2014**, *9*, e95534. https://doi.org/10.1371/journal.pone.0095534.
58. Lebreton, L.; Guillerm-Erckelboudt, A.-Y.; Gazengel, K.; Linglin, J.; Ourry, M.; Glory, P.; Sarniguet, A.; Daval, S.; Manzanares-Dauleux, M.J.; Mougel, C. Temporal Dynamics of Bacterial and Fungal Communities during the Infection of *Brassica Rapa* Roots by the Protist *Plasmodiophora Brassicae*. *PLoS ONE* **2019**, *14*, e0204195. https://doi.org/10.1371/journal.pone.0204195.
59. Cui, Z.; Huntley, R.B.; Zeng, Q.; Steven, B. Temporal and Spatial Dynamics in the Apple Flower Microbiome in the Presence of the Phytopathogen *Erwinia Amylovora*. *ISME J* **2021**, *15*, 318–329. https://doi.org/10.1038/s41396-020-00784-y.
60. Li, Y.; Li, T.; Zhao, D.; Wang, Z.; Liao, Y. Different Tillage Practices Change Assembly, Composition, and Co-Occurrence Patterns of Wheat Rhizosphere Diazotrophs. *Sci. Total Environ.* **2021**, *767*, 144252. https://doi.org/10.1016/j.scitotenv.2020.144252.
61. De Morais, U.L.; Antunes, L. A Look at the Way We Look at Complex Networks Robustness and Resilience. *arXiv* **2019**, *arXiv:1909.06448*. https://doi.org/10.48550/ARXIV.1909.06448.
62. Albert, R.; Jeong, H.; Barabási, A.-L. Error and Attack Tolerance of Complex Networks. *Nature* **2000**, *406*, 378–382. https://doi.org/10.1038/35019019.
63. Schneider, C.M.; Moreira, A.A.; Andrade, J.S.; Havlin, S.; Herrmann, H.J. Mitigation of Malicious Attacks on Networks. *Proc. Natl. Acad. Sci. USA* **2011**, *108*, 3838–3841. https://doi.org/10.1073/pnas.1009440108.
64. Dey, A.K.; Gel, Y.R.; Poor, H.V. What Network Motifs Tell Us about Resilience and Reliability of Complex Networks. *Proc. Natl. Acad. Sci. USA* **2019**, *116*, 19368–19373. https://doi.org/10.1073/pnas.1819529116.
65. Milo, R.; Shen-Orr, S.; Itzkovitz, S.; Kashtan, N.; Chklovskii, D.; Alon, U. Network Motifs: Simple Building Blocks of Complex Networks. *Science* **2002**, *298*, 824–827. https://doi.org/10.1126/science.298.5594.824.
66. Menck, P.J.; Heitzig, J.; Kurths, J.; Joachim Schellnhuber, H. How Dead Ends Undermine Power Grid Stability. *Nat. Commun.* **2014**, *5*, 3969. https://doi.org/10.1038/ncomms4969.
67. Schultz, P.; Heitzig, J.; Kurths, J. Detours around Basin Stability in Power Networks. *New J. Phys.* **2014**, *16*, 125001. https://doi.org/10.1088/1367-2630/16/12/125001.
68. Mangan, S.; Alon, U. Structure and Function of the Feed-Forward Loop Network Motif. *Proc. Natl. Acad. Sci. USA* **2003**, *100*, 11980–11985. https://doi.org/10.1073/pnas.2133841100.
69. Gorochowski, T.E.; Grierson, C.S.; di Bernardo, M. Organization of Feed-Forward Loop Motifs Reveals Architectural Principles in Natural and Engineered Networks. *Sci. Adv.* **2018**, *4*, eaap9751. https://doi.org/10.1126/sciadv.aap9751.
70. Donnelly, E.; de Water, J.V.; Luckhart, S. Malaria-Induced Bacteremia as a Consequence of Multiple Parasite Survival Strategies. *Curr. Res. Microb. Sci.* **2021**, *2*, 100036. https://doi.org/10.1016/j.crmicr.2021.100036.
71. Babatunde, K.A.; Adenuga, O.F. Neutrophils in Malaria: A Double-Edged Sword Role. *Front. Immunol.* **2022**, *13*, 922377. https://doi.org/10.3389/fimmu.2022.922377.
72. Dodd, D.; Spitzer, M.H.; Van Treuren, W.; Merrill, B.D.; Hryckowian, A.J.; Higginbottom, S.K.; Le, A.; Cowan, T.M.; Nolan, G.P.; Fischbach, M.A.; et al. A Gut Bacterial Pathway Metabolizes Aromatic Amino Acids into Nine Circulating Metabolites. *Nature* **2017**, *551*, 648–652. https://doi.org/10.1038/nature24661.
73. Stough, J.M.A.; Dearth, S.P.; Denny, J.E.; LeCleir, G.R.; Schmidt, N.W.; Campagna, S.R.; Wilhelm, S.W. Functional Characteristics of the Gut Microbiome in C57BL/6 Mice Differentially Susceptible to Plasmodium Yoelii. *Front. Microbiol.* **2016**, *7*, 1520. https://doi.org/10.3389/fmicb.2016.01520.
74. Meireles, P.; Brás, D.; Fontinha, D.; Chora, Â.F.; Serre, K.; Mendes, A.M.; Prudêncio, M. Elimination of Hepatic Rodent Plasmodium Parasites by Amino Acid Supplementation. *iScience* **2020**, *23*, 101781. https://doi.org/10.1016/j.isci.2020.101781.
75. Loose, L.D.; Silkworth, J.B.; Pittman, K.A.; Benitz, K.F.; Mueller, W. Impaired Host Resistance to Endotoxin and Malaria in Polychlorinated Biphenyl- and Hexachlorobenzene-Treated Mice. *Infect. Immun.* **1978**, *20*, 30–35. https://doi.org/10.1128/iai.20.1.30-35.1978.
76. Correa, R.; Coronado, L.M.; Garrido, A.C.; Durant-Archibold, A.A.; Spadafora, C. Volatile Organic Compounds Associated with Plasmodium Falciparum Infection in Vitro. *Parasites Vectors* **2017**, *10*, 215. https://doi.org/10.1186/s13071-017-2157-x.
77. Kelly, M.; Su, C.-Y.; Schaber, C.; Crowley, J.R.; Hsu, F.-F.; Carlson, J.R.; Odom, A.R. Malaria Parasites Produce Volatile Mosquito Attractants. *mBio* **2015**, *6*, e00235-15. https://doi.org/10.1128/mBio.00235-15.
78. Yilmaz, B.; Portugal, S.; Tran, T.M.; Gozzelino, R.; Ramos, S.; Gomes, J.; Regalado, A.; Cowan, P.J.; d'Apice, A.J.F.; Chong, A.S.; et al. Gut Microbiota Elicits a Protective Immune Response against Malaria Transmission. *Cell* **2014**, *159*, 1277–1289. https://doi.org/10.1016/j.cell.2014.10.053.

PAPER V

Impact of *Plasmodium relictum* infection on the colonization resistance of bird gut microbiota: A preliminary study.

Aželytė J., Maitre A., Abuin-Denis L., Piloto-Sardiñas E., Wu-Chuang A., Žiegytė R., Mateos-Hernández L., Obregón D., Cabezas-Cruz A., Palinauskas V.

Pathogens, 2023, 13(1), 1-14
DOI 10.3390/pathogens13010091

pathogens

MDPI

Article

Impact of *Plasmodium relictum* Infection on the Colonization Resistance of Bird Gut Microbiota: A Preliminary Study

Justė Aželytė [1], Apolline Maitre [2,3,4], Lianet Abuin-Denis [2,5], Elianne Piloto-Sardiñas [2,6], Alejandra Wu-Chuang [2], Rita Žiegytė [1], Lourdes Mateos-Hernández [2], Dasiel Obregón [7], Alejandro Cabezas-Cruz [2,*,†] and Vaidas Palinauskas [1,*,†]

1 Nature Research Centre, Akademijos 2, LT-08412 Vilnius, Lithuania; juste.azelyte@gmail.com (J.A.); rita.ziegyte@gamtc.lt (R.Ž.)
2 Anses, National Research Institute for Agriculture, Food and the Environment (INRAE), Ecole Nationale Vétérinaire d'Alfort, UMR BIPAR, Laboratoire de Santé Animale, F-94700 Maisons-Alfort, France; apolline.maitre@anses.fr (A.M.); labuind@gmail.com (L.A.-D.); elianne9409@gmail.com (E.P.-S.); alewch29@gmail.com (A.W.-C.); lourdes.mateos@vet-alfort.fr (L.M.-H.)
3 INRAE, UR 0045 Laboratoire de Recherches Sur Le Développement de L'Elevage (SELMET-LRDE), F-20250 Corte, France
4 EA 7310, Laboratoire de Virologie, Université de Corse, F-20250 Corte, France
5 Animal Biotechnology Department, Center for Genetic Engineering and Biotechnology, Avenue 31 between 158 and 190, Havana CU-10600, Cuba
6 Direction of Animal Health, National Center for Animal and Plant Health, Carretera de Tapaste y Autopista Nacional, Apartado Postal 10, San José de las Lajas CU-32700, Cuba
7 School of Environmental Sciences, University of Guelph, Guelph, ON N1G 2W1, Canada; dasielogv@gmail.com
* Correspondence: alejandro.cabezas@vet-alfort.fr (A.C.-C.); palinauskas@gmail.com (V.P.)
† These authors contributed equally to this work.

check for updates

Citation: Aželytė, J.; Maitre, A.; Abuin-Denis, L.; Piloto-Sardiñas, E.; Wu-Chuang, A.; Žiegytė, R.; Mateos-Hernández, L.; Obregón, D.; Cabezas-Cruz, A.; Palinauskas, V. Impact of *Plasmodium relictum* Infection on the Colonization Resistance of Bird Gut Microbiota: A Preliminary Study. *Pathogens* **2024**, *13*, 91. https://doi.org/10.3390/pathogens13010091

Academic Editor: Hans-Peter Fuehrer

Received: 3 December 2023
Revised: 5 January 2024
Accepted: 18 January 2024
Published: 20 January 2024

Abstract: Avian malaria infection has been known to affect host microbiota, but the impact of *Plasmodium* infection on the colonization resistance in bird gut microbiota remains unexplored. This study investigated the dynamics of *Plasmodium relictum* infection in canaries, aiming to explore the hypothesis that microbiota modulation by *P. relictum* would reduce colonization resistance. Canaries were infected with *P. relictum*, while a control group was maintained. The results revealed the presence of *P. relictum* in the blood of all infected canaries. Analysis of the host microbiota showed no significant differences in alpha diversity metrics between infected and control groups. However, significant differences in beta diversity indicated alterations in the microbial taxa composition of infected birds. Differential abundance analysis identified specific taxa with varying prevalence between infected and control groups at different time points. Network analysis demonstrated a decrease in correlations and revealed that *P. relictum* infection compromised the bird microbiota's ability to resist the removal of taxa but did not affect network robustness with the addition of new nodes. These findings suggest that *P. relictum* infection reduces gut microbiota stability and has an impact on colonization resistance. Understanding these interactions is crucial for developing strategies to enhance colonization resistance and maintain host health in the face of parasitic infections.

Keywords: microbiota; avian malaria; colonization resistance; *Plasmodium relictum*

1. Introduction

Avian malaria, caused by various species of the *Plasmodium* parasite, has been recognized as a significant threat to avian populations worldwide [1]. Among these parasites, *Plasmodium relictum* (genetic lineage SGS1) stands out due to its ability to infect a diverse range of bird species, with more than 300 known hosts documented [2]. As an important pathogen affecting avian health, studying the interactions between *P. relictum* and its avian

hosts is crucial for understanding the ecological and evolutionary implications of this parasitic infection.

Colonization resistance, a concept originating from ecological theory, refers to the host's ability to resist the establishment and proliferation of potential pathogens within its microbiota [3–6]. The microbiota, consisting of a complex community of microorganisms residing within the host, plays a critical role in maintaining host health and immune homeostasis [7,8]. Over the last few years, research on avian microbiota has markedly increased [8–10]. Due to birds inhabiting different environments and adapting to diverse living conditions, their microbiota is complex [11,12]. It can vary between bird species and individuals [11]. Perturbations to the microbiota can have profound effects on the host, potentially influencing disease susceptibility, immune response, and overall well-being [8,13].

While studies have investigated the impact of parasites on the host microbiota in various systems, the specific effects of avian malaria parasites on colonization resistance in birds remain relatively unexplored. Understanding how avian malaria parasites, such as *P. relictum*, influence the colonization resistance of their avian hosts is of great interest to comprehend the ecological dynamics of these infections and their potential implications for avian health.

Several studies have highlighted the importance of the microbiota in mediating host-pathogen interactions and disease outcomes [6,14]. For instance, research conducted on mammalian models has demonstrated that perturbations to the gut microbiota can affect the severity of parasitic infections and influence host immune responses [15–17]. Furthermore, the studies conducted by Taniguchi et al. [15] and Mooney et al. [18] revealed a significant correlation between infections of mice with *Plasmodium berghei* and *Plasmodium yoelli*, respectively, and alterations in the abundance of specific bacteria within the gut microbiota. Previous research has primarily focused on analyzing the composition of the microbiota when studying the interactions between avian malaria parasites and the host's microbiota [19–21]. However, it is important to note that the bacterial diversity of the microbiota alone does not fully capture the impact of parasite infection on the host's microbiota. A recent study by Aželyte et al. [22] investigated the effects of *Plasmodium homocircumflexum* infection on canaries' microbiota. Interestingly, they found that although the infection did not lead to significant changes in the overall diversity of the microbiota, notable alterations were observed in the bacterial networks within infected canaries at various time points during the infection. Despite advancements in avian microbiota research, it remains unclear whether interactions of *Plasmodium* with resident microbiota affect the response of the gut bacterial community to new invaders or taxa extinction events.

In this study, we aimed to examine the influence of *P. relictum* infection on the colonization resistance of canaries using network analysis. By characterizing the composition and dynamics of the canary gut microbiota in the presence and absence of *P. relictum* infection, we gained insights into the potential interactions between the parasite and the host microbiota. Furthermore, by employing network analysis, specifically node removal and node addition methods, we investigated the resilience and stability of the canary microbiota in the face of *P. relictum* infection.

Network analysis provides a powerful framework to explore the intricate relationships between individual microbial taxa within a microbiota [23,24], thereby elucidating the mechanisms underlying colonization resistance [25]. By applying node removal and addition methods within the microbiota network, we can assess the influence of specific microbial taxa on network structure [26], connectivity [26–28], and resistance [29]. Systematically removing nodes allows us to evaluate the impact on network robustness and identify key taxa that contribute to colonization resistance. Conversely, adding nodes helps us understand how the introduction of certain taxa influences network dynamics and colonization resistance. Through these robustness tests, we can gain insights into the essential microbial players and interactions that drive colonization resistance, providing

a comprehensive understanding of the interplay between the host, microbiota, and avian malaria parasite, *P. relictum*.

2. Methods

2.1. Data Source

To evaluate the impact of avian malaria infection on the bird gut microbiota, we analyzed preliminary data from a previous study on bird infection with *P. relictum* [30]. The study conducted by Aželytė et al. [30] investigated how anti-microbiota vaccination of host birds against commensal bacteria disrupted *P. relictum* sporogonic development by modulating mosquito microbiota. In this study, the 16S rRNA gene sequencing datasets from birds' fecal material of the *P. relictum* and PBS groups were used. Briefly, a group of 8-month-old canaries was inoculated with meront stages of *P. relictum*, referred to here as the *P. relictum*-infected group. Another group received PBS, referred to here as the control or the uninfected group. The blood was sampled at the indicated DPI (days post-infection) to microscopically calculate the parasitemia (Figure 1). Fecal samples were collected at 22 DPI and 38 DPI. The genomic DNA for microbiome analysis was extracted from feces and sent for amplicon sequencing. Aželytė et al. [30] provide a comprehensive description of the experimental design and procedures.

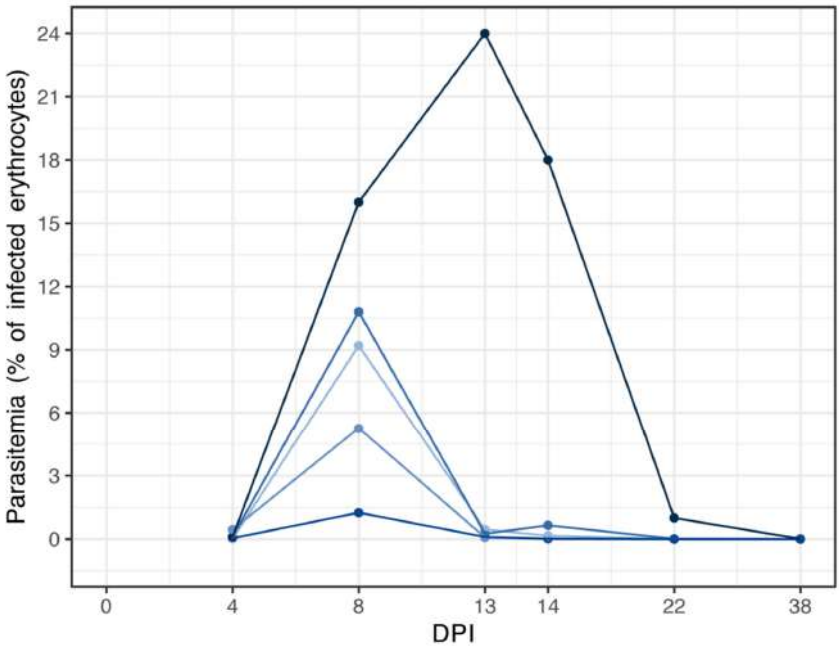

Figure 1. The dynamics of *P. relictum* parasitemia. Individual parasitemia values (% of infected erythrocytes) of *P. relictum* based on microscopy are presented. Different colors represent individual birds. DPI—days post-infection.

The 16S rRNA sequences were submitted to the SRA repository under Bioproject No. PRJNA971381. To analyze the raw sequences, we employed the QIIME 2 software package (ver. 2021.4) [31]. The paired-end reads, obtained in fastq files, were processed using

the DADA2 pipeline [32]. Taxonomy was assigned to the resulting amplicon sequence variants (ASVs) using a classify-sklearn naïve Bayes taxonomic classifier based on the SILVA database (release 138; [33]). To ensure data quality, we filtered the taxonomic table by removing taxa at the genus level that had a frequency of fewer than 10 reads and were present in less than 3 samples. The resulting data table was then used for microbiota assembly analysis.

2.2. Microbiota Diversity, Composition, and Abundance Analyses

To evaluate microbiota diversity and composition of *P. relictum*-infected and control birds at 22 DPI and 38 DPI, alpha and beta diversity of bacterial taxa were analyzed using rarefied ASVs with the q2-diversity plugin in Qiime2 [31]. Microbial richness between the groups was compared with the pairwise Kruskal–Wallis test ($p < 0.05$) using Faith's phylogenetic diversity [34] and observed features metrics (a measure of taxa inventory), while the evenness was calculated by Pielou's index [35]. The beta diversity between the groups was assessed using the Bray–Curtis dissimilarity index [36] with a PERMANOVA test ($p < 0.05$). Beta dispersion was calculated using the betadisper function of the Vegan package implemented in the R program (ver. 4.1.3) [37]. The dispersion was compared between the groups using a PERMANOVA test ($p < 0.05$).

Differences in taxa abundance between the groups were calculated using the ANOVA-like differential expression package 'ALDEx2' [38] in the R program (ver. 4.1.3) [37]. This method utilizes a centered log ratio (clr) transformation based on the geometric mean of read counts in the sample to measure relative abundance [39]. The comparisons were performed with a *t*-test ($p \leq 0.05$). The numbers of shared taxa in the microbiota of *P. relictum*-infected and control groups were visualized using Venn diagrams implemented in the online tool (http://bioinformatics.psb.ugent.be/webtools/Venn/; accessed on 10 May 2023).

By employing these methods and tools, this study aimed to comprehensively evaluate and compare the microbial diversity, composition, richness, evenness, beta diversity, dispersion, and taxa abundance between the *P. relictum*-infected and control groups of birds at two time points (22 DPI and 38 DPI).

2.3. Bacterial Co-Occurrence Networks

Co-occurrence microbial networks were constructed to visually represent the assembly of microbial communities under different conditions. These networks were based on taxonomic profiles at the genera level. In the network, nodes represent bacterial taxa, and the edges indicate significant positive (weight > 0.75) or negative (weight < −0.75) co-occurrence interactions between the nodes. The Sparse Correlations for Compositional data (SparCC) method [40] implemented in the R program (ver. 4.1.3) [37] was used to analyze constructed networks. Gephi 0.9.5 [41] software was employed for network visualization and measuring various topological features of each group, such as the number of nodes and edges, network diameter, average degree, weighted degree, average path length, modularity, and number of modules.

2.4. Comparative Network Analysis and Robustness

The microbial networks were compared between the conditions using various functions of the NetCoMi package [42] in the R program (ver. 4.1.3) [37]. To assess the similarities between networks based on shared nodes and edges, an association analysis was conducted. The degree of similarity between networks increases as the number of shared nodes and edges increases. For the comparison of the most central nodes in the networks, two *p*-values, P(J ≤ j) and P(J ≥ j), were calculated for each Jaccard index. These *p*-values represent the probability that the observed Jaccard index (J) value is either "less than or equal to" or "greater than or equal to" the expected Jaccard value at random (j). Differences were considered significant when $p < 0.05$.

The core association network (CAN) analysis function of the NetCoMi package [42] was used to evaluate the common nodes and edges between two different networks. The

core of the control and *P. relictum*-infected groups' networks was determined at two different time points using the Anuran toolbox [43] with default parameters. This analysis was conducted in the Anaconda Python environment (ver. 3.9.17) [44].

To test the robustness of the network to node removal, the Network Strengths and Weaknesses Analysis (NetSwan) package (ver. 0.1) was employed [45]. Various node removal attacks, including random, betweenness centrality, degree, and cascading, were performed to assess network tolerance based on connectivity loss. The standard error for loss of connectivity was calculated, considering variability, using a threshold of 0.975. The igraph package was utilized for network analysis and visualization [46,47].

The robustness of microbial networks to node addition was assessed using the network analysis and visualization package [48]. Nodes were incrementally added in sections ranging from 100 to 1000, and network connectivity was measured based on the degree metric of the largest connected component (LCC) and average path length. A Wilcoxon signed-rank test was conducted to calculate *p*-values for LCC and average path length. The *p*-values were adjusted using the Benjamini–Hochberg (BH) method to control the false discovery rate. Additionally, bootstrapping was performed to obtain confidence intervals for the variables. Significance was determined at a threshold of $p < 0.05$.

3. Results

3.1. Dynamics of Plasmodium relictum Infection

An experiment was conducted over a duration of 38 days to investigate the effects of *P. relictum* infection. A group of five canaries received an inoculation of infected blood containing *P. relictum* meronts, while another group of three canaries was injected with parasite-free PBS and served as the control. Four days after the infection, *P. relictum* was detected in the peripheral blood of all infected canaries (Figure 1). The highest parasitemia, which is measured by the percentage of infected erythrocytes, was observed at 8 days post-infection (DPI) in four *P. relictum*-infected birds, with an average of 6.6 ± 4.3% (mean ± SD). One bird reached the peak parasitemia of 24% at 13 DPI. Three birds showed low parasitemia in their peripheral blood at 22 DPI and 38 DPI (22 DPI—0.2 ± 0.4%; 38 DPI—0.004 ± 0.004%) (Figure 1).

3.2. The Impact of Plasmodium relictum Infection on Host Microbiota Diversity and Composition

We conducted an analysis of bird microbiota from fecal samples using amplicon sequence variants (ASV) to examine the impact of *P. relictum* infection on the host microbiota. We compared infected and control groups at two time points: 22 DPI and 38 DPI. To measure the diversity, we calculated three alpha diversity metrics, namely observed features (Figure 2A), phylogenetic diversity (Faith's phylogenetic diversity index) (Figure 2B), and evenness (Pielou's index) (Figure 2C). Surprisingly, there were no significant differences in these metrics between the infected and control groups (Kruskal–Wallis test, $p > 0.05$). However, we found significant differences in the observed features within the infected group between 22 DPI and 38 DPI (Figure 2A).

To assess microbial community composition, we used the Bray–Curtis index. We found a significant difference in the composition of the microbiota between the infected and control groups (PERMANOVA, $p = 0.007$; $F = 4.604$; Figure 2D,E), while beta dispersion showed no significant differences (PERMANOVA test, $p > 0.05$; Figure 2D,E).

Next, we conducted a differential abundance analysis to identify changes in specific taxa between *P. relictum*-infected and control birds. At 22 DPI, we observed a significantly higher abundance of three taxa in the microbiota of infected birds, while the control group had a higher abundance of seven taxa (Table S1, Figure S1). At 38 DPI, the control group had 23 taxa with a significantly increased abundance compared to the *P. relictum*-infected group. Interestingly, the bacterial taxa with significant differences in abundance were different at 22 DPI and 38 DPI and unique to the groups (Table S1, Figure S1).

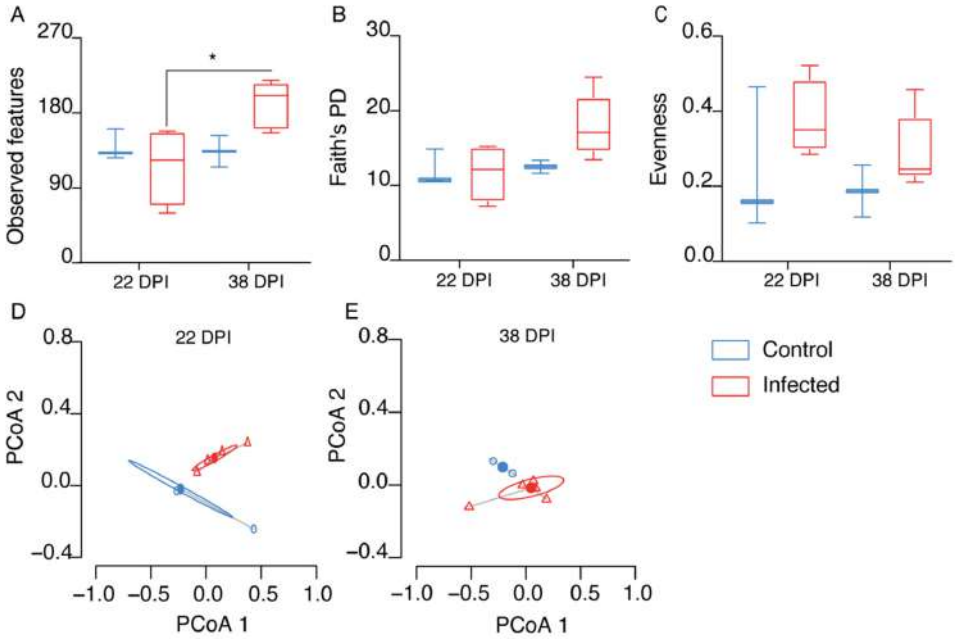

Figure 2. Comparison of microbial diversity to assess the impact of *P. relictum* infection on the microbiota in birds between infected and control groups at 22 and 38 days post-infection (DPI). (**A**) Observed features, (**B**) Faith's phylogenetic diversity (PD), and (**C**) Pielou's evenness index. Comparison of beta–diversity with Bray–Curtis dissimilarity index for infected (triangle) and control (circle) groups at 22 (**D**) and 38 DPI (**E**), represented in PCoA plot obtained by Betadisper function. * $p < 0.05$.

3.3. Changes in the Microbiota Assembly Due to Plasmodium relictum Infection

We compared the microbiota structure in uninfected and *P. relictum*-infected birds using bacterial co-occurrence networks. In the infected group, we observed fewer correlations between nodes compared to the control group at both 22 DPI and 38 DPI (Figure 3A). The correlation patterns between nodes in the two groups changed differently from 22 DPI to 38 DPI. At 22 DPI, both networks had the same number of nodes (Table 1). However, Venn analysis revealed that out of a total of 154 nodes, 64 (41.6%) were shared between the control and infected groups, with each group having 45 (29.2%) unique nodes (Figure 3B). From 22 DPI to 38 DPI, the number of nodes in the infected group's network increased, while the number of nodes declined in the control group. The bacterial network of infected birds comprised 84 (50.6%) unique nodes and 60 (36.1%) shared nodes with the control group, which, in turn, had 22 (33.3%) unique genera (Figure 3C). However, the number of correlations in the control group's network was notably higher at both time points compared to the infected birds (Table 1).

When comparing the modularity in the networks—referring to a degree of division into distinct communities—we found that this parameter was higher in the control group at 22 DPI compared to the infected group, while at 38 DPI, the pattern was inverted. Notably, the microbiota of the infected group showed greater interconnectedness with the presence of several distinct clusters (Figure 3A). In the control group's networks, both at 22 DPI and 38 DPI, a major cluster with nodes with the highest values of eigenvector centrality was

observed (Figure 3A, red nodes), but this pattern was not observed in the infected group's networks. Notably, only positive correlations were shared between the groups, while all negative correlations were specific to each group.

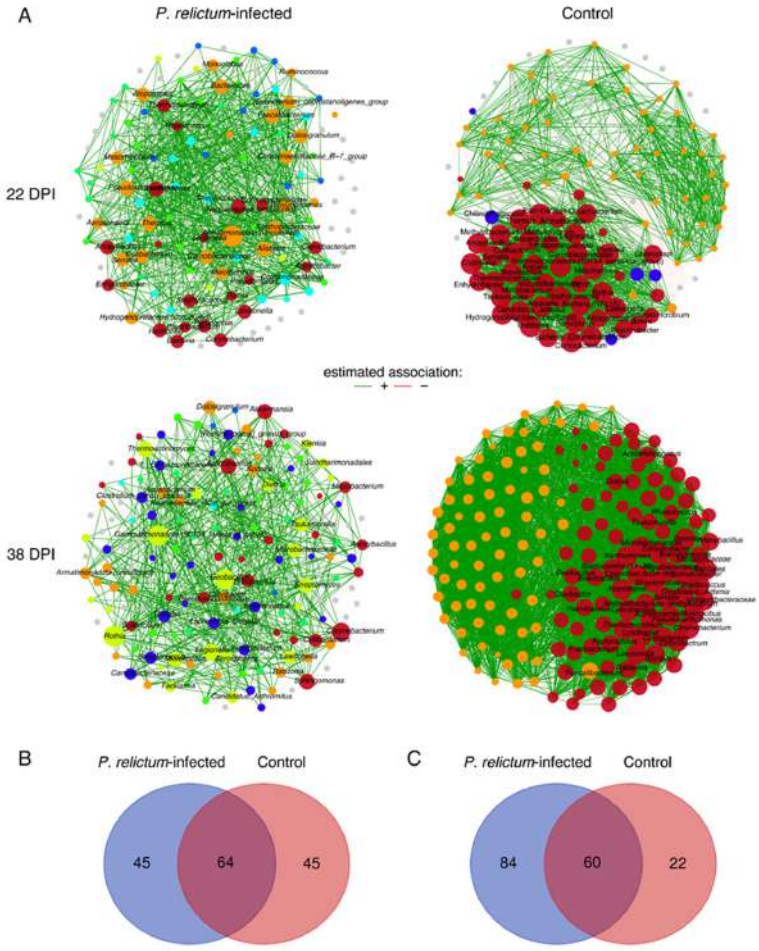

Figure 3. Microbial community assemblies in *P. relictum*-infected and uninfected birds. Co-occurrence networks (**A**) were extrapolated from the microbiota of *P. relictum*-infected and control birds at 22 DPI and 38 DPI. Bacterial taxa with at least one connection are symbolized by nodes, whilst connected edges represent a significant correlation between them. The width of the edges corresponds to the level of co-occurrence correlation (SparCC, weight ≥ 0.5 or ≤ -0.5). Green edges represent positive correlations. The colors of nodes specify clusters and modules in which taxa occur. The size of nodes is related to their eigenvector centrality. Venn diagrams displaying the number of shared and unique taxa detected within *P. relictum*-infected and control birds at 22 DPI (**B**) and 38 DPI (**C**).

Table 1. Topological parameters of co-occurrence networks.

Network Features	Uninfected		*P. relictum*-Infected	
	22 DPI	38 DPI	22 DPI	38 DPI
Nodes	109	82	109	139
Edges	2943	3235	1201	904
Positive	1482 (50.36%)	1558 (48.16%)	624 (51.96%)	461 (51%)
Negative	1461 (49.64%)	1677 (51.84%)	577 (48.04%)	443 (49%)
Network diameter	3	2	4	5
Average degree	54	78.902	22.037	13.007
Weighted degree	0.638	−2.286	0.877	0.257
Average path length	1.509	1.026	2.238	2.673
Modularity	19.062	−20.16	9.353	17.473
Number of modules	3	2	3	7
Average clustering coefficient	0.759	0.978	0.667	0.539

The observed Jaccard values for comparing degree and betweenness centrality between networks of *P. relictum*-infected and control birds were significantly lower than expected by random at 22 DPI. However, there were no significant differences in hub taxa, closeness, and eigenvector centrality (Table S2). At 38 DPI, all centrality measures showed significantly lower observed Jaccard values between the groups compared to random expectations. These significant values were all below 0.3, indicating a low similarity in centrality measures' distribution in the microbiota of *P. relictum*-infected and control birds (Table S2).

Despite the differences in the community assembly, the analysis of the core association network (CAN) revealed 62 core-associated nodes between the infected and control groups at 22 DPI (Figure 4). Among these core-associated nodes, we determined 72 (59% of the total 122) positive edges and 50 (41% of the total 122) negative edges, which were common in both groups. At 38 DPI, the core-associated network consisted of 52 nodes, with 38 (50% of the total 76) positive and 38 (50% of the total 76) negative edges.

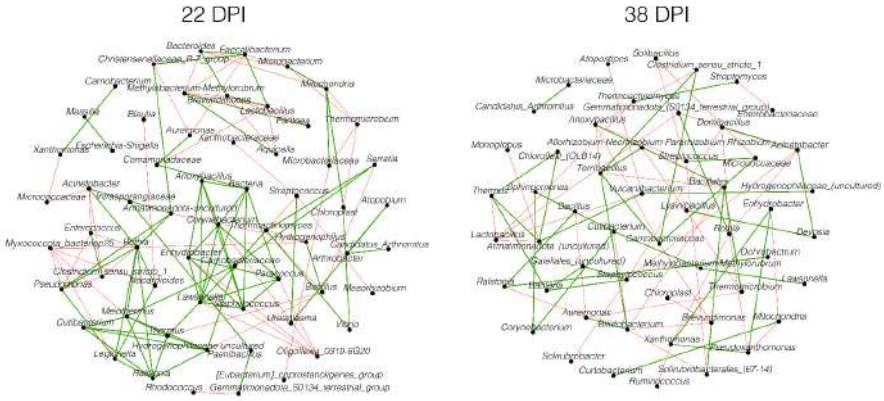

Figure 4. Core association networks inferred between *P. relictum*-infected and control groups at 22 DPI and 38 DPI. Positive (green) or negative (red) correlations are shown by the color of the edges. Nodes represent bacterial taxa.

3.4. Network Robustness

To assess the robustness of the bird microbiota networks during infection and in a healthy state at different time points, we tested the loss of connectivity due to node removal using different attack methods: direct, cascading, degree, or random. The results showed that the cascading method had the highest impact on network connectivity in infected birds compared to the control group. The most notable difference in network tolerance to perturbations between infected and control birds was observed at 80% connectivity loss. At 22 DPI, the infected group required the removal of 0.25 fraction of nodes in the network, while the control group required 0.42 to achieve the specified loss of connectivity (Figure 5A). At 38 DPI, the fraction of nodes removed increased to 0.30 for infected birds and 0.55 for the control group to achieve the same effect on the network (Figure 5B). Other node removal methods did not show a visible difference in connectivity loss between the groups (Figure S2).

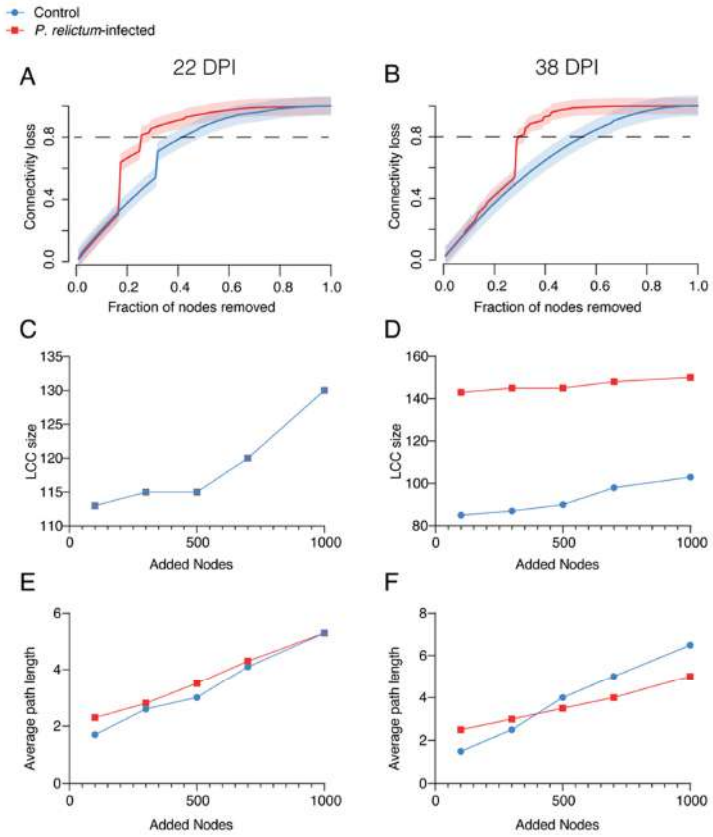

Figure 5. (**A**,**B**) Network robustness to node removal with cascading attack. Values of connectivity loss in *P. relictum*-infected (red) and control (blue) birds at 22 DPI and 38 DPI were compared. (**C**–**F**) Comparison of network robustness to node addition. The values of the largest connected component (LCC) (**C**,**D**) and average path length (**E**,**F**) are presented.

To compare the network stability of infected and control groups, we examined how the addition of new nodes affected network connectivity. The results revealed that the largest connected component (LCC) increased in both groups after adding more than 500 nodes to the networks at 22 DPI (Figure 5C,D). At 38 DPI, the infected group initially exhibited a high value of LCC, which did not significantly change even after adding more nodes, indicating a high stability of the network (Figure 5C). In contrast, the LCC in the control group remained relatively low compared to the infected group, with a minor increase when more nodes were added, suggesting less tolerance to changes in the microbiota (Figure 5D).

A similar pattern of changes in the average path length was observed in response to node additions in both infected and control groups (Figure 5E,F). Adding nodes to the networks increased the average path length in both groups at 22 DPI and 38 DPI (Figure 5E,F). However, at 38 DPI, the effects on the infected group's network were less pronounced compared to the control group.

4. Discussion

The influence of malaria parasites on the modulation of the microbiota has been established in previous studies [21,22]. In this study, we put forth the hypothesis that *P. relictum* plays a pivotal role in reshaping the microbial community within the host through intricate microbe–host interactions. Consequently, this process may result in a decreased ability of the microbiota to resist colonization. To investigate this phenomenon, we adopted a network-based approach to evaluate the effects of *P. relictum* on the composition of the microbiota in canaries.

We found no significant differences in alpha diversity metrics between the avian malaria parasite *P. relictum*-infected and control groups. This discovery aligns with the studies of Aželyte et al. [22] and Rohrer et al. [21], where an infection caused by avian malaria parasites did not greatly affect the alpha and beta diversity of the avian host. These results suggest that avian malaria infections have a negligible impact on the diversity of the host microbiota. In contrast, it is reported that the non-human primate and murine malaria parasites can significantly reduce alpha diversity [15,18,49]. Several studies showed that lower diversity of microbial species within the microbiota has been linked to reduced colonization resistance in other systems [50–52]. The current findings on the impact of avian *Plasmodium* on host-microbiota variety imply that it has a minimal impact on colonization resistance.

However, this study revealed noteworthy disparities in beta diversity between the *P. relictum*-infected and control groups, suggesting alterations in the microbiota composition of infected birds. This contrasts with the findings of Aželytė et al. [22] and Rohrer et al. [21], who reported no divergence in beta diversity between *Plasmodium*-infected birds and the control group. The observed changes in microbial composition in this study imply that *P. relictum* infection disturbs the normal equilibrium of bacterial taxa within the canaries' microbiota. Furthermore, upon analyzing differential abundance, we identified specific taxa with higher abundance, mostly in uninfected birds. These findings align with the studies conducted by Rohrer et al. [21], which observed fewer taxa with increased abundance in *Plasmodium*-infected birds compared to the control. Importantly, our findings are similar to the results of Aželytė et al. [22], who found no significant variations in taxa abundance between infected and uninfected birds at different time points. It is noteworthy that our results from the experiment conducted under controlled conditions are comparable to the study by Rohrer et al. [21], which investigated wild birds. Although the studies showed that microbiota composition is influenced by genetic background and other environmental factors [13,53], the alterations caused by infection can be recognized. The lack of change in alpha diversity suggests that overall microbial richness and evenness may remain relatively stable despite the presence of the parasite. However, the observed shifts in composition and abundance of commensal bacteria highlight the potential for specific taxa to be affected by the infection, which may have important implications for colonization resistance. Spragge et al. [52] showed that colonization resistance is not dependent on a single species but

rather on the associations of multiple bacteria cohesively living in a community. These findings suggest that while the overall diversity of the microbiota may not be impacted, specific microbial communities crucial for colonization resistance could be compromised by *P. relictum* infection.

In agreement with the findings of others in different parasites [14,22], this study reveals a decrease in network correlations, indicating that infection with *P. relictum* is linked to a reduction in the complexity and connectivity of the microbiota structure. As in *P. homocircumflexum* [22], we observed distinct changes in the correlation patterns between infected and control groups over time, suggesting that the infection dynamically affects the interactions among bacterial species within the community assembly, leading to alterations in the network structure. Furthermore, the varying proportions of unique and shared nodes between the groups indicate that *P. relictum*-related changes in the composition of the bacterial community result in changes in network membership. However, intriguingly, our CAN results imply that certain bacterial taxa maintain consistent associations despite the infection, while other associations may be specific to each group.

This disruption in community assembly may weaken the overall stability and resilience of the microbiota, potentially compromising its ability to resist colonization by pathogens. Disruption can occur due to drug administration, such as anthelmintics [54] or antibiotics [55], or pathogen infection [56], and these have been shown to affect colonization resistance [25]. For example, the administration of anthelmintic drugs significantly altered the microbial community of Welsh ponies, causing instability and disrupting the time-dependent network of interactions [54]. This disruption had long-term effects on microbial resilience [54]. Antibiotic use also disrupts the balance between host and microbiota, leading to *Clostridium difficile* infection [55]. Moreover, acute infection by *Yersinia* can induce long-term immune and microbiota changes, ultimately resulting in chronic inflammatory disease [56].

Furthermore, changes in centrality measures may impact the key microbial species involved in colonization resistance, potentially compromising the microbiota's ability to resist pathogen colonization. An example of this can be seen in the protective role of *Enterococcus faecalis* against *Staphylococcus aureus* in *Caenorhabditis elegans* [57], where *E. faecalis* becomes a keystone taxon in the nematode's microbiota [58]. Our findings on network robustness support the notion that *Plasmodium* infection has an impact on colonization resistance. Infected birds experienced greater disruption of network connectivity when taxa were removed, but their networks also showed higher stability and less pronounced changes after node additions.

5. Conclusions

In conclusion, this study on avian malaria parasite *P. relictum* infection suggests that, while overall microbial diversity remains stable, specific bacterial communities crucial for colonization resistance may be compromised. The infection disrupts the composition and connectivity of the microbiota, potentially weakening its ability to resist pathogen colonization. These findings have broader implications beyond avian malaria infections. Disruptions in community assembly, alterations in network structure, and changes in microbial abundances have been linked to compromised colonization resistance in other systems. Similar disruptions have been observed due to drug administration or pathogen infections, highlighting the importance of maintaining a healthy and stable microbiota for the host defense. Further research is needed to understand the intricate mechanisms underlying these interactions and develop strategies to enhance colonization resistance and host health.

Supplementary Materials: The following supporting information can be downloaded at https://www.mdpi.com/article/10.3390/pathogens13010091/s1. Figure S1: Heatmaps representing the relative abundance (expressed as centered log ratio) of taxa with significant differences between uninfected and *P. relictum*-infected birds at 22 DPI (A) and 38 DPI (B). Figure S2: Network tolerance to node removal. The resistance of the networks to directed, degree, cascading, and random attacks

in control and *P. relictum*-infected groups at 22 DPI and 38 DPI. Table S1: List of unique and differentially abundant taxa identified by the ALDEx2 method between the gut microbiota of infected and uninfected birds at 22 DPI and 38 DPI. Table S2: Jaccard indexes of local centrality measures. The two *p*-values, P(J $\leq$ j) and P(J $\geq$ j), for each Jaccard's index were added.

Author Contributions: A.C.-C. and V.P. conceived the study and supervised the work. J.A., A.M., L.A.-D., E.P.-S., D.O., A.W.-C., L.M.-H. and R.Ž. performed the analyses. J.A., A.M., L.A.-D. and E.P.-S. prepared the figures. L.A.-D., A.W.-C. and D.O. provided software. J.A. and A.C.-C. drafted the manuscript. All authors revised and accepted the last version of the manuscript.

Funding: This research was funded by the French Government's Investissement d'Avenir program, Laboratoire d'Excellence "Integrative Biology of Emerging Infectious Diseases" (Grant No. ANR-10-LABX-62-IBEID). Funding for V.P. was provided by the Research Council of Lithuania (LMTLT) (Project No. S-MIP-22-52). A.W.-C. was supported by Programa Nacional de Becas de Postgrado en el Exterior "Don Carlos Antonio López" (Grant No. 205/2018). A.M. was supported by the 'Collectivité de Corse', grant: 'Formations superieures' (SGCE-RAPPORT No. 0300).

Institutional Review Board Statement: All procedures were performed at the Nature Research Centre in Vilnius, Lithuania, according to Lithuanian and International Guiding Principles for Biomedical Research Involving Animals (2012). Infection experiments and other procedures were reviewed and approved by the Lithuanian State Food and Veterinary Service, Ref. No. 2020/07/24-G2-84. The assessment of the animal health and all described procedures were implemented by trained professionals (under licenses 2012/02/06-No-208, 2016/01/29-No-344, and 2021/02/05-No-527).

Informed Consent Statement: Not applicable.

Data Availability Statement: The datasets generated and analyzed in this study are available on the SRA repository under Bioproject No. PRJNA971381.

Conflicts of Interest: The authors declare no conflicts of interest.

References

1. Valkiūnas, G. *Avian Malaria Parasites and Other Haemosporidia*; CRC Press: Boca Raton, FL, USA, 2005; ISBN 978-0-415-30097-1.
2. Ducarmon, Q.R.; Zwittink, R.D.; Hornung, B.V.H.; van Schaik, W.; Young, V.B.; Kuijper, E.J. Gut Microbiota and Colonization Resistance against Bacterial Enteric Infection. *Microbiol. Mol. Biol. Rev.* **2019**, *83*, e00007-19. [CrossRef] [PubMed]
3. Karita, Y.; Limmer, D.T.; Hallatschek, O. Scale-Dependent Tipping Points of Bacterial Colonization Resistance. *Proc. Natl. Acad. Sci. USA* **2022**, *119*, e2115496119. [CrossRef] [PubMed]
4. Mullineaux-Sanders, C.; Suez, J.; Elinav, E.; Frankel, G. Sieving through Gut Models of Colonization Resistance. *Nat. Microbiol.* **2018**, *3*, 132–140. [CrossRef] [PubMed]
5. Stacy, A.; Andrade-Oliveira, V.; McCulloch, J.A.; Hild, B.; Oh, J.H.; Perez-Chaparro, P.J.; Sim, C.K.; Lim, A.I.; Link, V.M.; Enamorado, M.; et al. Infection Trains the Host for Microbiota-Enhanced Resistance to Pathogens. *Cell* **2021**, *184*, 615–627.e17. [CrossRef]
6. Martínez-de la Puente, J.; Santiago-Alarcon, D.; Palinauskas, V.; Bensch, S. Plasmodium Relictum. *Trends Parasitol.* **2021**, *37*, 355–356. [CrossRef]
7. Chen, Y.; Li, H. Avian Leukosis Virus Subgroup J Infection Influences the Gut Microbiota Composition in Huiyang Bearded Chickens. *Lett. Appl. Microbiol.* **2022**, *74*, 344–353. [CrossRef]
8. Sun, F.; Chen, J.; Liu, K.; Tang, M.; Yang, Y. The Avian Gut Microbiota: Diversity, Influencing Factors, and Future Directions. *Front. Microbiol.* **2022**, *13*, 934272. [CrossRef]
9. Waite, D.W.; Taylor, M.W. Exploring the Avian Gut Microbiota: Current Trends and Future Directions. *Front. Microbiol.* **2015**, *6*, 673. [CrossRef]
10. Palinauskas, V.; Mateos-Hernandez, L.; Wu-Chuang, A.; de la Fuente, J.; Aželytė, J.; Obregon, D.; Cabezas-Cruz, A. Exploring the Ecological Implications of Microbiota Diversity in Birds: Natural Barriers against Avian Malaria. *Front. Immunol.* **2022**, *13*, 807682. [CrossRef]
11. Cisek, A.A.; Binek, M. Chicken Intestinal Microbiota Function with a Special Emphasis on the Role of Probiotic Bacteria. *Pol. J. Vet. Sci.* **2014**, *17*, 385–394. [CrossRef]
12. Hird, S.M.; Sánchez, C.; Carstens, B.C.; Brumfield, R.T. Comparative Gut Microbiota of 59 Neotropical Bird Species. *Front. Microbiol.* **2015**, *6*, 1403. [CrossRef] [PubMed]
13. Grond, K.; Santo Domingo, J.W.; Lanctot, R.B.; Jumpponen, A.; Bentzen, R.L.; Boldenow, M.L.; Brown, S.C.; Casler, B.; Cunningham, J.A.; Doll, A.C.; et al. Composition and Drivers of Gut Microbial Communities in Arctic-Breeding Shorebirds. *Front. Microbiol.* **2019**, *10*, 2258. [CrossRef] [PubMed]

14. Mammeri, M.; Obregón, D.A.; Chevillot, A.; Polack, B.; Julien, C.; Pollet, T.; Cabezas-Cruz, A.; Adjou, K.T. Cryptosporidium Parvum Infection Depletes Butyrate Producer Bacteria in Goat Kid Microbiome. *Front. Microbiol.* **2020**, *11*, 548737. [CrossRef] [PubMed]
15. Taniguchi, T.; Miyauchi, E.; Nakamura, S.; Hirai, M.; Suzue, K.; Imai, T.; Nomura, T.; Handa, T.; Okada, H.; Shimokawa, C.; et al. Plasmodium Berghei ANKA Causes Intestinal Malaria Associated with Dysbiosis. *Sci. Rep.* **2015**, *5*, 15699. [CrossRef] [PubMed]
16. Stough, J.M.A.; Dearth, S.P.; Denny, J.E.; LeCleir, G.R.; Schmidt, N.W.; Campagna, S.R.; Wilhelm, S.W. Functional Characteristics of the Gut Microbiome in C57BL/6 Mice Differentially Susceptible to *Plasmodium yoelii*. *Front. Microbiol.* **2016**, *7*, 1520. [CrossRef] [PubMed]
17. Yilmaz, B.; Portugal, S.; Tran, T.M.; Gozzelino, R.; Ramos, S.; Gomes, J.; Regalado, A.; Cowan, P.J.; d'Apice, A.J.F.; Chong, A.S.; et al. Gut Microbiota Elicits a Protective Immune Response against Malaria Transmission. *Cell* **2014**, *159*, 1277–1289. [CrossRef]
18. Mooney, J.P.; Lokken, K.L.; Byndloss, M.X.; George, M.D.; Velazquez, E.M.; Faber, F.; Butler, B.P.; Walker, G.T.; Ali, M.M.; Potts, R.; et al. Inflammation-Associated Alterations to the Intestinal Microbiota Reduce Colonization Resistance against Non-Typhoidal Salmonella during Concurrent Malaria Parasite Infection. *Sci. Rep.* **2015**, *5*, 14603. [CrossRef]
19. Navine, A.K.; Paxton, K.L.; Paxton, E.H.; Hart, P.J.; Foster, J.T.; McInerney, N.; Fleischer, R.C.; Videvall, E. Microbiomes Associated with Avian Malaria Survival Differ between Susceptible Hawaiian Honeycreepers and Sympatric Malaria-resistant Introduced Birds. *Mol. Ecol.* **2023**, *32*, 6659–6670. [CrossRef]
20. Videvall, E.; Marzal, A.; Magallanes, S.; Fleischer, R.C.; Espinoza, K.; García-Longoria, L. The Uropygial Gland Microbiome of House Sparrows with Malaria Infection. *J. Avian Biol.* **2021**, *52*, jav.02686. [CrossRef]
21. Rohrer, S.D.; Robertson, B.Q.; Chubiz, L.M.; Parker, P.G. Gut Microbiome Composition Associated with *Plasmodium* Infection in the Eurasian Tree Sparrow. *J. Avian Biol.* **2023**, *2023*, e03027. [CrossRef]
22. Aželytė, J.; Wu-Chuang, A.; Maitre, A.; Žiegytė, R.; Mateos-Hernández, L.; Obregón, D.; Palinauskas, V.; Cabezas-Cruz, A. Avian Malaria Parasites Modulate Gut Microbiome Assembly in Canaries. *Microorganisms* **2023**, *11*, 563. [CrossRef] [PubMed]
23. Faust, K.; Raes, J. Microbial Interactions: From Networks to Models. *Nat. Rev. Microbiol.* **2012**, *10*, 538–550. [CrossRef] [PubMed]
24. Röttjers, L.; Faust, K. From Hairballs to Hypotheses–Biological Insights from Microbial Networks. *FEMS Microbiol. Rev.* **2018**, *42*, 761–780. [CrossRef] [PubMed]
25. Shade, A.; Peter, H.; Allison, S.D.; Baho, D.L.; Berga, M.; Bürgmann, H.; Huber, D.H.; Langenheder, S.; Lennon, J.T.; Martiny, J.B.H.; et al. Fundamentals of Microbial Community Resistance and Resilience. *Front. Microbio* **2012**, *3*, 417. [CrossRef] [PubMed]
26. Maitre, A.; Wu-Chuang, A.; Mateos-Hernández, L.; Piloto-Sardiñas, E.; Foucault-Simonin, A.; Cicculli, V.; Moutailler, S.; Paoli, J.; Falchi, A.; Obregón, D.; et al. Rickettsial Pathogens Drive Microbiota Assembly in *Hyalomma Marginatum* and *Rhipicephalus Bursa* Ticks. *Mol. Ecol.* **2023**, *32*, 4660–4676. [CrossRef] [PubMed]
27. Maitre, A.; Wu-Chuang, A.; Mateos-Hernández, L.; Foucault-Simonin, A.; Moutailler, S.; Paoli, J.-C.; Falchi, A.; Díaz-Sánchez, A.A.; Banović, P.; Obregón, D.; et al. Rickettsia Helvetica Infection Is Associated with Microbiome Modulation in Ixodes Ricinus Collected from Humans in Serbia. *Sci. Rep.* **2022**, *12*, 11464. [CrossRef]
28. Mateos-Hernández, L.; Obregón, D.; Wu-Chuang, A.; Maye, J.; Bornères, J.; Versillé, N.; de la Fuente, J.; Díaz-Sánchez, S.; Bermúdez-Humarán, L.G.; Torres-Maravilla, E.; et al. Anti-Microbiota Vaccines Modulate the Tick Microbiome in a Taxon-Specific Manner. *Front. Immunol.* **2021**, *12*, 704621. [CrossRef]
29. Estrada-Peña, A.; Cabezas-Cruz, A.; Obregón, D. Resistance of Tick Gut Microbiome to Anti-Tick Vaccines, Pathogen Infection and Antimicrobial Peptides. *Pathogens* **2020**, *9*, 309. [CrossRef]
30. Aželytė, J.; Wu-Chuang, A.; Žiegytė, R.; Platonova, E.; Mateos-Hernandez, L.; Maye, J.; Obregon, D.; Palinauskas, V.; Cabezas-Cruz, A. Anti-Microbiota Vaccine Reduces Avian Malaria Infection within Mosquito Vectors. *Front. Immunol.* **2022**, *13*, 841835. [CrossRef]
31. Bolyen, E.; Rideout, J.R.; Dillon, M.R.; Bokulich, N.A.; Abnet, C.C.; Al-Ghalith, G.A.; Alexander, H.; Alm, E.J.; Arumugam, M.; Asnicar, F.; et al. Reproducible, Interactive, Scalable and Extensible Microbiome Data Science Using QIIME 2. *Nat. Biotechnol.* **2019**, *37*, 852–857. [CrossRef]
32. Callahan, B.J.; McMurdie, P.J.; Rosen, M.J.; Han, A.W.; Johnson, A.J.A.; Holmes, S.P. DADA2: High-Resolution Sample Inference from Illumina Amplicon Data. *Nat. Methods* **2016**, *13*, 581–583. [CrossRef] [PubMed]
33. Yarza, P.; Yilmaz, P.; Pruesse, E.; Glöckner, F.O.; Ludwig, W.; Schleifer, K.-H.; Whitman, W.B.; Euzéby, J.; Amann, R.; Rosselló-Móra, R. Uniting the Classification of Cultured and Uncultured Bacteria and Archaea Using 16S rRNA Gene Sequences. *Nat. Rev. Microbiol.* **2014**, *12*, 635–645. [CrossRef] [PubMed]
34. Faith, D.P. Conservation Evaluation and Phylogenetic Diversity. *Biol. Conserv.* **1992**, *61*, 1–10. [CrossRef]
35. Bray, J.R.; Curtis, J.T. An Ordination of the Upland Forest Communities of Southern Wisconsin. *Ecol. Monogr.* **1957**, *27*, 325–349. [CrossRef]
36. Pielou, E.C. The Measurement of Diversity in Different Types of Biological Collections. *J. Theor. Biol.* **1966**, *13*, 131–144. [CrossRef]
37. R Core Team. *R: A Language and Environment for Statistical Computing*; R Foundation for Statistical Computing: Vienna, Austria, 2021. Available online: https://www.r-project.org/ (accessed on 10 May 2023).
38. Gloor, G.B.; Macklaim, J.M.; Fernandes, A.D. Displaying Variation in Large Datasets: Plotting a Visual Summary of Effect Sizes. *J. Comput. Graph. Stat.* **2016**, *25*, 971–979. [CrossRef]
39. Aitchison, J. *The Statistical Analysis of Compositional Data*; Springer: Dordrecht, The Netherlands, 1986; ISBN 978-94-010-8324-9.

40. Friedman, J.; Alm, E.J. Inferring Correlation Networks from Genomic Survey Data. *PLoS Comput. Biol.* **2012**, *8*, e1002687. [CrossRef]
41. Bastian, M.; Heymann, S.; Jacomy, M. Gephi: An Open Source Software for Exploring and Manipulating Networks. *ICWSM* **2009**, *3*, 361–362. [CrossRef]
42. Peschel, S.; Müller, C.L.; von Mutius, E.; Boulesteix, A.-L.; Depner, M. NetCoMi: Network Construction and Comparison for Microbiome Data in R. *Brief. Bioinform.* **2021**, *22*, bbaa290. [CrossRef]
43. Röttjers, L.; Vandeputte, D.; Raes, J.; Faust, K. Null-Model-Based Network Comparison Reveals Core Associations. *ISME Commun.* **2021**, *1*, 36. [CrossRef]
44. Anaconda Software Distribution. Anaconda Documentation. Anaconda Inc. 2023. Available online: https://docs.anaconda.com/ (accessed on 10 June 2023).
45. Lhomme, S. Analyse Spatiale de La Structure Des Réseaux Techniques Dans Un Contexte de Risques. *Cybergeo* **2015**. [CrossRef]
46. Csárdi, G.; Nepusz, T. The Igraph Software Package for Complex Network Research. *InterJournal Complex Syst.* **2006**, *1695*, 1–9.
47. Csárdi, G.; Nepusz, T.; Müller, K.; Horvát, S.; Traag, V.; Zanini, F.; Noom, D. Igraph for R: R Interface of the Igraph Library for Graph Theory and Network Analysis 2023. Zenodo. Available online: https://CRAN.R-project.org/package=igraph (accessed on 30 April 2023).
48. Freitas, S.; Yang, D.; Kumar, S.; Tong, H.; Chau, D.H. Evaluating Graph Vulnerability and Robustness Using TIGER. *arXiv* **2020**. [CrossRef]
49. Farinella, D.N.; Kaur, S.; Tran, V.; Cabrera-Mora, M.; Joyner, C.J.; Lapp, S.A.; Pakala, S.B.; Nural, M.V.; DeBarry, J.D.; Kissinger, J.C.; et al. Malaria Disrupts the Rhesus Macaque Gut Microbiome. *Front. Cell. Infect. Microbiol.* **2023**, *12*, 1058926. [CrossRef] [PubMed]
50. Robinson, C.J.; Schloss, P.; Ramos, Y.; Raffa, K.; Handelsman, J. Robustness of the Bacterial Community in the Cabbage White Butterfly Larval Midgut. *Microb. Ecol.* **2010**, *59*, 199–211. [CrossRef] [PubMed]
51. Shea, K. Community Ecology Theory as a Framework for Biological Invasions. *Trends Ecol. Evol.* **2002**, *17*, 170–176. [CrossRef]
52. Spragge, F.; Bakkeren, E.; Jahn, M.T.; Araujo, E.B.N.; Pearson, C.F.; Wang, X.; Pankhurst, L.; Cunrath, O.; Foster, K.R. Microbiome Diversity Protects against Pathogens by Nutrient Blocking. *Science* **2023**, *382*, eadj3502. [CrossRef] [PubMed]
53. Schokker, D.; Veninga, G.; Vastenhouw, S.A.; Bossers, A.; De Bree, F.M.; Kaal-Lansbergen, L.M.T.E.; Rebel, J.M.J.; Smits, M.A. Early Life Microbial Colonization of the Gut and Intestinal Development Differ between Genetically Divergent Broiler Lines. *BMC Genom.* **2015**, *16*, 418. [CrossRef] [PubMed]
54. Boisseau, M.; Dhorne-Pollet, S.; Bars-Cortina, D.; Courtot, É.; Serreau, D.; Annonay, G.; Lluch, J.; Gesbert, A.; Reigner, F.; Sallé, G.; et al. Species Interactions, Stability, and Resilience of the Gut Microbiota—Helminth Assemblage in Horses. *iScience* **2023**, *26*, 106044. [CrossRef]
55. Britton, R.A.; Young, V.B. Interaction between the Intestinal Microbiota and Host in Clostridium Difficile Colonization Resistance. *Trends Microbiol.* **2012**, *20*, 313–319. [CrossRef]
56. Kamdar, K.; Khakpour, S.; Chen, J.; Leone, V.; Brulc, J.; Mangatu, T.; Antonopoulos, D.A.; Chang, E.B.; Kahn, S.A.; Kirschner, B.S.; et al. Genetic and Metabolic Signals during Acute Enteric Bacterial Infection Alter the Microbiota and Drive Progression to Chronic Inflammatory Disease. *Cell Host Microbe* **2016**, *19*, 21–31. [CrossRef]
57. King, K.C.; Brockhurst, M.A.; Vasieva, O.; Paterson, S.; Betts, A.; Ford, S.A.; Frost, C.L.; Horsburgh, M.J.; Haldenby, S.; Hurst, G.D. Rapid Evolution of Microbe-Mediated Protection against Pathogens in a Worm Host. *ISME J.* **2016**, *10*, 1915–1924. [CrossRef] [PubMed]
58. Wu-Chuang, A.; Bates, K.A.; Obregon, D.; Estrada-Peña, A.; King, K.C.; Cabezas-Cruz, A. Rapid Evolution of a Novel Protective Symbiont into Keystone Taxon in Caenorhabditis Elegans Microbiota. *Sci. Rep.* **2022**, *12*, 14045. [CrossRef] [PubMed]

PAPER VI

Generalist Malaria Parasites and Host Imprinting: Unveiling Transcriptional Memory

García-Longoria L., Palinauskas V.**, Aželytė J.**, Marzal A., Ovelleiro D., Hellgren O.

Molecular Biology and Evolution, 2025, 1;42(9):msaf19
DOI 10.1093/molbev/msaf198

Molecular Biology and Evolution, 2025, **42**, 1–10
https://doi.org/10.1093/molbev/msaf198
Advance access publication 1 September 2025
Discoveries

MBE OXFORD

Generalist Malaria Parasites and Host Imprinting: Unveiling Transcriptional Memory

Luz García-Longoria [1,*] Vaidas Palinauskas [2] Justė Aželytė [2] Alfonso Marzal [1,3] David Ovelleiro [4] Olof Hellgren [5,*]

[1]Departamento de Anatomía, Biología celular y Zoología, Facultad de Ciencias, Universidad de Extremadura, Badajoz, Spain
[2]State Scientific Research Institute, Vilnius, Lithuania
[3]Widlife Research Group, Universidad Nacional de San Martín, Tarapoto, Perú
[4]Peripheral Nervous System, Vall d'Hebron Institut de Recerca (VHIR), Vall d'Hebron Hospital Universitari, Vall d'Hebron Barcelona Hospital Campus, Barcelona, Spain
[5]Evolutionary Ecology and Infection Biology, Department of Biology, Lund University, SE-22362 Lund, Sweden

***Corresponding authors**: E-mails: luzlongoria@unex.es; olof.hellgren@biol.lu.se.
Associate editor: Aurelien Tellier

Abstract

Generalist parasites must adapt to diverse host environments to ensure their survival and transmission. These adaptations can involve fixed genetic responses, transcriptional plasticity, or epigenetic mechanisms. The avian malaria parasite *Plasmodium homocircumflexum* offers an ideal model for studying transcriptional variation across hosts. We experimentally inoculated *P. homocircumflexum* into different bird species, bypassing the vector, to assess whether gene expression remains stable across hosts, resets in response to new environments, or reflects epigenetic inheritance. We tested two alternative hypotheses: (i) universal gene expression profile ("one key fits all"), where parasite expression remains consistent across hosts. Our outcomes revealed that gene expression differed significantly depending on the host species and time postinfection, rejecting this hypothesis. (ii) Transcriptional plasticity, where gene expression is determined by the recipient host. Contrary to this hypothesis, we observed that gene expression was primarily influenced by the donor at 8 d postinfection (dpi), whereas gene expression was more aligned with the recipient host at 16 dpi. We also explored two mechanisms to explain these patterns: (i) epigenetic inheritance, whereby early transcription reflects the donor environment but adjusts over time, and (ii) genetic differentiation selecting for specific haplotypes. Our data support mechanism (i): 2,647 differentially expressed genes (DEGs) were associated with the donor at 8 dpi, while only 271 DEGs were linked to the recipient at 16 dpi. Single Nucleotide Polymorphism analyses revealed low genetic differentiation, rejecting mechanism (ii). These findings suggest that *P. homocircumflexum* undergoes a shift from donor-dependent to recipient-dependent gene expression, likely driven by epigenetic regulation and transcriptional plasticity.

Keywords: transcriptomic plasticity, epigenetic regulation, *Plasmodium homocircumflexum*, adaptive strategies, avian malaria

Introduction

The survival of generalist parasites depends on their ability to adapt to new environments (Prati et al. 2022). When conducting host shifts, the parasite get exposed to varying immune responses, body temperatures, metabolism, and nutrient availability, all affecting survival and replication (Agosta et al. 2010; Gupta et al. 2020). Vector-transmitted parasites such as *Plasmodium* spp. must navigate in both vertebrate and invertebrate hosts, with the vertebrate immune system being a major challenge (Mandala et al. 2021; Matos et al. 2023). Just considering the vertebrate immune responses, they might further vary across species (Palinauskas et al. 2020; Galinski 2022) and geographic regions (Clark et al. 2020; Fecchio et al. 2021), requiring parasites to be highly flexible to overcome these challenges. One way to achieve this flexibility is by relying on transcriptional variation (Turnbull et al. 2022), where gene expression shifts in response to environmental changes, often regulated by epigenetic mechanisms such as DNA methylation (Serrano-Durán et al. 2022) and histone modifications (Connacher et al. 2022). These mechanisms enable adaptation without altering the genome (Hollin et al. 2023), helping parasites to evade host immunity and adjust to host metabolism within a single infection.

A key question is whether generalist parasites adapt through fixed genetic responses or flexible adjustments such as epigenetic modifications and real-time gene expression shifts. One possibility is a "universal key" strategy, where parasites maintain a static gene expression profile that enables infection across different hosts with minimal adjustment, relying on conserved gene responses (Schneider et al. 2023; Naidoo and Oliver 2024). Alternatively, selection-driven variation may favor specific haplotypes with expression profiles better suited to certain hosts (Ellis et al. 2023). Another strategy involves dynamic responses, in which gene expression adapts to different host immune defenses and metabolism (Guha et al. 2021). This plasticity may arise from epigenetic mechanisms or gene expression patterns inherited asexually from the parent population (Govindaraju and Rajavelu 2024), enabling the replication of successful adaptive responses. These inherited profiles may shift when environmental changes demand adaptation, optimizing parasite survival across hosts (Llorà-Batlle et al. 2019).

Plasmodium falciparum exemplifies transcriptional variation, with gene expression changes regulated through complex epigenetic mechanisms (Adejoh et al. 2023). Genes involved in antigenic variation and immune evasion exhibit

Received: May 15, 2025. **Revised:** July 15, 2025. **Accepted:** July 21, 2025

clonal variation, meaning genetically identical parasites express different gene sets (Wyss et al. 2024). This allows *P. falciparum* to maintain a diverse population, some better suited to withstand host changes (Schneider et al. 2023). Similarly, avian generalist *Plasmodium* species may employ analogous strategies, maintaining genetic and epigenetic diversity to adapt rapidly as they shift between avian hosts. However, this remains untested empirically.

Compared to mammalian *Plasmodium* species such as *Plasmodium falciparum*, avian *Plasmodium* species offer a unique model for examining the strategies of generalist versus specialist parasites. *Plasmodium homocircumflexum* is particularly relevant as it infects multiple host species that are phylogenetically diverse (Palinauskas et al. 2015). By analyzing gene expression changes in *P. homocircumflexum* across different hosts and over time, we can better understand how parasites navigate the balance between adaptation and specialization. The extent to which transcriptomic changes in generalist parasites stem from immediate host conditions versus retained adaptations from previous hosts remains unclear. It is likely that both factors contribute, as evidenced by *Plasmodium relictum* and *P. homocircumflexum*, which infect a variety of bird species (Bensch et al. 2009). These parasites may rely on multiple transcriptional variation sources to respond effectively to new immune challenges and physiological conditions (Manzoli et al. 2021). Identifying the specific sources utilized by *P. homocircumflexum* could enhance our understanding of how generalist parasites optimize their survival across different hosts. To investigate transcriptional variation, we conducted a crosswise infection experiment where we directly inoculated *P. homocircumflexum* into different host species after the parasites have had time to develop and adjust within either host. The method allowed us to bypass recombination in the vector, ensuring that the parasites initiating the new infection were directly exposed to either the same or a different host environment without time to "reset" their transcriptional profiles. This approach enabled us to assess how the parasite responds to the recipient host and how transcriptional variation unfolds across asexual generations. We considered two alternative hypotheses regarding the regulation of gene expression in *P. homocircumflexum*: (i) a "one key fits all" strategy, where gene expression remains consistent regardless of host environment, and (ii) transcriptomic plasticity, where gene expression reflects the recipient host environment, as clonal offspring adapt directly to new conditions. We also explored two possible mechanisms that could shape the observed transcriptional profiles: (i) epigenetic inheritance, where gene expression reflects a donor-derived program retained through asexual replication, and (b) selection on specific genotypes, which would result in expression divergence associated with genetic differentiation.

As the infection progresses, we hypothesize that *P. homocircumflexum* may shift gene expression through selection acting on epigenetically diverse asexually reproducing populations or through plastic responses triggered by host immune signals. By examining these scenarios, our study aims to determine whether gene expression in a generalist parasite is primarily shaped by adaptive responses to the recipient host environment or by retained adaptations from previous hosts. This research will deepen our understanding of the adaptability of generalist parasites and the evolutionary pressures that shape host–parasite interactions.

Results

Parasitemia

Parasitemia from all the individuals changed over the course of the infection (Fig. 1) achieving maximum values around 8 d post infection (dpi) in most of the individuals.

Principal Component Analysis

The principal component analysis (PCA) results obtained from normalized data show distinct clustering patterns for donors and recipients over time (Fig. 2). At 8 dpi, there was a

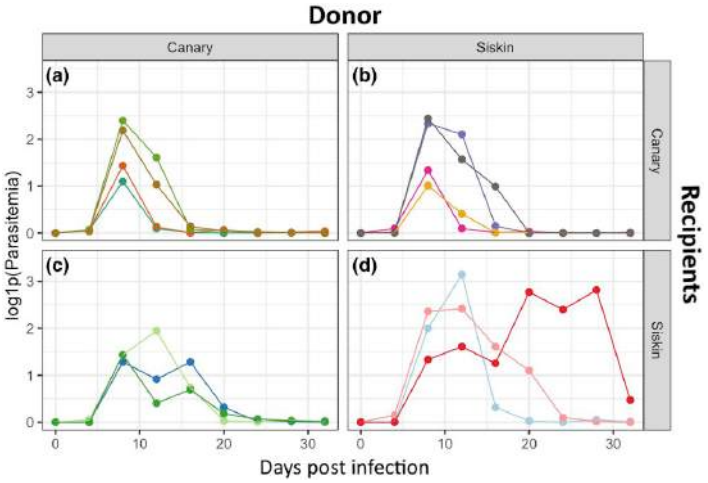

Fig. 1. Parasitemia levels for each experimental group, showing individual trajectories. Panels indicate combinations of donor and recipient species: a) canaries receiving infected blood from canaries, b) canaries receiving infected blood from siskins, c) siskins receiving infected blood from canaries, and d) siskins receiving infected blood from siskins. Each line represents an individual. Dashed lines indicate days of sampling for each group (8, 12, and 16 dpi).

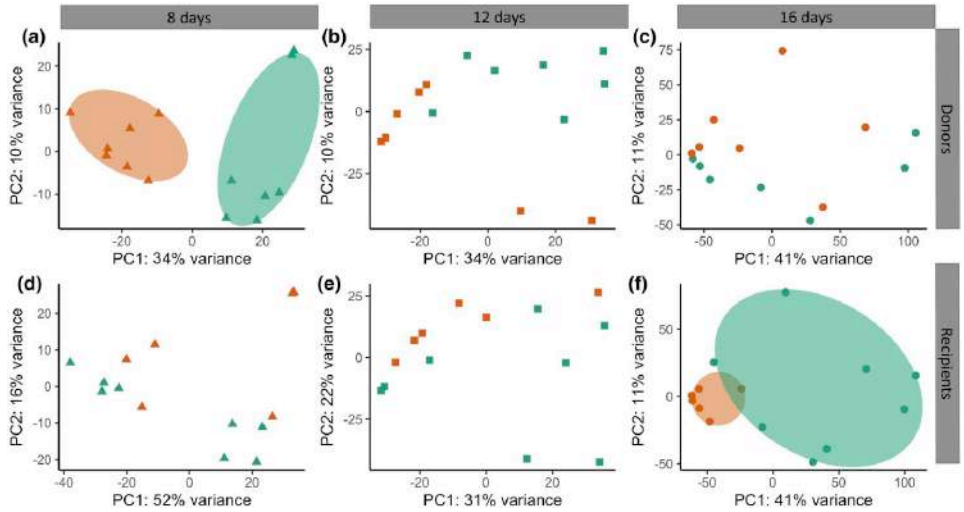

Fig. 2. Biplot from a PCA illustrating the variance in the data for donors and recipients at 8, 12, and 16 dpi. Shapes represent different time points: triangles for 8 dpi, squares for 12 dpi, and circles for 16 dpi. The first column shows PCA plots of donors (top row) and recipients (bottom row) at 8 dpi, the second column at 12 dpi, and the third column at 16 dpi. Each plot indicates the percentage of variance explained by the first two principal components (PC1 and PC2). Ellipses represent the 95% confidence intervals for each group.

clear separation based on the donor (Fig. 2a), indicating significant differences in their data profiles. However, this separation was not observed when considering the type of recipient (Fig. 2d). At 12 dpi, the distinction between the groups became less pronounced, suggesting a convergence of their data profiles (Fig. 2b–e). At 16 dpi, the PCA plots have shifted to form a tight clustering of samples in the recipient birds of siskins, regardless of the donor (Fig. 2f). In contrast, grouping by donor resulted in more dispersed data points with no clear clustering (Fig. 2).

Differential Expression Analyses

During the course of infection, *P. homocircumflexum* underwent transcriptional changes as it adapted to the host environment (Figs. 3 and 4). At 8 and 12 dpi, parasites originating from the same donor showed more homogeneous gene expression patterns, regardless of the species they infected. This observation suggests that early in the infection, parasites relied on preestablished gene expression profiles rather than immediately adapting to the new host environment. This pattern was reflected in the overall expression trends (Fig. 3) and the number of differentially expressed genes (DEGs), which were found to be higher when grouped by donor compared to recipient (Fig. 4). During this phase, parasites may prioritize strategies for immune evasion, red blood cell invasion, and replication while maintaining a transcriptional signature inherited from their original host.

However, by 16 dpi, the influence of the recipient species emerged as the primary factor shaping parasite gene expression (Fig. 3). At this stage, transcriptomic profiles were more distinct between host species, suggesting an active response to new physiological and immunological pressures. DEG patterns also shifted, with a higher percentage of DEGs associated with the recipient rather than the donor (Fig. 4). The most significant changes occurred between 8 and 16 dpi. At 8 dpi, 2,647 DEGs were detected when grouping by donors (Fig. 4a), while only 60 DEGs were observed when considering recipients (Fig. 4d). By 16 dpi, this trend reversed, with 271 DEGs when grouping by recipients (Fig. 4f) and only 19 DEGs by donors (Fig. 4c). These findings suggest that as infection progressed, parasites shifted from a generalist gene expression strategy to a more specialized adaptation tailored to the recipient host, likely involving metabolic adjustments and mechanisms for immune evasion. This highlights the plasticity of *P. homocircumflexum* in modulating its transcriptome to optimize survival across different host environments.

Variant Calling

A distribution of the samples according to their Single Nucleotide Polymorphism (SNP) was obtained for day 8 dpi (Fig. 5). As indicated in the Materials and Methods, similar analysis could not be performed for 12 and 16 dpi. The results indicate that samples do not cluster clearly when classified according to either recipient (Fig. 5a) or donor (Fig. 5b) species. The distribution of the samples showed no clear pattern when considering either the recipient (Fig. 5a) or donor (Fig. 5b) species. Additionally, two Fixation Index (FST) analyses were conducted. The first analysis yielded an FST value of 0.09 (95% CI 0.02 to 0.15) when considering donor species, while the second analysis resulted in an FST of 0.03 (95% CI 0.01 to 0.14) when considering recipient species. These FST values further support a lack of clear genetic differentiation among the samples based on the species classification.

Discussion

Our results provide insights into *P. homocircumflexum* infection in two avian host species, showing how generalist parasites adapt to phylogenetically distinct hosts. Parasitemia

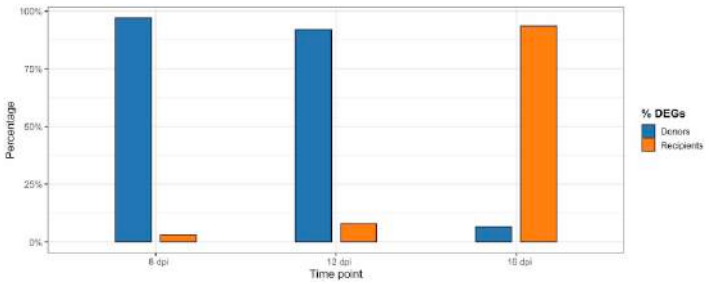

Fig. 3. Percentage of DEGs between donors and recipients at three time points: 8, 12, and 16 dpi. For each time point, two adjacent bars represent the percentages for donors and recipients, respectively, allowing direct comparison.

peaked at 8 dpi, with RNA expression shifting from donor-dependent at 8 dpi to recipient-dependent by 16 dpi. Regarding the scenarios, (i) the "one key fits all" strategy could be ruled out, as gene expression shifted according to the host environment, and (ii) transcriptomic plasticity could be partially supported, as expression in later stages reflected the recipient host environment, suggesting adaptation. Hence, our findings reject both extremes, revealing an intermediate profile with a shift from donor- to recipient-aligned expression. This pattern is consistent with the idea that gene expression is plastic but may initially reflect donor-derived regulation. We explored two mechanisms that could underlie this pattern: (i) epigenetic inheritance and (ii) selection-driven genetic divergence. While the first remains speculative, it aligns well with our data; the second is not supported by our genetic control analyses. Therefore, the observed pattern is consistent with epigenetic inheritance (i), whereby transcriptional profiles are retained from the donor via asexual replication and gradually adjust to the recipient host environment. While we did not directly measure epigenetic marks, this mechanism offers a plausible explanation for the early donor-driven expression. However, selection-driven differences (ii) are not supported, as our analysis of SNP variation served as a control to assess whether expression profiles could be explained by underlying genetic divergence. The low FST values and lack of clustering in PCA indicate that the observed transcriptional differences are unlikely to result from selection on divergent haplotypes. These findings underscore the plasticity and adaptability of generalist parasite plasticity in diverse host environments. Although we did not find evidence for selection acting on genetic variants (haplotypes), it is also possible that natural selection acts directly on gene expression levels (Nourmohammad et al. 2017; Cope et al. 2025). This form of selection could be considered an extension of the second mechanism, acting not on sequence variation but on regulatory variation. Below, we discuss these results in detail.

Although the infection dynamics of some parasites are well understood, classifying a parasite as a generalist or specialist depends on the density of its reservoir host (Fecchio et al. 2021). In this context, the biodiversity and abundance of species within an ecosystem may influence whether a parasite lineage is more or less generalist in its host range (de Angeli Dutra et al. 2021; Doussang et al. 2021; Prati et al. 2022). Indeed, previous studies have determined that the same parasite species can adapt to a more specialist role in environments with a limited number of potential host species, compared to scenarios where many potential hosts are available (de Angeli Dutra et al. 2021; Dharmarajan et al. 2021). The molecular mechanisms and adaptations that a generalist parasite population can undergo during infection and reproduction in different host species have been insufficiently analyzed. Our results provide new insights into this issue. Despite exhibiting similar levels of parasitemia, we revealed that the source of infection significantly influences the RNA expression patterns of the parasite. In essence, the donor species seems to dictate parasite expression in the days following infection. However, after 16 dpi, expression patterns appear to be primarily determined by the infected species (i.e. the recipient). According to the existing scientific literature, factors contributing to these changes in RNA expression patterns may include genetic variations such as SNPs, epigenetic modifications, or direct plasticity (Lorà-Batlle et al. 2019).

Single nucleotide polymorphisms in human malaria have been pivotal in identifying genetic factors that influence susceptibility to infection and drug resistance (Gill and Sharma 2022; Dinzouna-Boutamba et al. 2023). Over the last decade, SNP studies have been extensively used to uncover host–pathogen interactions and guide the development of targeted therapies and vaccines (e.g. Maïga-Ascofaré et al. 2010). In this study, we have used established SNP analysis workflows to determine whether the differences found during peak infection (8 dpi) could be due to natural selection within the parasite population. Our findings indicate that genetic selection during peak infection is 9% based on donor species and 3% based on recipient species. While these percentages suggest a small degree of selection at this stage of the infection cycle, we cannot definitively conclude that this process accounts for the observed differences. Additional methods (e.g. discriminant PCA or phylogenetics) could complement this analysis, but the limitations of our RNA-seq-derived SNP dataset restrict their applicability.

Epigenetic mechanisms, such as histone modifications and DNA methylation, have been recognized as significant drivers of transcriptional variation in parasites. These mechanisms enable heritable and reversible changes in chromatin state, which are crucial for the adaptive capacity of these organisms (Holliday 2006; Handel et al. 2010). This flexibility is particularly important for generalist parasites, as it facilitates their adaptation to changing environments during infection (Duraisingh and Skillman 2018; Hollin et al. 2023). In mammalian malaria systems, including *P. falciparum*, epigenetic factors have been shown to drive early gene expression changes (Adejoh et al. 2023). It is plausible that *P.*

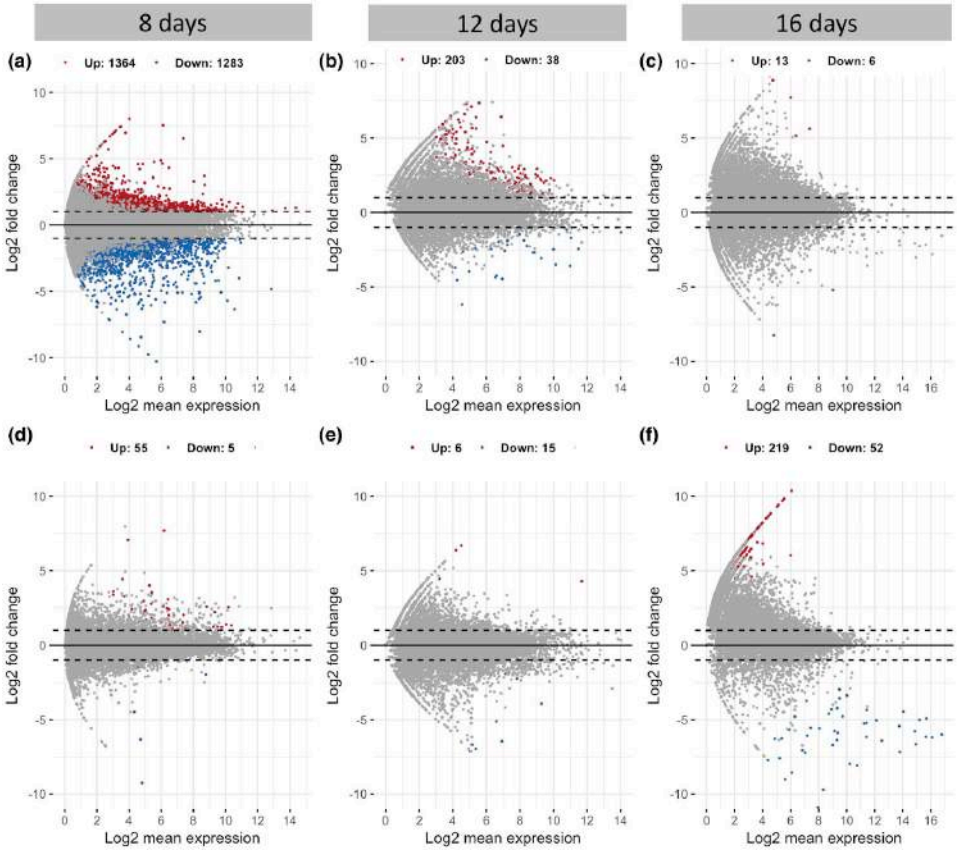

Fig. 4. Minus average plots showing differential gene expression analysis at 8, 12, and 16 dpi. The three plots on the top (a–c) show the results when analyzing the data by taking into account the donor species. The three plots on the bottom (d–f) show the results when analyzing the data by taking into account the recipient species. The *x* axis represents the $\log_2$ fold change, and the *y* axis shows the $-\log_{10}$–adjusted *P*–value. Points above the significance threshold indicate significantly upregulated or downregulated genes, while the remaining points are nonsignificant. Highlighted gene names correspond to the top 20 DEGs (FDR 2). The total number of DEGs is indicated for each plot.

homocircumflexum employs similar mechanisms inherited from the donor population to regulate gene expression at 8 dpi. These inherited epigenetic responses may provide a strategic advantage during the early stages of infection, allowing for rapid adaptation to the new host environment. As the infection progresses, the host immune system could exert selective pressure (Abdrabou et al. 2021), resulting in recipient-dependent patterns of gene expression. This shift underscores the parasite's dynamic adaptability in response to host-derived signals and immune challenges, highlighting the complexity of generalist parasite–host interactions. To test this hypothesis more directly, RNA expression data from the donor individuals at the moment of blood transfer would be required, enabling comparison with their corresponding derived 8 dpi populations. Although, these specific samples were not collected for transcriptomic analysis, such analyses could clarify whether transcriptional patterns reflect inherited epigenetic regulation or other adaptive processes.

Direct transcriptional variation refers to transient, nonheritable changes in gene expression that are triggered by environmental stressors (Llorà-Batlle et al. 2019). In the context of host–parasite interactions, these mechanisms can be influenced by the host immune response, which evolves dynamically over the course of an infection. Around 12 dpi, the host immune system transitions from innate to adaptive immunity (Sorci 2013; Delhaye et al. 2018), marking a critical turning point in the interaction between the host and the parasite. In our study, we observed a distinct shift in RNA expression patterns between 8 and 16 dpi. Early in the infection (8 dpi), parasite gene expression appeared to be dependent on the donor population. However, by 16 dpi, it was predominantly shaped by the recipient species. This temporal change aligns with the timing of immune system modulation, as the influence of the donor diminishes and the adaptive immune signals from the recipient take precedence. Our findings support the idea that parasite transcriptional responses are not only reactive

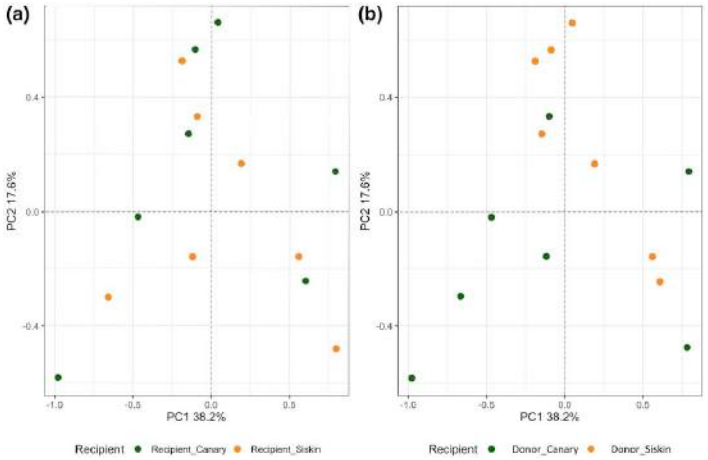

Fig. 5. PCA based on SNPs in expressed RNA in samples from 8 dpi classified based on two different criteria. a) The distribution of samples when classified according to the recipient species. b) The distribution of the same samples but classified based on the blood donor.

but also adaptive to the host immune environment. This highlights the role of immune system dynamics in shaping gene expression. These results provide valuable insights into how immune responses drive transcriptional variation, furthering our understanding of the complex interplay between host and parasite.

A critical next step is to investigate the host immune response over time, with a particular focus on distinct immune pathways or gene groups that are activated at different stages of infection. RNA-seq analyses could be instrumental in uncovering pathways associated with innate immunity during the early stages and adaptive immunity in the later stages of infection, thereby providing valuable insights into host–parasite dynamics. Furthermore, exploring cytokine responses, T-cell activation pathways, and other immune-related processes would help clarify the role of host immunity in shaping parasite gene expression. Such analyses could elucidate whether specific pathways are consistently targeted by *P. homocircumflexum* across hosts, which would improve our understanding of host-specific versus generalist responses.

Our experimental design, which involved blood inoculations, ensured that parasite populations began from the same starting point. This controlled setup allowed us to detect significant differences in RNA profiles influenced by donor species at 8 dpi and by recipient species at 16 dpi. The donor effect observed during early stages highlights the importance of parasite synchronization with the donor host. These results suggest that gene expression patterns may differ in natural infections transmitted by vectors due to the additional epigenetic regulation imposed by vector stages. Follow-up studies that include vector–host–parasite interactions would provide valuable insights into RNA expression dynamics and the influence of epigenetic regulation during transmission. Moreover, comparisons with human malaria experiments, where vector-stage regulation has been well documented (Yu et al. 2022), could further refine our understanding of these processes in avian systems.

In conclusion, our study highlights the dynamic transcriptional plasticity of *P. homocircumflexum* during infection in two avian host species, emphasizing how generalist parasites respond to distinct host environments. We observed that parasitemia peaked at 8 dpi, with RNA expression patterns initially influenced by the donor species before shifting to profiles driven by the recipient by 16 dpi. This transition may coincide with the progression of the host immune response from innate to adaptive immunity, suggesting that host-derived signals could influence parasite transcriptional responses. However, since we did not directly assess host immune markers, further studies are needed to confirm this relationship. Our SNP analyses revealed limited genetic selection, indicating that the observed transcriptional shifts are unlikely driven by genetic changes but may instead result from epigenetic mechanisms such as histone modifications or DNA methylation. These mechanisms may provide the parasite with transcriptional flexibility necessary to rapidly adjust to host-specific environments. Nonetheless, whether these changes are adaptive in the context of transmission remains unclear. In particular, the relationship between within-host transcriptional shifts and transmission success warrants further investigation. If the genes undergoing regulation are involved in gametocyte production, this could indicate an adaptive response facilitating transmission. Future research incorporating gametocyte-stage expression data and vector-mediated infections will be crucial to fully understand the interplay between host immunity, epigenetic regulation, and parasite adaptation.

Materials and Methods

Experimental Animals and Parasite Acquisition

The research was conducted in 2019 at the Nature Research Centre in Vilnius, Lithuania, using juvenile domestic canaries (*Serinus canaria domestica*) and Eurasian siskins (*Spinus spinus*) from commercial suppliers. All procedures complied with European and Lithuanian regulations on animal research, with ethical approval from the State Food and Veterinary Service of Lithuania (approval no. 2018/05/03-G2-84).

Birds were housed individually in cages, allowing social interaction, in a vector-free room with a stable 21 ± 1 °C

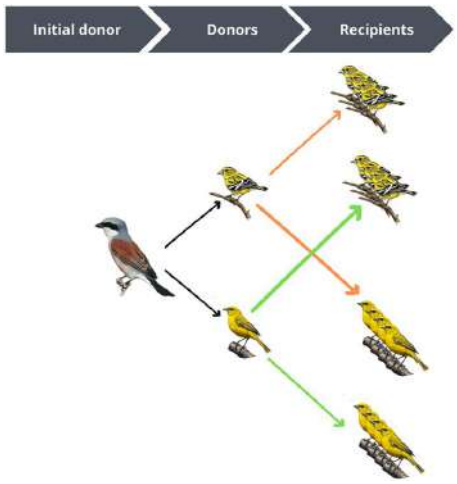

Fig. 6. Experimental design for this study involved using blood from an initial donor for consecutive experimental infections. One canary and one siskin served as blood donors, while a total of six siskins and eight canaries were used as recipients. Colored arrows indicate the origin of the infected blood: orange arrows represent blood from siskin donor, while green arrows represent blood from canary donor. (Drawings obtained with the artificial intelligence of Artbreeder and the final figure designed with Canva).

temperature and a natural light/dark cycle. Food and water were provided ad libitum. Before experiments, Polymerase Chain Reaction (PCR) and microscopy confirmed all birds were malaria-free. The parasite used was *P.* (Giovannolaia) *homocircumflexum*, lineage COLL4 (GenBank KC884250), originally isolated in 2010 from a wild red-backed shrike (*Lanius collurio*) captured at the Biological Station of the Zoological Institute of the Russian Academy of Sciences on the Curonian Spit, Baltic Sea. The strain was cryopreserved following Dimitrov et al. (2010) and later used for experiments.

Experimental Procedures

Eight canaries and six siskins were randomly assigned to four experimental groups (Fig. 6). The *P. homocircumflexum* strain COLL4, obtained from a canary, was used to infect four canaries and three siskins. The same strain, sourced from a siskin, was used to infect four additional canaries and three siskins. The experiments used the parasite's seventh passage.

To initiate infections, cryopreserved blood was introduced into a noninfected canary and siskin, which then served as donors: canary-derived parasites for canaries and siskins and siskin-derived parasites for canaries and siskins. Each bird received 100 µL of a freshly prepared suspension containing infected blood, 3.7% sodium citrate, and 0.9% saline (4:1:5 ratio), with an erythrocytic meront intensity of 0.4% and an estimated dose of 6×10^5 meronts. The mixture was injected into the pectoral muscle following Iezhova et al. (2005). Birds were monitored for 32 dpi, with blood samples collected every 4 d for microscopy and PCR. Additional samples for RNA sequencing were taken at 8, 16, and 24 dpi.

Sampling, Microscopy, and Molecular Analysis

Blood samples were obtained by puncturing the brachial vein. A small drop of blood from each bird was used to prepare two blood smears, while approximately 30 µl was stored in SET buffer (0.05 M Tris, 0.15 M NaCl, 0.5 ethylenediaminetetraacetic acid, pH 8.0) for molecular analysis (Hellgren et al. 2004). Samples for RNA analysis were preserved in TRIzol LS Reagent (Invitrogen, Carlsbad, CA). Blood samples were kept at −20 °C until processed. The blood smears were air-dried, fixed with absolute methanol, and stained with Giemsa (Valkiūnas et al. 2008). The slides were examined under an Olympus BX51 light microscope equipped with an Olympus DP12 (Olympus, Shinjuku City, Japan). Approximately 100 fields were reviewed at a magnification of 1000×. Parasitemia was quantified by counting the number of parasites per 1,000 erythrocytes, or per 10,000 erythrocytes in cases of low infection intensity, following the protocol recommended by Godfrey et al. (1987). Detailed procedures for preparing, staining, and examining blood smears were outlined by Valkiūnas et al. (2008).

DNA extraction was performed using the ammonium acetate protocol (Sambrook et al. 1989). A nested PCR protocol was employed for genetic analysis (Waldenström et al. 2004). Amplification products (1.5 µl) were resolved on a 2% agarose gel. Sequencing followed the protocol by Bensch et al. (2000), targeting the *5′* region with the primer HaemF. Dye terminator cycle sequencing (BigDye) was conducted on an ABI PRISMTM 3100 capillary sequencer (Applied Biosystems, USA). Sequence editing and alignment were carried out using BioEdit (Hall 1999).

RNA Extraction and Sequencing

Blood samples for RNA sequencing were collected at three different time points (8, 16, and 12 dpi). The samples were stored in TRIzol. Total RNA was extracted from 20 µL whole blood using 1000 µL TRIzol LS Reagent (Invitrogen, Carlsbad, CA) and homogenized by vortexing from all seven individuals. Samples were then incubated at room temperature for 5 min before the addition of 200 µl chloroform (Merck KGaA, Darmstadt, Germany). After a further incubation at room temperature for 3 min, the samples were centrifuged at 11,000 rpm for 17 min at 4 °C. The supernatant was then transferred to new tubes and processed using an RNeasy Mini Kit (Qiagen, GmbH, Hilden, Germany). Following the manufacturer's protocol, 1 volume of 70% ethanol was added to the lysate. The total extracted RNA was shipped on dry ice to Novogene Bioinformatics Technology, Hong Kong, for RNA quality control, DNAse treatment, and rRNA reduction and amplification using the SMARTer Ultra Low Kit (Clontech Laboratories, Inc.). Novogene performed library preparation, cDNA synthesis, and paired-end RNA sequencing using the Illumina HiSeq 2000. We quality checked all demultiplexed RNA-seq reads using FastQC (v.0.10.1) (Andrews 2010).

De Novo Transcriptome Assembly

As the genome of *P. homocircumflexum* is not available, alternative tools were employed in order to isolate information belonging exclusively to the *P. homocircumflexum* lineage pCOLL4. Initially, the canary genome (NCBI RefSeq assembly serCan2020) and a portion of the siskin genome (NCBI RefSeq assembly ASM3478079v1) were employed to eliminate reads belonging to the bird. Subsequently, the *P. relictum*

genome (NCBI RefSeq assembly GCA_900005765.1; Böhme et al. 2018) was utilized to keep reads belonging to the malaria parasite. Finally, the *P. homocircumflexum* transcriptome previously published (García-Longoria et al. 2020) was employed to obtain a greater number of reads and ensure that the reads used exclusively belonged to the malaria parasite. Analyses with and without the reference genome were performed using the bioinformatics software STAR (Dobin et al. 2013) and Bowtie (Langmead and Salzberg 2012). Standard adjustments were implemented to determine alignment sensitivity. Finally, the de novo assembly of the parasite was conducted using the transcriptome assembler Trinity (v. 2.15.1) (Grabherr et al. 2011), resulting in 14,649 contigs.

Guanine–Cytosine (GC) content varies across different eukaryotic organisms, with where *Plasmodium* species evolving toward a high Adenine–Thymine (AT) richness compared to its hosts (Galtier et al. 2001; Birdsell 2002; Hershberg and Petrov 2010; Videvall 2018), which provides a valuable tool for transcript separation in host–parasite studies. Consequently, the subsequent transcript was subjected to filtration based on GC content in order to exclude any host contigs and to include sequences with a mean GC content below 23% ($n = 12{,}058$).

Differential Gene Expression Level

The expression levels of the parasite genes were quantified using Salmon (v. 1.3.2) (Patro et al. 2017). Salmon is a software program that produces expected read counts for every contig and identifies genes that are expressed between species, along with the name of each contig. The read counts for every contig were stored in a file that was statistically analyzed inside the R statistical environment (v. 4.5.0) (R Core Team 2023). Read counts were normalized using regularized log transformation in order to account for potential variation in sequencing depth and the large differences in the number of parasites present in the blood (parasitemia levels). Regularized log transformation of counts was performed in order to represent the data without any prior knowledge of the sampling design in the PCA and sample distance calculations. This method of presenting counts without bias is preferable to variance stabilizing of counts when the size factors vary greatly between the samples, as is the case in our data. The package ggplot2 (Wickham 2016) was employed for the generation of all graphs.

Statistical Analyses

For the differential expression analyses, we used the R package DeSeq2 (love et al. 2014), which is designed for the specific task of performing this type of analysis. This package (version 1.16.1) was utilized to correct the variance–mean dependence in count data derived from high-throughput sequencing assays and to test for differential expression based on a model that employs the negative binomial distribution. When significant differences in expression were identified, and to circumvent potential issues associated with sequencing depth, gene length, or RNA composition, count data were initially normalized using the DeSeq2 method.

The statistical comparisons are presented in Fig. 6. Firstly, the samples were classified according to the donor. This distinction was made regardless of the species of bird receiving the blood (Fig. 6). Subsequently, the samples were classified based on the recipient of the blood (Fig. 6). In this instance, only the species of bird receiving the blood was considered. This approach enabled the number of DEGs to be determined in relation to either the origin of the blood (from birds of mixed species but with the same donor species) or the recipient (from birds of the same species but with infection originating from different species of donor).

Acknowledgments

Funding was provided by the Junta de Extremadura (PO17024, postdoc grant) to L.G.-L., the Spanish Ministry of Science and Innovation (PID2022-140397NB-I00) to A.M., and LA4 (R + D + I program in the Biodiversity Area financed with the funds of the FEDER Extremadura 2021–2027 Operational Program of the Recovery, Transformation and Resilience Plan) to L.G.-L., and A.M. V.P. obtained funding from the Research Council of Lithuania (LMTLT) (project no. S-MIP-22-52). O.H. obtained funding from the Swedish Research Council (VR 2016-03419 and 2021-03663). All the authors would like to thank Ananias Escalante for taking the time to read the manuscript and for his inspiring ideas.

Author Contributions

V.P. and J.A. performed all experimental work through experimental infections with and all the laboratory procedures. O.H. and V.P. conceived the study, designed the overall experiment, and contributed to the conceptual development. O.H., V.P., and A.M. secured funding for the research. L.G.-L. conducted all bioinformatics analyses and statistical assessments, drafted the manuscript, and contributed to the conceptual development and interpretation of results. D.O. provided support and assistance with bioinformatics analyses. All authors reviewed, edited, and approved the final version of the manuscript.

Data Availability

All the data used in this study has been uploaded to the National Center for Biotechnology Information (NCBI) under the accession number PRJNA1250583.

References

Abdrabou W, Dieng MM, Diawara A, Sermé SS, Almojil D, Sombié S, Henry NB, Kargougou D, Manikandan V, Soulama I, *et al.* Metabolome modulation of the host adaptive immunity in human malaria. *Nat Metab*. 2021:3(7):1001–1016. https://doi.org/10.1038/s42255-021-00404-9.

Adejoh J, Madu C, Egua M, Raheem AL, Okoh D, P M. Molecular and epigenetics mechanisms for the immune control of *Plasmodium* parasites infection: a comprehensive review. *Asian J Biol Sci*. 2023:16(4):636–669. https://doi.org/10.3923/ajbs.2023.636.669.

Agosta SJ, Janz N, Brooks DR. How specialists can be generalists: resolving the "parasite paradox" and implications for emerging infectious disease. *Zoologia*. 2010:27(2):151–162. https://doi.org/10.1590/S1984-46702010000200001.

Andrews S. FastQC: A quality control tool for high throughput sequence data. 2010. Unpublished data, [accessed 2025 Jul 10]. https://www.bioinformatics.babraham.ac.uk/projects/fastqc/.

Bensch S, Hellgren O, Pérez-Tris J. MalAvi: a public database of malaria parasites and related haemosporidians in avian hosts based on mitochondrial cytochrome b lineages. *Mol Ecol Resour*. 2009:9(5):1353–1358. https://doi.org/10.1111/j.1755-0998.2009.02692.x.

Bensch S, Stjernman M, Hasselquist D, Östman Ö, Hansson B, Westerdahl H, Pinheiro RT. Host specificity in avian blood parasites: a study of *Plasmodium* and *Haemoproteus* mitochondrial DNA amplified from birds. *Proc R Soc Lond B Biol Sci*. 2000:267(1452):1583–1589. https://doi.org/10.1098/rspb.2000.1181.

Birdsell JA. Integrating genomics, bioinformatics, and classical genetics to study the effects of recombination on genome evolution. *Mol Biol Evol*. 2002:19(7):1181–1197. https://doi.org/10.1093/oxfordjournals.molbev.a004176.

Böhme U, Otto TD, Cotton JA, Steinbiss S, Sanders M, Oyola SO, Nicot A, Gandon S, Patra KP, Herd C, *et al*. Complete avian malaria parasite genomes reveal features associated with lineage-specific evolution in birds and mammals. *Genome Res*. 2018:28(4):547–560. https://doi.org/10.1101/gr.218123.116.

Clark NJ, Drovetski SV, Voelker G. Robust geographical determinants of infection prevalence and a contrasting latitudinal diversity gradient for haemosporidian parasites in Western Palearctic birds. *Mol Ecol*. 2020:29(16):3131–3143. https://doi.org/10.1111/mec.15545.

Connacher J, Von Grüning H, Birkholtz L. Histone modification landscapes as a roadmap for malaria parasite development. *Front Cell Dev Biol*. 2022:10:848797. https://doi.org/10.3389/fcell.2022.848797.

Cope AL, Schraiber JG, Pennell M. Macroevolutionary divergence of gene expression driven by selection on protein abundance. *Science*. 2025:387(6738):1063–1068. https://doi.org/10.1126/science.ads2658.

de Angeli Dutra D, Moreira GF, Poulin P. Contrasting effects of host or local specialization: widespread haemosporidians are host generalists, whereas local specialists are locally abundant. *Glob Ecol Biogeogr*. 2021:30(12):2467–2476. https://doi.org/10.1111/geb.13403.

Delhaye J, Jenkins T, Glaizot O, Christe P. Avian malaria and bird humoral immune response. *Malar J*. 2018:17(1):1–7. https://doi.org/10.1186/s12936-018-2219-3.

Dharmarajan D, Gupta P, Vishudas CK, Robin VV. Anthropogenic disturbance favours generalist over specialist parasites in bird communities: implications for risk of disease emergence. *Ecol Lett*. 2021:24(9):1859–1868. https://doi.org/10.1111/ele.13818.

Dimitrov D, Zehtindjiev P, Bensch S. Genetic diversity of avian blood parasites in SE Europe: cytochrome b lineages of the genera *Plasmodium* and *Haemoproteus* (Haemosporida) from Bulgaria. *Acta Parasitol*. 2010:55(3):201–209. https://doi.org/10.2478/s11686-010-0029-z.

Dinzouna-Boutamba SD, Iroungou BA, Akombi FA, Yacka-Mouele L, Moon Z, Moon-Aung J, Lee S, Chung D, Hing Y, Goo YK. Assessment of genetic polymorphisms associated with malaria antifolate resistance among the population of Libreville, Gabon. *Malar J*. 2023:22(1):183. https://doi.org/10.1186/s12936-023-04615-1.

Dobin A, Davis CA, Schlesinger F, Drenkow J, Zaleski C, Jha S, Batut P, Chaisson M, Gingeras TR. STAR: ultrafast universal RNA-seq aligner. *Bioinformatics*. 2013:29(1):15–21. https://doi.org/10.1093/bioinformatics/bts635.

Doussang D, Sallaberry-Pincheira N, Cabanne GS, Litmaer DA, González-Acuña D, Vianna JA. Specialist versus generalist parasites: the interactions between host diversity, environment and geographic barriers in avian malaria. *Int J Parasitol*. 2021:51(11):899–911. https://doi.org/10.1016/j.ijpara.2021.04.003.

Duraisingh M, Skillman KM. Epigenetic variation and regulation in malaria parasites. *Annu Rev Microbiol*. 2018:72(1):355–375. https://doi.org/10.1146/annurev-micro-090817-062722.

Ellis VA, Ciloglu A, Yildirim A, Bensch S. Host shift and natural long-distance dispersal to an oceanic island of a host-specific parasite. *Biol Lett*. 2023:19(3):20220459. https://doi.org/10.1098/rsbl.2022.0459.

Fecchio A, Clark NJ, Bell JA, Skeen HR, Lutz HL, de la Torre GM, Wells K. Global drivers of avian haemosporidian infections vary across zoogeographical regions. *Glob Ecol Biogeogr*. 2021:30(12):2393–2406. https://doi.org/10.1111/geb.13390.

Galinski MR. Systems biology of malaria explored with nonhuman primates. *Malar J*. 2022:21(1):177. https://doi.org/10.1186/s12936-022-04199-2.

Galtier N, Piganeau G, Mouchiroud D, Duret L. GC-content evolution in mammalian genomes: the biased gene conversion hypothesis. *Genetics*. 2001:159(2):907–911. https://doi.org/10.1093/genetics/159.2.907.

García-Longoria L, Palinauskas V, Ilgūnas M, Valkiūnas G, Hellgren O. Differential gene expression of *Plasmodium homocircumflexum* (lineage pCOLL4) across two experimentally infected passerine bird species. *Genomics*. 2020:112(4):2857–2865. https://doi.org/10.1016/j.ygeno.2020.03.025.

Gill J, Sharma A. Genomic analysis of single nucleotide polymorphisms in malaria parasite drug targets. *Parasit Vectors*. 2022:15(1):309. https://doi.org/10.1186/s13071-022-05422-4.

Godfrey RD, Fedynich AM, Pence DB. Quantification of hematozoa in blood smears. *J Wildl Dis*. 1987:23(4):558–565. https://doi.org/10.7589/0090-3558-23.4.558.

Govindaraju G, Rajavelu A. Reading the epitranscriptome of the human malaria parasite. *Biomed J*. 2024:48(2):100703. https://doi.org/10.1016/j.bj.2024.100703.

Grabherr M, Haas BJ, Yassour M, Levin JZ, Thompson DA, Amit I, Adiconis X, Fan L, Raychowdhury R, Zeng Q, *et al*. Full-length transcriptome assembly from RNA-Seq data without a reference genome. *Nat Biotechnol*. 2011:29(7):644–652. https://doi.org/10.1038/nbt.1883.

Guha R, Mathioudaki A, Doumbo S, Doumtabe D, Skinner J, Arora G, Crompton PD. *Plasmodium falciparum* malaria drives epigenetic reprogramming of human monocytes toward a regulatory phenotype. *PLoS Pathog*. 2021:17(4):e1009430. https://doi.org/10.1371/journal.ppat.1009430.

Gupta P, Vishudas CK, Robin VV, Dharmarajan G. Host phylogeny matters: examining sources of variation in infection risk by blood parasites across a tropical montane bird community in India. *Parasit Vectors*. 2020:13(1):1–13. https://doi.org/10.1186/s13071-020-04404-8.

Hall A. BioEdit: a user-friendly biological sequence alignment editor and analysis program for Windows 95/98/NT. *Nucleic Acids Symp Ser*. 1999:41:95–98.

Handel AE, Ebers GC, Sreeram V. Epigenetics: molecular mechanisms and implications for disease. *Trends Mol Med*. 2010:16(1):7–16. https://doi.org/10.1016/j.molmed.2009.11.003.

Hellgren O, Waldenström J, Bensch S. A new PCR assay for simultaneous studies of *Leucocytozoon*, *Plasmodium*, and *Haemoproteus* from avian blood. *J Parasitol*. 2004:90(4):797–802. https://doi.org/10.1645/GE-184R1.

Hershberg R, Petrov DA. Evidence that mutation is universally biased towards AT in bacteria. *PLoS Genet*. 2010:6(9):e1001115. https://doi.org/10.1371/journal.pgen.1001115.

Holliday R. Epigenetics: a historical overview. *Epigenetics*. 2006:1(2):76–80. https://doi.org/10.4161/epi.1.2.2762.

Hollin T, Zeinab C, Roch L, G K. Epigenetic regulation and chromatin remodeling in malaria parasites. *Annu Rev Microbiol*. 2023:77(1):255–276. https://doi.org/10.1146/annurev-micro-032521-041554.

Iezhova TA, Valkiūnas G, Bairlein F. Vertebrate host specificity of two avian malaria parasites of the subgenus *Novyella*: *Plasmodium nucleophilum* and *Plasmodium vaughani*. *J Parasitol*. 2005:91(2):472–474. https://doi.org/10.1645/GE-3377RN.

Langmead B, Salzberg SL. Fast gapped-read alignment with Bowtie 2. *Nat Methods*. 2012:9(4):357–359. https://doi.org/10.1038/nmeth.1923.

Llorà-Batlle O, Tintó-Font E, Cortés A. Transcriptional variation in malaria parasites: why and how. *Brief Funct Genomics*. 2019:18(5):329–341. https://doi.org/10.1093/bfgp/elz009.

Love MI, Huber W, Anders S. Moderated estimation of fold change and dispersion for RNA-seq data with DESeq2. *Genome Biol*. 2014:15(12):1–21. https://doi.org/10.1186/s13059-014-0550-8.

Maïga-Ascofaré O, Le Bras J, Mazmouz R, Renard E, Falcao S, Broussier E, Clain J. Adaptive differentiation of *Plasmodium falciparum* populations inferred from single-nucleotide polymorphisms (SNPs) conferring drug resistance and from neutral SNP. *J Infect Dis*. 2010:202(7):1095–1103. https://doi.org/10.1086/656142.

Mandala WL, Harawa V, Dzinjalamala F, Tembo D. The role of different components of the immune system against *Plasmodium falciparum* malaria: possible contribution towards malaria vaccine development. *Mol Biochem Parasitol*. 2021:246:111425. https://doi.org/10.1016/j.molbiopara.2021.111425.

Manzoli DE, Saravia-Pietropaolo MJ, Arce SI, Percara A, Antoniazzi LR, Beldomenico PM. Specialist by preference, generalist by need: availability of quality hosts drives parasite choice in a natural multi-host–parasite system. *Int J Parasitol*. 2021:51(7):527–534. https://doi.org/10.1016/j.ijpara.2020.12.003.

Matos ADS, Soares IF, Baptista BDO, de Souza HADS, Chaves LB, Perce-da-Silva DDS, JDC L-J. Construction, expression, and evaluation of the naturally acquired humoral immune response against *Plasmodium vivax* RMC-1, a multistage chimeric protein. *Int J Mol Sci*. 2023:24(14):11571. https://doi.org/10.3390/ijms241411571.

Naidoo K, Oliver SV. Gene drives: an alternative approach to malaria control? *Gene Ther*. 2024:32(1):25–37. https://doi.org/10.1038/s41434-024-00468-8.

Nourmohammad A, Rambeau J, Held T, Kovacova V, Berg J, Lässig M. Adaptive evolution of gene expression in *Drosophila*. *Cell Rep*. 2017:20(6):1385–1395. https://doi.org/10.1016/j.celrep.2017.07.033.

Palinauskas V, de la Puente JM, Hernández-Soto SR, Marzal A. Experimental parasitology and ecoimmunology: concepts and opportunities in avian haemosporidian studies. In: Valkiūnas G, Atkinson CT, editors. *Avian malaria and related parasites in the tropics*. Germany: Springer; 2020. p. 527–558.

Palinauskas V, Žiegytė R, Ilgūnas M, Iezhova TA, Bernotienė R, Bolshakov C, Valkiūnas G. Description of the first cryptic avian malaria parasite, *Plasmodium homocircumflexum* n. sp., with experimental data on its virulence and development in avian hosts and mosquitoes. *Int J Parasitol*. 2015:45(1):51–62. https://doi.org/10.1016/j.ijpara.2014.08.012.

Patro R, Duggal G, Love MI, Irizarry RA, Kingsford C. Salmon provides fast and bias-aware quantification of transcript expression. *Nat Methods*. 2017:14(4):417–419. https://doi.org/10.1038/nmeth.4197.

Prati D, Grabner DS, Pfeifer SM, Lorenz AW, Sures B. Generalist parasites persist in degraded environments: a lesson learned from microsporidian diversity in amphipods. *Parasitology*. 2022:149(7):973–982. https://doi.org/10.1017/S0031182022000452.

R Core Team. *R: a language and environment for statistical computing*. Vienna, Austria: R Foundation for Statistical Computing; 2023. https://www.R-project.org/.

Sambrook J, Fritsch EF, Maniatis T. *Molecular cloning: a laboratory manual*. Long Island (NY): Cold Spring Harbor Laboratory Press; 1989.

Schneider VM, Visone JE, Harris CT, Florini F, Hadjimichael E, Zhang X, Deitsch KW. The human malaria parasite Plasmodium falciparum can sense environmental changes and respond by antigenic switching. *Proc Natl Acad Sci U S A*. 2023:120(17):e2302152120. https://doi.org/10.1073/pnas.2302152120.

Serrano-Durán R, López-Farfán D, Gómez-Díaz E. Epigenetic and epitranscriptomic gene regulation in *Plasmodium falciparum* and how we can use it against malaria. *Genes (Basel)*. 2022:13(10):1734. https://doi.org/10.3390/genes13101734.

Sorci G. Immunity, resistance and tolerance in bird-parasite interactions. *Parasite Immunol*. 2013:35(11):350–361. https://doi.org/10.1111/pim.12047.

Turnbull LB, Button-Simons KA, Agbayani N, Ferdig MT. Sources of transcription variation in *Plasmodium falciparum*. *J Genet Genomics*. 2022:49(10):965–974. https://doi.org/10.1016/j.jgg.2022.03.008.

Valkiūnas G, Iezhova TA, Loiseau C, Iezhova TA, Križanauskienė A, Palinauskas V, Sehgal RNM, Bensch S. A comparative analysis of microscopy and PCR-based detection methods for blood parasites. *J Parasitol*. 2008:94(6):1395–1401. https://doi.org/10.1645/GE-1570.1.

Videvall E. *Plasmodium* parasites of birds have the most AT-rich genes of eukaryotes. *Microb Genom*. 2018:4(2):e000150. https://doi.org/10.1099/mgen.0.000150.

Waldenström J, Bensch S, Kiboi S, Hasselquist D, Ottosson U. A new nested polymerase chain reaction method very efficient in detecting *Plasmodium* and *Haemoproteus* infections from avian blood. *J Parasitol*. 2004:90(1):191–194. https://doi.org/10.1645/GE-3221RN.

Wickham H. *Ggplot2: elegant graphics for data analysis*. New York: Springer-Verlag; 2016.

Wyss M, Kanyal A, Niederwieser I, Bartfai R, Voss TS. The *Plasmodium falciparum* histone methyltransferase PfSET10 is dispensable for the regulation of antigenic variation and gene expression in blood-stage parasites. *mSphere*. 2024:9:e0054624. https://doi.org/10.1128/msphere.00546-24.

Yu S, Wang J, Luo X, Zheng H, Wang L, Wang Y. Transmission-blocking strategies against malaria parasites during their mosquito stages. *Front Cell Infect Microbiol*. 2022:12:820650. https://doi.org/10.3389/fcimb.2022.820650.

NOTES

NOTES

Vilniaus universiteto leidykla
Saulėtekio al. 9, III rūmai, LT-10222 Vilnius
El. p. info@leidykla.vu.lt, www.leidykla.vu.lt
bookshop.vu.lt, journals.vu.lt
Tiražas 15 egz.